GROUNDWATER FLOW TO AN AGRICULTURAL TILE-DRAIN UNDER FLOOD IRRIGATION

BY

ROBERT C. REEDY

Submitted in Partial Fulfillment of the
Requirements for the Degree of
Master of Science in Hydrology

New Mexico Institute of Mining and Technology
Socorro, New Mexico
August, 1996

ABSTRACT

The Las Nutrias Groundwater Project was an investigation designed to quantify the effects of common agricultural practices on shallow groundwater at an operating commercial farm equipped with a tile-drainage system. The primary goals of the project were to investigate the quantities of nitrate-nitrogen and pesticide transported to the groundwater in response to flood irrigation and to develop and validate a variably-saturated two-dimensional finite-element flow and transport computer code. Investigations to date have revealed the presence of a strong preferential flow component immediately following an irrigation event characterized by rapid and extreme increases in chemical concentrations in the tile-drain water followed by abrupt decreases in those concentrations (Roth, 1995). This study focused on investigations designed to quantify both the amount of recharge occurring at the site and the amount of that recharge which was captured by the tile-drain system.

To those ends, the water inputs and outputs to the site were monitored in order to obtain a water balance. Tile-drain flow rate, chemistry, and head was monitored in an isolated section of one of the four tile-drain laterals at the site. A network of 55 monitoring wells and piezometers provided regional water table information and slug tests were performed in most of the wells to obtain estimates of the saturated hydraulic conductivity with depth. Precipitation and irrigation volumes were also measured. Evapotranspiration was estimated using a combination of methods. Instantaneous profile experiments were conducted at four locations at the site to quantify unsaturated hydraulic characteristics.

The measured tile-drain flow and chemical response to flood irrigation events during 1995 and early 1996 were compared to the tile-drain NO_3^- response data gathered during the 1994 season. The comparison indicated that of the total mass of NO_3^-N lost by all mechanisms during the 1994 season (840 kg), a range of 14% to 38% (21 to 55 kg/ha) was leached to the shallow groundwater. Tile-drain NO_3-N concentrations remained at essentially background levels for the duration of the 1995 and early 1996 irrigation seasons. Results of the water balance investigations revealed that evapotranspiration exceeded combined irrigation and effective precipitation during both the growing season (by at least 33.5 cm) and the calendar year (by about 5 cm). The net upward flux explains the persistent saline conditions in the soils. The tile-drain flow and chemistry responded rapidly to irrigation events, generally exhibiting an increase in electrical conductivity while flow rates either increased or decreased; the conductance of the tile-drain exhibited strongly non-linear hysteretic behavior that depended on irrigation sequence and timing. About 1.25% to 3.3% of the total recharge water was captured by the tile-drains. Computer simulations indicated that only particles located within a distance of a few centimeters immediately above or adjacent to the tile-drain exhibited travel times consistent with the responses observed. Most of the tile-drain flow originated from depths below the tile-drain.

TABLE OF CONTENTS

TABLE OF CONTENTS (CONTINUED)

LIST OF FIGURES

LIST OF FIGURES (CONTINUED)

LIST OF TABLES

ACKNOWLEDGMENTS

This thesis is dedicated to the memory of Jack Reedy, my father, and to my mother Gerri, for their unwavering support and love. Thanks, Dad. Thanks, Mom.

The Las Nutrias Groundwater Project was primarily funded by a grant from the United States Department of Agriculture - Cooperative State Research Service, Special Water Quality Grant No. 92-34214-7417 to the New Mexico Institute of Mining and Technology. Further funding was graciously provided by the Socorro Soil and Water Conservation District.

I would like to thank my advisor Dr. Jan M. H. Hendrickx, for his friendship and for the consulting work he threw my way. The extra income and experience is greatly appreciated. I also thank my thesis committee members Dr. Robert S. Bowman and Dr. John L. Wilson for their friendship, support, and guidance throughout this project and in my graduate career.

I would also like to extend thanks to my fellow graduate students and partners in crime Tracy Roth, Jeff Chaves, and Steve Roy. They made the long hours in the heat, cold, wind, rain, dust, bugs, etc., bearable and even, at times, fun. Additional thanks go to Will Holoman, Leo Porta, and Günter Hilmes for their help in both the field and the lab. I also thank the landowner and Darrel Reasner of the NRCS for their input. Further help was provided by Binayak Mohanty of the U.S. Salinity Lab.

Finally, I thank my wife Andrea for her love and patience. I am a lucky man. I never knew life could be this good.

1. INTRODUCTION

The hydrogeology of the Rio Grande Valley has been the subject of intense scrutiny in recent years due to the importance of its aquifer system as one of the major groundwater reservoirs in the southwestern United States. Investigations began early in this century and continue to date in an effort to characterize and model groundwater flow and the interactions between surface water and groundwater. Concepts of both the nature and extent of the aquifer system have evolved considerably. Estimates of the actual volume of available, high-quality groundwater have decreased while the present and projected water demands of population, agricultural, and industrial growth have increased.

Irrigated agriculture is by far the dominant consumer of both surface water and groundwater withdrawals, accounting for approximately 80% of total water use in the state. In the Albuquerque Basin, 98% of agricultural irrigation water is withdrawn from surface water sources (Wilson, 1992). Essentially all of the agricultural activity in New Mexico occurs in or near river valleys due to the fertile soils present there. These valleys are also the location of most of the state's population. Groundwater derived from the aquifer systems present in these valleys represents approximately 90% of non-agricultural water needs (Wilson, 1992). Agricultural chemicals, in the form of fertilizers and pesticides, therefore represent a significant potential hazard to both surface water and groundwater quality and hence to the value of those waters as a commercial and domestic resource. The possible leaching of applied fertilizers and pesticides may degrade groundwater quality. Surface water quality may also be affected

through direct runoff or through leaching to and subsequent return by inflow of contaminated shallow groundwater.

There has been relatively little effort expended to date in characterizing the impact of agricultural chemicals on shallow groundwater in the southwestern United States. Most previous studies have been conducted at experimental test sites where the investigators had essentially complete control over all aspects of the investigation. Additionally, many of these investigations have concentrated their efforts in areas where soil conditions, climate, and farming practices differ substantially from those experienced in New Mexico. To date, no comprehensive studies concerning the impacts of agriculture on shallow groundwater quality have been completed in New Mexico.

1.1 Scope of the Las Nutrias Groundwater Project

Our investigation, christened "The Las Nutrias Groundwater Project" (LNGP), was designed to study the impacts of common agricultural practices on shallow groundwater on an operating commercial farm. Specifically, the impacts of applied pesticides and nitrogen fertilizers were investigated. Methods and materials utilized in the investigation were designed not to hamper the farming operation: the land owner continued his standard operating procedures and we observed the groundwater responses.

There were two main objectives of the project. The primary objective was the collection and analysis of field data to characterize the hydrology of the site and to quantify the effects of standard agricultural practices on the shallow groundwater under the site. The second objective was the development of a deterministic, two-dimensional, variably saturated, dual-domain flow code coupled with a solute transport code. Data collection and field investigations were designed to obtain estimates of the parameters required for the model and were also utilized in the validation stages of model development.

The computer model was developed by coinvestigators at the US Salinity Laboratory (USDA-ARS) in Riverside, California, as an extension of their SWMS_2D and CHAIN_2D codes (Šimünek, et al., 1994). The model utilizes linear finite element methods with triangular elements to simulate water, solute, and heat transport. Water flow is simulated using a two-dimensional form of the Richard's equation modified to account for plant water uptake. The model incorporates scaling parameters to simplify the spatial variability of unsaturated

hydraulic properties and their temperature dependence. A bimodal unsaturated hydraulic conductivity function was developed to simulate preferential flow at low water tension values due to macropore structure.

Solute transport is simulated using a generalized form of the advection-dispersion equation which allows for linear and nonlinear equilibrium reactions between the liquid, gas and solid phases. The model incorporates zero-order production, independent first-order degradation, and dependent first-order decay/production of solutes which experience sequential first-order reactions. Conductive and convective heat movement in the solid and liquid phases is also incorporated, though latent heat transfer by vapor movement is ignored.

1.2 Scope and Organization of this Thesis

The focus of this thesis is the characterization of the physical aspects of groundwater flow at the site; specifically, to characterize tile-drain flow dynamics and to determine regional and local flow components to the tile-drain system during and following flood irrigation events. This is approached through the characterization and estimation of the hydrologic properties of the soils and aquifer at the site. These parameters, coupled with the results of previous investigations at the site (Roth, 1996) are utilized in the computer model Visual MODFLOW (Guiguer and Franz, 1996) in an attempt to quantify travel times to the tile-drain of particles originating at various lateral distances from the tile-drain and at or near the water table.

This thesis is organized under eight main headings: (1) Introduction, (2) Methods, (3) Results and Discussion, (4) Computer Modeling, (5) Conclusions, (6) Recommendations, (7) References, and (8) Appendices. Each of the first three headings is divided into sections. Sections *1.3* and *1.4* provide background information relating to the physical location and description of the LNGP site and its context in relation to the regional hydrogeology. Section *1.5* is a brief overview of regional agricultural practices. Section *1.6* describes site irrigation system and practices and the tile-drainage system. Sections *1.7* and *1.8* discuss the results of a site soil survey and the results of previous investigations conducted at the LNGP site. Section *1.9* discusses agricultural practices conducted by the landowner with respect to cropping pattern, fertilizer/pesticide applications, and crop yields.

The "Methods" heading outlines the methods and materials used to obtain the model parameter estimates as well as background information concerning the instrumentation and specific methods of data collection and analysis. Where appropriate, the accuracy and precision of the various methods is discussed. Each section under this heading corresponds numerically with a section under the "Results and Discussion" heading.

The "Results and Discussion" heading presents the results of the respective experiments and calculation procedures. Where appropriate, problems encountered during the data collection and the reliability of the results are discussed. The last, section *3.8*, presents simple water balance calculations based on the results of the relevant previous sections for both the growing season and for the calendar year 1995.

The "Modeling" heading presents the computer modeling setup and results. The final four headings are self-explanatory.

1.3 Location and Physical Description of the Site

The Las Nutrias Groundwater Project field site is located approximately 56 km (35 mi) north of Socorro, New Mexico, near the village of Las Nutrias at the southern end of the Albuquerque Basin (Figure 1). The site is reached by taking Interstate 25 exit 175 at Bernardo, east 5.6 km (3.5 mi) on US Highway 60, then north 5.3 km (3.3 mi) on NM Highway 304 to the village of Las Nutrias (Figure 2). The project site is approximately 1.4 km (0.9 mi) west of the village along a dirt road. The western edge of the site is about 0.4 km (0.25 mi) east of the Rio Grande and covers an area of approximately 25 ha (60 ac). The site is divided by berms into three benches (Figure 3 and Figure 4). The benches lie at progressively lower elevations toward the west and are hereafter referred to as the east, center, and west benches. The center bench (Figure 5) is the most heavily instrumented and hence the most intensely studied portion of the site. Other irrigated farms lie adjacent to the north, east, and south of the site with bosque (riparian) lands adjacent to the west between the site and the Rio Grande.

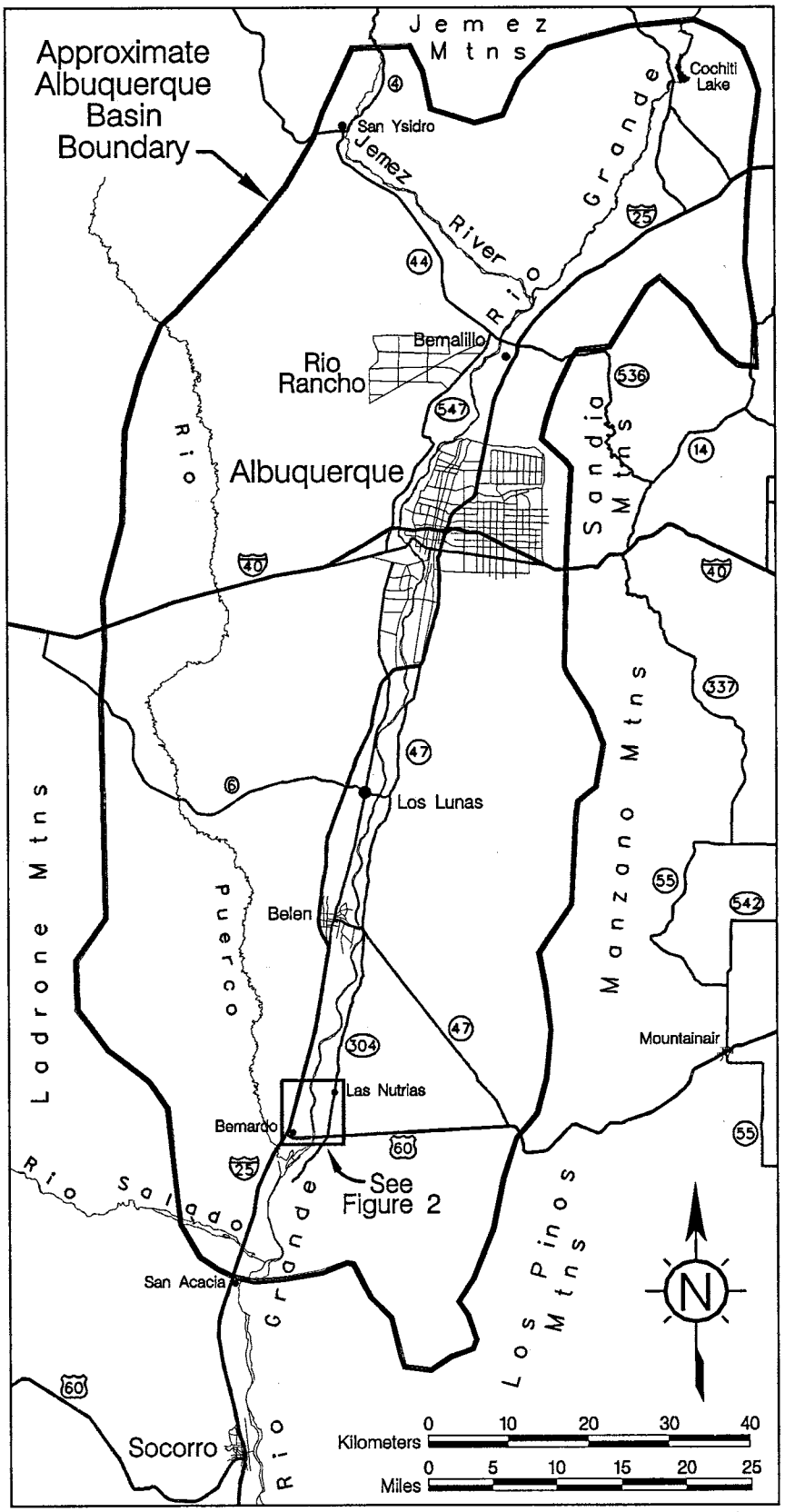

Figure 1: Albuquerque Basin (approximate boundary)

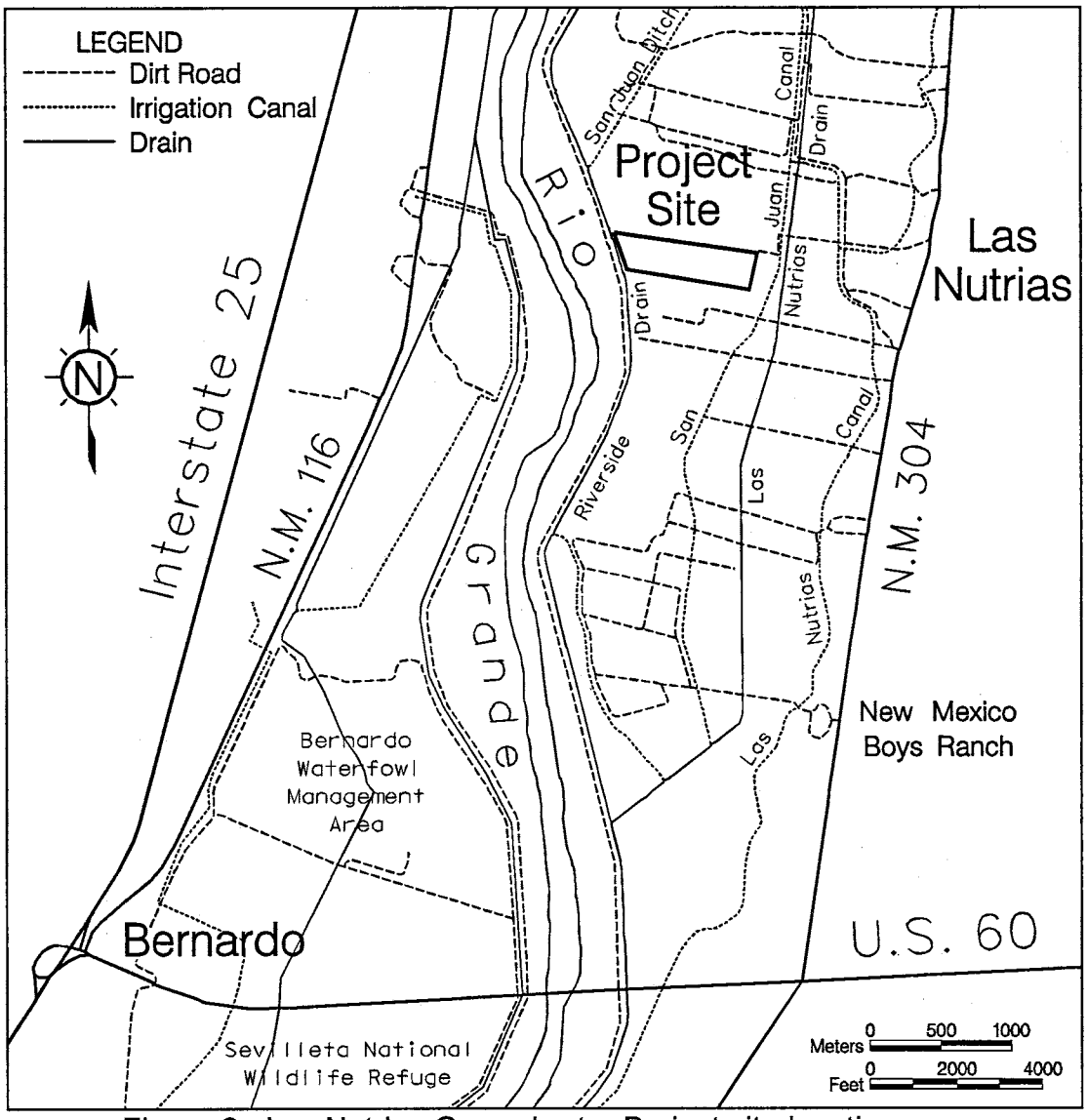

Figure 2: Las Nutrias Groundwater Project site location map

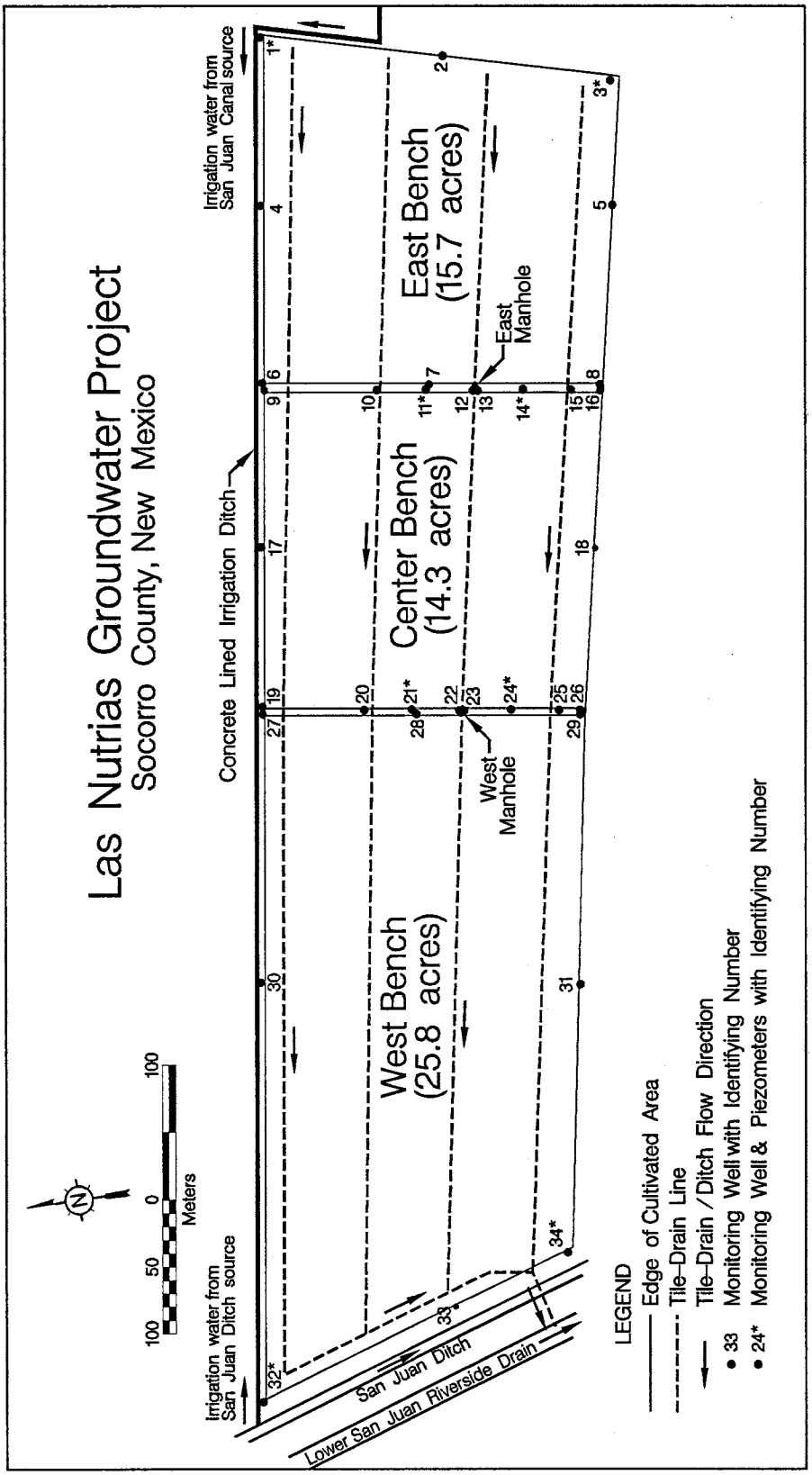

Figure 3: Las Nutrias Groundwater Project site map

Figure 4: 1984 aerial photograph of the Las Nutrias Groundwater Project site (Heavy lines indicate berms between benches)

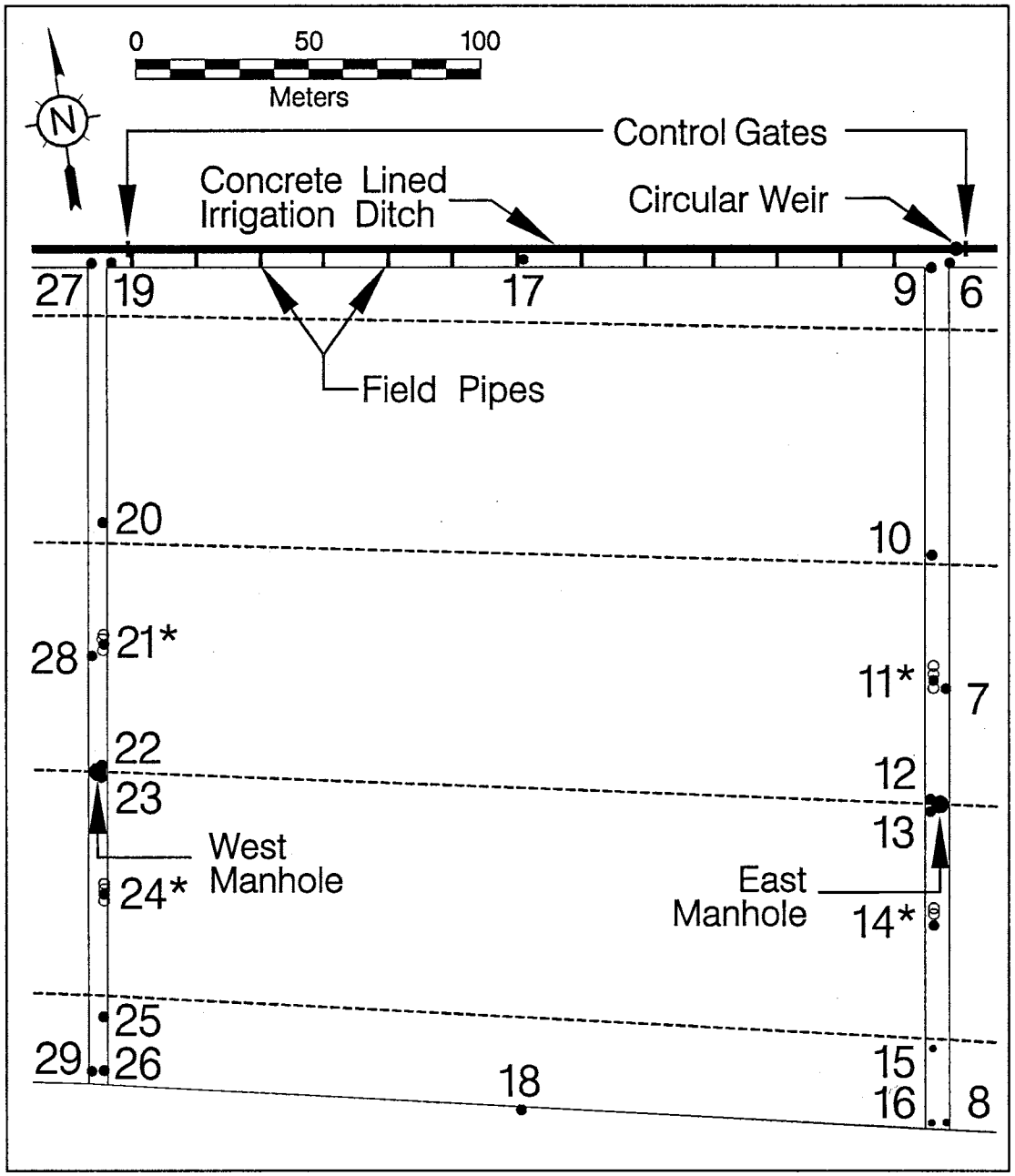

Figure 5: Center bench detail (numbers refer to wells - see legend in Figure 3)

The site lies at an elevation of approximately 1450 m (4760 ft) above mean sea level on the flood plain of the Rio Grande. The regional climate is arid to semi-arid, with annual precipitation averaging about 200 mm (8 in) in the valley to over 500 mm (20 in) in the mountains (USDA-SCS, 1988). About 50% of the annual precipitation in the valley is in the form of rain which falls from

(occasionally) intense, localized thunderstorms during the so-called monsoon season from early July through mid-September. More than 70% of the total annual precipitation occurs from May through October, the warmest six months of the year. (USDA-SCS, 1988)

The average annual temperature in the proximity of the LNGP site is 15°C (59°F) (USDA-SCS, 1988). Air temperatures vary widely through the year, based on a 37-year historical record of climatological data collected at the Agricultural Science Center (ASC), located about 32 km (20 mi) north of the LNGP site near Los Lunas, New Mexico. Winter daily temperatures range from -8 to 10°C (18 to 50°F) and summer daily temperatures range from 15 to 33°C (60 to 92°F). Relative humidity at the site also ranges widely and is not representative of the region in general due to the microclimatic conditions of the Rio Grande inner valley. Values at the ASC average about 45% for the year, with daily ranges of 10-60% in the summer to 30-100% in the winter. Daily maximum and minimum relative humidity values respectively coincide with the daily minimum and maximum temperature. Potential evapotranspiration for 1995, later discussed in detail, was about 2000 mm.

1.4 Hydrogeological Setting

There have been many extensive geologic and hydrologic investigations of the area performed by a host of investigators and agencies in an effort to characterize the structural and depositional history of the Albuquerque Basin. Many of these efforts have concentrated in recent years on the development of an understanding of the basin-scale hydrogeologic system. The following is a brief overview of the hydrogeologic features of the basin, chiefly derived from Hawley et al. (1995), Kelley (1977), Kernodle et al. (1995), and Thorn et al. (1993).

The dominant structural feature in the region is the Rio Grande Rift. Rifting began during the Oligocene (ca. 30 MA) and has continued episodically to the present. The rift extends approximately 1000 km (600 mi) from south-central Colorado, through New Mexico, into the western panhandle of Texas near El Paso, and into Chihuahua, Mexico. The site is located near the southern limit of the Albuquerque Basin (Figure 1), one of several basin structures located along the rift axis. The Albuquerque Basin, defined at the extent of Cenozoic deposits, extends from the La Bajada escarpment near Cochiti Reservoir to approximately San Acacia with an axial length of some 160 km (100 mi), an average width of 48 km (30 mi), and a surface area of about 7800 km^2 (3000mi^2).

The Albuquerque Basin was created from a series of *en-echelon* listric, normal faults trending north-south with an occasional left oblique shear component along basin boundary faults. The central portions of the structure have dropped while the marginal areas have been elevated, with major faults in

the basin interior exhibiting as much as 9000 m (30,000 ft) of vertical displacement. Some faults may constitute significant hydrologic features as barriers to flow where impermeable beds juxtapose permeable beds or where the faults are cemented. Conversely, faults which are not cemented may act as conduits for groundwater flow.

The eastern margin of the basin is dominated by the Sandia, Manzano, and Los Piños Mountains with maximum elevations of 3255 m (10,685 ft) at Sandia Peak to about 2350 m (7700 ft) in the Los Piños. These mountains consist primarily of Precambrian igneous and metamorphic rocks unconformably overlain by late Paleozoic (Pennsylvanian and Permian) limestones, sandstones, and mudstones. They generally exhibit steep, western-facing escarpments and gentle eastern-dipping slopes. The western edge of the basin is flanked by the southern extension of the Colorado Plateau and is significantly lower in elevation compared to the eastern uplifts, with maximum elevations ranging from 2400 to 2800 m (7800 to 9200 ft). Along the northern half of the western flank, formations consist of Mesozoic (Triassic through upper Cretaceous) sandstones and mudstones while along the southern half the Ladrone Mountains consist of late Paleozoic units as described above.

The basin interior is structurally divided into a northern, east-dipping half graben and a southern west-dipping half graben, with the demarcation between the two lying just south of Albuquerque. Elevations of the valley floor range from 1300 to 1550 m (4300 to 5100 ft) along the Rio Grande to as much as 1830 m (6000 ft) at the base of the eastern uplift. Basin stratigraphy is divided into three

major subdivisions based on depositional environment, lithofacies, and age: (1) pre-Santa Fe Tertiary rocks, (2) Santa Fe Group basin-fill sediments, and (3) post-Santa Fe river-valley and basin-fill sediments.

Pre-Santa Fe Tertiary rocks consist of lower and middle Tertiary sediments, primarily sandstones and mudstones, and silicic to basaltic intrusive and volcanic rocks of (late?) Oligocene to Miocene age. These units were deposited in two structural basins that predate the Albuquerque Basin and range in thickness up to 2100 m (7000 ft). They are not considered an important component of the hydrologic system due to their low permeability and depth of burial (>~4000m).

The Santa Fe Group is informally divided into the Lower (LSF), Middle (MSF), and Upper (USF) units. The LSF consists of alluvial, playa lake, and locally thick eolian facies in the middle of the basin which grade laterally into conglomeratic sandstones and mudstones at the basin margins. Deposited during early rifting in the late Oligocene and early Miocene (15-25 MA), these deposits range up to 1100 m (3500 ft) thick in the central basin. The LSF, along with the MSF, was deposited on the central plains of an internally drained basin complex. Due to the finer grained material, partial induration, and deep (>3000m) burial, the LSF is also generally not considered a major component of the aquifer system. Water quality is poor except in the local eolian deposits.

The MSF unit ranges from 1500 to 3000 m (5000 to 10,000 ft) thick in the center of the basin and was deposited during the middle to late Miocene (5-15 MA) during an episode of rapid basin subsidence/filling that also witnessed

much of the uplifting of the eastern mountain ranges. Deposits are similar in character to the LSF with the addition of localized, interbedded, basaltic to silicic volcanic flows and tuffs and local braided stream deposits. As with the LSF, water quality is generally poor though the upper sections of the unit, particularly the braided stream deposits, may locally have a significant hydrological role.

The USF is characterized by wide spread, coarse- to fine-grained fluvial (channel) deposits of the ancestral Rio Grande, Rio Puerco, and Rio Salado systems that grade laterally into piedmont-alluvial facies at the margins of the basin. There are also locally present eolian and volcanic flows and pyroclastic units. USF deposits were laid down during the late Miocene to early Pleistocene (1-5 MA) after through-flow conditions of the ancestral Rio Grande were established. Thickness of the USF is generally less than 300 m (1000 ft) though locally exceeds 600 m (2000 ft). The USF, in combination with inner-valley, post-Santa Fe units, forms the major aquifer system in the region.

Post-Santa Fe units consist of middle to late Pleistocene through Holocene (1-0 MA) alluvial and fluvial deposits. Piedmont-slope alluvium deposits at the margins of the basin range from 0 to 45 m (0 to 150 ft) thick and intertounge basin-ward with valley-border and river-terrace deposits up to 60 m (200 ft) thick. These deposits lie mostly in the vadose zone. River fluvial, channel, floodplain, and lower terrace deposits of the inner Rio Grande, Rio Puerco, and Rio Salado valleys range up to 37 m (120 ft) in thickness and are in contact with the USF. These deposits form the upper part of the shallow aquifer system and are present immediately under the project site.

The most significant recharge to the basin occurs as mountain-front recharge along the uplifts to the east and through the beds of intermittent streams and arroyos during and following flash flooding. Another major component is recharge from the Rio Grande and leakage from the Middle Rio Grande Conservancy District (MRGCD) irrigation ditches. Shallow groundwater elevations in the area of the site are controlled primarily by the MRGCD network of ditches and drains (Figure 2). Due to the extent of the network and the lack of funds, the system is rather poorly maintained, particularly the drains which have not been dredged for many years. The result is that the drains have silted and no longer operate efficiently. Thus, the drainage of discharged irrigation water or return flow is impaired and water levels under the LNGP site remain quite shallow for most of the irrigation season.

1.5 Regional Agricultural Practices

Most crops grown in the Albuquerque Basin are for consumption or grazing by livestock. The most significant crops grown in the area of the site are alfalfa, corn, sorghum-sudan, oats, and green chili (Darrel Reasner, NRCS, per. com., 1996). The average growing season, defined as frost-free days, is from late-April or early-May to about mid-October, a period of approximately 165 days. Flood irrigation methods are utilized for approximately 98% of irrigated land in the Albuquerque Basin. Irrigation water is available from March 1 through October 31 and is conveyed through a system of diversion dams, ditches, and drains administered by the MRGCD.

The amount of fertilizers administered depends on the crop requirements, soil conditions, and type of fertilizer. Commonly used fertilizers include ammonium sulfate, ammonium nitrate, urea, and nitrogen-phosphorous-potassium-sulfur formulations. Alfalfa, which is a nitrogen-fixing plant and therefore requires little or no nitrogen fertilization, generally demands less supplemental nutrients. There are literally thousands of pesticide formulations approved for use in New Mexico. Application of pesticides varies in both amount and timing. Often, pesticides are applied as a preventive measure while at other times they are applied on an as-needed basis.

1.6 Site Irrigation and Tile-Drainage Systems

Irrigation water is supplied to the site from two sources: the San Juan Canal to the east and the San Juan Ditch to the west (Figure 3 and Figure 4). Water is conveyed to the site fields from these sources through a trapezoidal concrete-lined irrigation ditch adjacent to the north of all three benches. The ditch has a bottom width of 30.5 cm (1 ft) with 45° sloping sides and a depth of approximately 76 cm (2.5 ft). Due to the elevation of the conveyance channels relative to the benches, the standard practice is to irrigate the east and center benches from the San Juan Canal source and the west bench from the San Juan Ditch source. Occasionally, both sources are used simultaneously to irrigate the west bench. There are gates set across the ditch near each of the two berms to facilitate the selective irrigation of each bench. Water is applied to the fields through a series of 25 cm (10 in) ID field pipes set in the southern wall of the concrete ditch, each with a separate gate mounted flush against the ditch wall. The center bench has 13 such field pipes spaced at approximate 18.3 m (60 ft) intervals (Figure 5).

The farm is equipped with a subsurface tile-drainage system which provides a means for measuring both the average quality and quantity of groundwater flowing beneath the field. The tile-drainage system was installed in 1979 in an effort to abate soil salinization by lowering the local water table. Since that time, disturbances of the soil profile due to installation have been mitigated by cultivation (Bowman et al., 1992). A cross-sectional view of the theoretical groundwater response to a tile-drain system in a single-layer,

homogeneous, and isotropic soil profile is presented in Figure 6. In designing the tile-drain system, the lateral distance between drains is a function of the hydraulic conductivity of the aquifer, the rate of recharge, the desired maximum water table elevation, and time. Under equilibrium conditions, atmospheric pressure should exist inside the tile-drain pipes.

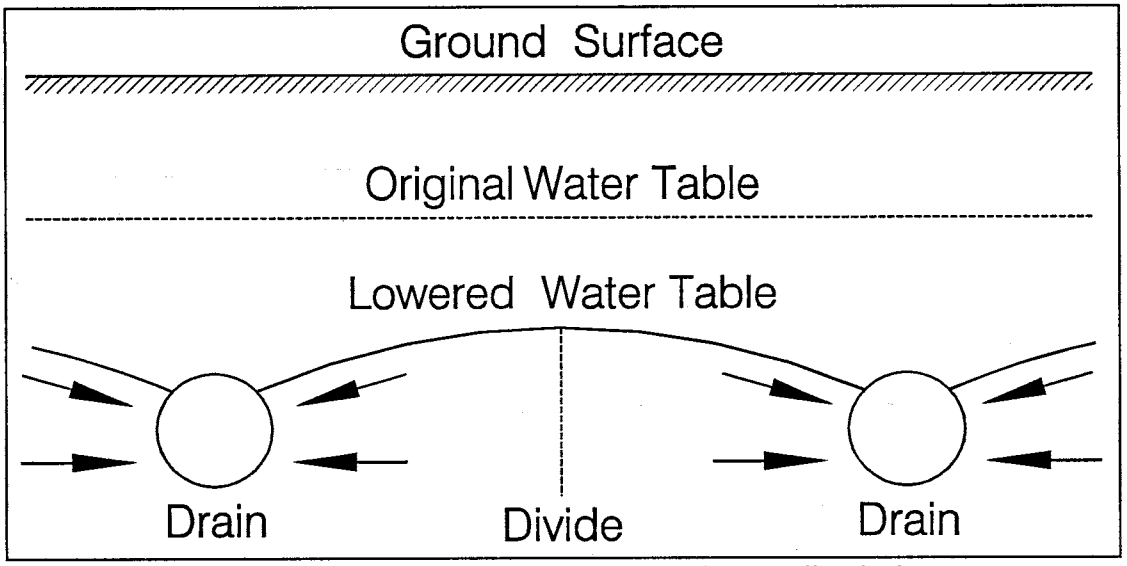

Figure 6: Theoretical groundwater flow to tile-drains

The tile-drainage system at the site consists of four lateral pipes, numbered 1 through 4 from north to south, respectively (see Figure 3 and Figure 5). See Table 1 for a summary of drain lateral design plan lengths and diameters. The tile-drains are perforated plastic pipe wrapped with nylon filtersock and buried approximately 1.2 to 1.8 m (4 to 6 ft) below ground surface. The laterals are spaced at approximate 65 m (215 ft) intervals trending east-west with a design gradient of 0.1% under the east bench and 0.05% under the center and west benches. However, a survey of the tile-drain pipe elevations in the manholes, discussed later, revealed that the actual gradient below the center bench is closer to 0.025%. The lateral spacing gradually increases from west to

east. The pipes are 10.2 cm (4 in) ID under the east bench while under the center bench they are 12.7 cm (5in) ID. Under the west bench, laterals #1 and #2 change to 15.2 cm (6 in) ID pipe 91 m (300 ft) and 61 m (200 ft), respectively, from their western ends. Laterals #3 and #4 remain at 12.7 cm ID under the entire west bench. All four laterals are joined at their western ends by a southerly flowing 15.2 cm ID collection pipe which enlarges to 20.3 cm (8 in) ID at the junction with lateral #3. At the junction with lateral #4, the collection pipe turns southwest for 44 m (145 ft) to the system effluence into the Lower San Juan Riverside Drain, the last 6 m (20 ft) enlarging to 25.4 cm (10 in) ID. Tile-drain density is approximately 164 m/ha (215 ft/ac).

Table 1: Summary of tile drain pipe lengths

	West Bench		Center Bench	East Bench	
Lateral #	Length of 6" pipe (ft)	Length of 5" pipe (ft)	Length of 5" pipe (ft)	Length of 4" pipe (ft)	Total Length (ft)
1	300	1320	800	835	3255
2	200	1320	800	810	3130
3	-	1420	800	770	2990
4	-	1370	800	730	2900
Total	500	5430	3200	3145	12275

Tile-drainage waters normally flow to the west and are collected in the Riverside Drain, which lies at a lower elevation adjacent to and west of the San Juan Ditch (Figure 3). Due to silting of the Riverside Drain, the tile-drainage system outflow pipe is submerged throughout the irrigation season and for much of the winter. This inhibits drainage of the tile-drains and results in a decrease in the efficiency of the entire system.

1.7 Soils

A detailed soil survey conducted by the Soil Conservation Service (SCS), now the Natural Resource Conservation Service (NRCS), in April and July, 1993, described soil profiles at 196 locations on the center bench to a depth of 152 cm (5 ft). Four main soil series were identified: Saneli, Glendale, Anthony, and Harkey. A description of the Harkey series does not exist in the reference material (USDA-SCS, 1988). Additionally, two Glendale units were mapped though no differentiating features were reported or were evident in the reference material. A map of the soil series distribution is presented in Figure 7. Locations of the series boundaries and survey location points are somewhat subjective as the original survey notes contained ambiguities as to sample point locations. The original survey map was published by Chaves (1995). There are no substantial differences between the original map and that depicted in Figure 7.

The Anthony series is classified as a coarse-loamy, mixed (calcareous), thermic Typic Torrifluvent that is well drained and has a moderately rapid permeability. The Ap horizon ranges from fine sand to sandy loam in texture. The C horizon above about 100 cm is fine sand, loamy very fine sand, or very fine sandy loam. Below 100 cm, the C horizon is fine to very fine sand or silt loam. Clay contents are generally less than 18% with some thin clayey strata possible. Pore structure is described as very fine interstitial grading downward to very fine tabular.

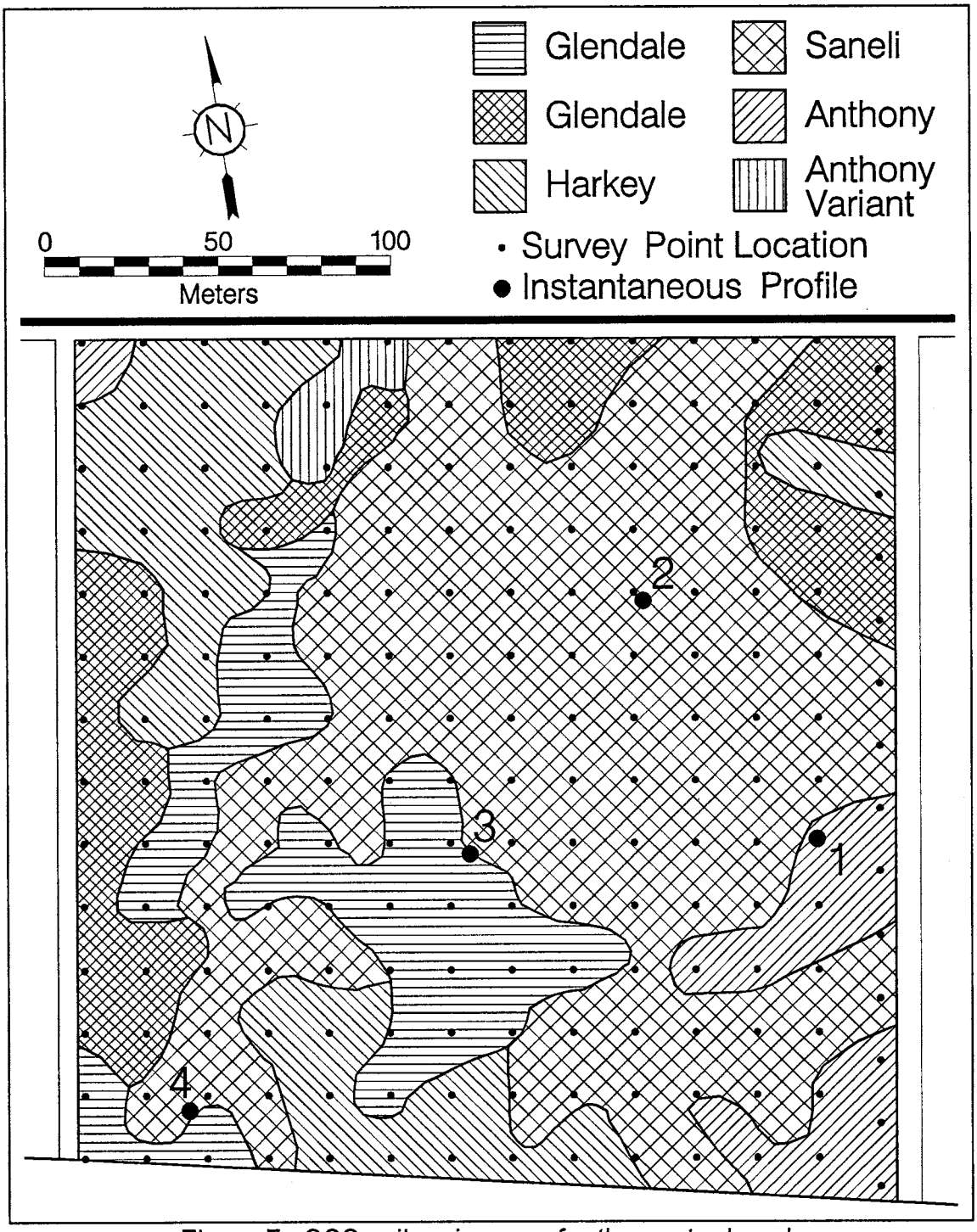

Figure 7: SCS soil series map for the center bench

The Anthony Variant series is classified as a coarse-loamy over clayey, mixed (calcareous), thermic Typic Ustifluvent that is well drained and has a slow

permeability. It is similar to the Anthony series but with a 20 to 40 cm thick clay layer at a depth of 60 to 95 cm.

The Glendale series is classified as a fine-silty, mixed (calcareous), thermic Typic Torrifluvent that is well drained and has a moderately slow permeability. The Ap horizon ranges from sandy loam to clay loam while the C horizon is stratified clay loam, silty clay loam, sandy loam or silt loam. Pore structure is described as commonly medium- grading downward to very fine tabular.

The Saneli series is classified as a clayey over sandy or sandy-skeletal, montmorillonitic (calcareous), thermic Vertic Torrifluvent that is well drained and has a very slow permeability. The Ap horizon is clay or silty clay. The upper C horizon is clay or silty clay while the lower C horizon is sand, fine sand, loamy sand, or loamy fine sand. The clay layer is 40 to 80 cm thick at depths from 20 to 75 cm. Cracks up to 2 cm in width are noted to extend from the surface through the clay layer.

Among other properties, the survey identified soil layer textural classifications, thicknesses to within 1 in, and "feel" method estimates of clay weight content. Those results are tabulated in Appendix A1. At least four distinct horizons were identified in 178 (89%) of the profiles: Ap, C1, C2, and C3. To illustrate the high degree of both lateral and vertical variability in the site soils, Figure 8 plots the percentile scores of clay content versus depth along with the average soil horizon depths. The Ap horizon exhibits fairly normally distributed clay contents. At the top of the C horizon, median clay content

increases dramatically reflecting the Saneli series clay layer. With increasing depth in the C horizon, clay content distributions display negative skewness grading downward to positive skewness as median textures become coarser grained and clay content decreases. Once sand is encountered (commonly the C3 horizon), there are generally no underlying, finer grained materials to a depth of 152 cm. The soils exhibit a full range of textures from clayey through sandy, with the clayey areas developing well defined shrinkage cracks at the surface as they dry.

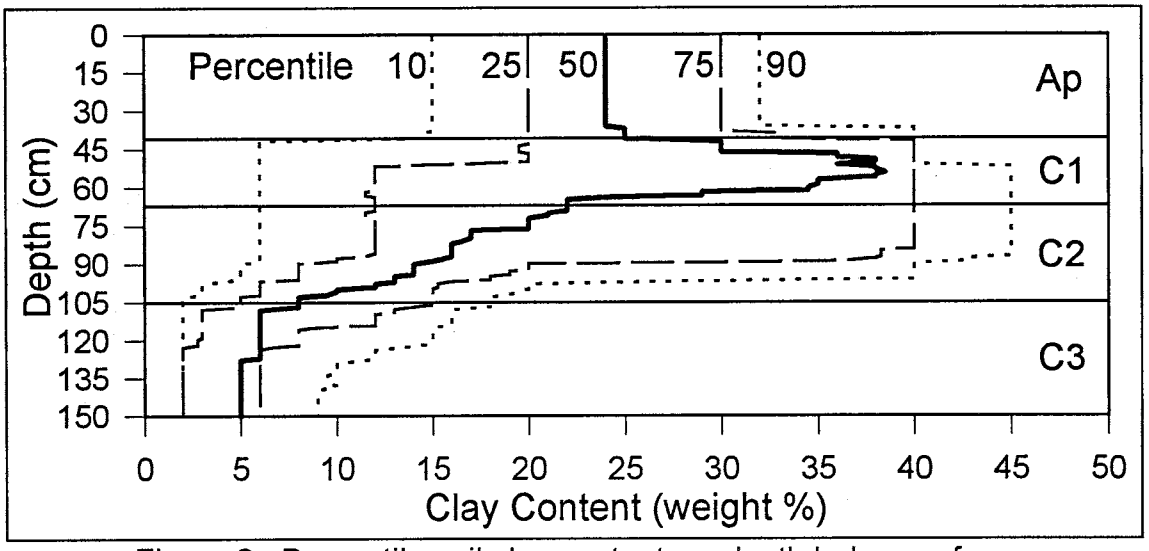

Figure 8: Percentile soil clay content vs. depth below surface

The Saneli series dominates much of the center bench. With the noted macropore structure of this series and, though to a lesser extent, of the other mapped series, there is a high potential for preferential flow pathways through the clayey upper soil layers to the sands below. The system of macropores is further enhanced by both floral and faunal activity in the form of root channels, earthworm burrows, and gopher tunnel networks. The latter have been observed to be extensive, especially during the early part of the irrigation season

near the berms where irrigation water applied to an adjacent higher-elevation bench wells up through the tunnels at substantial rates. Gopher tunnel networks were also noted in the more sandy regions within the central regions of the fields.

1.8 Previous Investigations

Investigations conducted during the 1994 growing season were conducted by Chaves (1995) and Roth (1996). Chaves investigated the spatial and temporal distribution of saturated and unsaturated hydraulic conductivity of surface soils utilizing both ponded and tension infiltrometers. Hydraulic conductivities were measured at 104 locations in the center bench at 0-, 3-, 6-, and 15 cm tensions. Soil core samples were obtained at nine of those locations and returned to the laboratory for more intensive characterization of the volumetric water content vs. pressure head relationship up to 170-cm tension using hanging water columns. Chaves (1995) concluded that there was no spatial correlation of infiltration rates, though there was an overall increase in infiltration rates as the growing season progressed.

Roth (1996) investigated nitrate-nitrogen and chloride concentrations in both the center bench soils and in the tile-drain. Over the course of the 1994 growing season, Roth determined that approximately 81% of the nitrate-nitrogen present in the center bench soil profile was either leached to the groundwater, utilized by the (sorghum-sudangrass hybrid) crop, or underwent bacterial denitrification. Roth collected soil core samples at 54 locations to a depth of 120 cm in 10 cm increments. The sample locations were spaced at 1.5 m intervals along a north-south transect centered on lateral #3 in the center of the center bench. The samples were then composited into four 30 cm intervals and analyzed for nitrate-nitrogen concentration. Analysis of the composited samples revealed that nitrate-nitrogen concentrations decreased with depth, both before

and after the 1994 irrigation season. More than 81% of the total mass of nitrate-nitrogen lost (by whatever mechanism) originated in the top 60 cm of the soil profile while more than 60% originated in the top 30 cm. Tile-drain water samples were collected using automated samplers, discussed later in the "Methods" section of this thesis.

Estimates ranged from 6% to 55% of nitrate-nitrogen leached to the groundwater. This rather wide range of values was due primarily to uncertainty concerning the tile-drain capture zone and flow dynamics. As will be discussed later, determination of return flow to the tile-drain was problematic in that the flow response depended strongly on the sequence and timing of east-center-west bench irrigation. Tile-drain nitrate concentrations exhibited a rapid increase, followed by a period of sustained high concentration, then a rapid decrease after an irrigation event with relatively little tailing, indicating a strong preferential flow component. By the beginning of the 1995 irrigation season, this observed nitrate concentration response had decreased to essentially background levels. Unfortunately, a reliable tile-drain flow measurement system was not in place until the beginning of the 1995 growing season, disallowing a direct determination of the actual mass intercepted by the tile-drain during the 1994 growing season. The estimate of the mass of nitrate-nitrogen leached to the shallow groundwater was therefore based on a water/mass-balance approach using the average irrigation return flows as observed during the 1995 irrigation season, the measured volumes of applied irrigation water and precipitation, and an estimated evapotranspiration volume.

1.9 Agricultural Practices at the Site

Crops planted on the fields of our study site included alfalfa, corn, sorghum-sudangrass hybrid, and winter wheat. Table 2 summarizes the crop and harvest schedule during the project, as well as fertilizer and pesticide application rates and formulations at the site, partially after Roth (1996).

Table 2: Site crop rotation, harvest, and chemical application schedule.

			Bench		
Year	Date	Event	West	Center	East
<1991	---	(Crop)	Corn	Corn	Alfalfa
1993	6/25	Fert. (400 lb/ac $(NH_4)_2SO_4$)	X[1]	X	---[2]
	10/5	Harvest	X	X	---
	10/10	Plant	WW[3]	WW	---
	10/15	Fert. (200 lb/ac Urea)	X	---	---
	10/25	Fert. (200 lb/ac Urea)	---	X	---
1994	3/7	Fert. (400 lb/ac $(NH_4)_2SO_4$)	X	---	---
	4/19	Pesticide (Lorsban)	---	---	X
	5/13	Harvest	X	nc[4]	---
	5/13	Plant	SS[5]	SS	---
	5/13	Fert. (200 lb/ac Urea)	X	---	---
	5/30	Harvest	---	---	X
	7/19	Harvest	X	X	---
	7/23	Pesticide (Lorsban, 1 pt/ac)	---	---	X
	9/14	Harvest	X	X	---
	9/25	Plant	Alfalfa	Alfalfa	---
1995	4/3	Fert. (250 lb/ac 8-36-4-4 N-P-K-S)	X	X	X
	4/20	Pesticide (Lorsban, 1.5 pt/ac)	---	---	X
	5/29	Harvest	X	X	X
	7/3	Harvest	X	X	X
	8/4	Harvest	X	X	X
	9/5	Harvest	X	X	X
	10/14	Harvest	X	X	X
1996	3/21	Fert. (250 lb/ac 8-36-4-4 N-P-K-S)	X	X	X
	4/18	Pesticide (Dimate 4E 0.75 pt/ac)	X	X	X
	4/18	Pesticide (Baythroid 2 3.2 oz/ac)	X	X	X
	5/15	Harvest	X	X	X

[1]event occurred [2]event did not occur [3]winter wheat [4]no crop [5]sorghum-sudan

The winter wheat crop planted on the center bench in October, 1993, did not grow. This is thought to be due to the sensitivity of winter wheat to saline soil conditions, which exist on the center bench. The fact that this crop did not grow and, subsequently, that the applied fertilizer was not utilized, is thought to be the primary reason for the observed extreme increase of nitrate levels in the tile-drain water through the 1994 growing season (Roth, 1996).

1995 alfalfa harvest tonnage and moisture contents per cutting as reported by the landowner are given in Table 3. Separate tonnage figures for the center bench were not recorded except for the final cutting of the season. Total dry matter harvested throughout the 1995 growing season was approximately 265 metric tons (292 English tons) based on a total cultivated area of 22.9 ha (56.5 ac) for all three benches. Not included in the cultivated acreage is an approximate 0.8 ha (2 ac) area in the southeast corner of the west bench which has been essentially abandoned due to high salinity. It is noted that, for the single harvest for which a separate yield figure was available for the center bench, yield was essentially identical to the average per acre yield for the east and west benches on the preceding day. This is in spite of the fact that there are several areas of the center bench which support little or no crop activity due to high salinity conditions.

Table 3: 1995 Alfalfa Harvest Tonnage

Harvest Date	Bench	English tons/ac[1]	Moisture Content[2]	Dry Matter	
				English tons/ac	Metric tons/ha
May 28-30	All	4.43	0.70	1.33	2.98
July 3-4	All	4.10	0.70	1.23	2.76
August 4-5	All	3.00	0.70	0.90	2.02
September 5	All	3.30	0.70	0.99	2.22
October 14	Center	0.85	0.12	0.75	1.68
October 13	W+E	2.40	0.70	0.72	1.61
			Total	5.18	11.65

[1]Wet weight. [2]Weight fraction.

2. METHODS

2.1 Precipitation

In April, 1994, three plastic rain gauges were mounted in unobstructed areas on 4x4 in posts located at the north-central edge of the center bench near monitoring well #17 and at each of the two manholes (Figure 5). The posts rose approximately 1.8 m (6 ft) above the elevation of the center bench. The gauges, manufactured by Productive Alternatives, Inc., Fergus Falls, MN., consisted of a top funnel which channels precipitation into a measuring tube. The capacity of the measuring tube was 25 mm (1 in.). Precipitation in excess of 25 mm was collected in a surrounding overflow chamber. The measurement scale accuracy was 0.1 mm.

During the months of November, 1994, through February, 1995, cattle were allowed to graze on the west bench. During this time, the rain gauge located at the west manhole was damaged and was not subsequently replaced. During the months of November, 1995, through February, 1996, cattle were again allowed access, though on all three benches. None of the three gauges could be maintained operational during this time.

Precipitation measurements were recorded manually. Thus, there were inevitable losses due to evaporation following an event and before the next field visit, possibly also leading to entirely unrecorded events. However, frequent visits to the field did occur during the months of highest precipitation.

2.2 Evapotranspiration

No direct measurements of evapotranspiration (ET) were made at the field site. Therefore, estimation of ET was required. Two general approaches were employed: (1) estimated ET based upon climatological data coupled with crop coefficients and capillary flux simulations and (2) estimated ET based upon crop yield tonnage.

In the first approach, daily reference (potential) evapotranspiration (ET_o) values were calculated based on hourly climatological data collected at the Agricultural Science Center (ASC) located three miles south of Los Lunas, New Mexico, approximately 32 km (20 mi) north of the field site. Weather conditions at the ASC were assumed to be, on average, substantially similar to those at the site to allow for a meaningful calculation. This assumption is justified by the small difference in elevation between the sites (approximately 30 m). Additionally, both sites are located in irrigated agricultural areas within the inner Rio Grande Valley where microclimatic conditions of wind speed, humidity, oasis effect, etc., should be very similar.

Daily ET_o values were calculated using two methods, both based on the modified Penman equation (Penman, 1963). See Appendix C1 for a listing of the equations and constants used in the calculations. The Penman method is the preferable method when, as in this case, adequate meteorological data are available. The first calculation procedure used the method employed by the ASC, the second method used the procedure suggested by the Food and Agriculture Organization (FAO) of the United Nations (Doorenbos and Pruitt,

1977). Both methods utilized the same daily climatological data: air temperature, relative humidity, wind speed, and solar radiation, all of which were measured and recorded on an hourly basis at the ASC location. The ASC method employed a direct calculation. The FAO method utilized published tables and was originally intended to be used for a more gross estimate of ET_o for irrigation scheduling. As a result, several of the tabulated data were not sufficient for determining daily values of the parameters required for the calculation. Where this situation existed, the given tabulated data were plotted and regression techniques applied to obtain polynomial coefficients resulting in a high (>0.99) coefficient of determination. In all cases, second-order polynomials were satisfactory. These polynomial relationships were then used to interpolate daily values for the FAO ET_o calculation. The results of the parallel ET_o calculations using both methods were then compared.

The calculated value of ET_o determined with the FAO method was then multiplied by an experimentally determined crop coefficient, *kc*. The *kc* is a dimensionless value which is a measure of the crops ability to hinder or enhance the evaporation process. In the case of alfalfa, the FAO published a curve relating a 28-day harvesting cycle to the *kc* for dry climates with light to moderate winds, conditions similar to those found in New Mexico (Doorenbos and Pruitt, 1977). The curve rises non-linearly from approximately 0.40 after a harvest to 1.18 prior to the next harvest to form an S-shape. The shape of this 28-day curve was mapped linearly to the time intervals between LNGP site harvests and with respect to the (slightly extended) ASC published frost-free

growing season in order to obtain daily *kc* values. The growing season was extended to the final harvest on October 14 to match observed minor growth following the official season.

Published values for alfalfa *kc* were not available outside the frost-free period, a time when the crop was dormant and plant root activity is assumed negligible. Following the 1994 irrigation season and prior to the first 1995 irrigation, the surface soils were dry and the water table had steadily lowered to approximately 1.3 m below the ground surface. Following the last 1995 irrigation in late October and the end of the growing season, the water table elevation again dropped due to the cessation of irrigation, thereby increasing tension on the soil profile and probably resulting in a net downward flow of soil water. Ignoring this complicating factor and, in the presumed absence of significant plant root uptake activity during the winter months, the remaining mechanisms for transport of water to the surface for evaporation are capillary rise and vapor-phase transport. No attempt was made to quantify vapor-phase transport at the site. In order to estimate the maximum depth of water that might have evaporated during the winter months, capillary flux simulations for the center bench soils were performed using the program CAPSEV (Wesseling, 1991). The program calculates the maximally possible capillary flux through a defined soil texture profile for a given water table depth. The flux is calculated for a specified depth location within the soil profile for a range of prescribed soil water tension values at that depth. Steady-state conditions are assumed.

The van Genuchten soil parameters obtained from both the instantaneous profile experiment (see Results section) and those published by Carsel and Parrish (1988) (Table 4) were used to define the soil texture profiles at each of the 196 SCS soil survey locations. Where instantaneous profile results for a given soil texture were available, those values were used in preference to the corresponding Carsel and Parrish values. Additionally, the parameters for fine sand were used for all horizons logged as sand in the SCS soil survey profiles. It is noted that, in general, the site soil parameters do not differ greatly from those of Carsel and Parrish. A range of soil water tension values from 100 to 10,000 cm was specified at a proscribed depth of 4 cm below the ground surface to generate simulated capillary flux values at each location, each over a range of water table depths from 70 to 175 cm. The area-weighted average capillary flux values for each water table depth and tension value was then determined.

Daily average water table depths were then calculated and used in the determination of a daily averaged capillary flux value. Daily average water table depth values were calculated using an area-weighted method as described later in section 2.4. An exponential regression function was fitted to the average water table elevation data collected from November 2, 1995, through March 2, 1996, and used to directly calculate the average depth to the water table as a function of time. Use of the average value resulted in a deviation of ±4 cm from the actual value for over 90% of the center bench area. The remaining 10% was deeper. The area-weighted daily average capillary flux values were finally

compared with the FAO daily ET_o to ensure that the flux value did not exceed the reference value.

Table 4: Carsel and Parrish (1988) soil parameters

Texture	θ_r	θ_s	K_s (cm/day)	α(/cm)	n
Sand	0.045	0.43	712.80	0.145	2.68
Loamy Sand	0.057	0.41	350.20	0.124	2.28
Sandy Loam	0.065	0.41	106.10	0.075	1.89
Loam	0.078	0.43	24.96	0.036	1.56
Silt	0.034	0.46	6.00	0.016	1.37
Silt Loam	0.067	0.45	10.80	0.020	1.41
Sandy Clay Loam	0.100	0.39	31.44	0.059	1.48
Clay Loam	0.095	0.41	6.24	0.019	1.31
Silty Clay Loam	0.089	0.43	1.68	0.010	1.23
Sandy Clay	0.100	0.38	2.88	0.027	1.23
Silty Clay	0.070	0.36	0.48	0.005	1.09
Clay	0.068	0.38	4.80	0.008	1.09

The second method employed to estimate ET utilized a linear crop yield function developed by Sammis and others (1979) which relates New Mexico alfalfa crop yield to consumptive water use. The empirical equation, presented in equation 2.2-1, was developed from lysimeter studies located at widely spaced geographical locations throughout New Mexico and had a coefficient of determination, r^2, of 0.89.

$$y = -1.36 + 0.11ET \tag{2.2-1}$$

where:

y = alfalfa yield (Metric tons/ha at near 0% moisture content)
ET = consumptive water use (cm)

While this relationship is not appropriate for a daily estimate of consumptive water use, it can provide a comparison value for total seasonal consumptive use as determined by the FAO method. Additionally, Mapel and

others (1985) developed a third-order polynomial model for estimating average monthly crop coefficients based on the concept of growing degree days. The number of growing degree days for any given day is the daily average number of degrees above some base temperature. The base temperature is the temperature below which growth for a given crop ceases. For alfalfa the base temperature is 5°C. Determination of the number of alfalfa growing degree days, G_d, on a given day during the growing season is thus:

$$G_d = T_{AVE} - 5 \tag{2.2-2}$$

where T_{AVE} is the average of the high and low temperatures for a given day. The total growing degree days in the season, G_T, is:

$$G_T = \sum_{d=1}^{n} G_d \tag{2.2-3}$$

where n is the number of days in the growing season. The relationship for the average monthly crop coefficient, *AKC*, was developed based on the same lysimeter studies mentioned above and had a somewhat lower r^2 of 0.69. The equation is:

$$AKC = 0.405 + \left(1.11 \times 10^{-3}\right) G_T - \left(4.25 \times 10^{-7}\right) G_T^2 + \left(3.65 \times 10^{-11}\right) G_T^3 \tag{2.2-4}$$

2.3 Unsaturated Soil Hydraulic Properties

Instantaneous profile (IP) experiments were conducted in April, 1995, at four locations on the center bench (Figure 7). The IP method is capable of determining estimates for the unsaturated hydraulic conductivity and water characteristic functions of a soil profile (Watson, 1966). The method consists of measuring simultaneously and at successive times the volumetric water content and pressure head at different depths within a soil profile as the initially saturated profile drains.

Experimental locations were chosen which, as best as possible, reflected the most commonly occurring vertical textural sequences in the center bench. Figure 9 displays the soil textures and thicknesses at the chosen locations and the tensiometer installation depths. The experimental installations consisted of a 5.1 cm (2 in) ID aluminum neutron probe access tube surrounded at a radius of approximately 60 cm (2 ft) by an array of tensiometers set at various depths. Access tubes were installed with a 5.1 cm (2 in) soil auger to a depth of approximately 1 m (3.3 ft) below ground surface and plugged at the bottom to prevent water entry. Tensiometers consisted of 5.1 cm (2 in) porous ceramic cups cemented to 7/8 in CPVC pipe of varying lengths and were installed in slightly under-sized holes. The top 3 to 4 cm of the tensiometers consisted of a clear plastic section capped with a septum. Pairs of tensiometers were installed vertically to a given depth on opposite sides of the neutron probe access tube and 6 to 8 depths were monitored at each installation. Surrounding each tensiometer array was a barrier constructed of soil. A protective plastic covering

was secured over the plot after ponding to prevent evaporative water loss and to exclude precipitation.

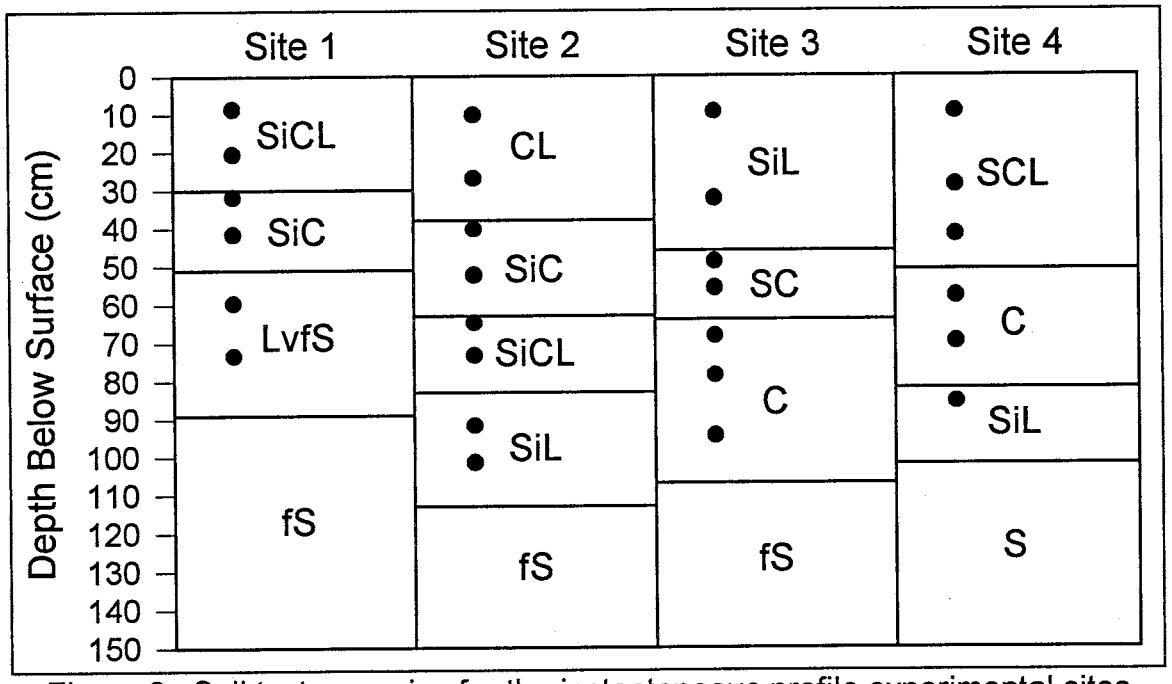

Figure 9: Soil texture series for the instantaneous profile experimental sites (Circular symbols represent tensiometer depths at each site)

Water was maintained ponded within the plot barriers and soil water pressures were monitored. Experimental data collection commenced when pressures ceased to change under ponding, typically after 4 to 5 hours. For approximately the following two weeks (i.e., until the next irrigation event), simultaneous measurements of water content and pressure were taken.

Soil water pressure was measured using a Tensimeter electronic vacuum gauge (Soil Measurement Systems, Las Cruces, NM) connected to a hypodermic needle. The needle was inserted through the tensiometer septum to measure the pressure of the volume of air just above the tensiometer water column. The Tensimeter provided a pressure measurement in millibars (mb) relative to (zero) atmospheric pressure. Soil water pressure was determined by adding the height

of the water column within the tensiometer, in centimeters, to the (negative) pressure measurements. The height of the water column was determined as the length measured from the center of the exposed porous cup to the top of the water column.

Volumetric water content measurements were obtained with a Model 503DR Hydroprobe® Moisture Depth Gauge (CPN Co., Martinez, CA), serial number H34045324. The meter consists of a fast neutron source (50mCi ^{241}Am), a slow neutron detector, and electronics for counting and converting the detected slow neutrons. Counts displayed by the meter are biased by a factor of 100, then normalized to a 16-second period. The probe is stored in the instrument housing and sheathed in a silicon-based paraffin substance having an apparent volumetric water content of 20.0%.

The emitted fast neutrons are slowed primarily by collisions with the nuclei of hydrogen molecules. Some elements, particularly boron, have an affinity for neutrons and if present in significant concentrations can result in a lowered count of the slow neutrons and thus an underestimate of the amount of water in the vicinity of the detector. In the absence of this complication, the number of slow neutrons detected is a direct measure of the amount of water in the vicinity of the source/detector.

The decay rate of the neutron source is assumed to have a normal distribution. The precision of a single neutron probe measurement increases as a function of the number of slow neutrons detected during the measurement period. Thus, higher water contents result in higher counts and greater

precision. In a homogeneous and uniformly saturated soil, the sampled region is spherical in shape and is referred to as the sphere of importance. Soils with higher water content result in a smaller sampled soil volume as the neutrons cannot penetrate as far as within soils having lower water content. Thus, changes in water content at soil texture boundaries tend to be smoothed and the geometry of the sampled area becomes irregular. Neutron probe measurements also become less reliable with proximity to the soil surface boundary as the spherically sampled region intersects the atmosphere, leading to an underestimate of water content. An empirical relationship by Visvalingam and Tandy (1972) is presented in Figure 10 which relates the radius of the sphere of importance, R_i, to the volumetric water content, θ_v.

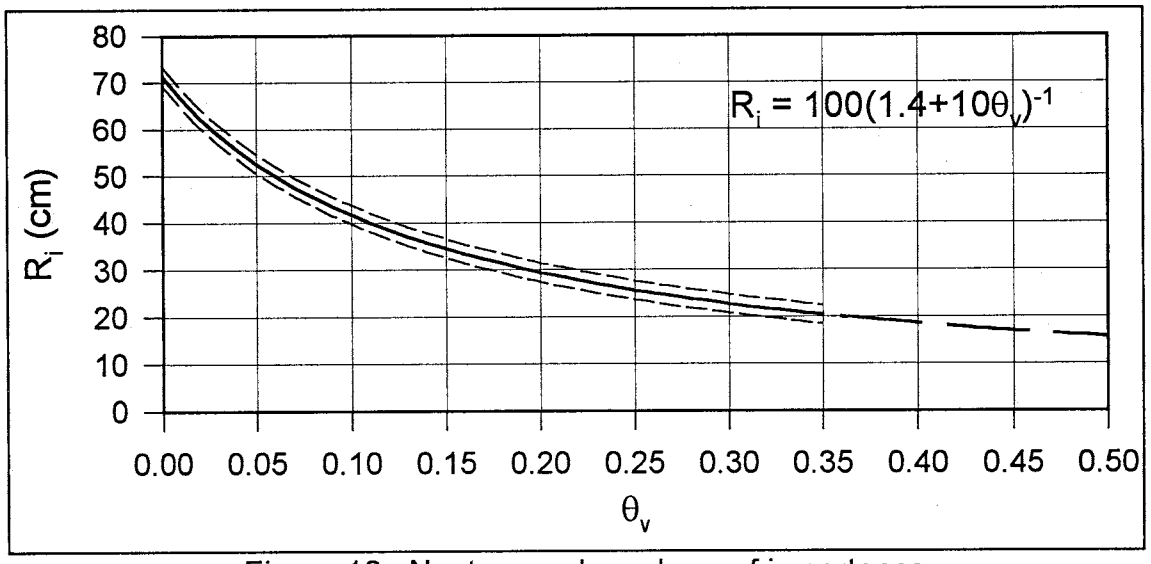

Figure 10: Neutron probe sphere of importance

The relationship was determined only up to θ_v=0.35 with a stated accuracy of ±2 cm (short-dashed lines). However, projecting the relationship to higher θ_v values (long-dashed line) should not introduce too much error and should provide a reasonable estimate of R_i. It is evident that for θ_v>0.35,

measurements closer than about 16 to 20 cm (6 to 8 in) to a boundary will result in a biasing of measurements across that boundary.

In addition to the soil measurements, five standard measurements were obtained on each date with the probe housed in the unit surrounded by the paraffin. Results of the standard measurements indicated that the probe was functioning within the accepted precision guidelines as published by the manufacturer. All neutron probe measurements consisted of a 32-second count period which was normalized by the probe electronics to a 16-second period. Neutron probe measurements obtained during the course of the experiment ranged from 6782 to 9684 counts (normalized to 16-second periods) resulting in single-measurement precision ranging from ±0.9% to ±0.7%, respectively.

Following the experiment, soil samples were obtained at several of the monitored depths at experimental locations 3 and 4 for bulk density and volumetric water content analysis in order to obtain a calibration for the neutron probe. Three soil samples of approximately 200 cm^3 each were collected at each depth, each within 10 to 20 cm of the neutron probe access tube, using cylindrical metal sample tubes. Samples of 100 cm^3 volume were also obtained at four depths at a location just southeast of the east bench in an area which receives no irrigation water. All samples were sealed in plastic bags as they were collected. The samples were later weighed, broken up into small (<0.5 cm^3) pieces, oven-dried at 105°C for 24 hours, then weighed again for determination of soil bulk density and volumetric water content. Just prior to sample collection, neutron probe counts were obtained at the sample depths.

The (normalized) neutron probe counts for a given depth were then plotted against the 3-sample averaged volumetric water content at that depth. A linear regression was performed to obtain the calibration equation.

Analysis of the IP data was performed by Benayak Mohanty of the US Salinity Laboratory, Riverside, Ca., using both the method outlined by Watson (1966) and the RETC code (van Genuchten et al., 1991) to obtain estimates of the unsaturated hydraulic soil characteristics.

2.4 Monitoring Wells, Piezometers, and Ground Elevation Survey

To monitor the water table and local hydraulic gradients, a total of 34 groundwater monitoring wells and 23 piezometers were installed at the site around the perimeter of the cultivated areas during February-March, 1993. Their locations and identifying numbers are shown in Figure 3. Drilling methods employed both jet pumping and hollow-stem augering. All wells were drilled with 7.6 cm (3 in) diameter holes. The well pipes were fitted with nylon filtersocks and the annuli back-filled with sand. Well screens consist of 1.27 cm (0.5 in) diameter holes spaced vertically 5.1 cm (2 in) apart at 90^0 intervals around the pipe. Holes on opposite sides of the pipe are offset vertically by 2.5 cm (1 in).

All well pipes were originally set with an above-ground extension. Due to subsequent damage from farming equipment, the wells were cut off below ground level and plastic valve boxes were installed around the wellheads. All wells were capped with removable PVC caps. Monitoring wells were 5.1 cm (2 in) ID PVC pipe installed at 34 locations at a nominal depth of 2 m (6.5 ft) below ground surface and were screened for their entire length. Monitoring wells were assigned names consisting of a number followed by the letter "A". Piezometers were 2.5 cm (1 in) ID PVC pipe installed at 8 of the monitoring well locations at nominal depths of 3-, 5-, and 7 m below ground surface and were screened over the bottom 20 cm. Piezometers were assigned names consisting of the number of the associated monitoring well followed by the letter "B", "C", or "E" for the 3-, 5-, or 7 m depth, respectively.

A wellhead elevation survey was conducted in August, 1993. Elevations were in feet relative to a benchmark (5/8 in diameter rebar stake) set near the fence corner in the extreme southwest of the west bench which was assigned an arbitrary 100 ft elevation. Elevations were recorded with 0.05 ft (1.5 cm) resolution. Wellhead elevation measuring points were marked with black ink for consistency of depth to water measurements. A second survey was conducted in February-March, 1996. This survey determined elevations with a resolution of 0.01ft (0.3cm) for the measuring points of all wells. See Appendix E1 for monitoring well and piezometer physical data. All elevations were converted to metric equivalents based on an arbitrary 100 m elevation assigned to the benchmark. Additionally, ground surface elevations were determined at 45 locations within the cultivated area of the center bench and surface elevation contours were generated with SURFER version 5.00 software (Golden Software, 1994) using triangulation and linear interpolation algorithms.

Water level surveys were conducted at varying time intervals. Two water level meters (Solinst, Inc., Ontario, Canada), were employed for the depth-to-water measurements. Meter #1 consisted of a 30 m long, flat insulated wire with a centimeter increment scale and a metal weight below the zero reference point having a displacement volume of approximately 5.5 cm^3. Meter #2 consisted of a 15 m long, round insulated wire having no marked scale and with metal weights above the zero reference point resulting in a displacement volume of <0.2 cm^3. Both meters functioned by lowering the weighted wire end into the well where contact with the water surface caused the circuit to close and an

audible signal was subsequently sounded by the meter. The weight at the end of Meter #1, which displaced water levels in the monitoring wells by only about 2.5 mm, caused significant displacement of water (about 11 mm) in the smaller diameter piezometers. Thus, Meter #2 was required which caused negligible displacement in the piezometers (~0.4 mm). No corrections were made for displacements caused by the meters as the vertical displacements were less than the resolution of the well head measurement point elevation survey. Additionally, most of the wells were set in porous media having a saturated hydraulic conductivity high enough to allow for significant recovery of the displaced volumes during the measurement process.

Water elevations in each well were determined by subtracting the depth to water measurements from the surveyed elevation of the measuring point for each well. Water contour maps were generated with SURFER using universal kriging algorithms (quadratic surface trend removal) based on the monitoring well water elevations. Residual vertical distances (at the monitoring well locations) between the measured and interpolated water table surfaces were analyzed for significant deviations. Vertical pressure gradients for adjacent "B", "C", and "E" piezometers were determined by dividing the change in total head between a pair of wells by the difference of their respective average screen elevations. Vertical gradients between the "A" and "B" wells were determined similarly but using the elevation of the mid-point of the saturated interval of the "A" well.

2.5 Slug Tests

Slug tests were performed in 31 monitoring wells and 23 piezometers in order to obtain estimates of the saturated hydraulic conductivity for the lower soil horizons and underlying aquifer sands. Instantaneous lowering of water levels in the wells was achieved through the rapid removal of a sealed and weighted section of PVC pipe or "slug" as described below. Recovery of water levels was monitored with Druck Model 35D differential (6-wire) pressure transducers (RST Instruments, Yakima, WA) and recorded using a Model CR-10 data logger (Campbell Scientific, Inc., Logan, UT) connected to a portable computer. Recovery data was logged on a quasi-logarithmic time scale ranging from 0.25 to 5.00 second intervals. Calibration equations for each of five pressure transducers were incorporated into the data logger software and water depths were recorded in meters.

Five pressure transducers were calibrated at approximately 10 points over a range of water depths from 0.015 to 2.800 m (0.05 to 9.19 ft). See Appendix F1 for calibration data. The pressure transducers and their wire leads were taped to 1.83 m (6.0 ft) lengths of 0.64 cm (0.25 in) or 0.48 cm (0.188 in) all-thread metal rod. The all-thread served three purposes: to aid in the calibration process, to prevent the transducer from moving upon slug removal from the well being tested, and to prevent the wire leads from becoming entangled with the slug in the small diameter wells being tested.

Slugs were constructed from PVC pipe, filled with sand for weighting, and plugged at each end. A metal screw-eye was attached to one plug and a length

of 0.5 cm corded nylon rope attached to the screw-eye. There were two slug length/diameter configurations: monitoring well slugs were 3.3 cm (1.3 in) OD with a 1 m length while piezometer well slugs were 1.65 cm (0.65 in) OD with a 1.5 m length.

Slug test data for all wells were analyzed using the Bouwer and RIce (B-R) technique (Bouwer and Rice, 1976). This empirical technique is based on the steady-state Thiem equation and generates estimates of hydraulic conductivity for either a partially- or completely penetrating well. The method assumes that the aquifer is unconfined, isotropic, homogeneous, and radially infinite. The method additionally assumes that the matrix is incompressible (negligible specific storage) and that flow is radial (negligible vertical flow component). The mathematical solution for hydraulic conductivity incorporates either one or two dimensionless coefficients depending upon whether the well is fully- or partially penetrating, respectively. The coefficient values were determined empirically by Bouwer and Rice with an electrical analog. The geometry and symbols utilized in the technique are presented in Figure 11.

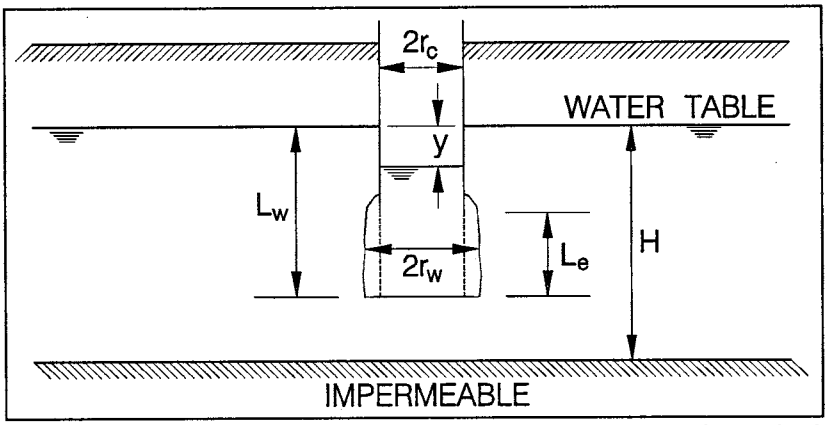

Figure 11: Bouwer and Rice (1976) geometry and symbols

The equation that Bouwer and Rice present is:

$$K = \frac{r_c^2 \ln(R_e/r_w)}{2L_e} \frac{1}{t} \ln \frac{y_0}{y_t} \qquad (2.5\text{-}1)$$

where symbols not defined in Figure 11 are:

K = saturated hydraulic conductivity (L/T)
R_e = effective radius of the well (L)
r_c = radius of well casing (L)
r_w = radius of well, including disturbed/developed zone (L)
H = saturated aquifer thickness (L)
L_w = length of well below the water table (L)
L_e = length of well screen (L)
t = time elapsed from slug removal (T)
y_0 = head level in the well immediately after slug removal (L)
y_t = head level in the well at a given recovery time t, (L)

The effective radius of the well represents the area of aquifer over which the slug perturbation is dissipated and is the only unknown value in Equation 2.6-1. The electrical analog analysis evaluated R_e for various system geometries and, for partially penetrating wells, was expressed as:

$$\ln \frac{R_e}{r_w} = \left[\frac{1.1}{\ln(L_w/r_w)} + \frac{A + B \ln[(H - L_w)/r_w]}{L_e/r_w} \right]^{-1} \qquad (2.5\text{-}2)$$

A and B are dimensionless coefficients obtained from a graph published by Bouwer and Rice (1976) which plots the coefficients as a function of L_e/r_w. Thus, with the stated assumptions, the effective radius is uniquely defined by the well geometry. By obtaining a plot of log drawdown ($\log_{10}$ s) vs. time (t) and regressing the early time straight-line section formed by the data points, the t=0 intercept value becomes y_0.. Any convenient t-y_t pair of values is subsequently chosen from the regressed line and the hydraulic conductivity is directly calculated.

The appropriateness of the B-R simplifying assumptions has been tested by various investigators for the purpose of quantifying any error that may be introduced into the hydraulic conductivity estimate based on the violation of those assumptions. Brown and Narasimhan (1995) used a numerical model to test the results of the B-R technique when the screened interval intersects the water table, a situation similar to the LNGP site monitoring wells. They found that in this situation the B-R method underestimated hydraulic conductivity by 50% or more relative to their simulated value.

Hyder et al. (1995) also used a numerical approach to test the B-R method assumptions. They investigated the effects of well geometry, aquifer anisotropy and specific storage (compressibility), and the proximity of the well screened interval to an aquifer boundary on the accuracy of the B-R hydraulic conductivity estimate. They developed a computer model (KGSMOD) which generates time-drawdown data given well geometry parameters, formation physical and hydrologic parameters, and initial head displacement. Among other findings, they determined that in situations of both small (<50) well aspect ratio (ratio of screen length to well radius) and small (<10) normalized distance to the water table (ratio of screen depth to screen length), the B-R hydraulic conductivity was underestimated. All of the piezometers at the LNGP site have aspect ratios of 5.25 and the monitoring well aspect ratios ranged from approximately 15 to 30 during the tests. Additionally, all of the monitoring wells were screened across the water table. Thus, in order to estimate the possible error introduced by these compounding situations, KGSMOD was executed for

each well using the respective B-R hydraulic conductivity value. Results of the KGSMOD simulations were then compared with the actual test data. If a noticeable difference was noted, adjustments made to the calculated B-R hydraulic conductivity values and KGSMOD was re-run until reasonably close matches between the slug test well-response data and the simulated well-response data were obtained.

2.6 Irrigations

The weir structure for measuring irrigation water application rates was installed in late May, 1994. Irrigation events were not recorded automatically and thus required the physical presence of field personnel. Only four of the eight 1994 season center bench irrigation events were recorded. The situation improved in the 1995 season, when eleven of the thirteen center bench irrigations were recorded.

Measurements of applied irrigation water volumes were determined using a circular weir located in the irrigation ditch at the northeast corner of the center bench (Figure 5). The irrigation ditch is trapezoidal in cross-section having a base width of 30.5 cm (1 ft) and 45° (1:1) sloping sides. Schematic diagrams of the circular weir are presented in Figure 12. The weir consists of a 25.4 cm (10 in) OD PVC pipe set vertically in the center of the irrigation ditch. Critical flow conditions are achieved with this weir when the ratio of the weir diameter to channel base width exceeds 0.75 and when down-stream flow conditions are less than 80% submerged (Samani and Magallanez, 1993). The weir diameter to channel base ratio here is 0.83. The weir was installed about 2 m up-stream from a 4 m long section of irrigation ditch having a greatly increased slope. During irrigations, a standing wave was consistently observed at the end of this steeper ditch section. Thus, at no time was there any hydraulically connected down-stream flow and critical flow at the weir was consistently maintained.

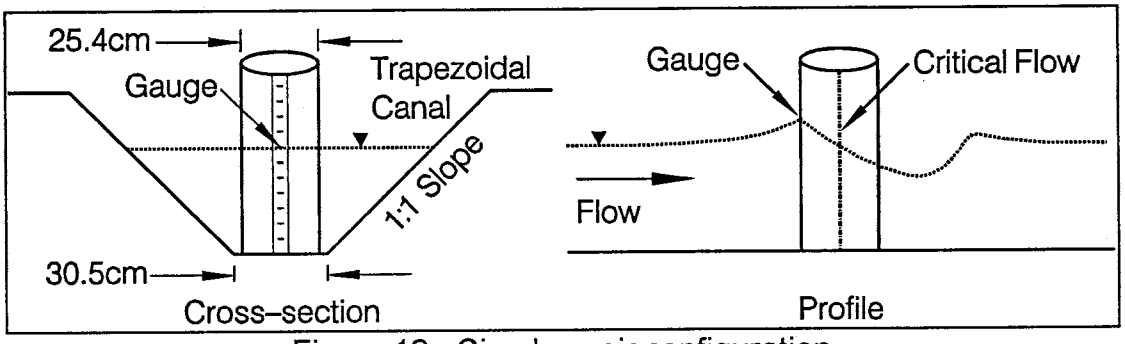

Figure 12: Circular weir configuration

Flow measurements during an irrigation event consisted of the depth of water on the gauge attached to the upstream side of the weir. Readings were typically obtained every 15 minutes throughout the irrigation event, with more frequent readings gathered during the initial and final stages or when relatively rapid fluctuations were otherwise noted.

Volumetric flow rates of irrigation waters were determined using the computer program FLUME, written and provided by Z. Samani (per. com., 1994). Input parameters consisted of the ditch geometry, weir diameter, and water depth observations. The calculations solve a system of equations based on energy conservation and on an empirical relationship between measured and actual flow rates. The stated accuracy of flow measurements obtained with this weir configuration is within ±5% as determined through laboratory comparison of actual flow rates with flow rates determined using the equations (Samani and Magallanez, 1993).

During the May 15, 1995 irrigation, concurrent flow velocity measurements were obtained with an electronic FLO-MATE™ Model 2000 Portable Water Flowmeter, (Marsh-McBirney, Inc., Frederick, MD). Water levels in the irrigation ditch remained essentially constant throughout the time of

measurement. Velocity profile measurements were taken at 20%, 60%, and 80% depths (measured from the water surface) and flow rates calculated by averaging the average of the 20% and 80% rates with the 60% rate and multiplying by the cross-sectional area of the ditch. Taking into consideration the stated accuracy for both the weir and the flowmeter, the calculated flow rates determined with the flowmeter ranged 3.4-5.6% lower than the weir measurements (see Appendix G2). This was expected as the method for determining flow rates with the meter was developed for a rectangular flow cross-section, which has a lower flow rate than a trapezoidal flow cross-section with the same cross-sectional flow area. Thus, the circular weir appeared to measure flow rates to within the stated accuracy.

2.7 Tile-drain Flow and Chemical Sampling

In order to isolate a tile-drain section, two manholes were installed in 1992 which intersected tile-drain #3 in the center bench (Figure 5). By monitoring flow rates and chemical concentrations in both manholes, the quantity and chemistry of the water entering the tile-drain from the center bench can be determined. The manholes are approximately 1.5 m (5 ft) diameter corrugated galvanized steel with a welded bottom plate installed to a depth of approximately 0.3 m (1 ft) below the bottom of the tile-drain pipe. The tile drain line was cut and attached to flanges mounted inside the manholes at both the inflow and outflow sides.

Figure 13 is a schematic diagram of the manholes and instrumentation. As the manholes were located several hundred meters from the nearest electrical transmission lines, power was provided with a photovoltaic/battery storage system. Solar panels mounted near the manholes provided 40 volts DC regulated to approximately 27 volts to charge banks of 12-volt lead-acid storage batteries. The battery banks were wired to provide both 12- and 24-volt DC supplies for manhole instrumentation.

Measurement of tile-drain flow rates was achieved with a paddle-wheel type Signet 2530 Low Flow Sensor (Signet Scientific Co., El Monte, CA). The flow sensor was capable of measuring fluid velocities of 0.1 to 3 m/s (0.3 to 10 ft/s) with a stated accuracy of ±1%. The flow sensor was mounted in a specialized Schedule 80 PVC T-fitting having an inflow and outflow control section connected, in turn, to Schedule 40 PVC plumbing at the tile-drain inflow

and outflow flanges. The inside diameter of the control section and other plumbing was dictated by balancing the anticipated range of flow velocity with the head loss required to increase the flow velocity to a measurable rate. In the east manhole, the up-gradient tile-drain pipe is 10.3 cm (4 in) ID while in the west manhole, the up-gradient tile-drain pipe is 12.7 cm (5 in) ID. At these diameters, a minimum measurable velocity of 0.1 m/s corresponded to flow rates of 40- and 65 l/min, respectively. These rates were much higher than those encountered and thus required that the flow sensor control sections be of a smaller diameter.

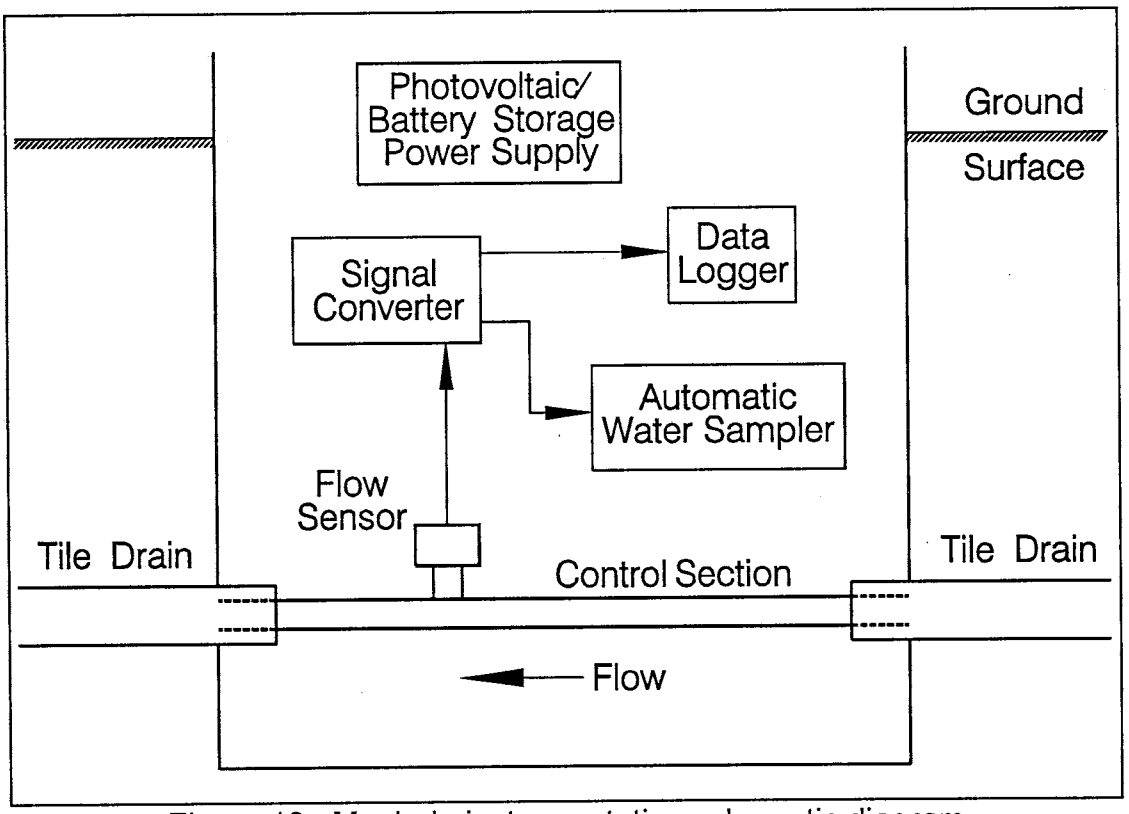

Figure 13: Manhole instrumentation schematic diagram

A 5.1 cm (2 in) ID control section was first installed in the west manhole on March 3, 1995, 12 days prior to the first irrigation of the season. Flow rates

were too low during non-irrigation times and as a result no discharge could be measured. Thus, 2.5 cm (1 in) ID control sections were subsequently installed in the west manhole on April 3 and in the east manhole on May 19. The flow control section in the east manhole was later replaced with a 1.27 cm (0.5 in) ID system on December 2.

The flow sensor generated a sine-wave signal having a frequency proportional to flow velocity. The signal was transmitted via wiring to a Signet 9010 Intelec-Pro™ Flow Controller (Signet Scientific Co., El Monte, CA) which converted the sensor signal to a volumetric flow rate using a programmed conversion factor. The flow controller additionally contained circuitry to output a DC voltage programmably proportional to the flow rate. The DC output was scaled from approximately 0.500 to 4.000 volts to represent flow rates in the range of 0 to 35 l/min, respectively, with a resolution of approximately 0.05 l/min. The DC output was connected to a Model 812 FIELD Data Logger (Tumut Gadara Corp., Columbus, OH) and recorded at various time intervals ranging from 3 to 10 minutes. Data was periodically retrieved from the data loggers with a portable lap-top computer.

Both manhole plumbing inflow sections contained a T-fitting and trap configuration leading to a stand-pipe for monitoring water levels in the tile-drain. Also, 5.1 cm (2 in) ID brass ball valves were mounted to the inflow and outflow flanges of both manholes to facilitate manhole repairs and maintenance. Beginning in early March, 1996, and lasting for a period of several weeks, a pressure transducer/data logger system (described in section 2.5) was installed

in the west manhole to concurrently monitor water levels in the tile-drain and in monitoring wells 22 and 23.

A manual calibration of flow rates in the west manhole was performed on April 7, 1995, with the 1.27 cm plumbing installed. The results are tabulated in Appendix H1. Flow rate measurements were obtained by observing flow rates reported by the flow controller while simultaneously collecting the outflow in a graduated container. Ten measurements were taken at reported flow rates from 12 to 28 l/min. Manually measured flow rates ranged from 0 to 9% higher, averaging 5% higher than those reported by the controller. The difference can be explained by the fact that the controller reported a 10-second averaged flow rate. Maintaining a constant flow rate during the tests was impossible and the reported flow rates fluctuated thus requiring a visual averaging. It is therefore probable that the flow controller reported a flow rate which was more accurate than could be obtained by the calibration procedure.

An upstream head increase in the tile-drain would be induced by the installed flow measurement system due to the constriction of the tile-drain diameter and the resulting increase in frictional head losses. Assuming all other factors were equal, this would imply that the other tile-drain laterals would function somewhat more efficiently as they would not be subject to these (additional) frictional losses. In order to estimate the impact of the installed flow measurement system on head levels in the tile drain, a standardized table of frictional losses for Schedule 80 PVC pipe was consulted. As presented in the 1995 Ryan Herco catalogue (Ryan Herco Products Corporation, Burbank, CA),

the tabulated frictional loss data were generated using the Williams and Hazen equation, which expresses the frictional head loss, in English units, as:

$$H = \frac{3.023V^{1.852}}{C^{1.852}D^{1.167}} \qquad (2.7\text{-}1)$$

where:

H = head loss (ft per 100 ft of pipe)
V = fluid velocity (ft/sec)
D = inside pipe diameter (ft)
C = coefficient of roughness of pipe interior surface
(C = 150 for schedule 80 PVC pipe, units not given)

In addition to the approximately 0.75 m (2.5 ft) of 2.54 cm (1 in) ID control section piping, various fittings and valves were installed. Figure 14 presents the predicted frictional head loss as a function of flow rate, assuming a combined effective length of 3.35 m (11 ft) of 2.54 cm ID pipe. The additional 2.6 m (8.5 ft) were included to account for the frictional head losses due to the installed fittings and valves (Pnueli and Gutfinger, 1992). Thus, over the observed range of non-irrigation flow rates (about 10 to 20 l/min, as discussed later), an increase in the water table elevation near the tile-drain under the center and east benches of from 2 to 9 cm was predicted.

Finally, water samples were collected in each manhole with ISCO® (Lincoln, NE) Model 2900 automated water samplers having a 12-sample capacity, each with 350 ml volume. Samples were collected at varying time intervals ranging from 2 hours during and following irrigation events to 3.5 days or longer between irrigations and during the non-irrigation season. At various times, the samples were analyzed for nitrate, chloride, and bromide concentrations using HPLC techniques and for chlorpyrifose (pesticide)

concentrations using amino assay techniques. Additionally, the electrical conductivity of samples was measured. Refer to Roth (1996) for a discussion of the chemical analytical methods and results.

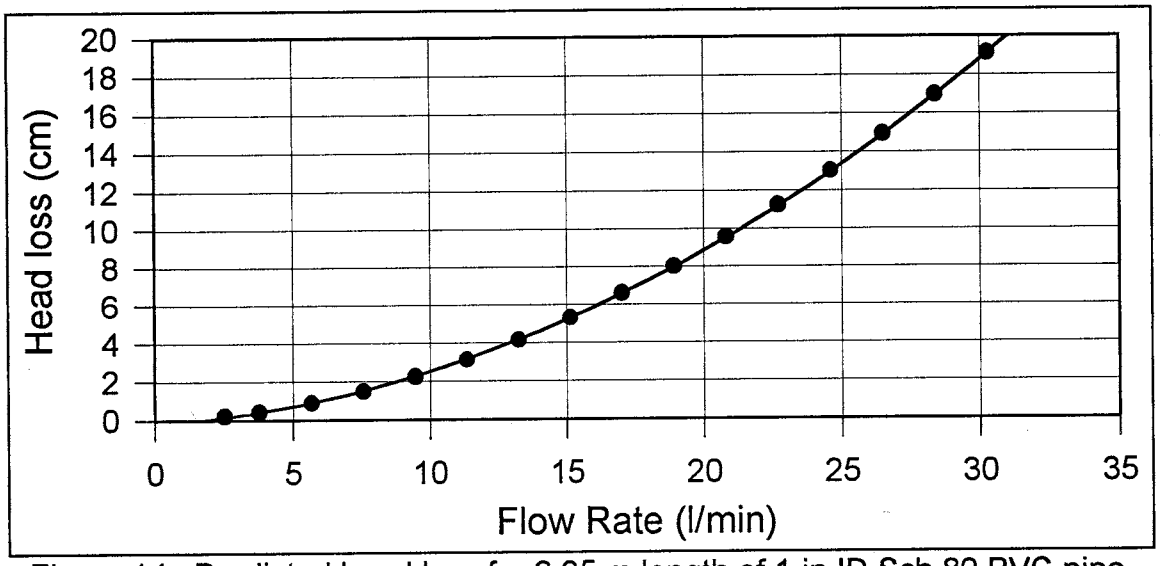

Figure 14: Predicted head loss for 3.35 m length of 1 in ID Sch 80 PVC pipe.

3. RESULTS & DISCUSSION

3.1 Precipitation

Measured precipitation for 1995 is summarized in Figure 15. Measurements are tabulated in Appendix B. The 1995 total amount of measured precipitation at the LNGP site was only 10.28 cm (4.05 in). This compares with the 13.64 cm (5.37 in) recorded at the Agricultural Science Center (ASC), Los Lunas, New Mexico, about 32 km (20 mi) to the north, which generally receives about 10% greater precipitation than the LNGP site in an average year (J. Hooks, ASC, pers. com., 1996). As mentioned previously, there were inevitably unrecorded events at the LNGP site as the rain gauges were not automated. However, due to the frequency of visits to the site, it is estimated that the recorded amount of precipitation is probably no more than about 10% below the actual amount, resulting in an estimated total precipitation of 11.3 cm (4.45 in). Additionally, any unrecorded events were probably small (<0.1 to 1.5 mm) as there was insufficient time for greater amounts to evaporate from the rain gauges between site visits.

Flow rates in the metered tile-drain line were not noticeably affected by any of the precipitation events. Therefore, it is assumed that the precipitation rates and amounts were insufficient to cause saturated flow. Rainfall was intercepted by the crop canopy and/or went into storage in the upper soil layers. As the rain gauges were not automated, no information is available concerning rainfall intensity. Thus, runoff is a possibility. However, due to the very flat nature of the fields, the high available detention storage, and the fact that no

standing water was observed after any of the events, runoff is considered negligible. Interception storage per event was probably on the order of 0.5 to 1.0 mm (0.02 to 0.04 in) (Viessman and Lewis, 1996). Using this range of interception for the recorded events and an estimated interception of 33% of the unrecorded events (~0.3 cm), total effective annual rainfall for 1995 is estimated to range from 8.4 to 9.6 cm (3.31 to 3.78 in).

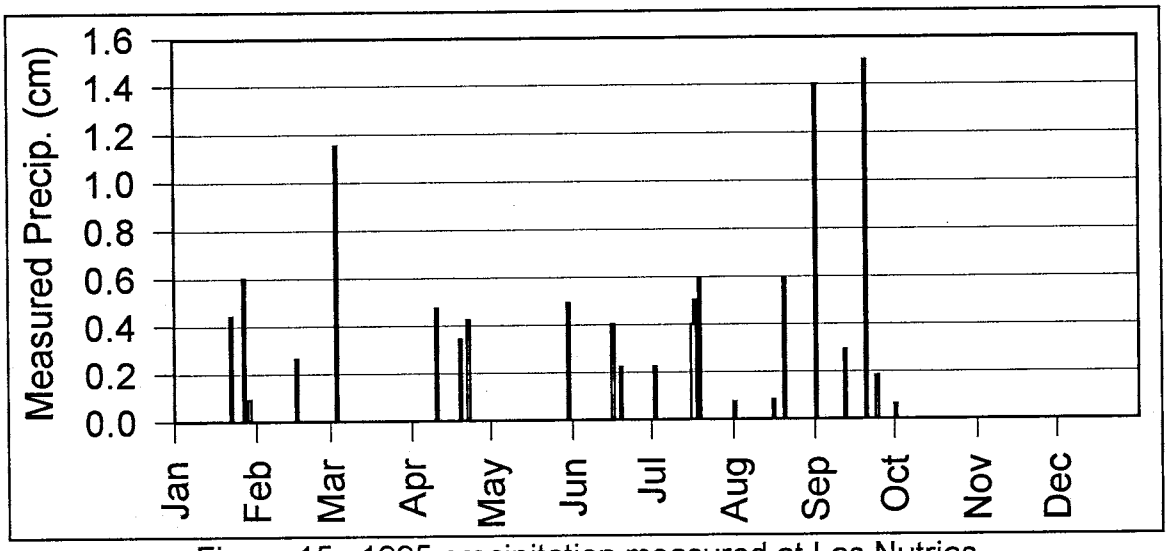

Figure 15: 1995 precipitation measured at Las Nutrias

3.2 Evapotranspiration

Results of the estimated daily reference evapotranspiration (ET_o), along with selected weather data, are tabulated in Appendix C2. The ASC method estimated an ET_o consistently lower than the FAO method by about 5%. This was due primarily to how the respective values for the average daily humidity and temperature were determined (see Appendix C1), to the determination of net long-wave radiation, and the use of slightly different crop reflection (albedo) coefficients. Monthly cumulative and daily average ET_o as determined by both methods are given in Table 5.

Table 5: Summary of 1995 ET_o

	ASC Method		FAO Method	
	Total ET_o (cm)	Ave. ET_o (cm/d)	Total ET_o (cm)	Ave. ET_o (cm/d)
January	5.62	0.18	6.57	0.21
February	9.59	0.34	10.08	0.36
March	13.69	0.44	14.52	0.47
April	16.68	0.56	17.76	0.59
May	22.10	0.71	23.45	0.76
June	24.46	0.82	25.43	0.85
July	26.68	0.86	27.46	0.89
August	22.04	0.71	23.10	0.75
September	16.12	0.54	17.13	0.57
October	15.25	0.49	15.48	0.50
November	9.42	0.31	10.07	0.34
December	6.52	0.21	7.31	0.24
Year	188.17	0.52	198.36	0.54

With respect to the uncertainty involved in estimating the actual amount of evapotranspiration that did occur, the difference between the methods is essentially negligible. The available crop coefficients were developed using the FAO method, which specifically warns against using ET_o values obtained with

the ASC method in conjunction with those crop coefficients. Thus, the ET_o values generated using that FAO method were used. The calculated values for ET_o are shown graphically below.

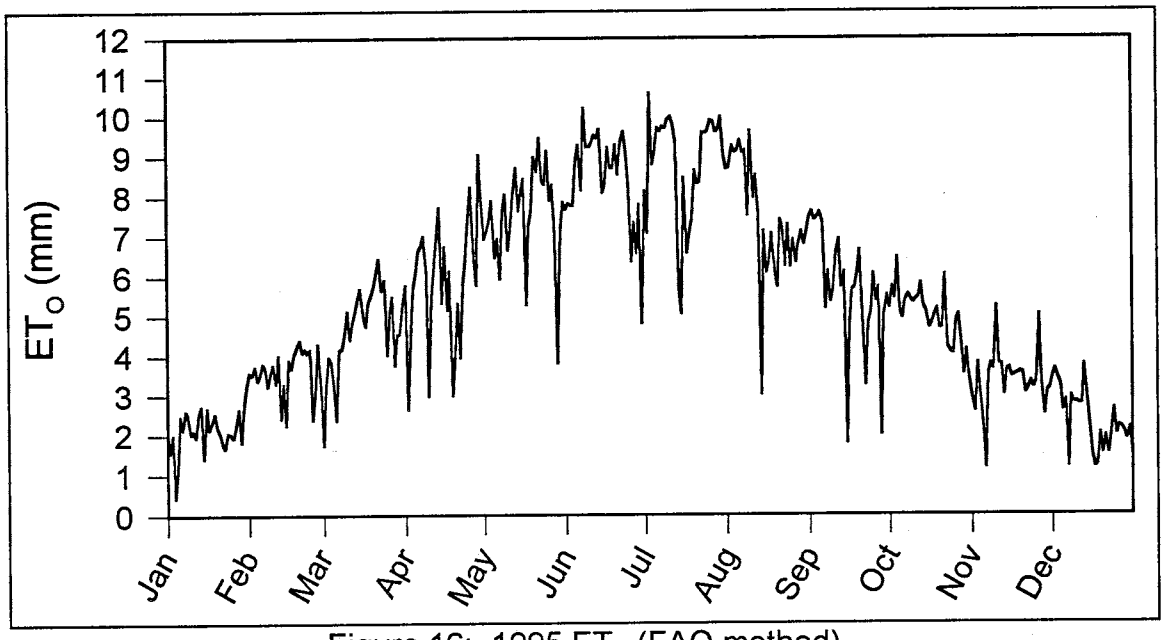

Figure 16: 1995 ET_o (FAO method)

While potential evapotranspiration is a function only of climatological conditions, actual evapotranspiration is additionally a function of the type of vegetation present and its ability or efficiency to withdraw water from the soil. This ability is a function of root system development, soil water content, and soil water quality. The alfalfa crop was planted just prior to the final 1994 irrigation and was therefore a relatively new crop when growth commenced in the spring of 1995. The root system likely required some time to develop fully. Growth was noted prior to the beginning of the official growing season (April 23) and continued for some time after the final cutting. Also, there were zones of elevated soil salinity levels where little or no growth occurred. These factors

were not considered in the determination of the crop coefficient as the published functions do not extend into the off-season, they do not account for growth of the root system, and they do not account for possible plant stress factors such as excessive soil water tensions and/or salinity. The crop coefficient function for the irrigation season is presented in Figure 17.

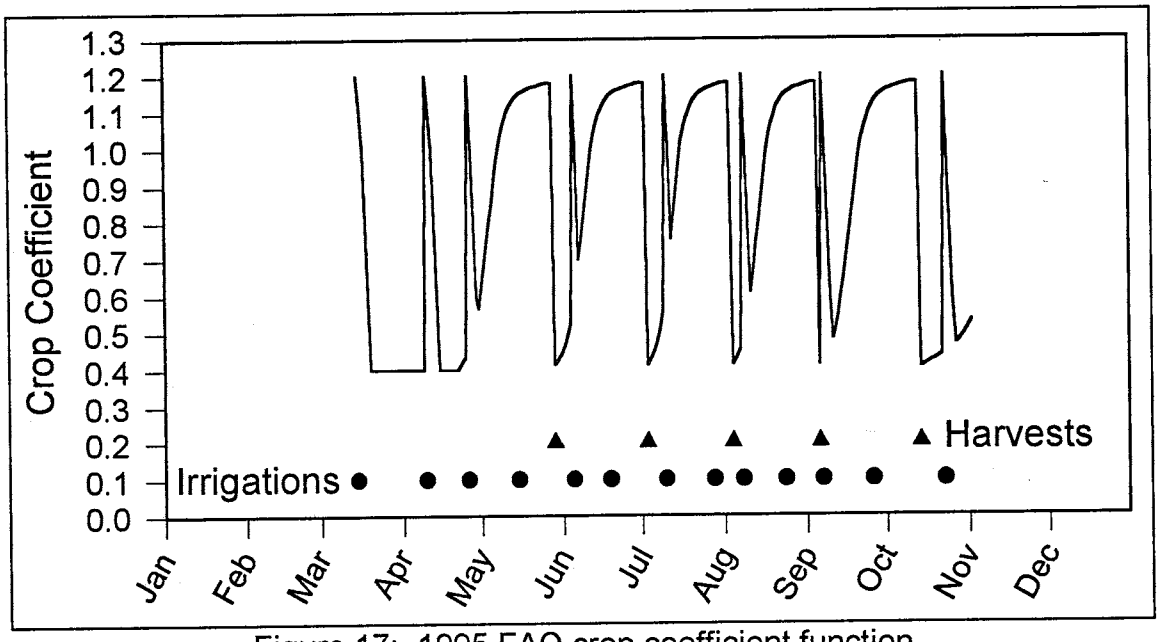

Figure 17: 1995 FAO crop coefficient function

In addition to the generally S-shaped appearance of the function as previously discussed, there are several superimposed spikes which represent evaporative losses during and following irrigation events that took place when there was no significant crop canopy cover. The average crop coefficient between harvests ranges from 0.90 to 0.98, averaging about 0.95. Prior to the official beginning of the growing season on April 23, there were two irrigations (March 15 and April 10) between which the crop coefficient was estimated at the minimum value of 0.40. The curve ends on November 2, the beginning of an

extended period of freezing night-time temperatures which probably halted further significant crop growth.

The area-averaged results of the CAPSEV capillary flux simulations for all the profiled locations are presented graphically in Figure 18.

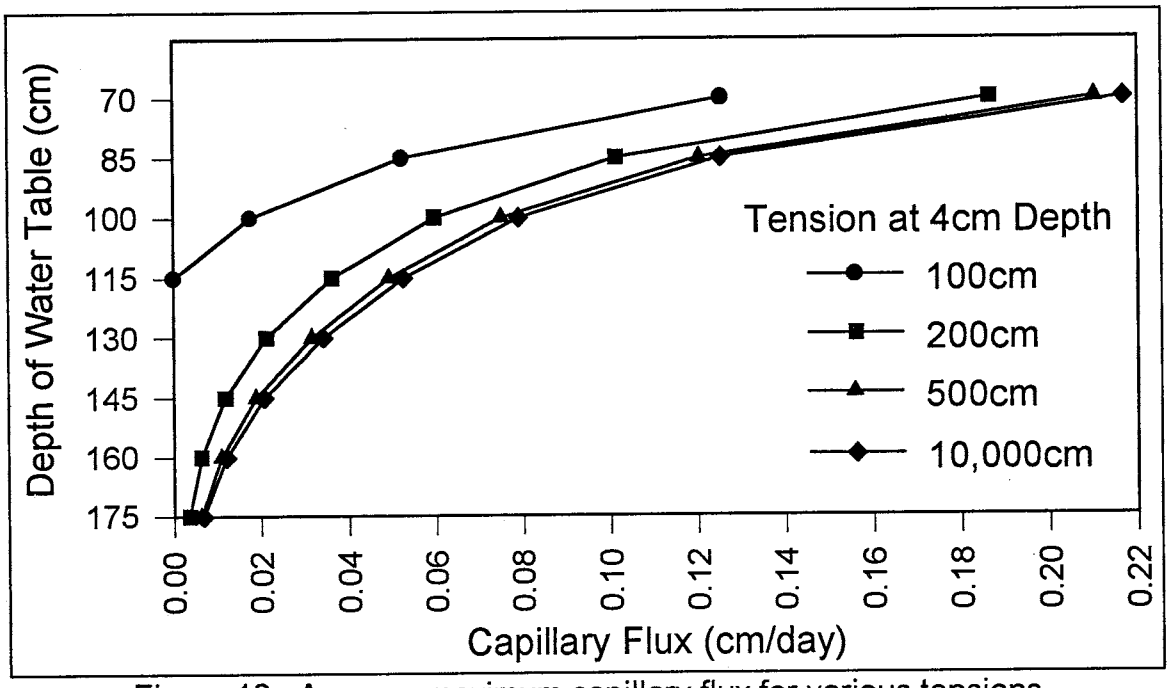

Figure 18: Average maximum capillary flux for various tensions

The figure illustrates that as the water table drops, the maximum possible flux at a given tension decreases rapidly. Additionally, there is a negligible increase in capillary flux as near-surface tensions surpass about 500 cm. If it is assumed that the dominant non-climatic factor controlling evaporation during the winter months is the depth to the water table and assuming that capillary flux maintains an equilibrium state for a given depth to the water table, the upper limit of evaporation can be estimated from the depth to the water table and a reasonable estimate of the near-surface tension.

Thus, using the daily FAO *kc* curve multiplied by the daily FAO ET_o during the irrigation season combined with the simulated maximum capillary flux values during the off-season at a near-surface soil water tension of 1000 cm, the estimated daily evapotranspiration was calculated and is presented in Figure 19.

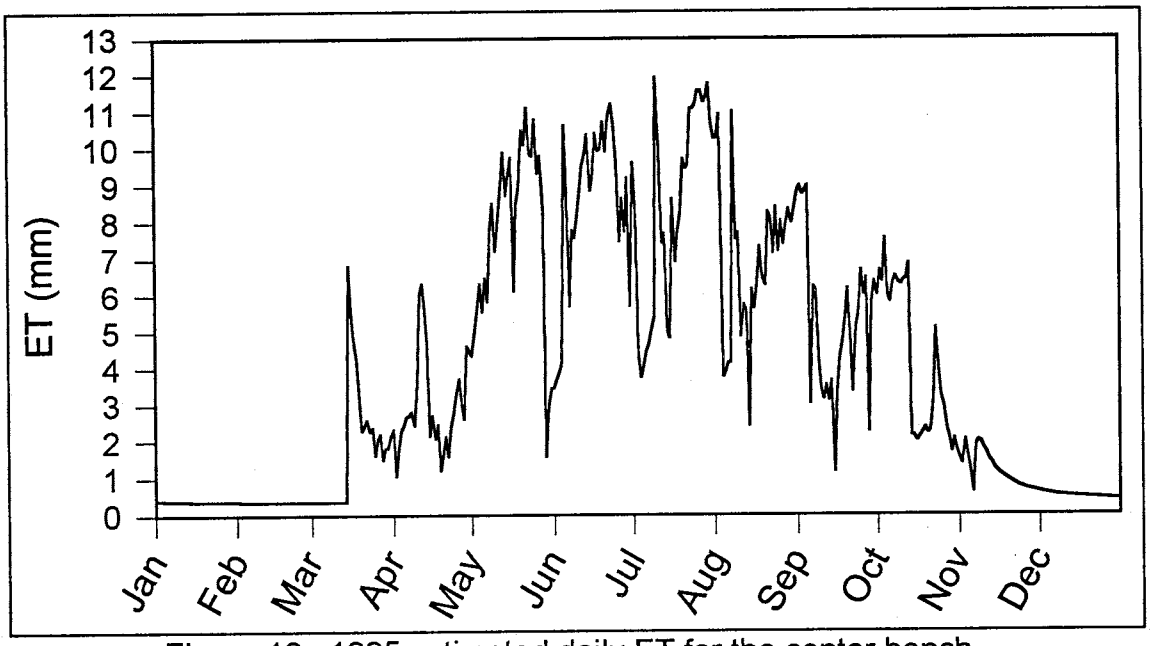

Figure 19: 1995 estimated daily ET for the center bench

The total estimated ET for 1995 was 148.4 cm. During the five harvesting cycles, starting with the beginning of the growing season on April 23 and ending with the final harvest on October 14, the FAO method estimated a total of 124.9 cm of water consumed by the crop (see Table 6) By comparison, the consumptive use crop function relationship presented by Sammis and others (1979), calculates a consumptive use of 118.3 cm for the total season harvest of 11.65 t/ha, a difference of only 5%. The FAO method had an average crop coefficient of 0.92 over the season while the Mapel and others (1985) growing

degree day-based polynomial calculated an average monthly crop coefficient of 0.91 for the 2909 growing degree days accumulated during the same period.

Table 6: Growing season ET summary

Harvest Cycle	Duration (days)	ET_o (cm)	ET (alfalfa) (cm)
1	36	27.3	27.0
2	35	28.8	27.9
3	32	28.6	27.2
4	33	24.2	23.1
5	38	20.5	19.8
Total	174	129.4	124.9

3.3 Unsaturated Soil Hydraulic Properties

Results of the soil bulk density and volumetric water content analyses are tabulated in Appendix D1. The neutron probe calibration regression is presented in Appendix D2. The instantaneous profile (IP) experimental data are presented in Appendix D3.

Assuming a soil particle density of 2.65 g/cm^3, soil porosities for 45 samples ranged from 35% to 60% with an average of 51%. There were no consistent vertical trends or within textural layers and porosity values at individual sampled depths exhibited ranges of 0.8% to 9.0%, averaging 4.5%, indicating a fair degree of both lateral and vertical heterogeneity.

Ponding of the sites prior to the collection of head and neutron probe data may not have been performed for a sufficient length of time. A clay layer existed at both IP experimental locations #3 and #4. The average porosity determined from 12 samples of those clay layers was 55%. Tensiometer measurements within the clay layers indicated that positive pressures existed throughout the course of the experiment. However, the neutron probe measurements indicated a (very consistent) average volumetric water content in the clay of only about 46%. Thus, despite positive pressures, the clay was apparently undersaturated by approximately 16% (9% apparent available storage). Undersaturation was also indicated for many of the remaining 33 soil samples, though to a lesser degree. Undersaturation may be attributed to either entrapped air, the presence of neutron absorbing elements, disturbance of the samples during collection, an over-estimate of soil particle density, or a combination of these factors.

The results of the experiment were difficult to analyze and provided unsaturated soil characteristics of limited usefulness as the soils remained very close to saturation over the duration of the experiment (B. Mohanty, per. com., 1995). As an example,

Figure 20 depicts the neutron probe volumetric water content and soil tension values for selected depths at experimental location 4 over the course of the experiment.

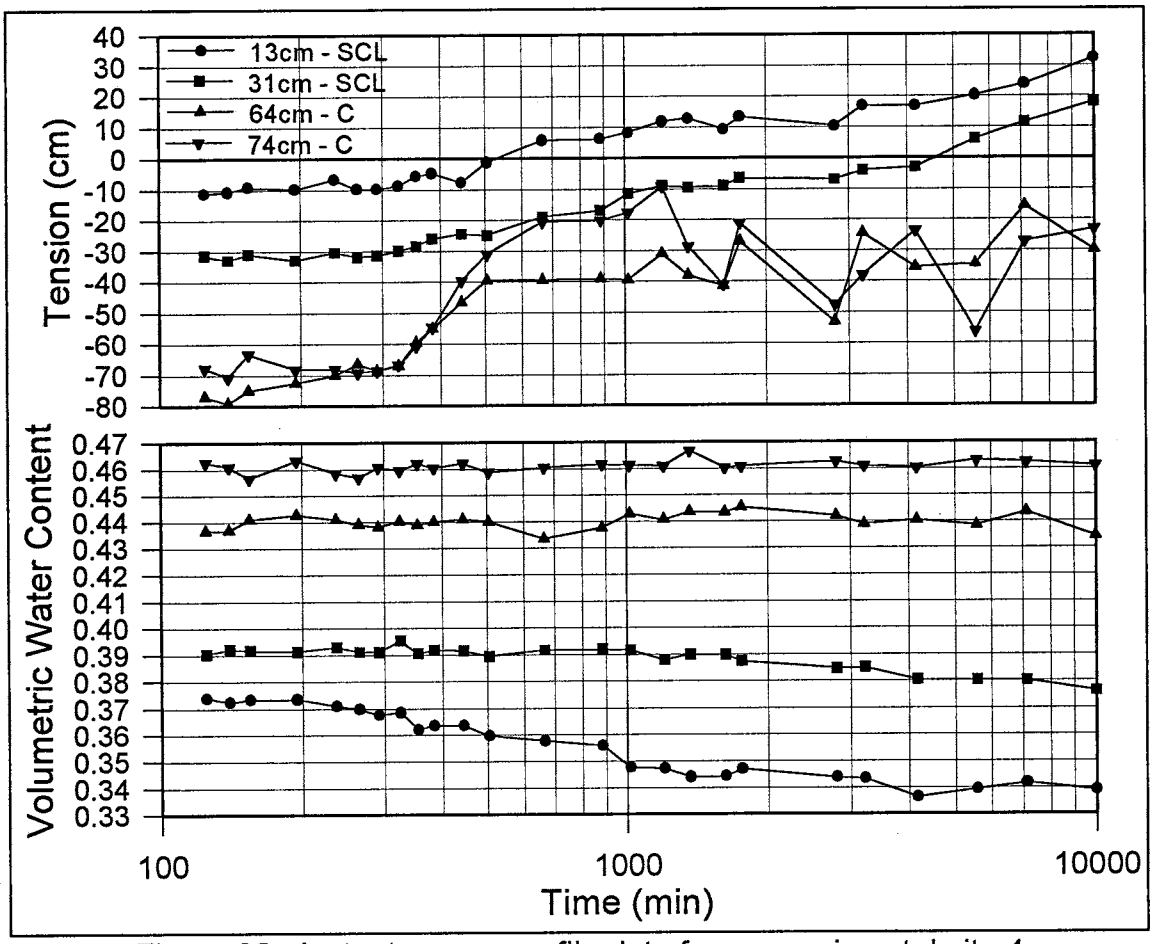

Figure 20: Instantaneous profile data from experimental site 4

As can be seen, very little change in water content was observed at depth and many of the measurements fluctuated only within the range of precision of

the neutron probe. Additionally, pressure values remained positive for many of the layers at depth, indicating saturated conditions. The most significant increases in soil tension occurred only in the near-surface levels, where neutron probe measurements are less reliable due to proximity to the soil surface. Note that at the 13 cm (5 in) depth, positive tension values were obtained after 500 min had elapsed, yet water contents exhibited a slight decrease before that time was reached. This indicates that the neutron probe sphere of importance (discussed earlier) intersected the surface and the decreasing measured water contents over this period indicated the decrease in the ponding level. This phenomenon was also noted to varying degree at all of the other three experimental locations. Also noted are the large fluctuations in pressure at later times during the experiment, again a feature at the other experimental locations. These fluctuations additionally confounded the analytical process and may be in part due to horizontal flow components as there were no lateral barriers to flow installed at the experimental locations.

The generally poor overall results of the experiment can be attributed to the shallow groundwater table, which limited the drainage of the soils, and to the very limited time period over which data was collected. A straight-forward analysis using the original method (Watson, 1966) provided questionable results and was therefore supplemented with an iterative, best-fit process using the RETC computer code (van Genuchten et al., 1991). As there were no high-tension soil water measurements available, estimates of the residual water contents were necessary. Characteristic curves were obtained that agreed

reasonably well with the (very) limited useable experimental data. The curves are presented in Figure 21. Table 7 lists the van Genuchten soil parameters obtained from the IP experiments. Many of the soil textures monitored during the experiment provided no useable data. Given the considerations stated above, these results should not be trusted too greatly and should therefore not be used for any detailed analysis of unsaturated flow at the site.

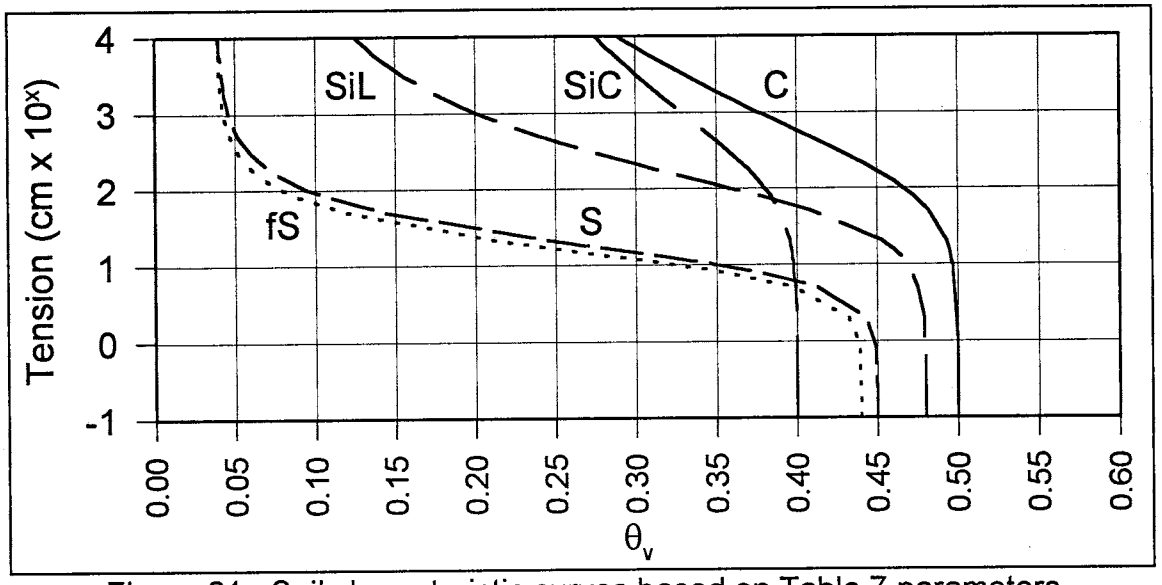

Figure 21: Soil characteristic curves based on Table 7 parameters

Table 7: Instantaneous profile soil parameters (B. Mohanty, per. com., 1996)

Texture	θ_r	θ_s	K_s (cm/day)	α(/cm)	n
Sand	0.039	0.45	120.52	0.090	1.90
Fine Sand	0.039	0.44	105.0	0.100	2.00
Silty Loam	0.070	0.48	28.32	0.020	1.38
Silty Clay	0.100	0.40	20.10	0.009	1.12
Clay	0.070	0.50	11.10	0.009	1.15

3.4 Monitoring Wells, Piezometers, and Ground Elevation Survey

Ground surface contours for the center bench are presented in Figure 22. There was a 16-cm change in elevation with an average southerly gradient of 0.07%. Center bench ground elevation survey data are presented in Appendix I.

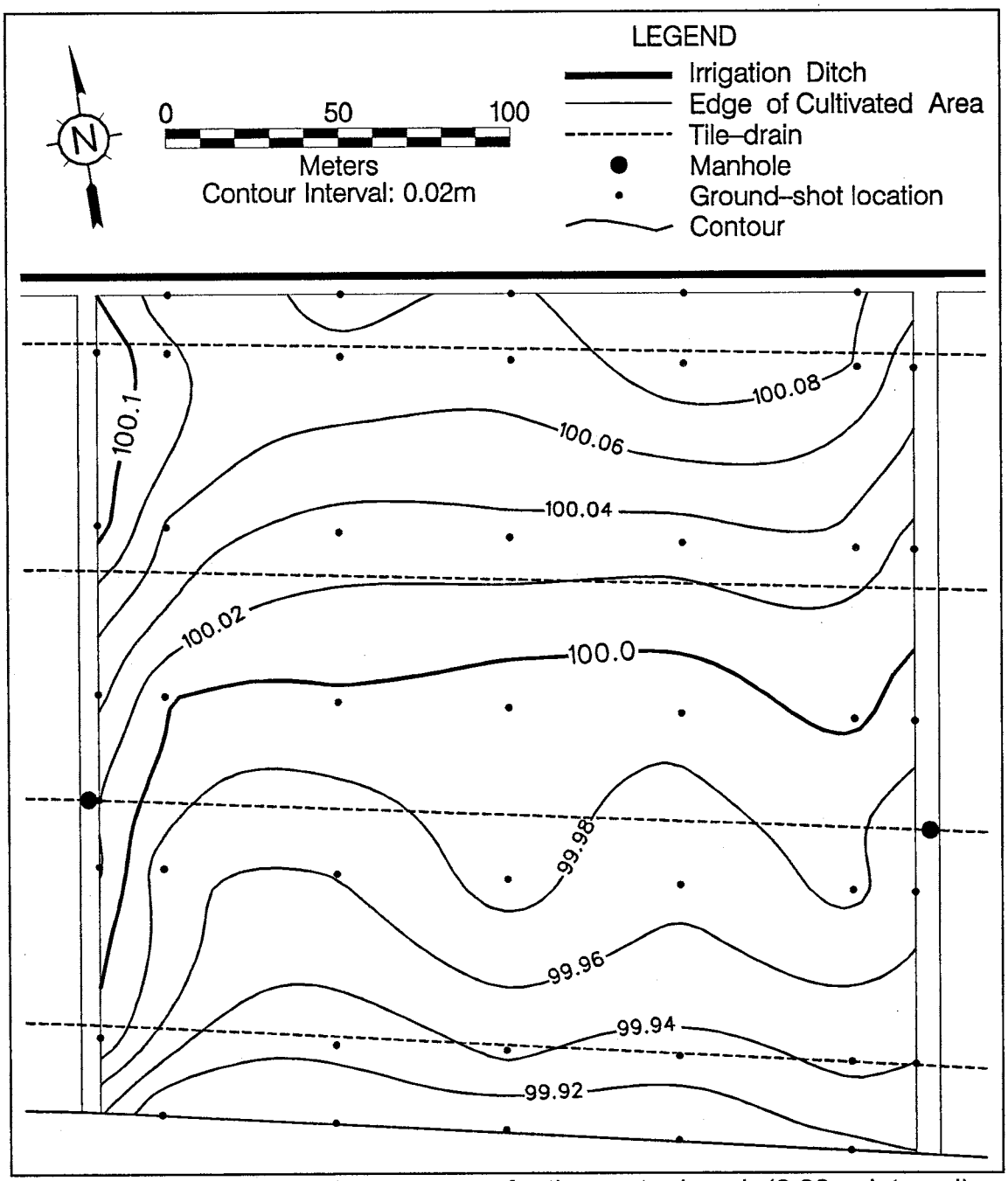

Figure 22: Ground surface contours for the center bench (0.02 m interval)

During irrigation, water was observed advancing at a much faster rate along the eastern edge of the field, as indicated by the slightly lower elevations there. In the central areas of the field, irregularities in the originally leveled surface have developed, probably due to differential soil compaction through repeated wetting and drying cycles. These irregularities result in slightly more water being applied in the lower elevation, or trough areas, though the furrows created during crop planting persist and tend to maintain a southerly-directed channeling of irrigation water. Additionally, the irregularities lead to an uneven advancement of flooding irrigation water. Along the west berm, there is a rise in elevation indicating that this strip of the field receives less water overall.

Monitoring well water level survey results are tabulated in Appendix E2. Kriged contour maps for each complete water level survey performed in 1995 are presented in Appendix E5. An analysis of residuals revealed that they were normally distributed about zero, with 75% to 90% of the measured water table elevations falling within ±1 cm of the kriged surfaces while 97% of measured water table elevations were within ±2 cm of the kriged surfaces. During the non-irrigation season, the water table contour maps indicated a south-southwest direction of groundwater flow under the east bench changing to a slightly more southwesterly direction under the west bench (see Figure 23).

Water table gradients under the east and center benches were uniformly about 0.08%. Gradients under the west bench were greater, especially on the western half where they were about 0.13%, possibly due to proximity to the surface drain. Water table data on the west bench were sketchy due to the

absence of data from abandoned monitoring wells 29 and 31, located at the southeast and south-central edge of the bench, respectively (Figure 3).

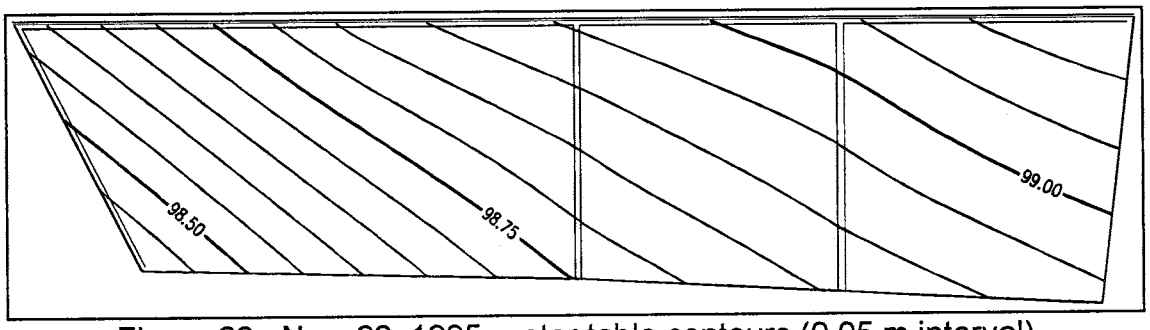

Figure 23: Nov. 22, 1995, water table contours (0.05 m interval)

During the irrigation season, gradients under the east and center benches still averaged about 0.08%, though variability increased due to irrigations on those benches and on the surrounding fields. Gradients under the west bench increased to an average of about 0.16% and exhibited less variability than the other two benches. Flow directions during the irrigation season changed erratically, depending on irrigations of the site and surrounding fields. Beginning in about late-July and lasting through mid-October, a more westerly flow direction was established and gradients averaged from 0.06% to 0.07% under the east and center benches, respectively. Figure 24 illustrates this change. Additionally, the figure depicts the effects of an irrigation of the fields to the north and northwest, which occurred on the same day as the survey and illustrates the rapid response of water levels to an irrigation event.

A feature which is conspicuously absent from the water table contour plots is the influence of the tile-drains. The tile-drain lines should create a series of undulations in the water table surface with high points approximately mid-way

between the lines (Figure 6). The regularity of the contour surface during non-irrigation times and in the presence of measurable flow rates in the tile-drain lines suggests that the tile-drains are not operating efficiently.

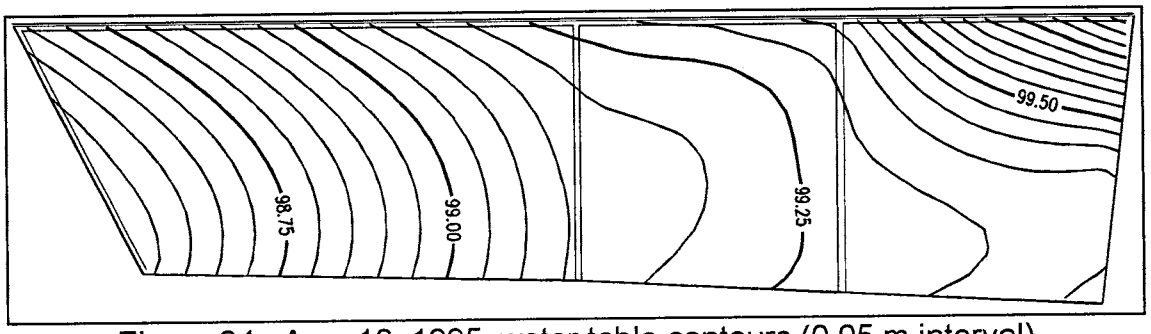

Figure 24: Aug. 18, 1995, water table contours (0.05 m interval)

As there were no monitoring wells located in the cultivated areas, the lack of these undulations could be an artifact of the mapping procedure and the well spacing. To investigate this possibility, five holes were augured at 50 m (164 ft) intervals along a north-south transect through the middle of the center bench at locations of known ground surface elevation. Water table elevations were measured at those points. The inclusion of those points resulted in no substantial differences in the water table surface as determined by omitting those points, indicating that the monitoring well network and mapping methods provided a reasonable estimate of the water table surface.

Figure 25 depicts a cross-sectional profile of water levels in wells 19 through 26 for several dates from November, 1995, through January, 1996. The wells were located along the west berm of the center bench. Lateral 3 was the location of the west manhole, where water levels were sharply lower than in the immediately adjacent wells 22 and 23, less than 2m distant.

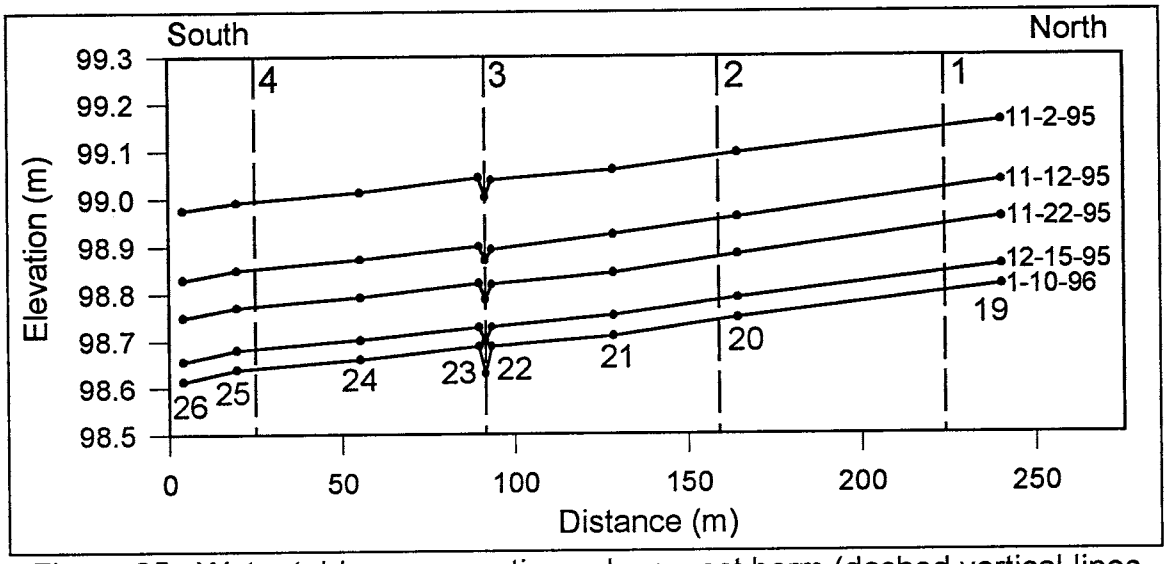

Figure 25: Water table cross-sections along west berm (dashed vertical lines represent tile-drain lateral locations. Numbers 1-4 across top of figure indicate lateral drain number. Numbers 19-26 indicate monitoring well numbers.)

Though the locations of laterals 1, 2 and 4 were determined from design plans only, their displayed locations should be within about ±5 m of their true location. The water levels in wells 20 and 25, located near laterals 2 and 4, respectively, do not appear to differ significantly from the regional gradient. Thus, it can be inferred that the unmonitored laterals were behaving similarly to lateral 3 and that the regional water table gradient dominated the flow regime in areas shortly distant from the tile-drains.

Figure 26 displays the average depth to water under the center bench for all 1995 water level surveys. Depths were determined by subtracting the water table surface from the ground surface. The surfaces were generated with SURFER using universal kriging algorithms for the water table surfaces and triangulation with linear interpolation algorithms for the ground surface, as discussed in the Methods section. Each surface had a 5-m square cell size on the same coordinate system resulting in corresponding cells with identical x-y

locations but with different elevations. For each cell, the water table surface elevation was subtracted from the corresponding ground surface elevation. The depths were thus area weighted, removing the effect of the irregular well spacing.

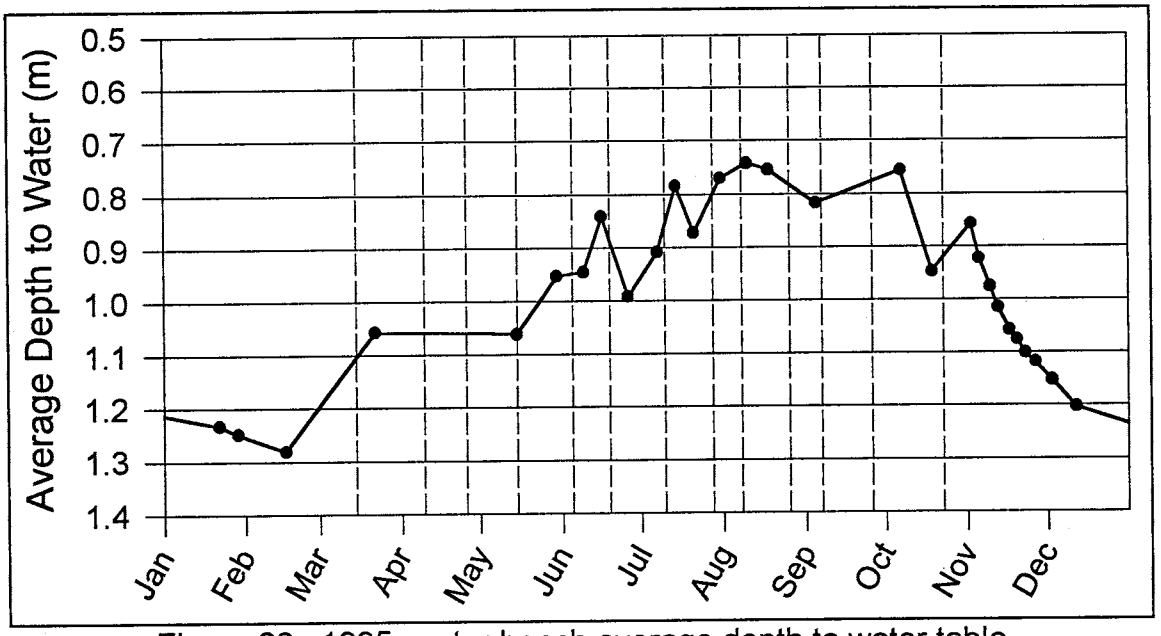

Figure 26: 1995 center bench average depth to water table
(vertical dashed lines represent irrigation events)

Following the irrigation season, water levels receded in a very smooth, exponential manner as depicted. During the irrigation season, water levels fluctuated between irrigations at the site and as a result of irrigations on the adjacent fields. The overall average water table elevation increased as irrigation frequency increased with water levels rising in late summer to an average of about 0.55 m above winter levels.

Water elevations and vertical gradients determined from the piezometer water level surveys are presented in Appendices B3 and B4, respectively. In general, vertical gradients were close to zero, ranging ±1.5%. Exceptions

occurred following irrigation events, when larger upward (positive) and downward (negative) gradients were encountered. Vertical gradients having the greatest magnitude occurred between the A and B well elevations (i.e., between the water table and a depth below the water table of about 2 m) beginning in May and lasting until late June, when strong (10-20%) upward gradients persisted. This coincided with the period during which the average water table elevation rose to a level coincident with the base of the clayey C2 soil horizon (~1.0 m depth).

3.5 Slug Tests

The time-drawdown data for each well are tabulated in Appendix F2. Slug test data were analyzed using the Bouwer and Rice method (Bouwer and Rice, 1976; Bouwer, 1989). The results were then compared with simulated slug tests using KGSMOD, a computer model developed by the Kansas Geological Survey to simulate slug tests in partially penetrating wells (Hyder et al., 1995). The B-R method assumes negligible specific storage, S_s. KGSMOD results indicate that for specific storage values $<10^{-3}$ m^{-1}, the B-R method does provide good results. The effect of increasing specific storage is a pronounced concave-upward appearance to the time vs. log drawdown data. Violation of another B-R assumption, significant anisotropy (k_H:k_Z>10), results in the same effect.

With the exception of piezometers 11C and 11E, all of the LNGP wells exhibited extremely straight time vs. log drawdown plots until late time. Therefore, a value of S_s $=10^{-4}$ m^{-1} was used and isotropic conditions were assumed for all KGSMOD simulations. This S_s is within the normal range of values for unconsolidated sands (Freeze and Cherry, 1979). As stated previously in the Methods section, the results of the B-R analyses of k_{sat} were utilized in the KGSMOD simulations and the resulting simulations were compared to the experimental data. The correction factor consisted of a multiplying factor applied to the B-R value for k_{sat} which resulted in a reasonably close fit for the KGSMOD simulation to the experimental data. Comparisons between the B-R analyses and the KGSMOD simulations resulted in correction factors ranging from 0.3 to 2.0 for k_{sat}, indicating that the B-R analysis did

provide quite reasonable estimates of hydraulic conductivity. A plot of the corrected B-R hydraulic conductivity versus the applied KGSMOD correction factor is presented in Figure 27. The high degree of correlation indicates that a systematic error was present in the KGSMOD simulations. During development and testing, KGSMOD was exhaustively evaluated for just this relationship and a similar correlation was not then indicated (J. Butler, pers. comm., 1996). The error here may be due to either an incorrect specific storage, the presence of a low degree of anisotropy ($10 > k_H : k_Z > 1$), or a combination of these factors. By any measure, however, the hydraulic conductivity estimates generated with the B-R method should be considered as reasonable estimates. In this case, approximately 90% of the B-R conductivity values were within ±100% of the KGSMOD simulated values while 65% of the B-R values were within ±65% of the simulated values. Therefore, the B-R values will henceforth be used.

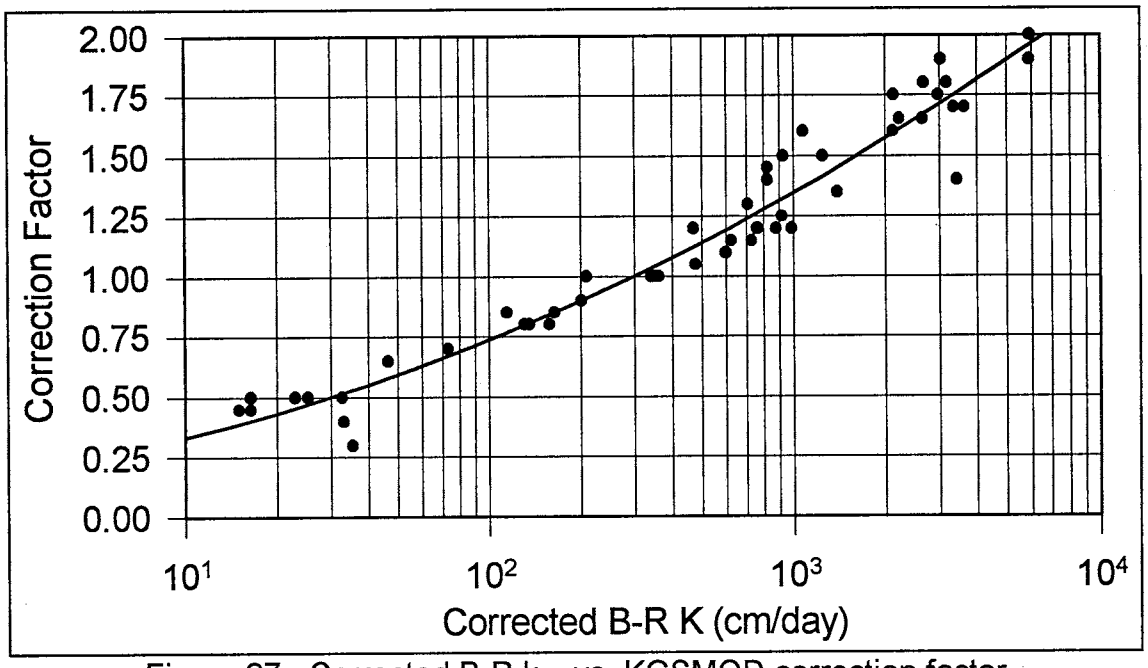

Figure 27: Corrected B-R k_{sat} vs. KGSMOD correction factor

There is an overall increase in hydraulic conductivity and an overall decrease in variability with increasing depth below ground surface, as illustrated in Figure 28. Piezometers 3E, 11C, and 11E are exceptions and are apparently set in clay-rich horizons, indicating the presence at those locations of clayey lenses within the sands underlying the site. The presence of clay layer at the depth and location of piezometer 3E was corroborated by well drilling logs, though no logs exist for wells 11C and 11E. Elevations above 98 m in the figure represent monitoring ("A") wells with elevations given as the center of the screened interval below the water table at the time of the test. Elevations below 98 m in the figure represent piezometers and are elevations at the center of the screened interval: "B" wells were screened between 96.5 and 97.5 m, "C" wells were screened between 95.0 and 96.0 m, and "E" wells were screened below 94.0 m. Results of the B-R analysis for each well tested are tabulated in Table 8.

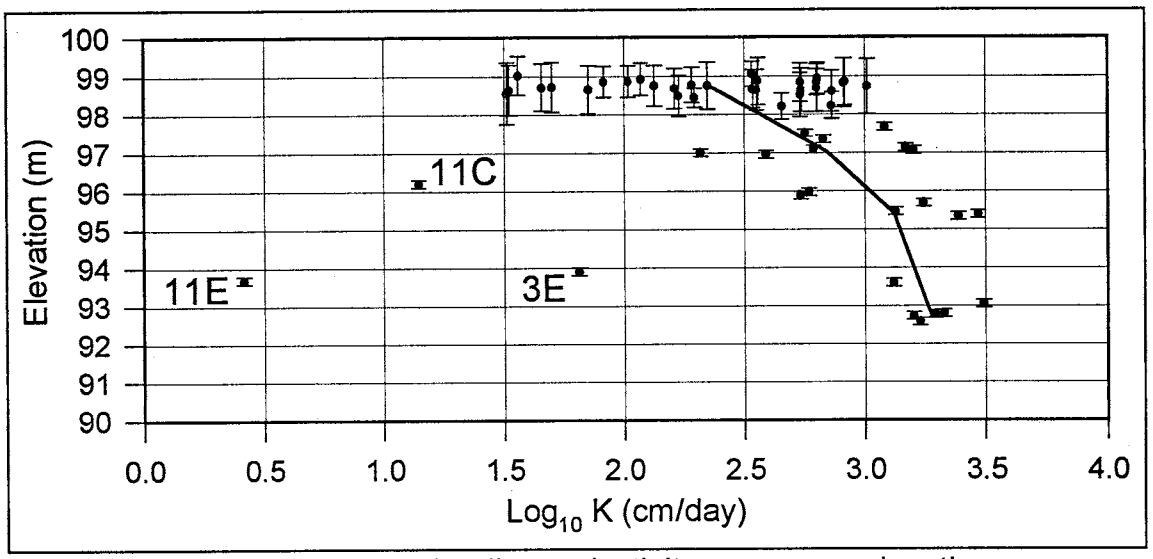

Figure 28: B-R hydraulic conductivity vs. screen elevation
(Fitted line represents the geometric mean k_{sat} value for the four well groupings, excluding labeled points. Error bars indicate well screen interval.)

Table 8: Slug test hydraulic conductivities - Bouwer and Rice Method

Well	$log_{10}K$ (cm/d)	K (cm/d)
1A	2.531	340
1B	3.084	1214
1C	2.769	588
1E	3.122	1324
2A	2.805	638
3A	1.917	83
3B	2.753	567
3C	2.735	543
3E	1.815	65
4A	2.072	118
5A	2.284	192
6A	1.560	36
7A	2.019	104
8A	2.801	632
9A	2.557	361
10A	2.348	223
11A	2.130	135
11B	2.827	672
11C	1.146	14
11E	0.417	3
13A	2.212	163
14A	2.738	547
14B	2.789	615
14E	3.492	3102
15A	2.536	343
16A	2.552	356
17A	2.914	821
18A	2.734	542
19A	2.918	828
20A	2.734	542
21A	2.802	634
21B	3.171	1483
21C	3.245	1758
21E	3.293	1964
22A	1.854	71
23A	1.523	33
24A	2.229	170
24B	2.591	390
24C	3.129	1347
24E	3.205	1603
25A	1.660	46
26A	1.702	50
27A	3.013	1030
28A	1.514	33
30A	2.864	732
32A	2.295	197
32B	3.203	1597
32C	3.470	2950
32E	3.328	2129
33A	2.863	730
34A	2.656	453
34B	2.319	209
34C	3.388	2444
34E	3.230	1698

3.6 Irrigations

Volumes for the 1995 season center bench irrigations are summarized in Table 9, below. Weir measurements and calculated flow rates for each of the monitored 1995 irrigation events are tabulated in Appendix G1.

Table 9: 1995 center bench irrigation volume summary

Date	Start Time	Duration	Average flow	Totals			
(1995)		(hr)	(gal/min)	gal x 10^3	ac-ft	in/ac	cm/ac
Mar 15	(missed)	---	---	(1678)	(5.15)	(4.32)	(11.0)
Apr 10	7:30 AM	6.10	4672	1710	5.25	4.41	11.2
Apr 26	7:26 AM	6.67	3548	1419	4.36	3.66	9.3
May 15	1:20 PM	6.15	4844	1788	5.49	4.61	11.7
Jun 5	1:13 PM	5.97	4551	1629	5.00	4.20	10.7
Jun 19	11:40 AM	7.67	3551	1633	5.02	4.21	10.7
Jul 10	2:24 PM	7.25	4157	1808	5.55	4.66	11.8
Jul 28	12:38 PM	7.37	3976	1757	5.40	4.53	11.5
Aug 8	12:29 PM	4.77	4597	1315	4.04	3.39	8.6
Aug 24	(missed)	---	---	(1244)	(3.82)	(3.21)	(8.1)
Sep 7	3:15 PM	4.55	3949	1078	3.31	2.78	7.1
Sep 26	1:30 PM	4.82	4636	1340	4.12	3.45	8.8
Oct 23	11:30 AM	7.60	4505	2054	6.31	5.30	13.4
	Average	6.27	4272	1594	4.90	4.09	10.3
			Season Total	20,455	62.83	52.7	133.9

(values shown in parenthesis are estimated values - see text)

The duration of irrigation events was decreased from an average of 6.5 hr to 4.6 hr during August-September. The result was a decrease of approximately 1-2 inches of water applied per irrigation. Prior to August, the practice was to allow flooding of the entire field before the water was shut off. This inevitably led to standing water in the southern portion of the field due to runoff from the northern part of the field. The problem became more acute as irrigation frequency increased which tended to keep soil moisture levels high. This problem was abated by shutting off the water when the flooding front was

approximately 30 to 40 meters from the southern edge of the field. The final irrigation of the season was by far the greatest as it was desired to get as much water into the soil as possible in anticipation of a dry winter season (landowner, pers. com., 1996).

For the eleven monitored irrigation events, an average of 10.4 cm (4.09 in) of water was applied over the 5.79 ha (14.3 ac) of the center bench. Assuming 10.97 cm (4.32 in) (average of the first seven monitored events) and 8.15 cm (3.21 in) (average of the three monitored events in August and September) was applied during the first and second missed irrigation events, respectively, a total of 133.9 cm (52.7 in) was applied during the irrigation season.

Figure 29 displays the time required for flooding irrigation waters to advance to a position over tile-drain lateral #3 for two different irrigation events. The time required to flood the field was a function of the application rate and the soil moisture conditions. The two events shown had similar application rates but quite different soil moisture contents as the June 5 (average application rate of 4525 gal/min) event was in the middle of the 1995 season and the March 26 (average application rate of 4250 gal/min) event was the first event of the 1996 season and the surface soils were very dry. In both cases, and as observed during other irrigations not shown, irrigation waters generally required from 3 to 4 hr to traverse the 150 m distance from the north edge of the center bench to a position over the monitored tile-drain. Occasionally the time required would somewhat exceed 4 hr if average application rates were low (<~4000 gal/min).

There was generally about 10 to 25 m of variability in the position of the advancing front due to irregularities and undulations of the ground surface.

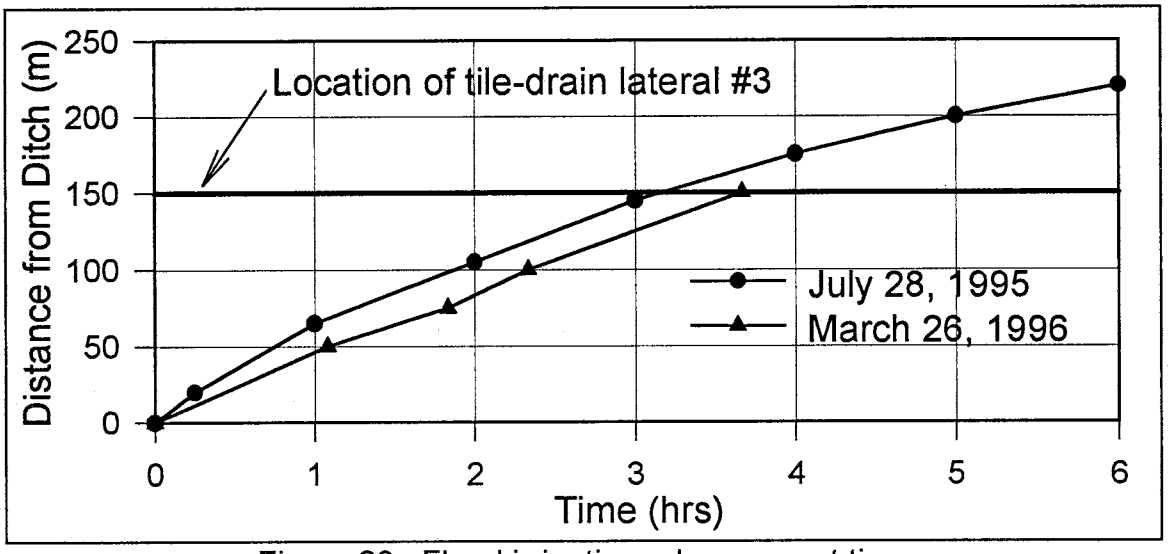

Figure 29: Flood irrigation advancement time

3.7 Tile-drain Flow and Chemical Sampling

As discussed in Section 2.7, the flow measurement system installed in the manholes resulted in the constriction of the tile-drain diameter in order to increase flow velocities to a measurable rate. The effect of this constriction was to cause an increase in the water levels in the soils adjacent to the tile-drain line above the 1994 levels of about 6 to 8 cm in the vicinity of the west manhole inlet and a slight increase in the east-west gradient within the tile-drain under the center bench. These measurements are presented graphically in Appendix H2. This increase equated to an approximate 10% increase with respect to the tile-drain elevation and therefore probably had a negligible impact on the tile-drain hydraulics.

Automated collection of tile-drain flow rate measurements commenced for the west manhole in March, 1995, and for the east manhole in May, 1995. Interruptions in the collection of data occasionally occurred, usually due to power failures in the east manhole. Other interruptions were caused by probable sticking or clogging of the flow sensor paddle-wheels and, in one case, by a lightning strike which caused the west manhole data logger to fail. Flow rate data was collected throughout the remainder of the year and into the 1996 irrigation season, ending in late May, 1996.

Flow measurements are presented in Appendix H3. As the quantity of flow measurement data is great, they are presented in graphical form as 0.5-hour averages. Upon inspection of the graphs, it is apparent that flow rates in the tile-drain line were rapidly and strongly influenced by site irrigations and by

both the sequence and relative timing of those irrigations with respect to the three benches. Less dramatic fluctuations occurred as a result of irrigations of the fields to the north and northeast. Long-term trends in the flow rate were influenced by the depth of submergence below the water table, with average flow rates increasing as submergence increased through the irrigation season. Additionally, flow from the east bench generally accounted for more than half of the total flow measured in the west manhole.

A combination of factors seemed to contribute to the flow rate in the drain at any given time: (1) the degree of submergence below the water table, (2) the regional gradient (i.e., gradient on the bench scale), (3) the local gradient (i.e., the gradient immediately adjacent to the drain), and (4) the gradient within the drain itself (i.e., the overall gradient from the flow rate measurement point to the system effluence). During an irrigation on the site, factors (1) and (4) became dominant. Figure 30 illustrates an east bench to west bench irrigation sequence. As water infiltrated during and following flooding of the east bench, the tile drain there became more submerged and the east-to-center bench gradient in the pipe was increased, thus increasing the flow through both manholes. This also resulted in a slight net loss of flow from the center bench due to the decreased local gradient there (factor 3). Subsequent to flooding and infiltration in the center bench, net flow rates there increased for the same reasons as they did when the east bench was flooded. Then, however, flow rates from the east bench decreased as the east-to-center bench gradient decreased (factor 4). Eventually, flow rates from the east bench decreased to unmeasureable rates

and may temporarily have stagnated or even reversed direction. Subsequent to flooding and infiltration on the west bench, the center-to-west gradient was reduced (factor 4) and net flow rates from the center bench declined rapidly to unmeasurable rates, which again may temporarily have stagnated or reversed direction. Unmeasureable flow rates persisted for a period of time until the east-to-west gradient in the drain recovered sufficiently to establish measurable westerly flow rates.

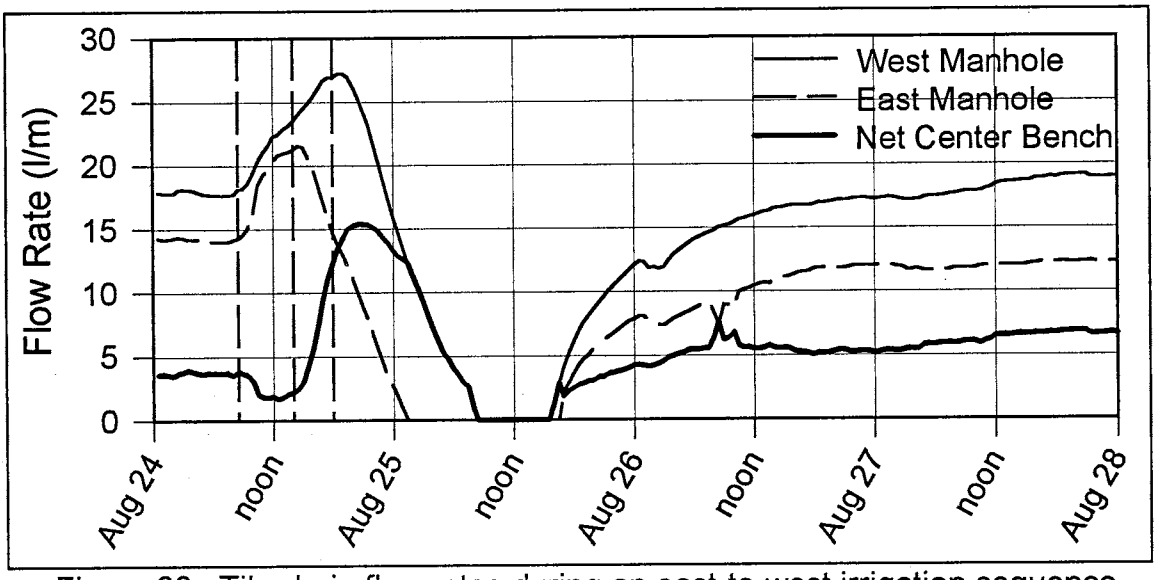

Figure 30: Tile-drain flow rates during an east-to-west irrigation sequence (dashed vertical lines represent east-center-west start times, respectively)

Another noteworthy feature in Figure 30, and which is evident in all LNGP site irrigations for which there is data, is the rapid response of the tile-drain flow rates. Flow rates in lateral #3 noticeably began to change within one hour of instigation of flooding, long before the 3 to 4 hours normally required for the advancing flood to reach the ground surface above the lateral (see Figure 29). This feature indicates the presence of preferential pathways through the soils and a highly dynamic saturated flow system.

Figure 31 illustrates a west-to-east irrigation sequence. Following flooding and infiltration in the west bench, flow rates from both the center, then the east bench rapidly stagnated or reversed Westerly flow was reestablished following flooding of the center and east benches. The observed peak in the net center bench flow rate following the irrigation event, also noted to a lesser degree in Figure 30, is an artifact of the flow meters, which were incapable of measuring flow rates below about 1.5 l/min. The net center bench flow was determined simply by subtracting the flow measured in the east manhole from the flow measured in the west manhole. The peaks are due to the recovery of measurable flow rates in the west manhole prior to their recovery in the east manhole.

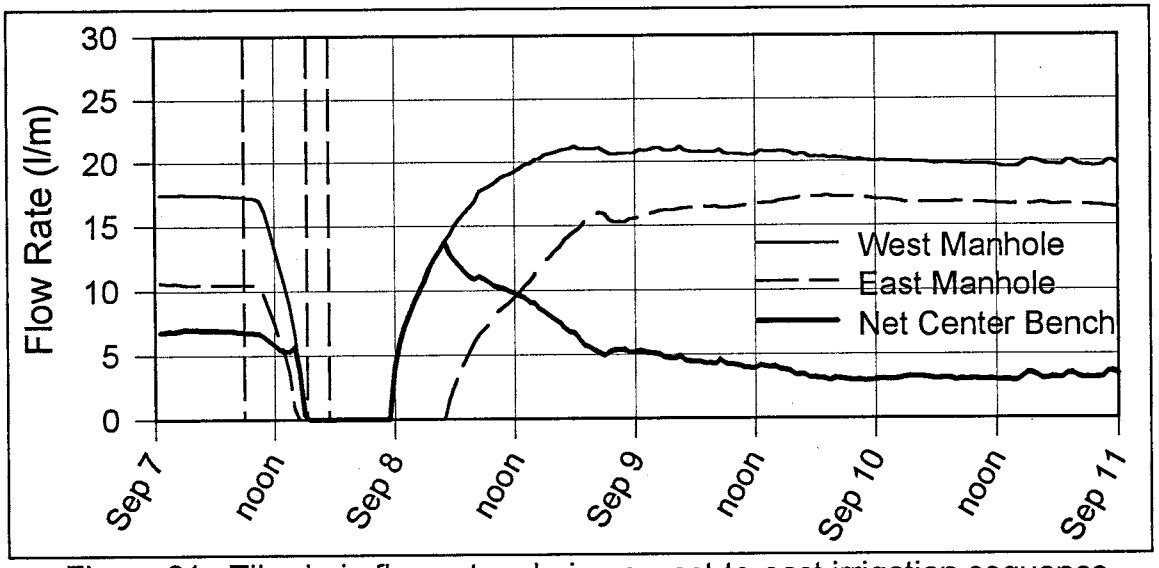

Figure 31: Tile-drain flow rates during a west-to-east irrigation sequence (vertical dashed lines represent west-center-east starting times, respectively)

Figure 32 displays the effects of an irrigation on the fields adjacent to the northeast on October 2 and to the north on October 5. The response is a

dampened and delayed profile of an irrigation on the center and east benches (in the absence of an irrigation on the west bench).

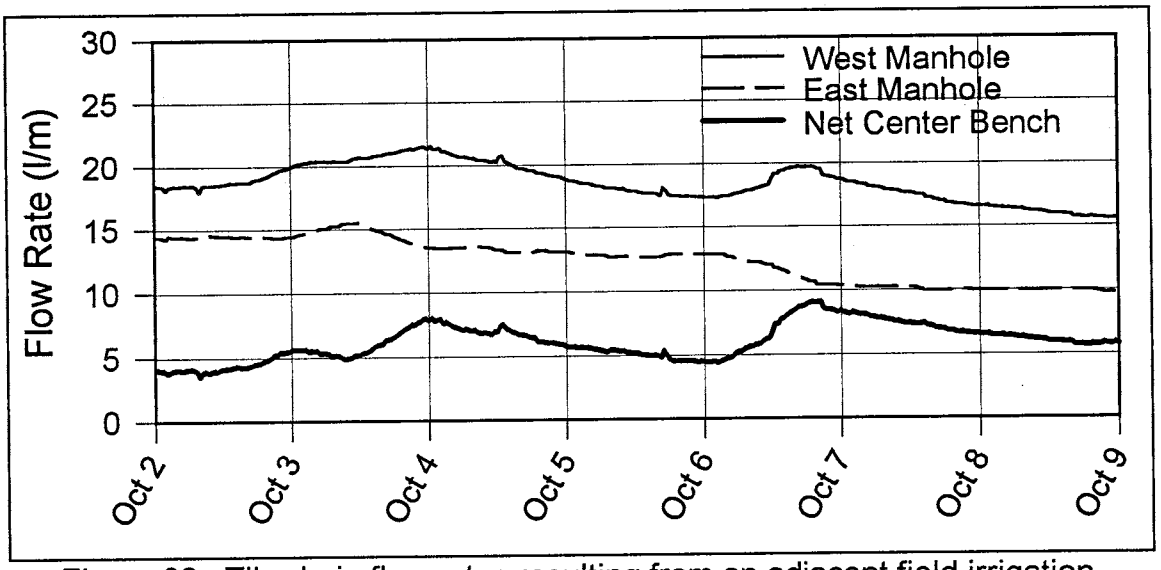

Figure 32: Tile-drain flow rates resulting from an adjacent field irrigation

It is noted that the flow meters used at the LNGP site measured only the magnitude of flow in excess of about 1.5 l/min and were incapable of directly indicating flow direction. Flow rates below about 1.5 l/min were recorded as 0.0 l/min. If the direction of flow had reversed at rates in excess of 1.5 l/min, positive values would have been recorded that would necessarily be bracketed by periods of zero recorded flow as flow rates passed through the "dead zone" of the flow meter. While not indicated in the figures just presented, this situation might have occurred during other irrigations when measurable flow rates were observed bracketed by periods of zero recorded flow (see Appendix H3). This was particularly evident in the east manhole during and following the June, 1995, irrigations. These observations may alternatively be attributed simply to debris temporarily clogging the flow meter paddle-wheel mechanism. This

seems likely in many cases as the transition from zero recorded flow to significantly high flow rates (>4.0 l/min) occurred abruptly (i.e., between successive 5-minute measurements). However, the existence of temporary reversal in the direction of flow still remains a possibility and cannot be definitively resolved without detailed head information along the length of the tile-drain lateral or a flow meter capable of distinguishing flow direction and the low (<1.5 l/min) flow rates.

Pressure transducers were installed in monitoring wells #22 and #23 and in the tile-drain stand-pipe in the west manhole in mid-March, 1996, just prior to the 1996 irrigation season. The transducers were installed in an attempt to ascertain the conductance of the tile-drain, i.e., the relationship between tile-drain flow, head in the tile-drain, and head in the aquifer adjacent to the tile-drain. The transducers, which were the same instruments utilized for the slug tests, monitored heads concurrent with the flow rate in the west manhole. The locations of the monitored heads created what in effect was a cross-sectional view of head adjacent to and in the tile-drain.

A concentrated bromide tracer solution was also applied to the ground surface at this time (just prior to the first 1996 season irrigation) along a line above the monitored tile-drain across most of the center bench, stopping approximately 9 m (30 ft) from each berm. The total amount of bromide applied was 20.0 kg (44.1 lb). In order to minimize dilution of the bromide tracer, the ball valves in the east manhole were closed, thus preventing inflow from the tile-drain under the east bench.

Figure 33 depicts the tile-drain conductance function during the first three irrigation events of the 1996 season. Conductance is the slope of the function defining the relationship between the head drop in the vicinity of the tile-drain (m) and tile-drain flow rate (m^3/day) per meter of pipe. Tile-drain submergence is used here and is the vertical distance between the bottom tile-drain elevation and total head elevation as measured in monitoring well 22.

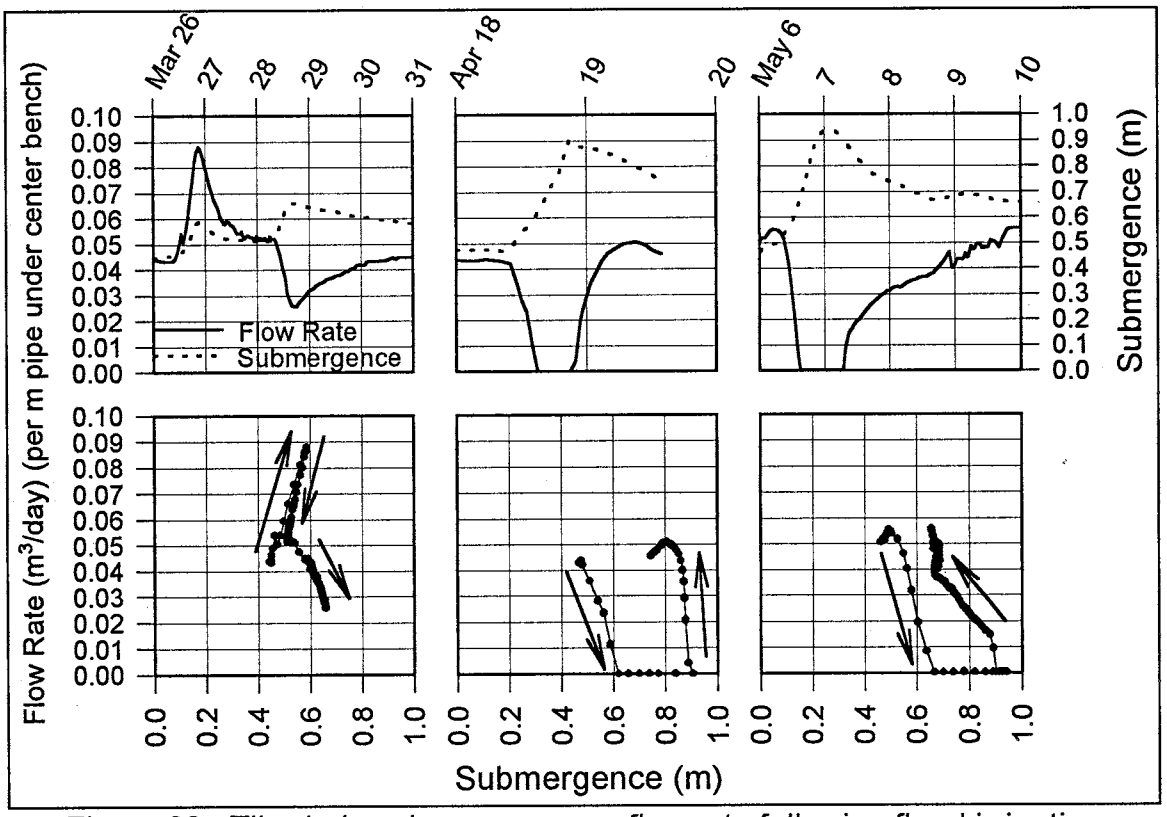

Figure 33: Tile-drain submergence vs. flow rate following flood irrigation (1996 irrigation events. Upper graphs depict temporal data. Lower graphs depict conductance function during the period corresponding to the graph immediately above. Arrows point in the direction of increasing time and symbols are separated in time by 1 hr.)

As can easily be seen, no unique relationship existed between tile-drain flow rate and tile-drain submergence during irrigation events. During the March 26, 1996, irrigation event the conductance function traced out a two-legged

pattern. The ascending and descending portions of the upper leg corresponded to the center bench irrigation and indicated a positive slope for the conductance function (with hysteresis) with values ranging from 0.32 to 0.44 m^2/day per meter of pipe, respectively. The west bench irrigation event two days later resulted in a negative slope for the conductance function and is depicted by the leg descending to the lower right as flow rates decreased while submergence increased. Though not apparent in Figure 33, an ascending trace returned along the same path as flow rates increased and submergence decreased following the west bench irrigation. Thus, no hysteresis was evident at this later time and conductance ranged from approximately -0.43 m^2/day per meter of pipe during the early time (following recovery of measurable flow rates) back to zero and then positive values about 3 days later.

Both of the later two events shown in Figure 33 were west- then center bench irrigation sequences. There was a significant amount of hysteresis in the conductance function for these events. The descending legs of both irrigations indicated conductance values of about -0.30 m^2/day per meter of pipe. The ascending (post-zero flow) legs displayed conductance values of about -1.50 m^2/day per meter of pipe during early recovery times. The conductance function slopes ranged back to zero then positive slopes over periods ranging from 12 to 72+ hours, when slopes of about 0.09 m^2/day were established.

Data collected during the 1995 water level surveys was used to quantify tile-drain conductance in the presence of flow contributed by the tile-drain under the east bench. The data required were head in the tile-drain in the west

manhole and both east- and west manhole flow rates so that the center bench contribution to flow could be calculated. Figure 34 displays points representing all of the monitoring well water level survey dates for which the required data were available (appendix E2). Only water level surveys conducted on days which were removed in time from perturbations induced by on- or off-site irrigation events were selected. The presence of perturbations was determined by inspecting the tile-drain flow rates (appendix H3). Thus, the dates selected presumably represent times during which both regional and local gradients to the tile-drain were fairly uniform.

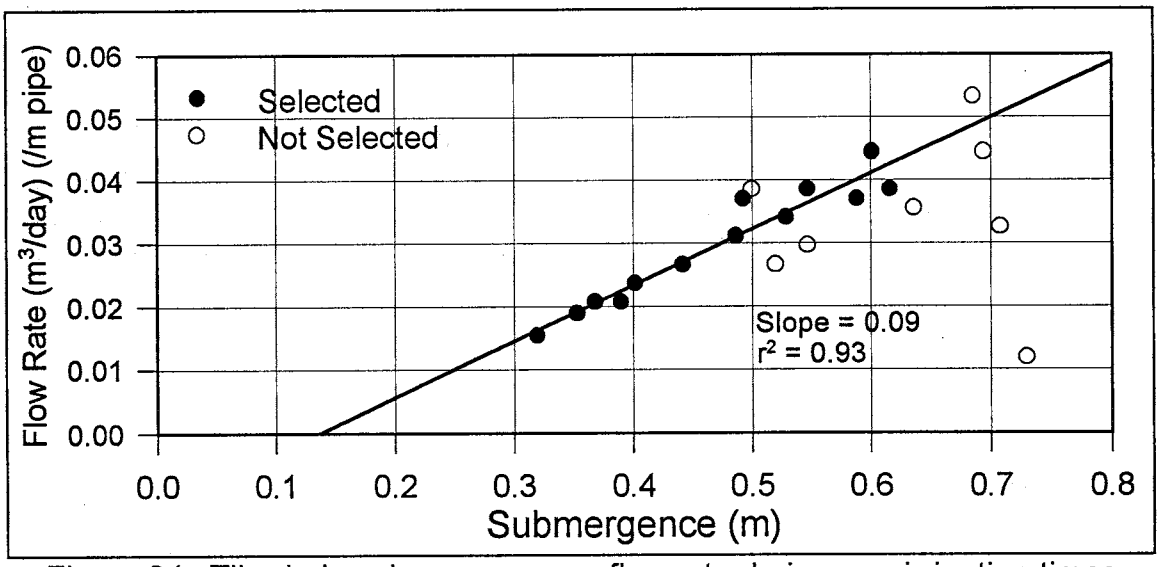

Figure 34: Tile-drain submergence vs. flow rate during non-irrigation times (1995 water level surveys with east bench contribution to tile-drain flow)

Regressing the 13 selected points resulted in a (very linear) tile-drain conductance of approximately 0.09 m^2/day per meter of pipe, similar to values during non-irrigation times in the early part of the 1996 irrigation season. Thus, during a center bench irrigation in the absence of a west bench irrigation, the slope of the conductance function of the monitored tile-drain under the center

bench increased by a factor ranging from approximately 3.5 to 5.0 for a period of at least 48 hours. In the presence of a west bench irrigation, the slope of the conductance function became negative and was followed by unmeasureable flow rates which persisted for approximately 6 to 24 hours. The recovery of a positive conductance function slope then required an additional 24 to 72+ hours.

Simple experiments were conducted to determine whether silting of the tile-drain filter sock or effluence submergence was the primary cause of the low efficiency of the tile-drain. The experiments were conducted on several occasions between March and May, 1994, when a pumping system was installed in the west manhole (Chaves, 1995). The pump effluent was directed into the outflow tile-drain while the inflow (up-gradient) tile-drain was allowed to flow freely. Initial water levels in the west manhole were approximately 50 cm above the center of the tile-drain. The pump lowered the water level in the west manhole creating free-fall (non-submerged) inflow. At various times, pumping was maintained for 2 to 4 hours. At the end of these periods, the volumetric flow rate of the inflow was estimated by obtaining multiple measured volumes of the inflow while noting the times required to obtain those volumes. The measured volumetric flow rates ranged from 52 to 130 l/min at the end of the pumping periods. The storage volume of the tile-drain under the east and center benches totaled approximately 5.0 m^3 and the drainable volumes in the east and west manholes totaled approximately 2.6 m^3, giving a total system storage volume of 7.6 m^3. Over the range of measured flow rates, the times required to drain that storage volume ranged from 1.0 to 2.4 hr. Following the removal of the stored

volume, tile-drain flow rates would have decreased to similar levels as those observed under similar submergence conditions if silting of the tile-drain filter sock was the limiting factor controlling flow into the tile-drain. However, at that time in the irrigation season and in the absence of effluence submergence, the tile-drain was capable of sustaining combined flow rates from the east and center benches that ranged up to almost one order of magnitude higher than those observed during the same period in 1995 (i.e., when water levels were approximately similar) (see Appendix H3). It can therefore be concluded that the primary condition influencing tile-drain efficiency is submergence of the effluence leading to a decrease in the gradient within the tile-drain. There is an insufficient head drop to allow the tile-drain system to drain efficiently.

Flow, head, and chemical results for the March 26, 1996, irrigation are presented in the graphs displayed in Figure 35. Head, tile-drain flow rate, and chemical concentrations remained fairly stable prior to the irrigation event. Head in the tile-drain (labeled "West Manhole" in the figure) exhibited exponential growth/decay variations with a 24-hr period prior to and following the irrigation event. These daily fluctuations are thought to be due to changes of the water level in the Riverside Drain as a result of runoff and return flow from irrigations to the north of the LNGP site. The fluctuations lead to changes in the degree of submergence of the system effluence. Though no direct data was collected as to the magnitude of the change, these fluctuations have been observed (Darrel Reasner, NRCS, per. comm., 1996).

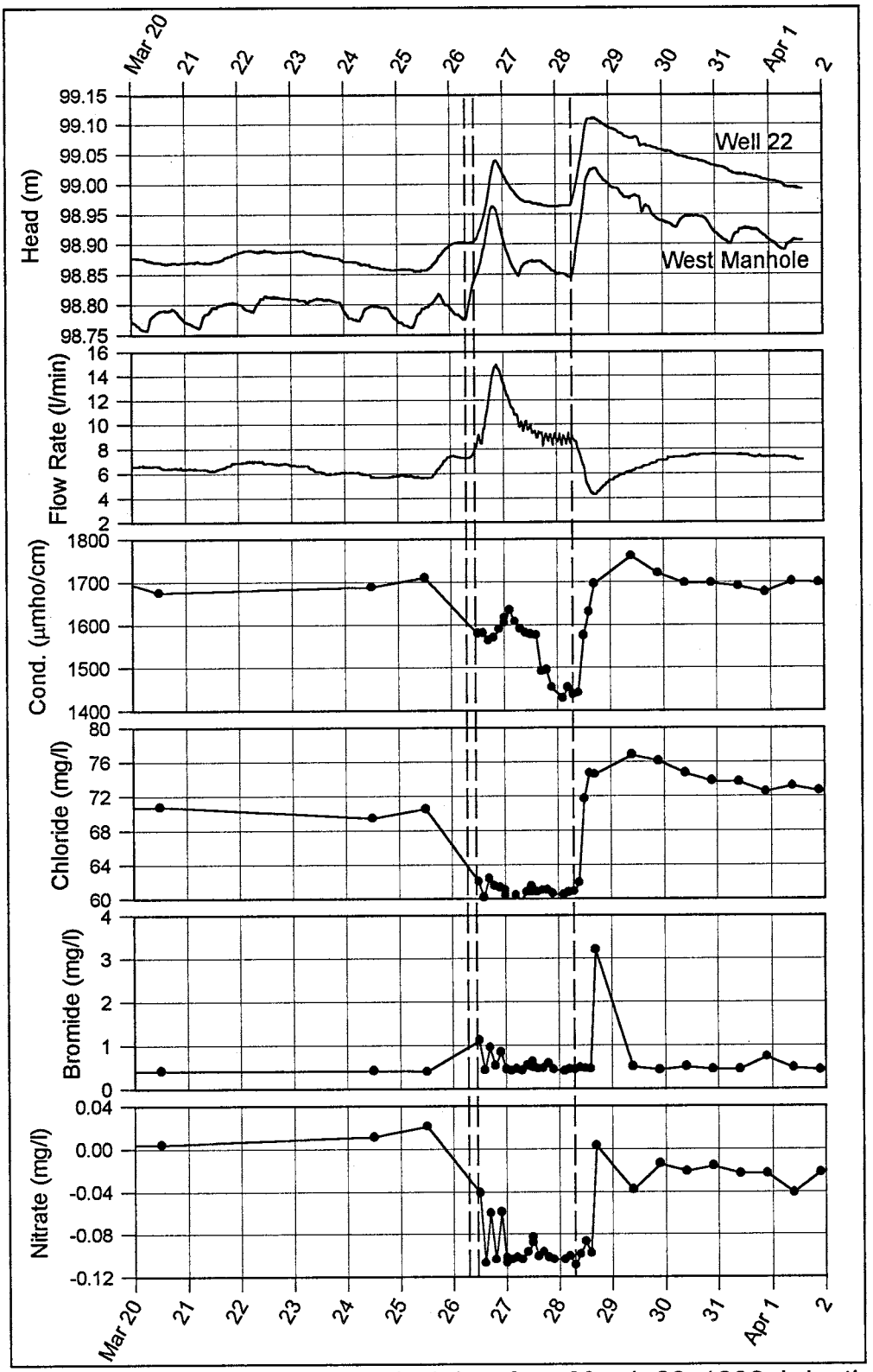

Figure 35: Head, flow, and chemical data from March 26, 1996, irrigation (vertical dashed lines represent start of east-center-west flooding, respectively)

At no time during or following that irrigation did the head in the tile-drain at the west manhole exceed that of the neighboring monitoring wells indicating that, at least at that location, flow was constantly into the tile-drain. The maximum tile-drain flow rate corresponded with the maximum tile-drain head following flooding of the east and center benches due to the increased center-to-west bench gradient. Flooding of the west bench, however, resulted in a reduction of the center-to-west bench gradient and the maximum tile-drain head then corresponded with the minimum tile-drain flow rate. Thus, the conductance of the tile-drain is non-linear and varies between positive and negative depending on irrigation sequence and timing.

Prior to the irrigation, the tile-drain chemistry was fairly consistent and was presumably representative of the regional groundwater at that depth and time as the March 26 irrigation was the first of the season on the LNGP site fields. The chemistry of the applied irrigation water is presented in Table 10. During the irrigation, chemical response in the tile-drain displayed a rapid decrease in concentration of both chloride and nitrate, indicating some degree of mixing of the applied irrigation water with the regional water. Electrical conductivity, which is subject to more processes, did not decrease as rapidly nor did it level off at a particular value as did the chloride and nitrate concentrations. Of the 20.0 kg of bromide applied to the center bench, only 0.0095 kg (0.05%) was measured in the tile-drain during the 7-day period following the irrigation event (assuming a background concentration of 0.4 mg/l). The only significant bromide concentration occurred in the last 2-hr interval sample taken

approximately concurrent with the minimum flow rate subsequent to the west bench irrigation. It is also noted that the tile-drain nitrate concentrations were low, being very close to the detection limit of the method used (Roth, 1995). The negative values shown are obviously impossible and negate their quantitative use. However, the relative changes in nitrate concentration are evident, allowing a qualitative inspection of the data.

Table 10: Irrigation water chemistry for March 26, 1996, irrigation

Date	Hour	Conductivity (μmho/cm)	Cl^- (mg/l)	Br^- (mg/l)	NO_3^- (mg/l)
3/26/96	12:00	399	17.29	0.002	2.59
3/26/96	16:00	404	17.95	-0.022	2.72
Average		402	17.62	-.01	2.66

All chemical concentrations exhibited a rapid and substantial increase just after irrigation of the west bench two days later, as conductivity, chloride, and nitrate returned to close to their pre-irrigation values. Chloride and conductivity increased to slightly above their pre-irrigation values and exhibited a slow tailing toward those values, indicating an increased degree of soil matrix water having chloride concentrations and electrical conductivity higher than the regional groundwater. The observed increases in chemical concentrations during times of reduced or unmeasurable flow in the tile-drain can be explained. Irrigation flooding resulted in a transient downward flow which tended to reduce the proportion of regional flow to the tile-drain. Subsequent flooding on the west bench resulted in a decrease in the center-to-west hydraulic gradient in the tile-drain which, in turn, reduced the gradient adjacent to the tile-drain under the center bench and further suppressed the regional flow input. Thus, during times

of minimal flow following flooding, the regional flow input was at a minimum allowing more opportunity for mixing of the preferential flow input. Additionally, matrix flow probably became more important as the season progressed and water contents remained relatively high.

In order to determine the minimum percentage of the total recharge water captured by the drain, it was necessary to estimate the total amount of irrigation recharge. The soil profile moisture content prior to the irrigation event, which was not measured in the field, was also estimated. Prior to the irrigation event, the water table elevation was, for the most part, within the sand layers underlying the soils at a depth of about 1.15 m. As indicated in Figure 35, the irrigation resulted in an approximate 15 cm rise in the water table. If the reasonable assumption is made that the soil moisture content profile within the sands prior to the irrigation event was in equilibrium with an approximate 0.05 cm/day evaporative flux density (as determined using the steady-state flux calculations for evapotranspiration, Figure 18), then the amount of storage available within the sands over that 15 cm rise in the water table can be estimated. The program CAPSEV (Wesseling, 1991) was used to calculate this estimate. Performing those calculations indicated that, prior to the March 26, 1996, irrigation event, there was an average of 9% available storage over the 15 cm distance above the water table, which equated to 1.35 cm (0.53 in) of recharge. As the total irrigation application was approximately 8.4 cm (3.3 in), then irrigation recharge was approximately 16% of the total applied irrigation volume, equating to 770 m^3 (2.03 $x10^5$ gal) for that irrigation. The value of 16%

irrigation recharge should represent a minimum value for recharge during the irrigation season as the soil moisture deficit was at a maximum for the year just prior to the irrigation. Irrigation events of similar application volumes conducted later in the season should result in higher recharge percentages due to the increased soil moisture content. However, the crop water requirements exceeded the total irrigation depth during the growing season by about 18.3 cm. This deficit would necessarily have been supplied either by storage or capillary flux. By comparing average depths to water over the course of the 1995 growing season (Figure 26) with the maximum possible capillary fluxes for those depths (Figure 18), it was estimated that capillary flux was capable of supplying a total depth ranging from 18 to 21 cm during the growing season. The combined values of net ET and capillary flux would imply zero recharge, in spite of the fact that recharge was observed. The estimate of 16% recharge equates to 15.7 cm of water during the irrigation season. This amount of recharge would not be directly available for crop use and would therefore be subtracted from the irrigation input and requiring a total net ET of 34 cm, about 60% greater than the estimated maximum capillary flux. Though the capillary flux value is problematic in that it was based on a combination of generalized unsaturated soil hydraulic properties and poor instantaneous profile experimental results, the calculation error probably does not exceed 100%. It therefore seems unlikely that recharge could have exceeded about 21% (20.7 cm) of the total irrigation depth, which would require a total net ET of about 39 cm.

The chloride data was used to estimate the fraction of recharge water in the tile-drain for this irrigation event as it exhibited the most abrupt changes in concentration. The total mass of chloride in the tile-drain is the sum contributed by both the background (regional) and recharge flow:

$$Q_B C_B + Q_R C_R = Q_T C_T \tag{3.7-1}$$

where:

Q_B = Background (regional) flow rate to the tile-drain (VT^{-1})
Q_R = Recharge flow rate to the tile-drain (VT^{-1})
Q_T = Total tile-drain flow rate (VT^{-1})
C_B = Background (regional) chloride concentration (MV^{-1})
C_R = Recharge chloride concentration (MV^{-1})
C_T = Tile-drain chloride concentration (MV^{-1})

Further, the total tile-drain flow is the sum of the recharge and background flows:

$$Q_B + Q_R = Q_T \tag{3.7-2}$$

Substituting equation 3.7-2 into equation 3.7-1 and rearranging gives the proportion of recharge flow to background flow, P_{RB}:

$$P_{RB} = \frac{Q_R}{Q_B} = \frac{C_T - C_B}{C_R - C_T} \tag{3.7-3}$$

Equation 3.7-3 contains one unknown value, C_R, which would necessarily reflect some degree of mixing between the infiltrating irrigation water and the soil water:

$$C_R = P_I C_I + P_S C_S \quad where \quad P_I + P_S = 1 \tag{3.7-4}$$

where:

P_I = Proportion of irrigation water (unitless)
P_S = Proportion of soil water (unitless)
C_I = Irrigation water chloride concentration (MV^{-1})
C_S = Soil water chloride concentration (MV^{-1})

As the soil moisture deficit was at a yearly maximum prior to this irrigation and both the concentration and flow responses in the tile-drain were rapid, it is

reasonable to assume that there was little opportunity for mixing between the soil matrix water and the irrigation water infiltrating through the macropore structure. The soil matrix water additionally had a concentration greater than background due to evapotranspiration (i.e., $C_S > C_B$). Since the tile-drain chloride concentration decreased below background during the irrigation response, mixing between the infiltrating irrigation and the matrix water was limited. Thus, the recharge chloride concentration, C_R, was limited by extreme values. The minimum possible value was $C_R = C_I = 17.6$ mg/l, representing zero matrix water in the recharge water. The maximum possible value was $C_R = C_T = 61.0$ mg/l, representing 100% recharge water. That range of values for C_R generated minimum and maximum estimates of P_{RB} in the tile-drain at the time of a given sample. Thus, the recharge flow rate for a given sample can be estimated as:

$$Q_T = Q_R + Q_B = Q_R + \frac{Q_R}{P_{RB}} \quad \Rightarrow \quad Q_R = Q_T\left(1 + \frac{1}{P_{RB}}\right)^{-1} \tag{3.7-5}$$

By multiplying the recharge flow rates obtained from equation 3.7-5 for each sample by the time interval between samples and summing the resulting recharge volumes, the total volume of recharge water intercepted by the tile-drain over a given time interval can be estimated. Finally, by dividing that total volume of recharge water by the total measured flow during the same time interval, the average proportion of recharge water intercepted by the tile-drain can be calculated.

A background chloride concentration, C_B, of 70.5 mg/l (the chloride concentration of the last sample obtained prior to the irrigation event) and an average irrigation water chloride concentration, C_I, of 17.6 mg/l were used. The tile-drain chloride concentration, C_T, ranged from 59.6 to 62.3 mg/l, averaging 61.0 mg/l. The total flow during the 48-hr period following flooding of the center bench was 28.3 m^3. The calculated minimum fraction of recharge water in the tile-drain (equating to zero mixing between irrigation and matrix waters) during that period ranged from 15.5% to 20.7%, averaging 18.2%, and a cumulative minimum total of 5.1 m^3 (1300 gal) of recharge water was captured by the tile-drain.

A study of tile-drain flow and chemical response to flood irrigation was conducted by Deverel and Fro (1991). Their two tile-drains were located 1.8 and 2.7 m below ground surface in a 9-m thick clay loam soil which was underlaid by sands. Their results indicated a range of 70% to 100% recharge water in the shallow tile-drain and 40% to 70% recharge water in the deeper tile-drain following an irrigation event. It seems unlikely that the LNGP tile-drains were nearly as efficient with respect to recharge collection considering that the LNGP tile-drains were located in the higher hydraulic conductivity sands underlying the soil horizons and would thus probably collected a larger proportion of regional flow. It was therefore estimated that the proportion of recharge water in the tile-drain water probably did not exceed about 40%.

Thus, the minimum value of 5.1 m^3 of recharge water captured by the monitored tile-drain during the 48-hr period following the irrigation event

represented a minimum only about 0.66% of the 770 m^3 of recharge. The maximum percentage (i.e., 40% of the 28.3 m^3 total flow) equated to only 1.47% of the total recharge volume. In terms of surface area and assuming equal distribution of the applied irrigation water over the center bench, the tile-drain intercepted the recharge which infiltrated over an area ranging from 1.6 m to 3.5 m wide centered on the tile-drain (i.e., 0.8 m to 1.7 m on each side of the tile-drain over an east-west distance of 237 m with a depth of 1.35 cm). This range of values agrees reasonably well with the data from monitoring wells 12, 13, 22 and 23, which show no noticeable drawdown at distances from the tile-drain ranging from 1.6 to 2.2 m. Finally, assuming an equivalent range of volumes was captured by the remaining three laterals, a total of only 2.6% to 5.9% of the total recharge volume was captured by the entire tile-drain system under the center bench for this irrigation.

Irrigations conducted during the latter parts of the 1994 through 1996 growing seasons showed a very different chemical response. The typical response was an increase in electrical conductivity beginning rapidly after the commencement of flooding and lasting for periods ranging from about 1 to 3 days followed by a rapid decrease, indicating a strong preferential flow component. Peak electrical conductivity values following irrigation events ranged from 1400 to 1950 μmho/cm, The highest concentrations generally coincided with periods of reduced and/or unmeasurable tile-drain flow rates after west bench flooding, as depicted in Figure 36. When measurable flow rates were reestablished, concentrations decreased fairly rapidly to background levels.

This presents the possibility that the chemistry reflected processes occurring on the west bench, though the presence of higher conductivity values prior to unmeasurable flow would tend to disprove that possibility.

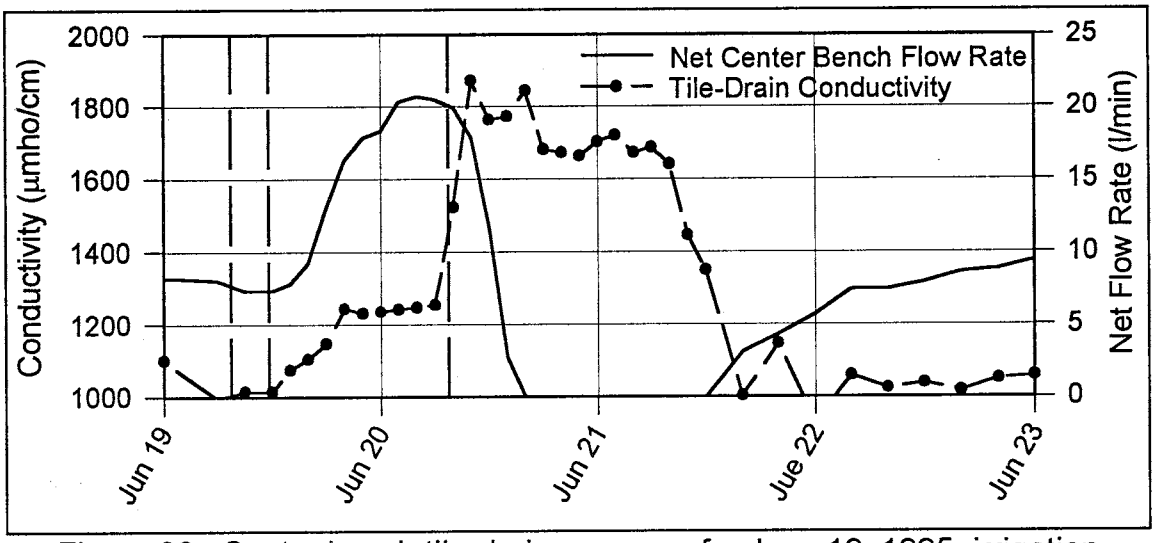

Figure 36: Center bench tile-drain response for June 19, 1995, irrigation (vertical dashed lines indicate start of east-center-west flooding, respectively.)

Figure 37 depicts the center bench response to the irrigation following that depicted in Figure 36. Measurable flow rates were maintained due to a coincidentally timed irrigation on the field adjacent to the north of the center bench. A higher proportion of regional flow to the tile-drain was maintained during this irrigation resulting in overall lower chemical concentrations relative to the previous irrigation response.

Figure 38 depicts the center bench response to a west-to-east irrigation sequence. Though samples were not collected during the early period of increasing concentrations, the tailing response is characteristic, typically being more gradual and lasting for longer periods (2+ days) than for an east-to-west sequence.

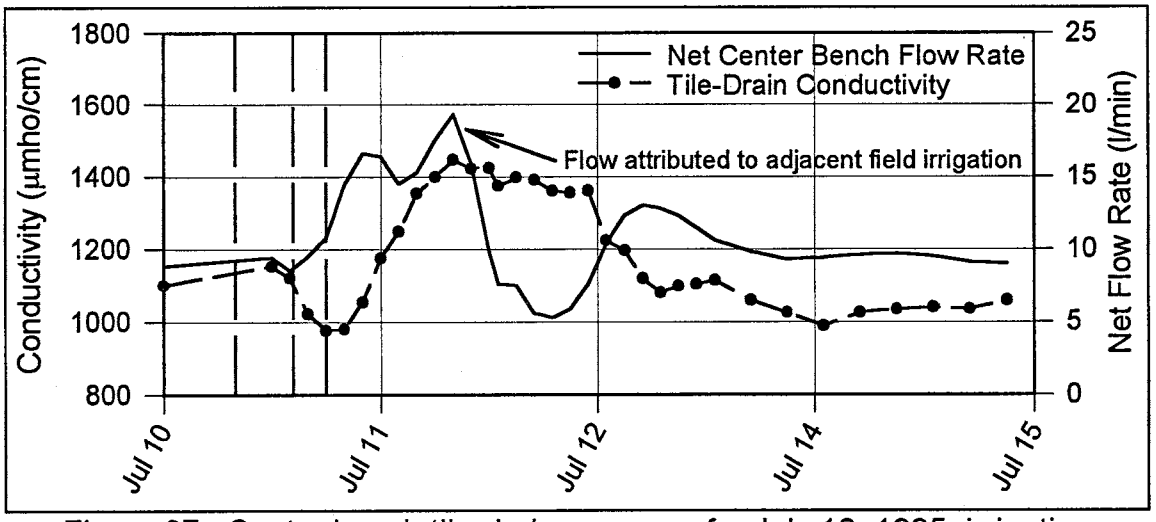

Figure 37: Center bench tile-drain response for July 10, 1995, irrigation (vertical dashed lines represent start of east-center-west flooding, respectively.)

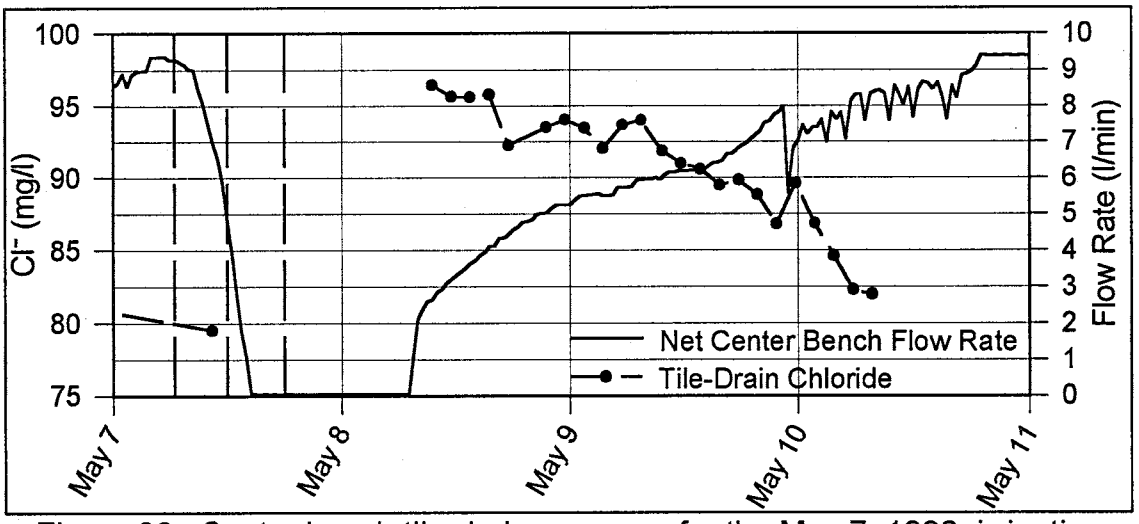

Figure 38: Center bench tile-drain response for the May 7, 1996, irrigation (vertical dashed lines represent start of west-center-east flooding, respectively.)

In order to determine the mass of NO_3-N that was leached to the shallow groundwater during the 1994 irrigation season, the total volume of recharge and the percentage of that recharge which was captured by the tile-drain must be known. The preceding discussion serves to highlight the high degree of uncertainty in the calculations of both of those values. The demonstrated low efficiency of the tile-drain and the uncertain percentages of captured recharge

(both of which changed substantially with time in response to on- and off-site irrigation events and sequences) complicate the determination of an "average" irrigation response. However, flow and chemical data were collected for several irrigations during the 1995 and 1996 seasons, allowing the determination of the percentages of the total response which occurred during different stages following irrigation. Table 11 lists total volumes of flow before, during, and after unmeasurable flow rates were established for six irrigation events grouped by irrigation sequence. Tile-drain flow volumes before unmeasurable flow rates were achieved were totaled beginning with the time at which a change in flow and/or chemical data relative to pre-irrigation conditions was discernible. Volumes totaled during unmeasurable flow rates assumed a flow rate of 1.5 l/min for the duration. Volume totals obtained after unmeasurable flow rates were totaled until flow and/or chemical data returned to approximately their pre-irrigation levels.

The analyses indicated that the reversal of irrigation sequence resulted in essentially identical, though reversed proportions of the total tile-drain flow response volumes relative to the period of unmeasurable flow rates. East-to-west irrigation sequences resulted in from 50% to 100% greater flow volumes as compared to west-to-east irrigation sequences, with the greatest volumes resulting from the delay of the west bench irrigation. Additionally, the total volume that could have entered the tile-drain during the period of unmeasurable flow rates ranged from only 2% to 10%, averaging 5% of the total response volume.

Table 11: Fractions of total flow response for different irrigation sequences

Irrigation Sequence	Irrigation Date	Total Volume of Flow* (m^3)				Fraction of Total (%)		
		Before	During	After	Total	Before	During	After
E-C-W	6/5/95	14.12	1.23	1.38	16.73	84	7	8
	6/19/95	25.75	2.09	2.39	30.23	85	7	8
	8/24/95	11.36	0.36	4.65	16.37	69	2	28
					Ave	80	5	15
W-C-E	9/7/95	1.45	0.49	11.72	13.66	11	4	86
	9/26/95	0.87	1.02	8.55	10.44	8	10	82
	4/18/96	1.63	0.63	8.99	11.25	14	6	80
					Ave	11	6	83

(*In the monitored tile-drain before, during, and after unmeasurable flow rates were established. 1.5 l/m flow rate was assumed during unmeasurable flow.)

The tile-drain NO_3-N concentration response to flood irrigations during the 1994 irrigation season exhibited rapid increases from background levels less than about 0.5 mg/l to peak concentrations ranging from 5 to 12.7 mg/l. These were followed by periods of sustained high concentrations which lasted generally for 1 to 2 days and were followed by periods of either rapid or gradual tailing to background levels, requiring up to another 1 to 3 days. In contrast, NO_3-N levels during the 1995 and early 1996 irrigation seasons remained at essentially background levels. Also, the chemical response to irrigation events lasted somewhat longer during the 1994 irrigation season as compared to those observed during the 1995 and early 1996 seasons. This was probably due to the duration of irrigation, which lasted for longer periods on the west bench during the 1994 season. (Following 1994 irrigation events, water was generally observed standing in both the center and west benches for periods lasting 1 to 2 days longer than periods following 1995 irrigation events.) The result was a

longer period of time was required for the gradient in the tile-drain to be reestablished.

With these considerations aside, the proportions of the total 1994 irrigation flow responses relative to periods of unmeasurable flow rates were assumed to be similar to those of the 1995 and early 1996 seasons. This assumption allowed for a comparison of the 1994 tile-drain NO_3-N response to the 1995 and early 1996 flow and chemical responses. The comparison was based on the proportion of flow analyses summarized in Table 11 and required an average NO_3-N concentration value for each of the three periods of an irrigation (i.e., before, during, and after unmeasurable flow rates). For this comparison, the tile-drain NO_3-N response for the June 28, 1994, irrigation was used and is shown in Figure 39, (Roth, 1995, Appendix 9.4). The data following that irrigation constituted the most complete data set for the 1994 season and witnessed the highest observed NO_3-N concentrations of any irrigation during the project. Thus, calculations based on that irrigation should represent a maximum value for average NO_3-N concentrations in the tile-drain.

The tailing in the chemical response is consistent with that observed for a west-to-east irrigation sequence. Thus, the average proportions of the total flow response for that sequence (see Table 11) were multiplied by the corresponding average NO_3-N concentrations and resulted in an overall average concentration of 6.75 mg/l during the irrigation response.

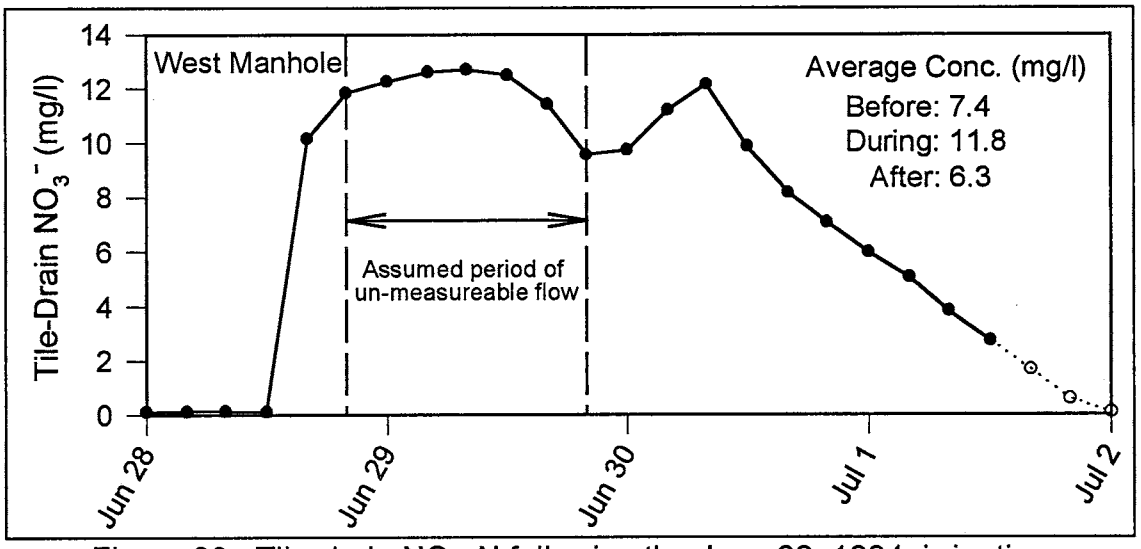

Figure 39: Tile-drain NO_3-N following the June 28, 1994, irrigation

Table 12 lists the applied volumes for ten irrigation events during the 1995 and early 1996 irrigation seasons along with the total net center bench flows to all of the tile-drains during each irrigation response, assuming each tile-drain received volumes similar to the monitored tile-drain. Also listed are the recharge volumes for the estimated range of recharge fractions of 16% to 21%.

Table 12: Irrigation volumes and tile-drain response volumes

Irrigation Date	Response Duration (days)	Irrigation Volume (m^3)	Recharge Volume (m^3)		Net Center Bench Flow* (m^3)
			16% of total	21% of total	
6/5/95	2.15	6167	987	1295	62.2
6/19/95	2.66	6182	989	1298	112.2
7/10/95	2.00	6844	1095	1437	135.5
8/8/95	1.18	4976	796	1045	30.0
8/24/95	2.68	4710	754	989	64.3
9/7/95	1.56	4081	653	857	53.0
9/26/95	1.83	5072	811	1065	37.9
10/23/95	2.03	7775	1244	1633	82.9
3/26/96	1.93	4824	772	1013	114.1
4/18/96	1.40	4474	716	940	42.7
Average	1.94	5511	882	1157	73.5

(*Total for all four tile-drains assuming volumes equal to monitored tile-drain)

Finally, the total mass of NO_3-N leached to the shallow groundwater is a function of the percentage of recharge in the tile-drain. Figure 40 displays this function for the two recharge volumes of 16% and 21% of the total irrigation volume. There were eight center bench irrigations during the 1994 season. Both curves are therefore based on an average NO_3-N concentration of 6.75×10^{-3} kg/m^3 (6.75 mg/l) for an average tile-drain irrigation response of 73.5 m^3 for each of the eight irrigations.

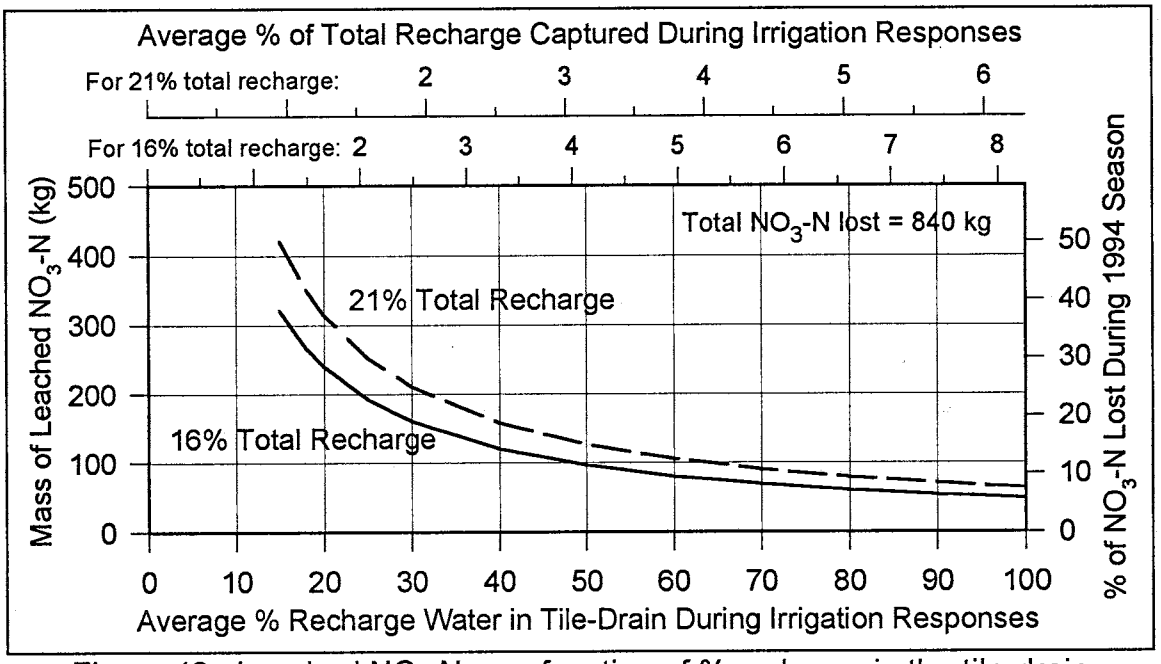

Figure 40: Leached NO_3-N as a function of % recharge in the tile-drain

The bottom axis of Figure 40 indicates the average percentage of recharge water in the tile-drain during the irrigation response periods. The top two axes indicate, for the total recharge volumes of 16% and 21%, respectively, the percentage of the total volume of recharge captured by the tile-drain during the irrigation response periods for the corresponding average percentage of recharge water in the tile-drain. For example, if the average percentage of

recharge water in the tile-drain was 40%, then 2.5% to 3.3% of the total recharge volume was captured by the tile-drain.

The total mass of NO_3-N which was lost from the center bench by all mechanisms during the 1994 growing season was 840 kg (Roth, 1995). The left-hand axis of Figure 40 indicates the mass of NO_3-N that was leached while the right-hand axis indicates the corresponding percentage of the 840 kg (i.e., 100%) lost. With the estimated average percentage of recharge water in the tile-drain during the irrigation response periods ranging from 20% to 40% and the estimated recharge ranging from 16% to 21% of the total irrigation volume, the mass of NO_3-N that was leached to the shallow groundwater during the 1994 irrigation season ranged from 120 to 316 kg, corresponding to 14% to 38% of the total mass that was lost. Over the surface area of the center bench, this equated to 21 to 55 kg/ha. Figure 40 further indicates that, of the total volume of irrigation recharge, only 1.25% to 3.3% was captured by the tile-drains during the irrigation response periods.

The calculation of the range of mass leached becomes increasingly sensitive to the percentage of recharge in the tile-drain as values decrease below about 50%. However, the crop probably utilized about 50% of the NO_3-N lost during the season (Roth, 1995), placing an approximate upper limit of about 50% on the mass that could have been leached. Thus, the calculated range of 14% to 38% of the NO_3-N mass leached to the shallow groundwater seems reasonable. The range falls within the wider range of 6% to 55% generated by Roth (1995). The analysis here is based on a larger data set which allowed a

more thorough analysis and an overall better understanding of the processes occurring at the field site than were available to Roth (1995). The range of mass lost determined here is somewhat higher than the 6% to 26% observed at a study area in Indiana (Kladivko, et. al., 1991) and somewhat lower than the 16% to 47% observed at a study area in Ohio (Owens, et. al., 1994), thought it overlaps both and agrees reasonable well with them.

3.8 Water Balance

It is interesting to note that during the interval of time between the start of the official growing season (April 23) and the final alfalfa cutting (October 13), the total irrigation application was 98.3 cm and total effective precipitation was 5.5 cm. Further, at least 15.7 cm of the of irrigation water was recharge (i.e., the minimum value of 16% recharge of irrigation water determined in the previous section). Thus, the total input during the growing season was 88.1 cm (98.3 + 5.5 - 15.7). Using the average of the FAO and Mapel et al. (1995) alfalfa consumptive water use values (121.6 cm), we see that at least 33.5 cm (121.6 - 88.1) of the crop use water was provided by capillary flux and/or changes in storage. Figure 18 indicates that the steady-state capillary flux would be approximately 0.2 cm/day for a water table depth of 0.75 m, a condition which existed for a large part of the irrigation season. While this calculation does not specifically account for changes in storage, the water table elevation was approximately the same at both the beginning and the end of the period and water contents were probably similar since irrigation began before and continued after the period. The net upward flux explains the persistent salinity problem observed on the center bench.

With respect to the entire calendar year, a simple water balance calculation revealed a net upward flux. Again, assuming there was no change in storage, total inputs (irrigation and precipitation) were approximately 143 cm while total outputs (ET) were approximately 148 cm, a net upward flux of 5 cm.

4. COMPUTER MODELING

The goal of the computer modeling was to obtain insight into the travel times to the tile-drain of particles appearing at the water table. The computer program Visual MODFLOW (Guiguer and Franz, 1996) was used to simulate steady-state, three-dimensional, saturated flow to a tile-drain system using parameters measured at the LNGP site. The computer program provides a convenient graphical user interface and is based on the U.S. Geological Survey modular three-dimensional finite-difference groundwater flow model commonly referred to as MODFLOW (McDonald and Harbaugh, 1988). Visual MODFLOW also incorporates particle tracking routines based on the U.S. Geological Survey program commonly referred to as MODPATH (Pollock, 1989). The particle tracking routines accommodated only steady-state simulations.

The area of the center-bench was simulated. The east-west grid spacing was approximately 10 m. The north-south grid spacing varied from 10 m away from the tile-drain locations to approximately 2.5 m at the tile-drains, with adjacent grid spacings changing by no more than a factor of 0.5. The simulations employed a 16-layered system to a depth of 10 m. Near-surface (<1.m depth) layers reflected a somewhat arbitrary textural sequence with average layer thicknesses and saturated hydraulic conductivity values reflecting results of the SCS soil survey and the instantaneous profile experiments. Deeper (>1 m depth) layers were simulated as sands having an increase in horizontal hydraulic conductivity, k_H, with depth, reflecting the results of the slug tests. Saturated k_H values for a given depth were obtained using the average

values indicated in Figure 28. Values for saturated vertical hydraulic conductivity, k_Z, were assumed such that k_H:k_Z ranged from 0 to 10 for a given layer, as also indicated by the slug test results.

Boundaries consisted of four parallel tile-drains spaced approximately as at the LNGP site. Elevations for the unmonitored tile-drains were interpolated based on those surveyed for the monitored tile-drain and the ground surface (i.e., they were placed at the same depth below the surface and having the same east-to-west gradient). Tile-drain conductance was set at 0.09 m^2/day per meter of pipe for all laterals. Multiple water table elevations within the observed range having a southwesterly 0.08% gradient were specified as constant head boundaries surrounding the model perimeter, excluding those cells above and those containing tile-drain boundaries.

The model was executed under steady-state conditions using successive uniform 20 cm increases in water table elevation. Particles were placed at and below the water table surface at various depths and lateral distances from the monitored tile-drain and the times required for the particles to reach the tile drain were noted.

The steady-state simulations indicated that the tile-drain conductance was the critical factor governing tile-drain flow. Variation of k_H values by factors of ±10 and of k_V values of 0.1 to 1.0 times k_H resulted in negligible variations of the water-table profile. The tile-drain conductance value of 0.09 m^2/day produced simulated tile-drain flow rates very close to those observed for a given water table elevation. With this value of conductance, atmospheric pressures

did not develop in the tile-drain under steady-state conditions. In order to obtain atmospheric pressure in the tile-drain, it was necessary to increase the conductance by about an order of magnitude. The observed inefficiency of the tile-drains is most likely due to the submerged conditions at the outflow, as discussed earlier, and also possibly to constrictions at the outflow due to observed silting of the effluence pipe.

Under steady-state conditions during non-irrigation (i.e., zero recharge) times and under all water table elevations simulated, particles in the upper-most regions of the saturated zone (i.e., within the near-surface clay layer and in the immediately underlying fine sands) required hundreds to thousands of days to reach the tile-drain from distances ranging from 2 to 20 meters up-gradient. Flow directly below the tile-drains was directed nearly vertically upward. Between the tile-drains at distances greater than about 8 to10 m from the tile-drains, flow was horizontal. Flow velocities increased with depth everywhere regardless of flow direction. The tile-drain capture zones were asymmetric due to the regional gradient, extending only about 3 to 5 m down-gradient from the pipes and to depths of about 4 m below the ground surface. The up-gradient capture zones extended laterally to within 3 to 5 m of the next up-gradient tile-drain to a depth of about 5 to 6 meters below the ground surface. The up-gradient capture zones of laterals 2, 3, and 4 included waters originating at greater depths which welled up due to the influence of, but were not captured by, the adjacent up-gradient lateral. Based on the steady-state velocity

distributions, the great majority of water entering the tile-drains originated from directly below the tile-drains.

Steady-state recharge rates ranging from 1 to 4 cm/day (assumed similar to the rates during irrigation events) applied to the entire center bench were also simulated. The results indicated that particles located at the (pre-irrigation) water table elevation immediately above the tile-drain required from 10 to 30 days to reach the tile-drain. This time is far longer than that of the observed chemical response.

The overall results of the computer modeling exercises served to reinforce the presence of preferential, or dual-mode saturated flow at the LNGP site. The computer model, which simulated only saturated, single-mode conductivity, indicated that travel times of particles in the upper meter of the water table and shortly distant from the tile-drain required much longer to reach the tile-drain than was observed in the chemical response of the tile-drains. These results indicate that the increased chemical concentrations observed during and following irrigation events were due to an increased proportion of inflow of water derived from the vicinity immediately above the tile-drain with a corresponding decrease in the contribution of flow from greater depths caused by the transient downward flow induced by the irrigation.

Conceptually, there were multiple process occurring at different times at the LNGP site. Prior to the beginning of the irrigation season, water levels and moisture contents were at their lowest points for the year. Inflow to the tile-drains was derived from off-site lateral inflow. The first irrigation of the season

served primarily to satisfy the soil moisture deficit, with most of the irrigation water going to storage while the excess infiltrated through the macropores. As the season progressed, on- and off-site irrigations raised the water table under the site and crops began to utilize water, deriving more of their water need from capillary rise and storage than was accounted for by irrigations and precipitation. Thus, there was net upward flow during the growing season punctuated by short periods of downward flow during and immediately following irrigations. During non-irrigation times, solutes in the upper saturated portions of the aquifer moved both laterally southeastward and upward in response to the regional gradient and capillary flux demand of the crop. However, due to the increasing hydraulic conductivity with depth, most of the tile-drain flow during non-irrigation times was derived from depth and thus diluted the chemistry of the (lesser) contribution of flow derived from the upper saturated zone.

During and immediately following irrigations, solutes in the upper saturated portions of the aquifer moved predominantly downward as irrigation water infiltrated directly through the macropore structure and additionally induced saturated matrix flow acting to flush downward the evapoconcentrated solutes. The conductance of the tile-drain was temporarily enhanced and/or reduced, depending on irrigation amounts, sequence, and relative timing of irrigation applications. Flow to the tile-drain during those times consisted of a greater, though unknown, percentage of recharge water, as evidenced by the generally increased chemical concentrations.

5. CONCLUSIONS

- Nitrate leaching at the LNPG site does not appear to create a major or persistant problem with regard to shallow groundwater quality. During the 1994 irrigation season, NO_3-N concentrations in excess of 10 mg/l in the monitored tile-drain lasted for only short periods of time immediately following a flood irrigation event. Samples collected from the tile-drain system effluence never exceeded the drinking water standard of 10 mg/l, despite the (temporarily) elevated NO_3-N concentrations under the center bench. Background concentrations under the center bench during the 1994 season averaged about 0.30 mg/l. During the 1995 and early 1996 irrigation seasons, nitrate concentrations in the monitored tile-drain averaged 0.30 and 0.25 mg/l, respectively, and rarely exceeded 1.0 mg/l.

- From 14% to 38% (120 to 316 kg) of the 840 kg of NO_3-N lost from the center bench by all mechanisms (i.e., crop uptake, bacterial denitrification, and leaching to shallow groundwater) was leached to the shallow groundwater during the 1994 irrigation season, equating to 21 to 55 kg/ha. The elevated NO_3-N concentrations were anomalous and probably resulted from the winter wheat crop's failure to grow and resulting failure to utilize the applied nitrogen fertilizer (Roth, 1995). This estimate was based on five assumptions: (1) the observed 1995 and 1996 tile-drain flow and chemical responses to irrigation events were, on average, similar to those of 1994, (2) the elevated 1994 tile-drain NO_3-N concentrations averaged no more than 6.75 mg/l during the irrigation response periods, (3) the fraction of recharge water in the tile-drain averaged 20% to 40%

during the irrigation response periods, (4) the volume of recharge did not exceed 16% to 21% of the total applied irrigation volume, and (5) the three unmonitored tile-drains under the center bench responded to irrigation events in a fashion similar to the monitored tile-drain.

- The fraction of recharge captured by the tile-drain during the irrigation response periods averaged from 1.25% to 3.3% of the total recharge volume. This estimate was based on the same five assumptions enumerated above.
- There was a strong preferential flow component in the LNGP soils. This conclusion was supported by the rapid head, flow, and chemical response in the tile-drain to both on- and off-site flood irrigation events.
- The low efficiency of the tile-drain system was due to the submerged conditions of the system effluence, as confirmed by field experiments. Silting of the filter-socks and/or in the tile-drains did not appear to be the limiting factor governing flow in the tile-drain. Agricultural operators considering the installation of tile-drain systems should take note of the inefficiency of the LNGP site tile-drain system. Drainage canal water elevations must be maintained below tile-drain system effluence outfall elevations by proper ditch maintenance. Also, while designing tile-drain installations for areas having both an increase in hydraulic conductivity with depth and a substantial regional flow, the tile-drain spacing and pipe diameter calculations should include provisions to account for an increased regional flow input.
- With the reasonable assumption that there was no significant change in soil water storage over the periods analyzed, evapotranspiration from the center

bench at the LNGP site exceeded the sum of irrigation and effective precipitation. A net upward flux of 5 cm existed for the calendar year and of at least 33.5 cm for the growing season. The net upward flux explains the persistent saline soil conditions present on the center bench.

- Results of the instantaneous profile experiments were poor due to the extremely limited duration of the experiments and the very small changes in water content and matrix pressure. Thus, the unsaturated flow characteristics of the vadose zone at the LNGP site remain largely unquantified.

- The slug test results indicated that, with depth, there was an overall increase in saturated hydraulic conductivity of the sands underlying the LNGP site. Additionally, the anisotropy ratio (k_H:k_Z) was less than 10 as indicated by the highly linear log-drawdown recovery rates. Saturated hydraulic conductivity values, as determined by the Bouwer and Rice (1976) technique, increased from an average of 230 cm/d in the upper 1.0 to 1.5 m of the aquifer to an average of 1900 cm/d at a depth of about 6.5 m. These averages exclude three piezometers apparently set in a discontinuous clayey layer at about 4 to 6.5 m depth, which had a average k_H of 27 cm/d. The presence of a clayey layer was confirmed at a depth of 6.4 m from the drilling log for piezometer 3E. Logs for piezometers 1E and 14E, the only other logs available, showed a possible clayey layer about 0.4 m thich at a depth of 3.2 m at piezometer 11E and no evidence of a clayey layer at piezometer 14E.

- One of the initially attractive aspects of this project was the fact that a commercial operation rather than an experimental installation was the object of

the study. While that aspect may still have merits, complications arose during the course of the study which warrant critical review. Probably the single most important was the lack of control over when and where irrigation waters were applied, both on- and off-site, which complicated the mass balance calculations. Due to the nature and management practices of the irrigation delivery system, irrigations on fields neighboring the center bench were more often than not performed within a day of a center bench irrigation. The influence of irrigations, both on the west bench and on the adjacent up-gradient fields had a profound impact on the monitored tile-drain flow and chemistry response. There were only rare occurrences which afforded the opportunity to monitor those influences individually. Many of those opportunities were lost, primarily because the physical location of the project site introduced logistical problems at odds with the obvious need for long term observations and frequent field visits.

6. RECOMMENDATIONS

Most of the following recommendations pertain to site-specific problems and the required implementation costs in both material and labor would probably be prohibitive in light of the possible benefits realized. Also, certain recommendations would hamper or otherwise infringe upon the normal commercial operations and practices at the site. These considerations aside, however, there are several recommendations that could be made in order to better quantify recharge and solute transport at the LNGP site.

The single most important improvement would be to dredge the Riverside Drain to a depth that would leave the tile-drain system effluence pipe above the water level in the drain. This would allow the system to operate as efficiently as possible without further modification. If drainage was still insufficient, collection pipes for each field could be installed, thus creating separate and unrelated drainage systems for each bench.

Many of the problems encountered stem from the irrigation sequence and timing. Having experimental control over that sequence and timing would allow for a more methodical approach to determining the tile-drain flow response under different conditions. It would also eliminate the problems associated with missed irrigations. Another improvement would be the installation of an instrumented manhole at the system effluence. This would have the advantage of monitoring the flow and chemical response of a much larger area than was employed here, though it would also require the measurement of irrigation application on the east and west benches.

In order to better quantify the unsaturated hydraulic properties of the soils, the instantaneous profile experiments could be repeated. Any new experiments should commence with the end of the irrigation season thus allowing the maximum time for drainage. Vertical barriers should be installed to the water table to prevent lateral flow. Tracers could be added to the ponded water in order to quantify the macropore-matrix exchange coefficients.

Tile-drain chemistry needs to be better understood in relation to changes in tile-drain flow. There were often large changes in chemical parameters between samples due to on- and off-site irrigation events for which we were not prepared, indicating the need to increase sampling frequency.

Finally, neutron probe access tubes should be permanently installed at several locations and monitored frequently in order to quantify pre- and post-irrigation water contents. This information, coupled with more complete information regarding the unsaturated hydraulic properties, would lead to a better estimate of recharge than can currently be determined.

7. REFERENCES

Bowman, R.S., J.M.H. Hendrickx, and S. Bulsterbaum. 1992. *Las Nutrias Groundwater Project.* Proc. of N.M. Conf. on the Env., Albuq., N.M.

Bowman, R.S., J.M.H. Hendrickx, T.L. Roth, R.C. Reedy, B.P. Mohanty, and M.Th. van Genuchten. 1995. *Preferential Flow of Nitrate and Pesticides in a Tile-Drained Field.* Agron. Abstr. 85:236.

Bouwer, H. 1989. *The Bouwer and Rice Slug Test - An Update.* Groundwater 27(3), 304-309.

Bouwer, H. and R.C. Rice. 1976. *A Slug Test for Determining Hydraulic Conductivity of Unconfined Aquifers With Completely or Partially Penetrating Wells.* Water Resour. Res., 12(3), 423-428.

Brown, D.L., and T.N. Narasimhan. 1995. *An Evaluation of the Bouwer and Rice Method of Slug Test Analysis.* Water Resour. Res. 31(5), 1239-1246.

Carsel, R.F., and R.S. Parrish. 1988. *Developing Joint Probability Distributions of Soil Water Retention Characteristics.* Water Resour. Res. 24(4), 755-769.

Chaves, J.S. 1995. *Variability in Hydraulic Conductivity and Soil Salinity in a Flood-irrigated Field: The Las Nutrias Groundwater Project.* M.S. Thesis, New Mexico Institute of Mining and Technology, Socorro, NM.

Cooper, H.H., Jr., J.D. Bredehoeft, and I.S. Papadopulos. 1967. *Response of a Finite-Diameter Well to an Instantaneous Charge of Water.* Water Resour. Res., 3(1), 263-269.

Deutsch, C.V., and A.G. Journel. 1992. *GSLIB Geostatistical Software Library and Users Guide*. Oxford University Press, New York, N.Y. pp. 340.

Deverel, S.J., and J.L. Fro. 1991. *Groundwater Flow and Solute Movement to Drain Laterals, Western San Joaquin Valley, California. 1. Geochemical Assessment.* Water Resour. Res., 27(9), 2233-2246.

Doorenbos, J., and Pruitt, W.O. 1977. *Crop Water Requirements.* Food and Agriculture Organization of the United Nations, Irrigation and Drainage Paper 24, 179 pp.

Faust, C.R., and Mercer, J.W. 1984. *Evaluation of Slug Tests in Wells Containing a Finite-Thickness Skin.* Water Resour. Res., 20(4), 504-506.

Freeze, R.A., and J.A. Cherry. 1979. *Groundwater*. Prentice Hall Publishers, Englewood Cliffs, N.J. 604 pp.

Fro, J.L., and S.J. Deverel. 1991. *Groundwater Flow and Solute Movement to Drain Laterals, Western San Joaquin Valley, California. 2. Quantitative Hydrologic Assessment.* Water Resour. Res., 27(9), 2247-2257.

Golden Software, 1994. *SURFER version 5.00 User Guide.* Golden Software, Golden, Co.

Guiguer, N. and T. Franz. 1996. *Visual MODFLOW, Version 1.5, The Integrated Modeling Enviromnent for MODFLOW and MODPATH.* Waterloo Hydrogeologic Software, Waterloo, ON, Canada.

Harbaugh, A.W. 1990. *A Computer Program for Calculating Subregional Water Budgets Using Results from the U.S. Geological Survey Modular Finite-Difference Ground-Water Flow Model.* U.S.G.S., Reston, VA. 23 pp.

Hawley, J.W., C.S. Hasse, and R.P. Lorinsky. 1995. *An Underground View of the Albuquerque Basin.* in Proc. of the 39th Ann. N.M. Water Conference. N.M. Water Resour. Res. Inst. Report No. 290.

Hill, M.C. 1990. *Preconditioned Conjugate-Gradient 2 (PCG2), A Computer Program for Solving Ground-Water Flow Equations.* U.S.G.S. Water Resour. Invest. Report 90-4048. 43 pp.

Hyder, Z. and J.J. Butler, Jr. 1995. *Slug Tests in Unconfined Formations: An Assessment of the Bouwer and Rice Technique.*Groundwater 33(1),16-22.

Hyder, Z., J.J. Butler, Jr., C.D. McElwee, and W. Liu. 1994. *Slug Tests in Partially Penetrating Wells.* Water Resour. Res., 30(11), 2945-2957.

Kelley, V.C. 1977. *Geology of Albuquerque Basin, New Mexico.* N.M. Bur. of Mines and Mineral Resour. Mem. 33, 59 pp.

Kernodle, J.M., D.P. McAda, and C.R. Thorn. 1995. *Simulation of Groundwater Flow in the Albuquerque Basin, Central New Mexico.* U.S.G.S. Water Resour. Invest. Report 94-4251, 114 pp.

Kladivko, E.J., G.E. Van Scoyoc, E.J. Monke, K.M. Oates, and W. Pask. 1991. *Pesticide and Nutrient Movement to Subsurface Tile Drains on a Silt Loam Soil in Indiana.* J. Environmental Quality, 20, 264-270.

Lorinsky, R.P., J.W. Hawley, and D.W. Love. 1991. *Geologic Overview and Pliocene-Quaternary History of the Albuquerque Basin, Central New Mexico.* N.M. Bur. of Mines & Mineral Resour. Bull. 137, pp. 157-162.

Mapel, C.L., Sammis, T.W., and Lansford, R.R. 1985. *Estimating Crop Water Production Functions Based on Transpiration and Crop Growth Curves Through Modeling.* N.M. Water Resour. Res. Inst. Report No. 191. 38 pp.

McDonald, M.G., and A.W. Harbaugh. 1988. *A Modular Three-Dimensional Finite-Difference Ground-Water Flow Model.* U.S.G.S. Techniques of Water Resour. Invest., Book 6. 14 ch.

McDonald, M.G., A.W. Harbaugh, B.R. Orr, and D.J. Ackerman. 1991. *A Method of Converting No-Flow Cells to Variable-Head Cells for the U.S. Geological Survey Modular Finite-Difference Ground-Water Flow Model.* U.S.G.S. Open-File Report 91-536. 98 pp.

McElwee, C.D., and J.J. Butler, Jr. 1992. *Effective Transmissivities From Slug Tests in Wells With a Skin.* Kansas Geol. Soc. Open-File Report #92-12.

New Mexico State University, 1959 to 1995. Climatological data collected at the Agricultural Science Center, Los Lunas, New Mexico.

Owens, L.B., M.W. Edwards, and R.W. Van Keuren. 1994. *Groundwater Nitrate Levels Under Fertilized Grass-Legume Pastures.* J. Environmental Quality, 23, 752-758

Pandit, N.S., and R.F. Miner. 1986. *Interpretation of Slug Test Data.* Groundwater, 24(6), 743-749.

Penman, H.L. 1963. *Vegetation and Hydrology.* Commonwealth Bureau of Soils Tech. Comm. No. 53, Horpenden, England. 125 pp.

Pnueli, D., and C Gutfinger. 1992. *Fluid Mechanics*. Cambridge University Press, New York, N.Y. 482 pp.

Pollock, W.P. 1989. *Documentation of Computer Programs to Compute and Display Pathlines Using Results form the U.S. Geological Survey Modular Finite-Difference Ground-Water Flow Model.* U.S.G.S. Open-File Report 89-381. 81 pp.

Roth, T.L. 1996. *Agricultural Chemical Transport to Shallow Groundwater in a Tile-drained, Flood Irrigated Field.* M.S. Thesis, New Mexico Institute of Mining and Technology, Socorro, NM.

Roybal, F.E. 1991. *Groundwater Resources of Socorro County, New Mexico.* U.S.G.S. Water Resour. Invest. Rpt 89-4083. 32 pp.

Samani, Z., and H. Magallanez. 1993. *Measuring Water in Trapezoidal Canals.* J. Irrigation and Drainage Eng., 119(1), 181-186.

Sammis, T.W., E.G. Hanson, C.E. Barnes, H.D. Fuehring, E.J. Gregory, R.F. Hooks, T.A. Howell, and M.D. Finkner. 1979. *Consumptive Use and Yields of Crops in New Mexico.* N. M. Water Resour. Res. Inst. Report No. 115, 108 pp.

Sammis, T.W., and J.A. Guitar. 1981. *Effects of Decreased Watering on Crop Yields.* N. M. Water Resour. Res. Inst. Report No. 136, 29 pp.

Shan, C., and D.B. Stephens. 1994. *Recommendations for Usage of SURFER to Gridding Model Results.* Groundwater 32(3), 503-506.

Šimünek, J., T. Vogel, and M.Th. van Genuchten. 1994. *The SWMS_2D Code for Simulating Water Flow and Solute Transport in Two-Dimensional Variable Saturated Media.* Research Report No. 132, 197 pp. U.S. Salinity Laboratory, USDA-ARS, Riverside, California.

Thorn, C.R., D.P. McAda, and J.M. Kernodle. 1993. *Geohydrologic Framework and Hydrologic Conditions in the Albuquerque Basin, Central New Mexico.* U.S.G.S. Water Resour. Invest. Report 93-4149. 106 pp.

United States Department of Agriculture, Soil Conservation Service, 1988. *Soil Survey of Socorro County Area, New Mexico.* U.S. Gov. Printing Office, Washington, D.C. pp. 328.

Van Genuchten, M.Th., F.J. Leij, and S.R. Yates. 1991. *The RETC Code for Quantifying the Hydraulic Functions of Unsaturated Soils.* US EPA Report No. 600/2-91/065. 83 pp.

Viessman, W. and Lewis, G.L. 1996. *Introduction to Hydrology*, 4th Edition. HarperCollins College Publishers. 760 pp.

Visvalingham, M., and J.D. Tandy. 1972. *The Neutron Method for Measuring Soil Moisture Content - A Review.* J. Soil Science, 23(4), 499-511.

Watson, K.K. 1966. *An Instantaneous Profile Method for Determining the Hydraulic Conductivity of Unsaturated Porous Materials.* Water Resour. Res., 2(4), 709-715.

Wesseling, J.G. 1991. *CAPSEV: Steady State Moisture Flow Theory, Program Description and User Manual.* Report 37, 51 pp. Winand Staring Centre for Integrated Land, Soil and Water Res., Wageningen, The Netherlands.

Wilson, B.C. 1992. *Water Use by Categories in New Mexico Counties and River Basins, and Irrigated Acreage in 1990.* N.M. State Engineer Technical Report 47. 141 pp.

Appendix A - Soil Texture, Thickness, and % Clay

Horizon	AP			C1			C2		
Site ID	texture	cm	%clay	texture	cm	%clay	texture	cm	%clay
1	SCL	25	24	SL	13	13	S	25	2
2	SiCL	36	28	S	43	2	LvfS	23	6
3	SCL	36	26	LS	25	5	S	91	2
4	SiCL	33	28	C	28	40	SiL	53	20
5	SiCL	33	29	SiC	23	40	SiL	58	16
6	SiCL	36	30	S	20	2	SiL	41	16
7	SCL	30	26	LS	28	10	LvfS	30	13
8	SCL	30	23	CL	20	38	S	76	2
9	SiCL	33	28	SiCL	18	38	S	25	2
10	SiCL	43	28	S	33	2	LvfS	38	14
11	SiCL	41	30	S	30	2	SiCL	18	30
12	SiL	41	25	SiCL	20	33	S	15	2
13	SiL	41	25	SiCL	15	34	SiL	33	16
14	SiL	51	25	vfS	30	2	S	33	2
16	SiL	41	20	SiCL	10	38	S,fS,vfS	102	6
17	SiL	38	20	SiCL	13	36	LfS	41	12
18	SiL	41	16	SiCL	20	30	LvfS	28	13
19	SiL	46	18	SiCL	36	34	LvfS,SiL	46	10
20	SiL	56	25	SiC	20	40	SiCL,SiL,S	25	17

Horizon	C3			C4			C5		
Site ID	texture	cm	%clay	texture	cm	%clay	texture	cm	%clay
1	vfS	23	2	LvfS	28	8	S	38	2
2	S	51	2	-	-	-	-	-	-
3	-	-	-	-	-	-	-	-	-
4	S	38	2	-	-	-	-	-	-
5	S	38	2	-	-	-	-	-	-
6	S	56	2	-	-	-	-	-	-
7	S	64	2	-	-	-	-	-	-
8	fS	25	5	-	-	-	-	-	-
9	SiL	33	16	S	43	2	-	-	-
10	S	38	2	-	-	-	-	-	-
11	LvfS	64	15	-	-	-	-	-	-
12	SiCL	13	33	LvfS	25	13	S	38	2
13	S,LvfS	64	25	-	-	-	-	-	-
14	LvfS	15	5	S	23	2	-	-	-
16	-	-	-	-	-	-	-	-	-
17	S,fS	61	6	-	-	-	-	-	-
18	SiL,LfS,S	38	9	S	25	2	-	-	-
19	S	25	2	-	-	-	-	-	-
20	S	36	2	SiC	15	40	-	-	-

- horizon does not exist

Appendix A (cont.) - Soil Texture, Thickness, and % Clay

Horizon	AP			C1			C2		
Site ID	texture	cm	%clay	texture	cm	%clay	texture	cm	%clay
21	SiCL	41	29	SiC	41	40	LvfS	33	13
22	SiCL	41	28	SiC	41	40	LvfS,SiL	33	13
23	SiL	46	24	SiC	30	40	fS	76	5
24	SiCL	30	30	SiC	20	40	LvfS,vfS,SiL	38	12
25	SiCL	38	30	SiC	18	40	fS,vfS	46	10
26	SCL	43	28	fS	20	8	S,vfS	18	3
27	SiCL	36	30	SiC	15	40	LfS	25	10
28	CL	36	30	SiC	20	40	S	20	2
29	SCL	30	25	SiC	20	40	S	25	5
31	SCL	25	30	C	18	40	S	20	5
32	CL	43	30	S	20	5	LvfS	38	12
33	CL	46	30	SiC	18	40	S	13	5
34	CL(SiCL)	43	32	SiC	10	40	LvfS	36	13
35	CL(SiCL)	46	33	fS	43	5	S	64	2
36	CL(SiCL)	30	30	SiC	20	40	LvfS	25	12
37	SiCL	46	28	SiC	30	40	LfS,fSL	76	14
38	SiCL(CL)	46	28	SiC	43	40	fS	64	5
39	SiL	36	24	SiCL	15	36	SiC	38	40
40	SiL	38	25	SiCL	13	36	SiC	41	40

Horizon	C3			C4			C5		
Site ID	texture	cm	%clay	texture	cm	%clay	texture	cm	%clay
21	fS,vfS	38	5	-	-	-	-	-	-
22	S	38	2	-	-	-	-	-	-
23	vfS			-	-	-	-	-	-
24	fS	64	5	-	-	-	-	-	-
25	S,fS	51	3	-	-	-	-	-	-
26	S,SiL	71	8	-	-	-	-	-	-
27	SiL	25	14	S	51	2	-	-	-
28	SiL	25	13	S,SiL	51	8	-	-	-
29	S,SiL	30	8	S	46	2	-	-	-
31	SiCL	13	30	SiL	25	15	S	51	2
32	S,LvfS	51	6	-	-	-	-	-	-
33	SiL,S	51	9	S	25	2	-	-	-
34	S	64	2	-	-	-	-	-	-
35	-	-	-	-	-	-	-	-	-
36	LfS	51	10	S	25	2	-	-	-
37	-	-	-	-	-	-	-	-	-
38	-	-	-	-	-	-	-	-	-
39	LvfS	25	5	fS	38	2	-	-	-
40	fS,SiCL	36	3	S	25		-	-	-

- horizon does not exist

Appendix A (cont.) - Soil Texture, Thickness, and % Clay

Horizon	AP			C1			C2		
Site ID	texture	cm	%clay	texture	cm	%clay	texture	cm	%clay
41	SiL	41	23	SiC	23	40	fS,SiL,LfS	89	10
42	SiL	41	20	SiC	30	40	SiL	43	15
43	SiCL	41	28	SiC	15	40	SiL,LvfS	53	13
44	SiCL	56	30	SiC	41	40	S	56	2
46	SiL	46	25	SiCL	15	38	SiC,LvfS	53	13
47	SiCL(SiL)	46	28	SiCL	18	37	SiL	43	14
48	SiCL	36	30	SiCL	18	36	SiL,LvfS	48	13
49	SiCL	43	32	SiC(SiCL)	20	40	SiL,LvfS	25	13
50	CL	36	30	SiC	23	40	LvfS,SiL	30	9
51	CL	38	32	SiC	58	40	SiL	18	14
52	CL	51	30	SiC	38	40	SiL	25	12
53	CL	46	32	SiC	38	40	SiL	15	12
54	CL	46	32	SiC	36	40	LfS	20	8
55	CL	51	32	SiC	43	40	SiL	20	14
56	CL	41	33	SiC	18	40	LfS,fSL	38	12
57	CL	25	32	CL	30	38	SiL,LfS,S	51	7
58	CL	46	32	SiC	15	40	LvfS	28	8
59	CL	36	32	SiC	18	40	LfS,fSL	23	13
61	CL	51	29	fS	30	5	SiL,LvfS	46	10

Horizon	C3			C4			C5		
Site ID	texture	cm	%clay	texture	cm	%clay	texture	cm	%clay
41	-	-	-	-	-	-	-	-	-
42	fS	38	5	-	-	-	-	-	-
43	S	43	2	-	-	-	-	-	-
44	-	-	-	-	-	-	-	-	-
46	S	38	2	-	-	-	-	-	-
47	S	46	2	-	-	-	-	-	-
48	S	51	2	-	-	-	-	-	-
49	LfS	25	8	S	38	2	-	-	-
50	S	64	2	-	-	-	-	-	-
51	S	38	2	-	-	-	-	-	-
52	S	38	5	-	-	-	-	-	-
53	fS	53	5	-	-	-	-	-	-
54	fS	51	2	-	-	-	-	-	-
55	S	38	2	-	-	-	-	-	-
56	fS	56	5	-	-	-	-	-	-
57	S	46	2	-	-	-	-	-	-
58	S	64	2	-	-	-	-	-	-
59	SiL	25	2	S	51	-	-	-	-
61	S	25	2	-	-	-	-	-	-

- horizon does not exist

Appendix A (cont.) - Soil Texture, Thickness, and % Clay

Horizon	AP			C1			C2		
Site ID	texture	cm	%clay	texture	cm	%clay	texture	cm	%clay
62	SCL	36	28	SiC	28	40	SiCL	41	30
63	CL	38	33	SiC	18	40	SiL,LfS	51	12
64	SCL	38	23	fS	38	2	SiL,LfS	36	10
65	CL	41	33	SiC	13	40	SiCL,SiL,LfS	69	18
66	CL	46	33	SiC	51	40	vfS	56	5
67	CL	48	28	SiC	33	40	fS	46	5
68	CL(SiCL)	33	28	SiC	43	40	fS,vfS	46	5
69	CL(SiCL)	33	28	SiC	56	40	SiL,LvfS,fS	64	10
70	CL	46	30	SiCL	25	45	SiL,LvfS	28	13
71	CL	38	30	SiC	23	40	SiCL	30	34
72	SiCL	38	28	SiC	38	40	LvfS	23	13
73	SiCL	36	30	SiC(SiCL)	15	40	vfS,LvfS	38	8
74	SiL	38	24	SiCL(SiC)	51	38	S,SiL	13	10
76	SiL	36	24	SiCL	10	36	vfS	69	8
77	SiL	46	20	SiCL	25	35	SiL,SiCL	36	24
78	SiCL	36	32	SiCL	13	38	SiL,vfS	66	12
79	SiCL	36	32	SiC	18	40	SiL,vfS	33	12
80	CL	51	30	SiC	20	40	SiCL	18	36
81	CL	46	32	SiC	25	40	SiCL	10	35

Horizon	C3			C4			C5		
Site ID	texture	cm	%clay	texture	cm	%clay	texture	cm	%clay
62	S	48	2	-	-	-	-	-	-
63	fS	46	2	-	-	-	-	-	-
64	S	41	2	-	-	-	-	-	-
65	S	30	2	-	-	-	-	-	-
66	-	-	-	-	-	-	-	-	-
67	S	25	2	-	-	-	-	-	-
68	S	30	2	-	-	-	-	-	-
69	-	-	-	-	-	-	-	-	-
70	fS	53	5	-	-	-	-	-	-
71	SiL	48	16	S	13	2	-	-	-
72	fS	53	5	-	-	-	-	-	-
73	S	64	2	-	-	-	-	-	-
74	S	51	2	-	-	-	-	-	-
76	S	38	2	-	-	-	-	-	-
77	S	46	2	-	-	-	-	-	-
78	S	38	2	-	-	-	-	-	-
79	S,SiL	28	9	S	38	2	-	-	-
80	SiL,vfS,S	64	9	-	-	-	-	-	-
81	SiL,LvfS,vfS L	33	12	A	38	2	-	-	-

- horizon does not exist

Appendix A (cont.) - Soil Texture, Thickness, and % Clay

Horizon	AP			C1			C2		
Site ID	texture	cm	%clay	texture	cm	%clay	texture	cm	%clay
82	CL	43	32	SiC	28	40	SiCL	10	35
83	CL(SCL)	48	30	SiCL	43	40	SiL,SiCL,vfS	28	19
84	CL	53	32	SIC	38	40	S	61	2
85	CL(SCL)	51	28	SiC	38	40	SiL	18	15
86	SiCL	38	30	CL	15	30	SiC	36	40
87	SiCL	36	28	SiC	20	40	LvfS,vfS	46	8
88	SiCL	30	28	SiC	41	40	SiCL,SiL,vfS	25	18
89	CL	46	30	SiC	25	40	LfS	18	10
90	SCL	46	22	CL	18	35	C	33	45
91	SCL	46	20	C	18	45	C	13	45
92	SiL	46	20	C	36	45	fS	28	6
93	SiL	46	18	C	18	40	C	33	45
94	SiL	41	20	C	10	40	C	33	45
95	SCL	41	20	C	20	40	C	28	45
96	SiCL	38	30	C	10	40	C	28	45
97	SCL	38	30	C	51	45	fS	18	6
98	SiCL	41	30	C,SiC	56	45	SiL	25	16
99	SiCL	46	28	C	30	45	SiCL	30	28
100	SiCL	38	30	C	18	40	SiL	33	20

Horizon	C3			C4			C5		
Site ID	texture	cm	%clay	texture	cm	%clay	texture	cm	%clay
82	SiL	15	15	S,SiL	56	9	-	-	-
83	S	33	2	-	-	-	-	-	-
84	-	-	-	-	-	-	-	-	-
85	S	46	2	-	-	-	-	-	-
86	SiCL	18	30	S	46	2	-	-	-
87	fS,SiL	51	9	-	-	-	-	-	-
88	S	56	2	-	-	-	-	-	-
89	fS,SiCL	25	18	fS	38	2	-	-	-
90	LfS	25	10	fS	30	6	-	-	-
91	SiL	15	16	fSL	25	12	S	36	3
92	SiL	43	15	-	-	-	-	-	-
93	fS	28	6	fS	28	6	-	-	-
94	fS,SiL,LfS	69	10	-	-	-	-	-	-
95	LfS	25	9	fS	38	6	-	-	-
96	fS	33	6	fS	43	6	-	-	-
97	fS	46	6	-	-	-	-	-	-
98	fS	30	6	-	-	-	-	-	-
99	fS	46	6	-	-	-	-	-	-
100	fS	64	6	-	-	-	-	-	-

- horizon does not exist

Appendix A (cont.) - Soil Texture, Thickness, and % Clay

Horizon	AP			C1			C2		
Site ID	texture	cm	%clay	texture	cm	%clay	texture	cm	%clay
101	SiCL	38	28	SiC,SiCL	33	38	SiL,SiCL	56	19
102	SiL	38	22	vfS	23	9	SiL	53	16
103	SiL	38	15	vfS	18	5	SiL	56	22
104	SiL	38	16	fS	10	6	SiL	66	18
105	SiL	36	16	SiC	10	40	SiL	64	16
106	SiL	46	16	SiCL	43	34	SiL	43	13
107	SiCL	46	30	SiL,SiCL	30	35	SiCL	13	32
108	SiCL	46	28	SiCL	36	34	SiL	25	15
109	SiCL	46	28	SiCL	18	39	SiL	43	17
110	SiL	41	25	SiCL	23	30	SiC	33	40
111	SiL	41	25	SiC	20	45	fS	91	6
112	SCL	38	25	CL	13	35	SiC	43	40
113	CL	51	30	CL	15	35	SiC	30	40
114	SiL	51	20	fS	18	6	C	18	45
115	SiL	46	30	C	30	45	SiL	30	12
116	SiL	46	20	C	10	40	C	41	45
117	SiL	46	22	C	30	45	SiL	20	16
118	SiL	46	25	fS	25	8	C	36	45
119	SiL	51	20	fS,SiL	20	15	C	28	45

Horizon	C3			C4			C5		
Site ID	texture	cm	%clay	texture	cm	%clay	texture	cm	%clay
101	fS	25	2	-	-	-	-	-	-
102	fS,SiL	38	11	-	-	-	-	-	-
103	S	41	5	-	-	-	-	-	-
104	fS	38	6	-	-	-	-	-	-
105	fS	43	6	-	-	-	-	-	-
106	fS	20	6	-	-	-	-	-	-
107	fS	13	6	SiL	30	13	vfS	20	6
108	vfS	33	8	fS	13	5	-	-	-
109	S,fS,vfS	46	6	-	-	-	-	-	-
110	SiL	13	15	fS	43	6	-	-	-
111			6	-	-	-	-	-	-
112	LfS	58	10	-	-	-	-	-	-
113	fS	30	6	SiL	25	10	-	-	-
114	fS	36	6	vfS	23	6	S	8	3
115	vfS	20	6	fS	25	6	-	-	-
116	fS	56	8	-	-	-	-	-	-
117	fS	56	6	-	-	-	-	-	-
118	fS	20	6	S	25	3	-	-	-
119	vfS	28	6	S	25	6	-	-	-

- horizon does not exist

Appendix A (cont.) - Soil Texture, Thickness, and % Clay

Horizon	AP			C1			C2		
Site ID	texture	cm	%clay	texture	cm	%clay	texture	cm	%clay
120	SiL	46	18	SiCL	23	38	C	23	45
121	SiL	38	20	SiCL	25	32	C	33	45
122	SiL	46	22	SiCL	20	35	C	30	45
123	SCL	41	20	SiCL	10	35	C	43	45
124	SCL	41	20	SiCL	10	35	C	30	45
125	SCL	38	20	C	33	45	vfS,SIL	43	12
126	SiL	41	18	C	28	45	vfS	23	8
127	SiL	41	16	SiC	30	40	SiL	43	25
128	SiL	41	20	SiCL	15	35	SiC	38	40
129	fS	41	6	fS	36	6	SiL	25	20
130	SiL	41	15	SiL	61	20	S	51	3
131	SiL	41	15	fS	15	6	SiL	46	22
132	SiL	41	15	fS	36	6	LvfS	25	13
133	SiL	46	15	fS	25	6	SiL,LvfS	36	15
134	fS	15	6	SiL	23	20	fS	13	6
135	SiL	36	18	SiCL	53	39	fS	64	6
136	SiL	41	18	SiC	58	40	fS	53	6
137	SiC	46	18	C	43	40	SiL	18	20
138	SiL	36	22	C	25	40	fS	30	6

Horizon	C3			C4			C5		
Site ID	texture	cm	%clay	texture	cm	%clay	texture	cm	%clay
120	SiL,vfS	23	14	fS	38	6	-	-	-
121	SiL	25	15	fS	30	6	-	-	-
122	SiL,fS	56	12	-	-	-	-	-	-
123	SiL	13	15	fS	46	6	-	-	-
124	vfS	41	6	fS	30	6	-	-	-
125	fS	38	6	-	-	-	-	-	-
126	vfS,SiL	36	12	fS	25	6	-	-	-
127	fS	38	6	-	-	-	-	-	-
128	fS	58	6	-	-	-	-	-	-
129	fS	51	3	-	-	-	-	-	-
130	-	-	-	-	-	-	-	-	-
131	fS	51	6	-	-	-	-	-	-
132	fS	51	6	-	-	-	-	-	-
133	S	46	6	-	-	-	-	-	-
134	SiL	38	15	fS	64	6	-	-	-
135	-	-	-	-	-	-	-	-	-
136	-	-	-	-	-	-	-	-	-
137	fS,SiL	46	15	-	-	-	-	-	-
138	SiL	23	18	fS	38	1	-	-	-

- horizon does not exist

Appendix A (cont.) - Soil Texture, Thickness, and % Clay

Horizon	AP			C1			C2		
Site ID	texture	cm	%clay	texture	cm	%clay	texture	cm	%clay
139	SiCL	46	28	C	43	40	SiL	38	16
140	SiCL	41	28	C	15	40	C	33	45
141	SiC	41	18	C	30	40	C	33	45
142	SCL	41	20	SiC	61	40	SiL	30	20
143	fSL	41	19	fS	13	6	C	36	40
144	fSL	41	40	fS	23	6	C	36	40
145	SiL	51	18	SiCL	13	39	C	46	45
146	fS	41	6	fS	30	6	SiL	15	15
147	SiL	46	18	fS,SiL	30	15	fS	38	6
148	SiL	46	18	SiL	51	16	fS	56	6
149	SiL	41	18	SiCL	28	32	vfS	58	8
150	LfS	41	18	fS	41	6	SiL	46	20
151	CL	46	32	SiC	13	40	SiL	79	18
152	SCL	41	20	C	10	40	SiL	51	16
153	SiCL	46	30	C	46	40	SiL	41	16
154	SCL	41	28	SCL	10	28	C	25	45
155	SiCL	46	30	C	25	40	SiL	36	15
156	CL	41	30	SiCL	15	30	C	25	45
157	SCL	51	20	SiL	13	20	C	36	40

Horizon	C3			C4			C5		
Site ID	texture	cm	%clay	texture	cm	%clay	texture	cm	%clay
139	S	25	6	-	-	-	-	-	-
140	SiL	33	14	fS	30	6	-	-	-
141	SiL,fS	48	16	-	-	-	-	-	-
142	fS	20	6	-	-	-	-	-	-
143	SiL	25	15	fS	38	6	-	-	-
144	SiL	23	16	fS	30	6	-	-	-
145	fS	43	6	-	-	-	-	-	-
146	S	66	3	-	-	-	-	-	-
147	S	38	3	-	-	-	-	-	-
148	-	-	-	-	-	-	-	-	-
149	fS	25	6	-	-	-	-	-	-
150	fS	25	3	-	-	-	-	-	-
151	fS	15	6	-	-	-	-	-	-
152	LvfS	51	12	-	-	-	-	-	-
153	fS	20	6	-	-	-	-	-	-
154	fS	25	6	fS,SiL	51	10	-	-	-
155	LvfS,SiCL	46	10	-	-	-	-	-	-
156	SiL	33	18	fS	38	6	-	-	-
157	SiL	53	12	-	-	-	-	-	-

- horizon does not exist

Appendix A (cont.) - Soil Texture, Thickness, and % Clay

Horizon	AP			C1			C2		
Site ID	texture	cm	%clay	texture	cm	%clay	texture	cm	%clay
158	SCL	41	20	C	58	45	fS	53	6
159	SiL	48	20	C	46	45	vfS	20	10
160	SCL	51	20	C	30	40	SiL	20	20
161	SCL	51	22	C	43	45	SiL	20	16
162	SCL	41	20	SiCL	10	30	C	38	45
163	SCL	51	20	C	13	40	SiL	33	15
164	SiL	30	25	C	33	40	fS	38	6
165	SiL	46	22	C	25	40	SiL	56	20
166	SiL	46	20	C	25	40	SiL	51	16
167	SCL	41	23	C	10	40	fS	38	6
168	SiL	38	20	C	13	40	SiL,LfS	43	12
169	fS	46	6	fS,SiL	30	10	SiL,fS	20	18
170	SiL	46	15	SiL,LS	30	15	LS,SiL	25	10
171	SiL	41	15	SiL	41	15	fS,S	71	5
172	LfS	41	10	LfS	10	10	SiL	56	15
173	LfS	46	10	LfS	30	10	SiL	20	15
174	LfS	38	10	fS	25	6	SiL	30	15
175	LfS	43	12	fS	64	6	S	46	3
176	LvfS	43	15	vfS	33	10	SiL	25	15

Horizon	C3			C4			C5		
Site ID	texture	cm	%clay	texture	cm	%clay	texture	cm	%clay
158	-	-	-	-	-	-	-	-	-
159	fS	38	6	-	-	-	-	-	-
160	fS	51	6	-	-	-	-	-	-
161	fS	38	6	-	-	-	-	-	-
162	SIL	13	12	fS	51	6	-	-	-
163	fS	56	6	-	-	-	-	-	-
164	S	51	3	-	-	-	-	-	-
165	fS	25	6	-	-	-	-	-	-
166	fS	30	6	-	-	-	-	-	-
167	SiL,LfS	13	12	fS	51	6	-	-	-
168	fS,vfS	58	8	-	-	-	-	-	-
169	fS	56	6	-	-	-	-	-	-
170	S	51	3	-	-	-	-	-	-
171	-	-	-	-	-	-	-	-	-
172	S	46	3	-	-	-	-	-	-
173	S	56	3	-	-	-	-	-	-
174	vfS	33	5	S	25	3	-	-	-
175	-	-	-	-	-	-	-	-	-
176	S	51	3	-	-	-	-	-	-

- horizon does not exist

Appendix A (cont.) - Soil Texture, Thickness, and % Clay

Horizon	AP			C1			C2		
Site ID	texture	cm	%clay	texture	cm	%clay	texture	cm	%clay
177	vfSL	43	15	vfS	15	8	SiL	18	15
178	SiL	41	18	SiL,vfSL	30	15	SiCL	18	38
179	SiL	36	18	SiC	15	40	fS	25	8
180	vfSL	41	15	fS	23	6	SiL,vfS	64	15
181	SCL	43	20	C	18	40	vfS,SiL	30	10
182	SCL	41	20	C	10	40	SiL	46	18
183	SiL	41	23	C	23	40	SiL	43	23
184	SiL	46	20	SiC	15	40	SiCL	36	28
185	SiL	46	22	SiCL	10	36	SiL,fS,vfS	33	15
186	SCL	51	22	SiCL	43	30	vfS	33	6
187	SCL	41	20	SiCL	10	32	C	38	45
188	SCL	38	22	SiL	30	25	C	20	40
189	SCL	43	32	CL	13	32	C	20	40
190	SCL	38	20	LfS	10	6	SiC	15	40
191	SCL	41	20	C	13	40	SiL,LvfS,vfS	69	15
192	SCL	41	22	LvfS,SiL	30	14	SiC	28	40
193	SCL	41	22	LfS	23	12	SiL	33	22
194	SCL	46	20	C	10	40	fS	25	8
195	SCL	38	23	SCL	10	30	C	15	40

Horizon	C3			C4			C5		
Site ID	texture	cm	%clay	texture	cm	%clay	texture	cm	%clay
177	vfS	25	8	S	51	3	-	-	-
178	S	64	3	-	-	-	-	-	-
179	SiL	30	15	fS	46	8	-	-	-
180	fS	25	3	-	-	-	-	-	-
181	S	61	3	-	-	-	-	-	-
182	S	56	3	-	-	-	-	-	-
183	S	46	3	-	-	-	-	-	-
184	fS	56	6	-	-	-	-	-	-
185	S	64	3	-	-	-	-	-	-
186	S	25	3	-	-	-	-	-	-
187	SiL,LvfS	10	15	S	53	3	-	-	-
188	SiL,fS,vfS	64	15	-	-	-	-	-	-
189	SiL,LvfS,vfSL	56	12	S	20	3	-	-	-
190	SiL	25	16	fS	38	8	S	25	3
191	S	30	3	-	-	-	-	-	-
192	fS	53	3	-	-	-	-	-	-
193	S	56	3	-	-	-	-	-	-
194	SiL	18	20	fS	53	6	-	-	-
195	S,fS	38	6	vfS,SiL	30	6	S	20	3

- horizon does not exist

Appendix A (cont.) - Soil Texture, Thickness, and % Clay

Horizon	AP			C1			C2		
Site ID	texture	cm	%clay	texture	cm	%clay	texture	cm	%clay
196	SCL	46	20	C	10	40	vfS	15	6
197	SiL	46	16	SiL	36	22	fS,S	71	3
198	vfSL	30	15	vfS	25	6	SiL	25	25
199	fSL	46	14	vfSL	23	15	SiL	36	18
200	fSL	46	15	LfS	25	10	LvfS,fSL,SiL	30	15
201	fSL	36	15	CL	10	38	S,fS	107	5

Horizon	C3			C4			C5		
Site ID	texture	cm	%clay	texture	cm	%clay	texture	cm	%clay
196	SiCL	25	30	S	56	3	-	-	-
197	-	-	-	-	-	-	-	-	-
198	S	33	3	fS	38	6	-	-	-
199	S	48	3	-	-	-	-	-	-
200	S	51	3	-	-	-	-	-	-
201	-	-	-	-	-	-	-	-	-

- horizon does not exist

Survey of sites 1-89 was conducted April 8-10, 1992

Survey of sites 90-201 was conducted July 13-16, 1992

No data was provided for sites 15, 30, 45, 60, or 75

Appendix B - Precipitation Data

Date (1995)	North Gauge (mm)	East Gauge (mm)	Average (mm)
22-Jan	4.4	-----	4.4
27-Jan	6.0	-----	6.0
29-Jan	0.9	-----	0.9
16-Feb	2.6	-----	2.6
3-Mar	11.5	-----	11.5
10-Apr	4.7	-----	4.7
19-Apr	3.2	3.5	3.4
22-Apr	4.2	4.1	4.2
30-May	4.8	5.0	4.9
16-Jun	4.0	4.0	4.0
19-Jun	2.2	2.1	2.2
2-Jul	2.2	2.1	2.2
16-Jul	4.0	4.0	4.0
17-Jul	0.5	0.5	0.5
19-Jul	5.8	6.0	5.9
1-Aug	0.8	0.6	0.7
15-Aug	0.8	0.7	0.8
19-Aug	6.0	5.7	5.9
1-Sep	15.0	13.0	14.0
12-Sep	3.0	2.8	2.9
20-Sep	15.0	15.0	15.0
24-Sep	1.8	1.8	1.8
1-Nov	0.6	0.6	0.6
		TOTAL	102.8

Appendix C1 - Evapotranspiration Calculation Methods

ASC Method

The method utilized by the Agricultural Science Center (ASC), Los Lunas, New Mexico, for is the modified Penman equation calcualtion of potential evapotranspiration from the surface of well watered short grass:

$$ET_o = \frac{\Delta R_n + \gamma E_a}{\Delta + \gamma}$$

where

$$\Delta = 33.8639\left(0.05904\left(0.00739T_{ave} + 0.8072\right)^7 - 0.0000342\right)$$

$$\gamma = \frac{C_p p}{0.622L}$$

$$R_n = 0.95(1-\alpha)R_s + R_l$$

$$E_a = 15.36\left(1.0 + 0.0062u_2\right)\left(e_s - e_a\right)$$

symbols:

ET_o = potential evapotranspiration (cm/day)
E_a = aerodynamic component related to wind spead and humidity
Δ = slope of the saturation vapor pressure vs. temperature curve at the air temperature (mb/°C)
T_{ave} = average daily temperature ($_o$C)
γ = psychrometric constant (mb/°C)
R_n = net solar radiation (ly/day)
R_s = short-wave radiation (ly/day)
R_l = long-wave radiation (=-64 ly/day)
α = albedo (reflection coefficient = 0.21)
C_p = specific heat of air (= 0.242 cal/g-°C)
p = atmospheric pressure (mb)
L = latent heat of vaporization (cal/g)
u_2 = average daily wind velocity at height of 2 meters (km/day)
e_s = saturation vapor pressure at mean air temperature (mb)
e_a = actual vapor pressure at mean air temperature (mb)

Saturation vapor pressure at mean air temperature is determined as the average of saturation vapor pressures at the minimum and maximum daily temperatures.

$$e_s = \frac{6.108\left(10^{p\min} + 10^{p\max}\right)}{2} \quad \text{where}$$

$$p\min(mb) = \frac{7.5T_{\min}}{T_{\min} + 237.3}, \; T_{\min} = \text{minimum daily temperature (°C)}$$

$$p\max(mb) = \frac{7.5T_{\max}}{T_{\max} + 237.3}, \; T_{\max} = \text{maximum daily temperature (°C)}$$

Appendix C1 (cont.) - Evapotranspiration Calculation Methods

Actual vapor pressure at mean air temperature is determined in a similar fashion. This assumes that maximum and minimum relative humidity values occur at the same times respectively with the minimum and maximum air temperature:

$$e_a = \frac{6.108\left(\left(\frac{rh_{\max}}{100}\right) \times 10^{p\min} + \left(\frac{rh_{\min}}{100}\right) \times 10^{p\max}\right)}{2}$$

Atmospheric pressure is determined by elevation in meters above mean sea level:

$$p = 1013.0 - 0.0155(elevation) = 1013.0 - 0.1055(1480) = 857mb$$

Correction for wind velocity u_h measured at a height h = 3.74 meters above ground surface:

$$u_2 = \left(\frac{2.00}{h}\right)^{0.2} u_h = \left(\frac{2.00}{3.74}\right)^{0.2} u_h = 0.882u_h$$

FAO Method

The Food and Agriculture Organization (FAO) of the United Nations method also utilizes the modified Penman equation (Doorenbos and Pruitt, 1977) rearranged as:

$$ET_o = WR_n + (1-W)f(u)(e_s - e_a)$$

where:

W = temperature-related weighting factor
R_n = net radiation in equivalent evaporation (mm/day)
$f(u)$ = wind-related function
e_s, e_a = as above (mb)

Values for these factors and functions are obtained from published tables, but are essentially identical to those obtained in the ASC method with three differences:

(1) e_s and e_a are determined using the average of the daily high and low temperatures and the average of the daily high and low relative humidity values (rather than the averages obtained from the 24 daily measurements as is used in the ASC method).

(2) R_l, the net long-wave radiation, is calculated as a function of temperature, e_a, and the percent cloudiness (rather than the constant value used in the ASC method).

(3) The albedo, α, is set to 0.25 (rather than 0.21 used in the ASC method)

Appendix C2 - Selected Climatological Data and Daily ET_o

	T_{ave}	RH_{ave}	u_2	R_n	ET_o
Date	(°C)	(%)	(km/d)	(ly)	(cm)
1/1/95	-1	26	34	263	0.18
1/2/95	1	20	34	158	0.11
1/3/95	1	38	34	265	0.19
1/4/95	1	82	34	60	-0.01
1/5/95	3	54	68	122	0.06
1/6/95	4	41	106	294	0.22
1/7/95	2	36	34	282	0.20
1/8/95	5	40	44	310	0.25
1/9/95	3	38	34	313	0.25
1/10/95	2	33	34	246	0.19
1/11/95	4	22	34	239	0.20
1/12/95	6	42	51	215	0.16
1/13/95	3	36	41	322	0.25
1/14/95	4	28	34	327	0.28
1/15/95	3	47	34	162	0.11
1/16/95	4	26	136	294	0.24
1/17/95	0	31	37	291	0.20
1/18/95	-2	19	41	344	0.24
1/19/95	-1	22	37	339	0.26
1/20/95	1	23	34	263	0.20
1/21/95	5	42	34	236	0.17
1/22/95	2	39	41	212	0.14
1/23/95	-1	39	34	248	0.16
1/24/95	2	30	34	246	0.19
1/25/95	4	30	44	220	0.18
1/26/95	6	38	44	212	0.16
1/27/95	5	37	89	227	0.18
1/28/95	1	24	37	368	0.28
1/29/95	-1	39	37	253	0.17
1/30/95	0	21	37	384	0.29
1/31/95	3	16	34	377	0.33

	T_{ave}	RH_{ave}	u_2	R_n	ET_o
Date	(°C)	(%)	(km/d)	(ly)	(cm)
2/1/95	7	19	37	370	0.35
2/2/95	8	16	37	387	0.37
2/3/95	7	14	37	396	0.38
2/4/95	4	15	34	401	0.37
2/5/95	5	14	34	406	0.38
2/6/95	6	14	34	411	0.40
2/7/95	6	16	34	411	0.38
2/8/95	5	22	51	380	0.33
2/9/95	7	15	58	391	0.37
2/10/95	6	17	55	418	0.37
2/11/95	7	22	68	322	0.28
2/12/95	8	15	58	430	0.40
2/13/95	7	33	41	263	0.22
2/14/95	11	25	129	270	0.27
2/15/95	10	47	37	229	0.18
2/16/95	7	16	44	454	0.41
2/17/95	5	16	34	413	0.37
2/18/95	7	14	44	458	0.43
2/19/95	8	15	37	454	0.42
2/20/95	8	13	34	461	0.46
2/21/95	11	14	51	377	0.38
2/22/95	10	16	34	444	0.43
2/23/95	11	17	37	384	0.38
2/24/95	12	20	34	434	0.41
2/25/95	9	45	37	258	0.21
2/26/95	8	35	37	344	0.29
2/27/95	9	17	37	487	0.45
2/28/95	8	31	41	360	0.32

Appendix C2 (cont.) - Selected Climatological Data and Daily ET_o

Date	T_{ave} (°C)	RH_{ave} (%)	u_2 (km/d)	R_n (ly)	ET_o (cm)
3/1/95	7	69	82	201	0.13
3/2/95	6	54	61	408	0.32
3/3/95	12	18	44	394	0.37
3/4/95	11	22	78	308	0.31
3/5/95	12	30	68	253	0.25
3/6/95	9	21	68	210	0.18
3/7/95	4	18	34	537	0.44
3/8/95	5	16	37	530	0.45
3/9/95	7	14	37	523	0.48
3/10/95	9	13	34	551	0.55
3/11/95	12	15	106	387	0.43
3/12/95	10	17	68	482	0.46
3/13/95	10	14	37	556	0.53
3/14/95	12	13	37	568	0.57
3/15/95	12	13	34	570	0.57
3/16/95	12	13	34	523	0.53
3/17/95	12	15	65	444	0.47
3/18/95	12	15	37	575	0.56
3/19/95	14	14	75	518	0.55
3/20/95	16	13	44	556	0.58
3/21/95	17	11	102	513	0.59
3/22/95	14	13	55	602	0.62
3/23/95	12	13	95	485	0.53
3/24/95	14	14	75	518	0.54
3/25/95	7	17	72	408	0.37
3/26/95	6	16	37	616	0.53
3/27/95	8	14	41	623	0.59
3/28/95	8	22	48	384	0.34
3/29/95	6	16	44	573	0.50
3/30/95	7	20	44	568	0.49
3/31/95	7	15	37	637	0.57

Date	T_{ave} (°C)	RH_{ave} (%)	u_2 (km/d)	R_n (ly)	ET_o (cm)
4/1/95	8	14	34	642	0.61
4/2/95	7	29	58	270	0.24
4/3/95	8	21	44	518	0.48
4/4/95	11	13	37	635	0.61
4/5/95	14	11	41	623	0.65
4/6/95	16	11	34	630	0.67
4/7/95	16	12	51	633	0.68
4/8/95	16	12	65	623	0.68
4/9/95	11	13	99	530	0.57
4/10/95	4	36	44	384	0.29
4/11/95	7	15	41	659	0.59
4/12/95	11	12	34	687	0.69
4/13/95	15	11	72	637	0.70
4/14/95	16	12	112	625	0.71
4/15/95	14	13	82	413	0.46
4/16/95	14	13	99	542	0.60
4/17/95	8	17	129	454	0.44
4/18/95	11	14	51	702	0.67
4/19/95	7	31	55	337	0.27
4/20/95	9	20	51	434	0.39
4/21/95	9	25	58	575	0.52
4/22/95	7	36	37	508	0.41
4/23/95	9	21	37	695	0.63
4/24/95	11	14	44	738	0.69
4/25/95	14	11	41	742	0.77
4/26/95	17	11	44	726	0.79
4/27/95	15	11	37	585	0.63
4/28/95	18	12	58	470	0.52
4/29/95	21	10	55	735	0.84
4/30/95	20	12	89	621	0.71

Appendix C2 (cont.) - Selected Climatological Data and Daily ET_o

	T_{ave}	RH_{ave}	u_2	R_n	ET_o
Date	(°C)	(%)	(km/d)	(ly)	(cm)
5/1/95	19	12	41	599	0.65
5/2/95	19	11	102	578	0.65
5/3/95	16	12	41	721	0.75
5/4/95	18	11	51	738	0.80
5/5/95	19	11	119	430	0.53
5/6/95	16	13	78	623	0.66
5/7/95	11	17	102	602	0.56
5/8/95	13	15	95	733	0.74
5/9/95	16	12	44	769	0.80
5/10/95	17	11	41	623	0.67
5/11/95	19	11	41	702	0.75
5/12/95	19	11	129	597	0.71
5/13/95	20	11	68	721	0.81
5/14/95	19	11	41	707	0.77
5/15/95	22	10	58	668	0.77
5/16/95	20	10	89	668	0.78
5/17/95	13	24	102	427	0.44
5/18/95	17	12	34	704	0.75
5/19/95	19	10	34	687	0.75
5/20/95	22	10	55	771	0.87
5/21/95	22	9	37	757	0.86
5/22/95	23	9	95	759	0.90
5/23/95	21	11	58	678	0.76
5/24/95	19	11	44	721	0.79
5/25/95	21	10	92	747	0.86
5/26/95	18	11	95	742	0.81
5/27/95	18	12	65	728	0.79
5/28/95	18	14	61	611	0.66
5/29/95	15	39	48	346	0.33
5/30/95	16	15	55	721	0.74
5/31/95	18	10	37	769	0.83

	T_{ave}	RH_{ave}	u_2	R_n	ET_o
Date	(°C)	(%)	(km/d)	(ly)	(cm)
6/1/95	21	10	34	702	0.78
6/2/95	23	10	68	642	0.74
6/3/95	20	11	51	659	0.74
6/4/95	22	10	44	683	0.76
6/5/95	23	9	48	792	0.90
6/6/95	23	9	48	788	0.91
6/7/95	21	10	48	702	0.79
6/8/95	22	10	102	802	0.93
6/9/95	19	10	34	814	0.90
6/10/95	21	10	44	809	0.91
6/11/95	21	10	37	802	0.90
6/12/95	23	8	34	802	0.95
6/13/95	26	7	37	769	0.93
6/14/95	26	7	55	750	0.92
6/15/95	26	8	44	618	0.75
6/16/95	24	9	78	613	0.74
6/17/95	24	10	106	687	0.82
6/18/95	23	10	37	738	0.84
6/19/95	26	9	58	733	0.85
6/20/95	26	8	37	773	0.90
6/21/95	25	9	37	716	0.83
6/22/95	24	8	34	795	0.92
6/23/95	25	8	34	814	0.95
6/24/95	26	9	37	726	0.85
6/25/95	23	12	44	647	0.75
6/26/95	21	12	51	532	0.60
6/27/95	23	9	44	616	0.72
6/28/95	22	9	65	542	0.65
6/29/95	22	10	51	676	0.78
6/30/95	19	41	37	449	0.44

Appendix C2 (cont.) - Selected Climatological Data and Daily ET_o

Date	T_{ave} (°C)	RH_{ave} (%)	u_2 (km/d)	R_n (ly)	ET_o (cm)
7/1/95	23	9	72	699	0.81
7/2/95	23	10	68	573	0.67
7/3/95	24	10	112	800	0.96
7/4/95	23	10	61	735	0.84
7/5/95	22	8	37	812	0.93
7/6/95	26	7	34	809	0.97
7/7/95	28	7	34	778	0.93
7/8/95	27	7	37	788	0.95
7/9/95	27	7	37	776	0.93
7/10/95	28	7	37	792	0.96
7/11/95	28	7	41	792	0.95
7/12/95	27	8	37	795	0.94
7/13/95	28	8	41	697	0.84
7/14/95	24	15	37	425	0.49
7/15/95	23	11	37	389	0.47
7/16/95	24	15	48	702	0.81
7/17/95	23	25	37	570	0.62
7/18/95	24	19	44	599	0.67
7/19/95	24	12	37	637	0.72
7/20/95	26	8	37	750	0.87
7/21/95	26	9	41	673	0.80
7/22/95	27	7	48	685	0.82
7/23/95	26	8	41	797	0.94
7/24/95	24	7	37	788	0.94
7/25/95	26	6	34	788	0.95
7/26/95	27	6	34	788	0.98
7/27/95	27	6	37	781	0.96
7/28/95	28	5	34	764	0.96
7/29/95	29	6	34	754	0.93
7/30/95	30	6	44	726	0.91
7/31/95	27	7	51	687	0.85

Date	T_{ave} (°C)	RH_{ave} (%)	u_2 (km/d)	R_n (ly)	ET_o (cm)
8/1/95	26	9	37	714	0.84
8/2/95	27	7	37	738	0.88
8/3/95	27	8	41	730	0.88
8/4/95	28	7	41	702	0.86
8/5/95	29	6	44	695	0.87
8/6/95	29	6	37	704	0.87
8/7/95	28	7	37	723	0.88
8/8/95	28	7	51	709	0.87
8/9/95	28	8	51	587	0.72
8/10/95	29	7	51	704	0.89
8/11/95	27	7	58	611	0.76
8/12/95	28	8	41	702	0.84
8/13/95	27	12	55	559	0.68
8/14/95	23	27	27	196	0.22
8/15/95	24	26	44	621	0.69
8/16/95	24	28	48	496	0.56
8/17/95	24	29	37	554	0.60
8/18/95	24	30	48	602	0.67
8/19/95	23	22	55	508	0.57
8/20/95	23	34	37	499	0.53
8/21/95	24	24	37	661	0.73
8/22/95	24	25	48	611	0.69
8/23/95	22	27	44	549	0.61
8/24/95	23	25	44	649	0.72
8/25/95	23	29	37	547	0.60
8/26/95	24	28	34	623	0.68
8/27/95	22	31	37	568	0.61
8/28/95	24	28	48	594	0.65
8/29/95	25	21	34	613	0.69
8/30/95	25	19	37	575	0.65
8/31/95	24	25	34	621	0.69

Appendix C2 (cont.) - Selected Climatological Data and Daily ET_o

Date	T_{ave} (°C)	RH_{ave} (%)	u_2 (km/d)	R_n (ly)	ET_o (cm)
9/1/95	26	14	34	637	0.74
9/2/95	24	15	34	659	0.75
9/3/95	24	18	34	644	0.74
9/4/95	24	16	34	647	0.75
9/5/95	24	13	34	642	0.76
9/6/95	24	15	61	590	0.72
9/7/95	22	27	48	422	0.47
9/8/95	21	30	48	544	0.58
9/9/95	19	42	37	520	0.51
9/10/95	21	29	34	501	0.53
9/11/95	21	22	34	604	0.65
9/12/95	21	14	34	628	0.69
9/13/95	19	22	41	513	0.56
9/14/95	21	21	37	537	0.59
9/15/95	17	52	37	143	0.10
9/16/95	19	34	34	437	0.44
9/17/95	20	30	34	518	0.54
9/18/95	20	29	41	523	0.55
9/19/95	19	22	34	575	0.61
9/20/95	21	13	55	580	0.65
9/21/95	16	33	58	456	0.46
9/22/95	10	49	37	351	0.29
9/23/95	16	23	37	480	0.49
9/24/95	19	16	58	444	0.49
9/25/95	17	20	37	561	0.58
9/26/95	18	19	37	468	0.51
9/27/95	19	17	48	513	0.57
9/28/95	16	54	48	191	0.15
9/29/95	18	22	72	456	0.48
9/30/95	14	22	37	561	0.55

Date	T_{ave} (°C)	RH_{ave} (%)	u_2 (km/d)	R_n (ly)	ET_o (cm)
10/1/95	15	24	34	523	0.53
10/2/95	15	12	37	549	0.57
10/3/95	14	15	34	547	0.57
10/4/95	14	12	150	537	0.64
10/5/95	10	13	61	539	0.53
10/6/95	9	15	37	530	0.52
10/7/95	15	16	41	496	0.55
10/8/95	14	12	44	523	0.56
10/9/95	14	12	48	516	0.56
10/10/95	13	12	37	513	0.55
10/11/95	14	11	34	508	0.56
10/12/95	16	16	58	496	0.54
10/13/95	16	8	55	504	0.56
10/14/95	12	11	48	499	0.54
10/15/95	13	12	34	494	0.53
10/16/95	15	15	48	415	0.46
10/17/95	13	15	37	437	0.47
10/18/95	15	13	41	458	0.50
10/19/95	14	10	48	465	0.52
10/20/95	11	18	41	458	0.47
10/21/95	13	10	44	454	0.50
10/22/95	13	14	167	422	0.53
10/23/95	6	14	55	451	0.41
10/24/95	9	18	48	396	0.40
10/25/95	9	14	37	413	0.41
10/26/95	12	10	85	432	0.50
10/27/95	14	11	65	427	0.48
10/28/95	12	14	41	391	0.43
10/29/95	12	17	37	289	0.31
10/30/95	12	15	41	375	0.41
10/31/95	13	27	58	282	0.29

Appendix C2 (cont.) - Selected Climatological Data and Daily ET_o

Date	T_{ave} (°C)	RH_{ave} (%)	u_2 (km/d)	R_n (ly)	ET_o (cm)
11/1/95	14	29	99	212	0.21
11/2/95	12	29	65	234	0.21
11/3/95	7	15	61	406	0.39
11/4/95	8	31	58	322	0.28
11/5/95	8	41	55	241	0.19
11/6/95	9	59	58	98	0.05
11/7/95	9	25	48	380	0.36
11/8/95	9	21	44	389	0.38
11/9/95	11	15	102	298	0.35
11/10/95	11	25	249	308	0.39
11/11/95	5	17	85	380	0.36
11/12/95	7	15	41	375	0.39
11/13/95	10	17	0	248	0.23
11/14/95	9	26	55	358	0.35
11/15/95	10	23	58	356	0.35
11/16/95	8	25	44	353	0.34
11/17/95	9	19	44	351	0.35
11/18/95	7	18	41	351	0.35
11/19/95	7	16	51	349	0.36
11/20/95	8	16	51	332	0.33
11/21/95	7	32	48	325	0.30
11/22/95	7	0	41	325	0.34
11/23/95	7	0	48	322	0.34
11/24/95	6	0	41	322	0.34
11/25/95	6	0	41	317	0.34
11/26/95	11	0	191	308	0.41
11/27/95	4	0	106	308	0.38
11/28/95	1	0	44	308	0.34
11/29/95	6	0	58	308	0.35
11/30/95	6	0	51	308	0.35

Date	T_{ave} (°C)	RH_{ave} (%)	u_2 (km/d)	R_n (ly)	ET_o (cm)
12/1/95	6	17	61	325	0.35
12/2/95	7	13	92	310	0.35
12/3/95	7	18	51	315	0.31
12/4/95	8	17	72	282	0.31
12/5/95	7	23	44	234	0.23
12/6/95	8	21	61	241	0.25
12/7/95	6	44	82	93	0.05
12/8/95	6	24	75	310	0.28
12/9/95	2	24	51	308	0.27
12/10/95	3	-	-	-	-
12/11/95	3	20	44	310	0.24
12/12/95	5	14	58	253	0.27
12/13/95	9	12	75	279	0.32
12/14/95	6	22	85	263	0.26
12/15/95	4	33	58	246	0.19
12/16/95	3	36	44	146	0.10
12/17/95	4	52	78	117	0.06
12/18/95	2	49	48	158	0.09
12/19/95	-1	38	44	289	0.20
12/20/95	-1	44	48	215	0.14
12/21/95	0	40	82	260	0.18
12/22/95	-1	44	51	198	0.12
12/23/95	-2	33	82	277	0.19
12/24/95	-2	27	129	284	0.22
12/25/95	-4	26	44	291	0.20
12/26/95	-3	20	41	301	0.23
12/27/95	-3	22	44	301	0.22
12/28/95	-1	27	61	282	0.22
12/29/95	1	30	65	234	0.17
12/30/95	1	34	82	255	0.20
12/31/95	4	31	58	253	0.19

Appendix D1 - Instantaneous Profile Soil Physical Data

Bulk density (ρ_b), volumetric water content (θ_v), and neutron probe (NP) data used to generate the neutron probe calibration, presented in Appendix D2. Porosity values, *n*, assume a particle density of 2.65 g/cm^3.

IP Location #3				
depth (cm)	ρ_b (g/cm^3)	θ_v (%)	n (%)	NP (cnts)
13	1.30	34.2	51	
13	1.28	35.5	52	7149
13	1.31	35.5	50	
36	1.33	36.7	50	
36	1.37	39.3	50	8287
36	1.36	37.4	48	
53	1.21	38.7	49	
53	1.19	40.0	54	9395
53	1.21	41.0	55	
58	1.16	47.7	54	
58	1.13	48.6	56	9576
58	1.07	48.4	57	
71	1.13	54.9	59	
71	1.07	54.4	57	9317
71	1.11	54.3	60	
81	1.31	40.1	58	
81	1.21	38.9	51	9015
81	1.45	45.1	54	

IP Location #4				
depth (cm)	ρ_b (g/cm^3)	θ_v (%)	n (%)	Probe (counts)
13	1.53	35.5	42	
13	1.52	32.2	43	7035
13	1.64	36.6	38	
31	1.47	33.2	45	
31	1.54	36.9	42	7435
31	1.60	35.3	40	
46	1.71	33.3	35	
46	1.55	28.4	41	7271
46	1.52	30.2	43	
64	1.41	43.6	47	
64	1.19	42.7	55	8967
64	1.39	38.4	48	
74	1.16	46.0	56	
74	1.08	53.2	59	9367
74	1.10	50.5	58	

Near SE Corner of East Bench				
depth (cm)	ρ_b (g/cm^3)	θ (vol%)	n (%)	Probe (counts)
15	1.25	11.0	53	
15	1.29	11.3	51	2305
15	1.39	11.8	47	
30	1.29	17.7	51	
30	1.12	17.0	58	3917
30	1.12	16.4	58	
46	1.36	25.4	49	
46	1.35	24.5	49	5165
46	1.58	27.7	40	
61	1.21	35.2	54	
61	1.18	34.4	56	5871
61	1.23	33.9	54	

Appendix D2 - Neutron Probe Calibration Curve

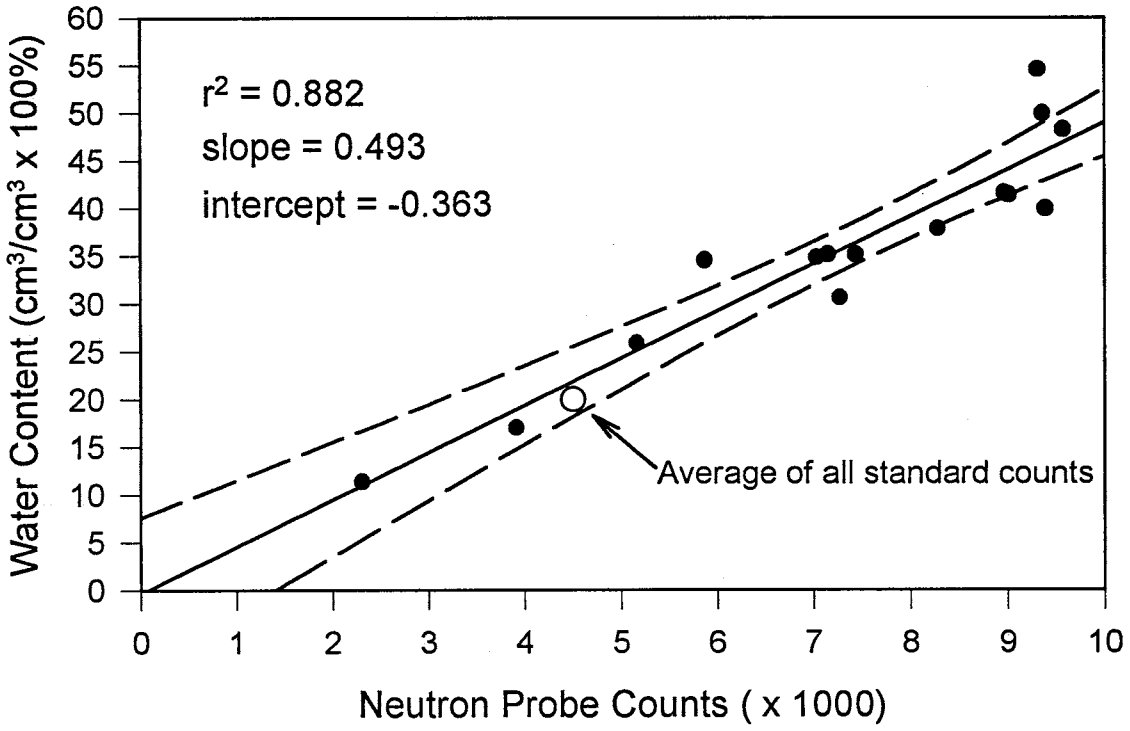

Notes: Solid points represent the 3-sample average water contents
Linear regression shown as solid line
95% confidence interval shown as dashed lines

Appendix D3 - Instantaneous Profile Experimental Data

IP Experimental Site #1

depth - texture	13cm-SiCL			20cm - SiCL			36cm - SiC		
tensiometer	a	b		a	b		a	b	
t (min)	h(cm)	h(cm)	θ_v	h(cm)	h(cm)	θ_v	h(cm)	h(cm)	θ_v
0	-17	-16	0.434	-23	-23	0.442	-36	-21	0.451
37	-17	-14	0.425	-21	-23	0.440	-32	-35	0.453
52	-12	-15	0.419	-19	-19	0.439	-29	-34	0.449
67	-15	-11	0.413	-19	-18	0.439	-28	-40	0.450
82	-12	-16	0.410	-18	-12	0.438	-26	-40	0.455
97	-13	-13	0.408	-15	-16	0.438	-26	-41	0.452
112	-8	-11	0.407	-14	-10	0.439	-25	-32	0.451
127	-7	-10	0.409	-14	-11	0.436	-24	-41	0.451
142	-10	-11	0.411	-13	-12	0.438	-23	-41	0.447
157	-8	-13	0.407	-13	-14	0.438	-23	-41	0.449
172	-5	-9	0.408	-12	-10	0.438	-22	-41	0.449
187	-6	-9	0.407	-13	-9	0.437	-20	-41	0.450
202	-4	-9	0.403	-10	-9	0.439	-23	-41	0.447
217	-3	-10	0.413	-9	-9	0.436	-22	-41	0.453
232	-5	-11	0.408	-10	-11	0.438	-22	-41	0.450
247	-4	-10	0.409	-9	-9	0.435	-20	-41	0.451
262	-4	-7	0.406	-10	-9	0.439	-21	-41	0.448
277	-6	-7	0.406	-8	-9	0.438	-21	-41	0.450
292	-8	-10	0.409	-9	-13	0.434	-21	-41	0.449
307	0	-4	0.406	-7	-6	0.437	-17	-36	0.449
322	2	-3	0.403	-6	-5	0.437	-13	-33	0.451
337	2	-3	0.405	-5	-6	0.433	-18	-26	0.455
352	-2	-6	0.403	-5	-8	0.436	-18	-30	0.452
367	1	-4	0.404	-4	-5	0.436	-16	-21	0.449
382	4	2	0.398	-2	-2	0.436	-15	-15	0.454
397	5	2	0.399	-2	-2	0.436	-13	-12	0.448
427	6	5	0.398	-1	-1	0.430	-12	-9	0.452
457	7	6	0.400	-1	-1	0.430	-11	-5	0.454
517	5	4	0.389	-1	-3	0.434	-13	-7	0.452
577	9	8	0.395	1	1	0.425	-12	4	0.449
637	8	7	0.393	0	-2	0.424	-12	2	0.450
817	10	10	0.392	2	1	0.424	-9	3	0.440
997	12	14	0.391	5	3	0.422	-7	5	0.439
1057	11	14	0.391	6	4	0.426	-7	5	0.436
1117	12	12	0.392	5	2	0.421	-6	-3	0.441
1177	8	11	0.390	5	0	0.422	-6	-10	0.436
1237	11	12	0.389	6	2	0.426	-5	-12	0.435
1297	6	8	0.391	5	-2	0.423	-5	-22	0.432
1357	5	5	0.386	8	-3	0.419	-1	-31	0.435

Note: Heads (h) are cm of tension.

Appendix D3 (cont.) - Instantaneous Profile Experimental Data

IP Experimental SIte #1 (continued)

depth - texture	13cm - SiCL			20cm - SiCL			36cm - SiC		
tensiometer	a	b		a	b		a	b	
t (min)	h(cm)	h(cm)	θ_v	h(cm)	h(cm)	θ_v	h(cm)	h(cm)	θ_v
1565	7	8	0.387	10	4	0.420	-1	-11	0.437
1813	16	18	0.382	12	7	0.421	-1	24	0.432
2020	16	13	0.384	11	5	0.424	-1	13	0.435
2257	18	17	0.384	12	7	0.421	-1	9	0.432
2445	21	19	0.383	12	10	0.418	0	8	0.432
2587	17	18	0.383	11	4	0.419	0	1	0.434
2737	23	23	0.385	15	12	0.419	2	6	0.433
3008	18	0	0.383	19	13	0.421	5	0	0.435
3147	15	10	0.385	16	12	0.422	3	17	0.433
4210	15	11	0.379	16	10	0.417	4	-28	0.433
4629	18	8	0.384	18	18	0.418	7	33	0.433
5250	27	6	0.383	23	20	0.414	7	11	0.434
6575	25	-3	0.374	20	10	0.415	10	-8	0.430
8135	21	28	0.376	19	15	0.418	8	-9	0.433
11065	10	14	0.385	23	15	0.414	8	-22	0.429
14165	-4	-7	0.383	26	15	0.415	15	-3	0.426
16630	18	5	0.380	22	21	0.417	17	10	0.424

Note: Heads (h) are cm of tension.

Appendix D3 (cont.) - Instantaneous Profile Experimental Data

IP Experimental Site #1 (continued)

depth - texture	43cm - SiC			64cm - LvfS			76cm - LvfS		
tensiometer	a	b		a	b		a	b	
t (min)	h(cm)	h(cm)	θ_v	h(cm)	h(cm)	θ_v	h(cm)	h(cm)	θ_v
0	-11	-14	0.440	21	15	0.433	12	10	0.423
37	-20	-23	0.440	16	9	0.437	7	8	0.420
52	-28	-27	0.441	13	8	0.438	6	11	0.426
67	-32	-33	0.441	10	5	0.436	4	11	0.421
82	-34	-36	0.441	10	6	0.437	7	12	0.424
97	-38	-39	0.441	10	5	0.428	6	11	0.421
112	-30	-32	0.442	17	13	0.432	14	14	0.426
127	-29	-31	0.444	19	14	0.437	14	13	0.424
142	-30	-31	0.445	18	14	0.435	13	13	0.423
157	-36	-37	0.437	13	9	0.435	8	10	0.424
172	-27	-31	0.440	20	15	0.434	15	13	0.423
187	-27	-28	0.442	21	16	0.433	14	14	0.424
202	-26	-28	0.441	22	16	0.434	15	14	0.424
217	-26	-28	0.443	21	7	0.433	5	15	0.425
232	-31	-33	0.440	18	11	0.437	9	8	0.425
247	-31	-33	0.439	18	12	0.435	9	12	0.420
262	-30	-31	0.441	19	14	0.437	11	13	0.422
277	-31	-32	0.442	18	14	0.437	10	13	0.422
292	-41	-40	0.438	12	7	0.434	4	7	0.421
307	-30	-30	0.439	22	17	0.435	15	16	0.422
322	-27	-28	0.443	24	17	0.437	16	15	0.425
337	-26	-25	0.442	25	20	0.438	15	15	0.421
352	-33	-32	0.441	19	14	0.439	11	11	0.423
367	-23	-24	0.443	26	20	0.435	17	17	0.427
382	-20	-18	0.438	28	21	0.438	19	17	0.424
397	-18	-16	0.439	29	23	0.436	18	17	0.424
427	-14	-11	0.440	30	25	0.435	18	18	0.427
457	-13	-9	0.440	31	26	0.437	19	18	0.419
517	-12	-9	0.439	30	23	0.433	17	15	0.426
577	-1	2	0.439	34	29	0.436	20	19	0.427
637	1	2	0.439	30	25	0.436	17	16	0.425
817	5	6	0.431	31	26	0.435	18	18	0.425
997	9	13	0.421	30	28	0.426	17	17	0.426
1057	9	11	0.418	30	27	0.420	17	18	0.420
1117	1	5	0.417	26	24	0.406	15	16	0.421
1177	-8	-1	0.419	23	23	0.404	14	17	0.415
1237	-12	-4	0.421	23	23	0.397	13	17	0.412
1297	-26	-18	0.418	17	16	0.397	9	14	0.411
1357	-41	-24	0.412	18	16	0.397	8	12	0.409

Note: Heads (h) are cm of tension.

Appendix D3 (cont.) - Instantaneous Profile Experimental Data

IP Experimental Site #1 (continued)

depth - texture	43cm - SiC			64cm - LvfS			76cm - LvfS		
tensiometer	a	b		a	b		a	b	
t (min)	h(cm)	h(cm)	θ_v	h(cm)	h(cm)	θ_v	h(cm)	h(cm)	θ_v
1565	-39	-15	0.420	30	30	0.395	21	23	0.409
1813	5	24	0.418	42	44	0.396	26	28	0.410
2020	15	30	0.409	32	31	0.396	19	22	0.413
2257	19	29	0.408	33	33	0.395	19	24	0.409
2445	23	31	0.407	34	35	0.393	20	41	0.403
2587	18	25	0.406	29	28	0.396	13	19	0.406
2737	16	26	0.409	34	37	0.397	21	27	0.414
3008	3	12	0.406	36	36	0.392	28	31	0.413
3147	13	24	0.407	40	35	0.392	26	25	0.411
4210	-21	-9	0.412	24	28	0.397	13	24	0.411
4629	7	25	0.408	45	44	0.393	30	33	0.410
5250	30	33	0.412	41	40	0.398	30	32	0.409
6575	-20	13	0.407	28	27	0.393	19	26	0.413
8135	1	14	0.405	27	28	0.393	17	22	0.408
11065	-6	2	0.406	27	29	0.394	16	26	0.409
14165	-35	-17	0.404	28	25	0.392	19	25	0.407
16630	44	44	0.405	13	12	0.396	1	13	0.412

Note: Heads (h) are cm of tension.

Appendix D3 (cont.) - Instantaneous Profile Experimental Data

IP Experimental SIte #2

depth - texture	13cm - CL			31cm - CL			46cm -SiC		
tensiometer	a	b		a	b		a	b	
t (min)	h(cm)	h(cm)	θ_v	h(cm)	h(cm)	θ_v	h(cm)	h(cm)	θ_v
0	-11	-14	0.406	-28	-31	0.420	-40	-42	0.440
50	-10	-14	0.402	-26	-31	0.422	-41	-42	0.441
80	-7	-7	0.405	-24	-25	0.421	-32	-37	0.440
110	-3	-8	0.402	-20	-14	0.421	-31	-27	0.444
140	4	2	0.397	-16	-7	0.422	-31	-26	0.440
170	5	-1	0.397	-16	-15	0.421	-33	-28	0.443
200	7	6	0.399	-11	-3	0.419	-25	-23	0.441
230	11	14	0.397	-8	-2	0.417	-12	-19	0.437
290	13	5	0.395	-8	-4	0.421	-30	-18	0.439
320	12	8	0.393	-9	-5	0.419	-23	-20	0.441
350	15	11	0.395	-6	1	0.426	-22	-16	0.440
380	14	12	0.397	-6	4	0.422	-22	-13	0.442
432	16	17	0.395	0	4	0.419	-11	-12	0.439
462	19	21	0.399	2	11	0.414	-7	-6	0.444
490	22	22	0.394	2	10	0.422	-4	-4	0.437
1530	29	27	0.388	14	18	0.415	2	5	0.441
1993	32	38	0.387	18	25	0.413	20	10	0.438
2950	37	44	0.390	24	32	0.415	16	13	0.412
4305	43	37	0.382	25	27	0.410	7	14	0.437
5860	45	48	0.382	30	36	0.410	15	20	0.435
8766	43	39	0.382	29	29	0.409	5	13	0.434
11890	40	32	0.388	28	31	0.405	2	17	0.431
14320	51	29	0.384	29	28	0.405	15	11	0.436

Note: Heads (h) are cm of tension.

Appendix D3 (cont.) - Instantaneous Profile Experimental Data

IP Experimental SIte #2 (continued)

depth - texture	56cm - SiC			69cm - SiCL			76cm - SiCL		
tensiometer	a	b		a	b		a	b	
t (min)	h(cm)	h(cm)	θ_v	h(cm)	h(cm)	θ_v	h(cm)	h(cm)	θ_v
0	-37	-38	0.440	-33	-39	0.412	-12	-18	0.417
50	-34	-49	0.446	-37	-46	0.416	-15	-20	0.416
80	-28	-39	0.442	-29	-36	0.417	-8	-15	0.419
110	-25	-30	0.445	-29	-30	0.418	-6	-11	0.418
140	-21	-34	0.446	-30	-32	0.420	-10	-15	0.415
170	-22	-45	0.445	-33	-41	0.415	-18	-25	0.417
200	-18	-29	0.448	-25	-27	0.420	-8	-12	0.416
230	-9	-14	0.443	-10	-13	0.418	5	2	0.415
290	-17	-36	0.443	-27	-30	0.414	-14	-19	0.418
320	-12	-30	0.443	-22	-26	0.416	-9	-13	0.419
350	-10	-29	0.445	-21	-25	0.415	-9	-14	0.417
380	-11	-19	0.447	-19	-18	0.421	-7	-5	0.418
432	-4	-16	0.448	-10	-14	0.419	2	-4	0.419
462	-1	-7	0.446	-6	-6	0.421	5	3	0.418
490	1	-5	0.446	-3	-3	0.415	5	5	0.420
1530	14	-9	0.440	2	-2	0.415	12	13	0.414
1993	27	15	0.442	29	17	0.416	29	26	0.414
2950	32	12	0.438	24	15	0.414	28	26	0.419
4305	27	7	0.440	12	5	0.411	21	19	0.414
5860	35	11	0.438	22	19	0.410	27	27	0.410
8766	28	-4	0.436	11	8	0.408	19	17	0.413
11890	27	5	0.433	9	10	0.411	20	19	0.411
14320	37	9	0.432	10	6	0.415	1	-2	0.418

depth - texture	94cm - SiL				94cm - SiL		
tensiometer	a	b			a	b	
t (min)	h(cm)	h(cm)	θ_v	t (min)	h(cm)	h(cm)	θ_v
0	-11	-6	0.459	432	-3	2	0.457
50	-16	-6	0.455	462	0	3	0.458
80	-10	-2	0.455	490	0	5	0.455
110	-5	-1	0.456	1530	-7	4	0.454
140	-13	0	0.454	1993	11	8	0.456
170	-23	-7	0.454	2950	11	10	0.451
200	-13	0	0.458	4305	2	8	0.446
230	4	3	0.458	5860	10	12	0.453
290	-18	2	0.454	8766	0	6	0.454
320	-15	-5	0.462	11890	-2	8	0.459
350	-16	-2	0.456	14320	-21	-11	0.468
380	-14	5	0.457				

Appendix D3 (cont.) - Instantaneous Profile Experimental Data

IP Experimental Site #3

depth - texture	13cm - SiL			36cm - SiL		53cm - SC		
tensiometer	a	b		a		a	b	
t (min)	h(cm)	h(cm)	θ_v	h(cm)	θ_v	h(cm)	h(cm)	θ_v
0	-12	-15	0.440	-37	0.422	-45	-52	0.457
44	-10	-15	0.441	-34	0.420	-46	-52	0.459
72	-10	-15	0.439	-33	0.420	-46	-52	0.463
100	-7	-12	0.437	-41	0.424	-44	-50	0.462
134	-4	-9	0.427	-28	0.421	-40	-48	0.463
164	0	-1	0.416	-23	0.422	-37	-42	0.455
194	3	0	0.406	-19	0.420	-32	-37	0.463
224	5	3	0.398	-18	0.421	-27	-34	0.464
254	9	4	0.396	-13	0.418	-19	-27	0.463
284	9	6	0.391	-13	0.418	-18	-24	0.463
314	11	7	0.391	-15	0.419	-18	-27	0.463
444	15	13	0.383	-8	0.418	-15	-21	0.463
666	21	19	0.376	-6	0.418	-10	-19	0.463
824	26	23	0.366	2	0.415	-7	-18	0.461
1006	30	24	0.366	7	0.419	1	-10	0.463
1189	33	26	0.363	9	0.417	-10	-25	0.458
1429	31	27	0.357	8	0.415	-5	-17	0.467
1563	38	31	0.361	20	0.414	15	3	0.459
2584	40	33	0.356	16	0.412	-9	-23	0.460
3044	47	37	0.351	29	0.410	27	16	0.457
3974	51	41	0.346	28	0.412	10	-1	0.464
5479	45	40	0.349	23	0.412	-6	-7	0.461
7034	54	45	0.349	34	0.413	15	8	0.463
9909	48	41	0.349	26	0.410	-5	-15	0.465
13069	44	42	0.353	28	0.406	-1	-13	0.461
15546	63	52	0.345	37	0.407	11	8	0.466

Note: Heads (h) are cm of tension.

Appendix D3 (cont.) - Instantaneous Profile Experimental Data

IP Experimental Site #3 (continued)

depth - texture	58cm - SC			71cm - C			81cm - C			97cm - C	
tensiometer	a	b		a	b		a	b		a	
t (min)	h(cm)	h(cm)	θ_v	h(cm)	h(cm)	θ_v	h(cm)	h(cm)	θ_v	h(cm)	θ_v
0	-54	-50	0.467	-58	-61	0.457	-47	-31	0.442	-10	0.468
44	-55	-51	0.473	-56	-62	0.459	-48	-35	0.436	-11	0.465
72	-56	-52	0.467	-56	-61	0.456	-48	-35	0.445	-10	0.465
100	-54	-52	0.466	-54	-58	0.452	-47	-32	0.438	-8	0.462
134	-52	-52	0.467	-49	-56	0.457	-48	-30	0.443	-6	0.465
164	-45	-49	0.469	-45	-53	0.453	-43	-24	0.443	-4	0.461
194	-41	-46	0.472	-42	-46	0.458	-41	-22	0.441	-4	0.464
224	-38	-42	0.471	-39	-42	0.460	-40	-18	0.445	1	0.461
254	-30	-33	0.466	-34	-35	0.454	-31	-12	0.444	3	0.459
284	-29	-31	0.465	-32	-34	0.458	-30	-13	0.438	3	0.465
314	-31	-33	0.468	-32	-34	0.458	-32	-15	0.441	1	0.464
444	-25	-29	0.467	-26	-24	0.459	-26	-14	0.445	1	0.462
666	-24	-29	0.467	-25	-24	0.458	-22	-12	0.444	1	0.462
824	-19	2	0.467	-25	-24	0.459	-20	-9	0.446	-1	0.468
1006	-11	-21	0.464	-18	-19	0.458	-13	-6	0.443	0	0.464
1189	-20	-39	0.467	-38	-43	0.457	-30	-13	0.440	-6	0.464
1429	-15	-37	0.466	-36	-42	0.456	-28	-7	0.440	-5	0.462
1563	4	-14	0.468	-6	-17	0.459	-3	9	0.443	10	0.465
2584	-17	-42	0.466	-43	-50	0.458	-36	-6	0.442	-9	0.460
3044	19	7	0.468	17	0	0.456	23	25	0.440	24	0.464
3974	2	-3	0.474	-5	-2	0.458	4	9	0.442	6	0.464
5479	-8	-19	0.466	-25	-31	0.456	-13	-1	0.443	-8	0.467
7034	8	-5	0.466	-9	-7	0.457	6	16	0.441	11	0.468
9909	-11	-27	0.470	-34	-34	0.453	-16	0	0.441	-6	0.465
13069	-12	-50	0.467	-38	-51	0.455	-30	6	0.437	1	0.461
15546	6	15	0.470	-1	15	0.453	11	-7	0.441	-21	0.466

Note: Heads (h) are cm of tension.

Appendix D3 (cont.) - Instantaneous Profile Experimental Data

IP Experimental Site #4

depth - texture	13cm - SCL			31cm - SCL			46cm - SCL		
tensiometer	a	b		a	b		a	b	
t (min)	h(cm)	h(cm)	θ_v	h(cm)	h(cm)	θ_v	h(cm)	h(cm)	θ_v
0	-18	-11	0.388	-31	-35	0.395	-41	-47	0.367
125	-16	-6	0.374	-29	-34	0.390	-51	-47	0.364
140	-11	-10	0.372	-30	-36	0.392	-51	-48	0.364
155	-9	-9	0.373	-30	-32	0.392	-49	-47	0.363
195	-11	-8	0.373	-33	-33	0.391	-49	-48	0.368
237	-8	-5	0.371	-31	-30	0.393	-48	-44	0.363
265	-9	-10	0.370	-32	-32	0.391	-46	-43	0.363
292	-8	-11	0.368	-30	-33	0.391	-45	-44	0.368
325	-8	-9	0.368	-28	-32	0.395	-43	-42	0.361
355	-6	-5	0.362	-25	-32	0.390	-37	-36	0.365
385	-4	-5	0.364	-25	-27	0.392	-33	-35	0.366
445	0	-15	0.363	-22	-27	0.391	-27	-31	0.367
505	-1	-1	0.360	-24	-26	0.389	-24	-31	0.364
665	8	4	0.358	-19	-19	0.392	-25	-29	0.362
885	8	5	0.356	-17	-17	0.392	-23	-24	0.362
1015	9	8	0.348	-10	-13	0.391	-20	-22	0.365
1201	12	12	0.347	-7	-11	0.388	-14	-20	0.369
1365	13	13	0.344	-8	-11	0.390	-17	-19	0.364
1622	8	11	0.344	-7	-11	0.390	-17	-16	0.365
1759	13	14	0.347	-5	-8	0.387	-7	-13	0.364
2800	11	10	0.344	-7	-7	0.385	-19	-19	0.367
3215	17	17	0.343	-2	-6	0.385	-5	-9	0.366
4165	18	16	0.336	-4	-2	0.380	-12	-15	0.362
5580	20	21	0.339	6	6	0.380	-8	-5	0.363
7130	24	24	0.342	14	9	0.380	5	5	0.362
9985	32	33	0.339	18	18	0.376	6	7	0.360
13115	28	26	0.334	20	22	0.373	0	8	0.356
15614	50	51	0.331	32	33	0.368	18	24	0.358

Note: Heads (h) are cm of tension.

Appendix D3 (cont.) - Instantaneous Profile Experimental Data

IP Experimental Site #4 (continued)

depth - texture	64cm - C			74cm - C			89cm - SiL		
tensiometer	a	b		a	b		a	b	
t (min)	h(cm)	h(cm)	θ_v	h(cm)	h(cm)	θ_v	h(cm)	h(cm)	θ_v
0	-60	-58	0.441	-37	-32	0.461	-19	-23	0.454
125	-79	-76	0.437	-55	-80	0.463	-39	-40	0.454
140	-79	-80	0.437	-57	-84	0.461	-46	-44	0.452
155	-76	-75	0.441	-56	-70	0.456	-41	-41	0.451
195	-74	-72	0.443	-56	-80	0.463	-42	-41	0.458
237	-70	-71	0.441	-56	-80	0.458	-42	-40	0.456
265	-66	-68	0.439	-59	-79	0.457	-40	-38	0.459
292	-68	-70	0.438	-57	-80	0.461	-41	-37	0.456
325	-65	-70	0.440	-55	-78	0.459	-37	-32	0.451
355	-59	-61	0.439	-49	-72	0.462	-26	-23	0.455
385	-53	-58	0.440	-43	-66	0.460	-22	-16	0.458
445	-46	-48	0.441	-28	-51	0.462	-15	0	0.460
505	-39	-41	0.440	-22	-40	0.459	-2	10	0.455
665	-42	-38	0.433	-13	-28	0.460	10	16	0.455
885	-41	-38	0.438	-13	-27	0.462	11	15	0.455
1015	-41	-39	0.443	-11	-24	0.461	13	12	0.455
1201	-33	-30	0.441	-4	-14	0.461	23	20	0.457
1365	-35	-42	0.444	-18	-39	0.467	1	-3	0.457
1622	-41	-43	0.443	-29	-53	0.460	-8	-10	0.457
1759	-27	-28	0.445	-8	-34	0.461	10	11	0.456
2800	-52	-55	0.442	-37	-58	0.463	-21	-22	0.456
3215	-22	-28	0.439	-21	-55	0.461	-3	5	0.456
4165	-34	-38	0.440	-14	-33	0.460	3	-1	0.456
5580	-29	-41	0.438	-38	-74	0.463	-19	-8	0.456
7130	-20	-12	0.443	-18	-36	0.462	-6	-2	0.452
9985	-26	-35	0.434	-15	-31	0.461	-14	-17	0.455
13115	-37	-45	0.443	-59	-76	0.463	-48	-48	0.453
15614	7	2	0.440	21	12	0.456	13	-5	0.441

Note: Heads (h) are cm of tension.

Appendix E1 - Manhole and Well Physical Data

Location	[1]Map X (m)	[1]Map Y (m)	[2]Platform Z (m)	[3]Invert Z (m)	[4]MP Z (m)	[5]MP Z (m)	[6]MP Z (m)
East MH	1240.9	1081.7	99.101	98.510	99.927	100.006	99.984
West MH	997.0	1091.4	99.086	98.451	99.535	---	---
R. Drain	558.9	1042.9	----	97.714	---	---	---

Well	[1]Map X (m)	[1]Map Y (m)	[7]MP Elev (ft)	[8]MP Elev (m)	[9]Pipe Length (m)	[10]TD Elev (m)
1A	1503.0	1241.1	2.00	100.610	1.892	98.718
1B	1501.7	1241.1	1.63	100.497	2.937	97.560
1C	1500.2	1240.8	1.47	100.448	4.590	95.858
1E	1496.8	1241.4	1.73	100.527	7.032	93.495
2A	1489.1	1105.1	0.95	100.290	1.766	98.524
3A	1470.9	981.1	0.91	100.277	1.839	98.438
3B	1470.0	980.3	0.81	100.247	2.847	97.400
3C	1468.4	979.5	1.01	100.308	4.538	95.770
3E	1467.0	978.9	0.99	100.302	6.517	93.785
4A	1376.4	1241.2	1.34	100.408	1.921	98.487
5A	1376.9	979.8	0.99	100.302	1.996	98.306
6A	1244.0	1240.0	1.31	100.399	1.896	98.503
7A	1242.6	1115.4	1.33	100.405	1.961	98.444
8A	1242.6	989.0	0.94	100.287	1.787	98.500
9A	1238.5	1238.6	0.49	100.149	1.900	98.249
10A	1238.6	1154.6	0.01	100.003	1.882	98.121
11A	1239.0	1117.9	0.18	100.055	1.842	98.213
11B	1239.0	1119.7	0.08	100.024	2.786	97.238
11C	1239.0	1122.1	-0.02	99.994	3.905	96.089
11E	1239.0	1115.6	-0.06	99.982	6.413	93.569
12A	1238.1	1083.2	-0.52	99.842	1.549	98.293
13A	1238.1	1079.6	-0.43	99.869	1.722	98.147
14A	1239.1	1046.1	0.00	100.000	1.938	98.062
14B	1239.0	1049.4	-0.36	99.890	2.908	96.982
14E	1239.0	1051.1	-0.16	99.951	7.013	92.938
15A	1238.8	1010.5	-0.27	99.918	1.766	98.152
16A	1238.4	988.9	-0.36	99.890	1.802	98.088
17A	1120.8	1241.0	0.54	100.165	1.995	98.170
18A	1120.0	992.6	-0.07	99.979	2.048	97.931
19A	1001.3	1240.1	0.45	100.137	1.907	98.230
20A	998.8	1164.3	0.17	100.052	1.719	98.333
21A	999.0	1128.5	-0.04	99.988	1.928	98.060
21B	998.9	1131.3	-0.17	99.950	2.927	97.023
21C	998.6	1130.0	0.17	100.052	4.468	95.584
21E	998.8	1126.7	-0.06	99.983	7.308	92.675

Appendix E1 (cont.) - Manhole and Well Physical Data

Well	[1]Map X (m)	[1]Map Y (m)	[2]MP Elev (ft)	[3]MP Elev (m)	[4]Pipe Length (m)	[5]TD Elev (m)
22A	998.4	1093.3	-0.06	99.982	1.969	98.013
23A	998.3	1089.7	-0.30	99.909	1.938	97.971
24A	999.0	1055.3	-0.32	99.902	1.952	97.950
24B	999.0	1058.4	-0.08	99.976	3.052	96.924
24C	999.0	1056.8	-0.06	99.983	4.622	95.361
24E	999.0	1053.4	-0.16	99.953	7.366	92.587
25A	998.8	1019.7	-0.15	99.954	1.864	98.090
26A	998.9	1004.2	-0.06	99.982	1.917	98.065
27A	996.0	1239.7	-0.22	99.933	1.937	97.996
28A	995.6	1125.1	-1.03	99.686	1.946	97.740
29A	995.4	1004.0	-1.20	99.634	-----	-----
30A	795.0	1242.0	-0.40	99.878	1.827	98.051
31A	794.0	1004.0	-1.10	99.665	-----	-----
32A	482.0	1239.0	-0.45	99.863	1.682	98.181
32B	481.0	1239.0	-0.43	99.869	2.905	96.964
32C	482.0	1240.0	-0.42	99.872	4.597	95.275
32E	484.0	1241.0	-0.24	99.928	7.237	92.691
33A	550.0	1095.0	-0.74	99.774	1.907	97.867
34A	595.0	1012.0	-0.74	99.774	1.919	97.855
34B	599.0	1013.0	-0.43	99.869	2.970	96.899
34C	597.0	1013.0	-0.70	99.787	4.564	95.223
34E	593.0	1015.0	-1.01	99.692	7.214	92.478

[1] Coordinates are based on arbitrary local coordinate system.

[2] Elevation of manhole platform relative to survey datum. Datum is 5/8" rebar stake located at the fence corner by southwest corner of west bench

[3] Invert (inside bottom) elevation of tile-drain pipe relative to survey datum

[4] MP (measuring point) elevation of standpipe. Valid for West manhole for all surveys. Valid for East manhole through 12-2-95.

[5] MP elevation of standpipe in East manhole for period 12-3-95 through 3-2-96.

[6] MP elevation of standpipe in East manhole after 3-2-96.

[7] MP elevation relative to survey datum.

[8] MP elevation generated by converting MP (ft) and adding arbitrary 100 meters.

[9] Pipe lengths as measured by sounding with water depth meter #2 (see text).

[10] TD (total depth) elevations for all monitoring (A) wells are actual elevation of bottom of pipe. TD elevations for all piezometer (B, C, & D) wells are for elevation of center of (20 cm) screened interval.

Appendix E2 - Monitoring Well Water Elevations

Monitoring well and tile drain water elevations given in meters above arbitrary datum. See Appendix B1 for monitoring well and piezometer measuring point elevations.

	1995 Survey Date							
Well	22-Jan	29-Jan	16-Feb	22-Mar	15-May	30-May	9-Jun	16-Jun
1A	98.946	98.938	98.912	99.063	99.183	99.260	99.237	99.435
2A	98.835	98.830	98.792	98.992	99.116	99.133	99.137	99.308
3A	98.727	98.723	98.699	99.005	98.977	99.119	99.048	99.166
4A	98.924	98.928	98.903	99.048	-----	99.227	99.213	99.479
5A	98.708	98.702	98.683	98.975	98.904	99.077	99.028	99.104
6A	98.891	98.884	98.857	99.015	99.067	99.159	99.167	99.299
7A	98.822	98.803	-----	98.970	99.050	99.082	99.094	99.204
8A	98.706	98.702	98.669	98.955	98.902	99.067	99.016	99.099
9A	98.889	98.881	98.859	99.013	99.054	99.158	99.161	99.381
10A	98.813	98.802	98.772	98.975	99.030	99.097	99.100	99.225
11A	98.804	98.793	98.764	98.972	99.031	99.084	99.091	99.198
12A	98.779	98.772	98.733	98.964	-----	99.071	99.074	99.160
13A	98.771	98.760	98.734	98.969	-----	99.056	99.078	99.156
14A	98.758	98.750	98.712	98.968	98.959	99.063	99.050	99.134
15A	98.721	98.710	98.671	98.949	98.915	99.049	99.020	99.098
16A	98.706	-----	98.661	98.948	98.900	99.058	99.010	99.093
17A	98.874	98.861	98.819	98.994	99.037	99.125	99.162	99.335
18A	98.683	98.657	98.630	98.899	98.849	99.012	98.967	99.061
19A	98.840	98.828	98.793	98.984	99.005	99.078	99.126	99.263
20A	98.764	98.750	98.717	98.931	98.913	99.014	99.055	99.140
21A	98.714	98.700	98.669	98.896	98.866	98.983	99.012	99.088
22A	98.694	98.682	98.654	98.888	98.843	98.971	98.998	99.067
23A	98.702	98.688	98.653	98.894	98.847	98.984	98.994	99.068
24A	98.681	98.664	98.630	98.871	98.822	98.964	98.972	99.038
25A	98.659	98.642	98.610	98.858	98.801	98.959	98.948	-----
26A	98.642	98.622	98.592	98.842	98.782	98.959	98.992	98.982
27A	98.830	98.808	98.782	98.975	99.002	99.074	99.118	99.259
28A	98.727	98.707	98.674	98.902	98.864	98.987	99.017	99.093
30A	98.778	98.747	98.717	98.918	98.940	99.000	99.070	99.188
32A	98.562	98.532	98.502	98.703	98.725	98.785	98.855	98.838
33A	98.474	98.377	98.376	98.522	98.532	98.579	98.621	98.723
34A	98.434	98.342	98.330	98.477	98.480	98.596	98.561	98.648

----- No data

Appendix E2 (cont.) - Monitoring Well Water Elevations

Monitoring well and tile drain water elevations given in meters above arbitrary datum. See Appendix B1 for monitoring well and piezometer measuring point elevations.

	1995 Survey Date							
Well	26-Jun	7-Jul	14-Jul	21-Jul	31-Jul	11-Aug	18-Aug	5-Sep
1A	99.270	99.416	99.433	99.368	99.439	99.469	99.919	99.408
2A	99.142	99.281	99.339	99.302	99.383	99.433	99.345	99.319
3A	99.025	99.182	99.287	99.230	99.334	99.379	99.375	99.356
4A	99.236	99.359	99.408	99.329	99.416	99.454	99.703	99.378
5A	99.005	99.132	99.239	99.167	99.308	99.324	99.307	99.299
6A	99.175	99.259	99.352	99.243	99.354	99.379	99.371	99.293
7A	99.080	99.159	99.291	99.194	99.325	99.355	99.291	99.247
8A	98.989	99.090	99.207	99.127	99.257	99.267	99.268	99.245
9A	99.168	99.249	99.349	99.248	99.338	99.372	99.369	99.293
10A	99.088	99.175	99.293	99.193	99.313	99.343	99.301	99.246
11A	99.083	99.162	99.282	99.183	99.315	99.340	99.286	99.245
12A	99.043	99.136	99.258	99.171	99.309	99.323	99.272	99.188
13A	99.056	99.129	99.257	99.168	99.308	99.331	99.252	99.255
14A	99.034	99.118	99.248	99.165	99.283	99.310	99.280	99.247
15A	99.005	99.092	99.215	99.148	99.261	99.271	99.267	99.230
16A	98.987	99.075	99.200	99.122	99.250	99.262	99.270	99.241
17A	-----	99.201	99.300	99.218	99.297	99.329	99.309	99.240
18A	98.937	99.015	99.129	99.059	99.151	99.168	99.233	99.159
19A	99.105	99.156	99.257	99.170	99.238	99.258	99.262	99.168
20A	99.016	99.057	99.183	99.093	99.171	99.206	99.192	99.114
21A	98.878	99.006	99.147	99.061	99.139	99.172	99.169	99.093
22A	98.951	98.998	99.136	99.052	99.146	99.181	99.159	99.087
23A	98.959	99.009	99.154	99.056	99.172	99.204	99.172	99.094
24A	98.930	98.962	99.111	99.022	99.112	99.143	99.171	99.093
25A	98.909	98.954	99.095	98.997	99.119	99.146	99.177	99.095
26A	98.889	98.934	99.098	98.902	99.210	99.278	99.172	99.084
27A	99.099	99.154	99.245	99.161	99.225	99.253	99.252	99.164
30A	99.044	99.078	99.173	99.086	99.137	99.171	99.078	99.025
32A	98.722	98.768	98.812	98.778	98.730	98.635	98.642	98.595
33A	98.613	98.624	98.705	98.673	98.647	98.560	98.523	98.500
34A	98.561	98.610	98.704	98.620	98.591	98.523	98.511	98.473

----- No data

Appendix E2 (cont.) - Monitoring Well Water Elevations

Monitoring well and tile drain water elevations given in meters above arbitrary datum. See Appendix B1 for monitoring well and piezometer measuring point elevations.

	1995 Survey Date							
Well	7-Oct	18-Oct	2-Nov	5-Nov	9-Nov	12-Nov	16-Nov	19-Nov
1A	99.435	99.297	99.375	99.319	99.258	99.224	99.175	99.158
2A	99.328	99.191	99.289	99.238	99.172	99.133	99.085	99.058
3A	99.392	99.135	99.298	99.167	99.090	99.042	98.997	98.965
4A	99.426	99.266	99.356	99.306	99.246	99.210	99.158	99.132
5A	99.342	99.107	99.241	99.123	99.052	99.010	98.952	98.928
6A	99.369	99.189	99.290	99.238	99.182	99.141	99.099	99.075
7A	99.294	99.114	99.220	99.157	99.097	99.053	99.015	98.989
8A	99.303	99.059	99.182	99.084	99.009	98.964	98.922	98.898
9A	99.355	99.186	99.287	99.229	99.176	99.144	99.089	99.067
10A	99.302	99.121	99.225	99.164	99.106	99.063	99.013	99.001
11A	99.301	99.102	99.209	99.140	99.083	99.039	98.995	98.973
12A	99.277	99.086	99.207	99.131	99.069	99.033	98.972	98.960
13A	99.259	99.085	99.187	99.127	99.065	99.024	98.969	98.959
14A	99.288	99.085	99.196	99.111	99.053	99.009	98.955	98.942
15A	99.287	99.058	99.178	99.085	99.014	98.973	98.928	98.901
16A	99.298	99.055	99.173	99.069	99.005	98.954	98.920	98.894
17A	99.315	99.132	99.233	99.176	99.127	99.083	99.046	99.024
18A	99.225	99.046	99.074	98.994	98.936	98.892	98.854	98.832
19A	99.227	99.070	99.161	99.112	99.068	99.035	98.997	98.978
20A	99.173	98.999	99.095	99.042	98.997	98.960	98.924	98.907
21A	99.152	98.960	99.053	98.998	98.952	98.916	98.879	98.863
22A	99.145	98.944	99.039	98.980	98.938	98.893	98.853	98.841
23A	99.154	98.949	99.044	98.988	98.938	98.899	98.859	98.848
24A	99.147	98.929	99.013	98.959	98.909	98.872	98.832	98.815
25A	99.148	98.909	98.992	98.927	98.883	98.849	98.804	98.794
26A	99.142	98.894	98.976	98.910	98.861	98.829	98.792	98.772
27A	99.222	99.064	99.157	99.111	99.066	99.032	98.993	98.971
28A	99.160	98.966	99.058	99.001	98.956	98.922	98.884	98.871
30A	99.092	98.953	99.042	98.997	98.959	98.928	98.903	98.888
32A	98.679	98.592	98.610	98.599	98.599	98.591	98.593	98.583
33A	98.579	98.490	98.501	98.491	98.489	98.478	98.464	98.471
34A	98.552	98.434	98.450	98.435	98.438	98.423	98.416	98.410
EMH	-----	98.926	99.127	99.073	99.004	98.971	98.907	98.906
WMH	-----	99.027	99.003	98.956	98.902	98.870	98.830	98.815

----- No data

Appendix E2 (cont.) - Monitoring Well Water Elevations

Monitoring well and tile drain water elevations given in meters above arbitrary datum. See Appendix B1 for monitoring well and piezometer measuring point elevations.

	1995 Survey Date				1996		
Well	22-Nov	26-Nov	2-Dec	15-Dec	10-Jan	2-Mar	1-Apr
1A	99.129	99.109	99.077	99.022	98.958	98.908	99.309
2A	99.033	99.004	98.968	98.911	98.850	98.791	99.185
3A	98.930	98.909	98.867	98.806	98.748	98.729	99.106
4A	99.110	99.094	99.055	99.000	98.942	98.886	99.287
5A	98.896	98.872	98.833	98.777	98.717	98.662	99.082
6A	99.048	99.039	98.998	98.946	98.884	98.847	99.226
7A	98.962	98.950	98.904	98.852	98.827	98.754	99.140
8A	98.865	98.845	98.806	98.751	98.695	98.658	99.057
9A	99.043	99.026	98.991	98.939	98.882	98.838	99.221
10A	98.971	98.950	98.913	98.861	98.805	98.769	99.148
11A	98.950	98.919	98.891	98.835	98.781	98.734	99.125
12A	98.927	98.904	98.871	98.819	98.767	98.722	99.105
13A	98.929	98.912	98.869	98.818	98.768	98.718	99.097
14A	98.917	98.900	98.853	98.802	98.748	98.697	99.087
15A	98.873	98.847	98.814	98.760	98.708	98.660	99.064
16A	98.866	98.842	98.800	98.749	98.694	98.659	99.058
17A	99.003	98.990	98.951	98.903	98.853	98.811	99.175
18A	98.808	98.789	98.774	98.708	98.661	98.621	98.996
19A	98.958	98.939	98.906	98.858	98.816	-----	99.122
20A	98.882	98.869	98.834	98.790	98.748	98.712	99.051
21A	98.836	98.820	98.788	98.745	98.703	98.667	99.009
22A	98.819	98.804	98.771	98.729	98.688	98.653	98.993
23A	98.821	98.807	98.772	98.728	98.688	98.647	98.996
24A	98.792	98.774	98.748	98.702	98.661	98.622	98.967
25A	98.771	98.754	98.723	98.681	98.639	98.600	98.941
26A	98.750	98.727	98.702	98.657	98.614	98.582	98.924
27A	98.950	98.934	98.898	98.854	98.807	98.773	99.113
28A	98.844	98.828	98.795	98.752	98.704	98.674	99.014
30A	98.868	98.854	98.824	98.783	98.740	98.715	99.025
32A	98.570	98.555	98.549	98.535	98.525	98.515	98.645
33A	98.460	98.443	98.434	98.421	98.412	98.401	98.545
34A	98.408	98.390	98.383	98.368	98.359	98.351	98.495
EMH	98.868	98.587	98.812	98.774	98.698	-----	99.180
WMH	98.788	98.779	98.738	98.698	98.630	-----	98.904

----- No data

Appendix E3 - Piezometer Water Elevations

Piezometer water elevations given in meters above arbitrary datum. See Appendix B1 for monitoring well and piezometer measuring point elevations.

	1995 Survey Date							
Well	22-Jan	29-Jan	16-Feb	22-Mar	15-May	30-May	9-Jun	16-Jun
1A	98.946	98.938	98.912	99.063	99.183	99.260	99.237	99.435
1B	98.930	98.937	98.902	99.056	99.172	99.242	99.018	99.312
1C	98.954	98.949	98.912	99.070	-----	99.074	99.035	99.336
1E	98.938	98.943	98.917	99.063	99.176	99.090	99.034	99.324
3A	98.727	98.723	98.699	99.005	98.977	99.119	99.048	99.166
3B	98.723	98.729	98.694	99.003	98.797	98.922	98.839	98.954
3C	98.725	98.723	98.690	99.001	98.948	98.916	98.837	98.955
3E	98.721	98.746	98.714	98.978	98.979	98.914	98.870	99.003
11A	98.804	98.793	98.764	98.972	99.031	99.084	99.091	99.198
11B	98.798	98.792	98.756	98.970	99.028	99.084	98.879	99.001
11C	98.786	98.805	98.755	98.990	99.006	98.930	98.892	98.998
11E	98.831	98.784	98.736	98.957	-----	98.942	98.876	98.986
14A	98.758	98.750	98.712	98.968	98.959	99.063	99.050	99.134
14B	98.748	98.746	98.707	98.953	98.753	98.843	98.839	98.917
14E	98.723	98.715	98.684	98.936	98.747	98.831	98.823	98.912
21A	98.714	98.700	98.669	98.896	98.866	98.983	99.012	99.088
21B	98.724	98.717	98.678	98.898	98.705	98.762	98.802	98.881
21C	98.701	98.688	98.637	98.876	98.660	98.760	98.791	98.868
21E	98.721	98.714	98.675	98.897	98.714	98.774	98.807	98.882
24A	98.681	98.664	98.630	98.871	98.822	98.964	98.972	99.038
24B	98.682	98.678	98.641	98.886	98.819	98.820	98.774	98.838
24C	98.676	98.674	98.627	98.866	98.813	98.760	98.759	98.828
24E	98.690	98.672	98.637	98.872	98.677	98.758	98.760	98.837
32A	98.562	99.863	99.863	99.863	99.863	99.863	99.863	99.863
32B	98.548	98.494	98.485	98.613	98.508	98.545	98.551	98.619
32C	98.550	98.500	98.498	98.618	98.512	98.532	98.556	98.626
32E	98.554	98.502	98.497	98.620	98.470	98.547	98.714	98.629
34A	98.437	98.345	98.333	98.480	98.483	98.599	98.564	98.651
34B	98.427	98.354	98.325	98.468	98.481	98.390	98.368	98.443
34C	98.424	98.335	98.315	98.462	98.479	98.509	98.357	98.437
34E	98.411	98.328	98.311	98.456	98.461	98.317	98.353	98.427

----- No data

Appendix E3 (cont.) - Piezometer Water Elevations

Piezometer water elevations given in meters above arbitrary datum. See Appendix B1 for monitoring well and piezometer measuring point elevations.

	1995 Survey Date							
Well	26-Jun	7-Jul	14-Jul	21-Jul	31-Jul	11-Aug	18-Aug	5-Sep
1A	99.270	99.416	99.433	99.368	99.439	99.469	99.919	99.408
1B	99.048	99.408	99.427	99.362	99.433	99.457	99.921	99.411
1C	99.056	99.414	99.453	99.377	99.450	99.450	99.928	99.428
1E	99.057	99.412	99.438	99.371	99.440	99.460	99.944	99.416
3A	99.025	99.182	99.287	99.230	99.334	99.379	99.375	99.356
3B	98.820	99.090	99.284	99.235	99.344	99.354	99.373	99.365
3C	98.812	99.188	99.276	99.234	99.322	99.356	99.372	99.467
3E	98.840	99.199	99.290	99.247	99.343	99.350	99.382	99.342
11A	99.083	99.162	99.322	99.183	99.315	99.340	99.286	99.245
11B	98.855	99.160	99.283	99.197	99.306	99.324	99.288	99.246
11C	98.868	99.162	99.295	99.209	99.333	99.349	99.289	99.284
11E	98.860	99.151	99.281	99.190	99.330	99.336	99.281	99.267
14A	99.034	99.118	99.248	99.165	99.283	99.310	99.280	99.247
14B	98.814	99.111	99.240	99.162	99.278	99.296	99.272	99.242
14E	98.801	99.097	99.222	99.146	99.261	99.274	99.262	99.218
21A	98.879	99.006	99.147	99.061	99.139	99.172	99.169	99.093
21B	98.764	99.026	99.159	99.071	99.145	99.159	99.168	99.097
21C	98.740	99.011	99.137	98.962	99.123	99.138	99.153	99.072
21E	98.756	99.028	99.149	99.071	99.141	99.160	99.174	99.091
24A	98.930	98.962	99.111	99.022	99.112	99.143	99.171	99.093
24B	98.730	98.987	99.133	99.029	99.126	99.130	99.267	99.108
24C	98.737	98.977	99.113	99.021	99.119	99.153	99.172	99.091
24E	98.719	98.951	99.120	99.025	99.114	99.130	99.182	99.101
32A	99.863	98.768	98.809	98.778	98.730	98.635	98.642	98.595
32B	98.497	98.719	98.805	98.770	98.721	98.629	98.634	98.591
32C	98.506	98.772	98.807	98.774	98.729	98.638	98.653	98.592
32E	98.509	98.773	98.810	98.772	98.733	98.638	98.654	98.581
34A	98.564	98.613	98.707	98.623	98.656	98.526	98.514	98.476
34B	98.365	98.624	98.736	98.638	98.612	98.513	98.517	98.501
34C	98.349	98.619	98.708	98.628	98.601	98.514	98.508	98.485
34E	98.346	98.603	98.699	98.630	98.591	98.509	98.494	98.471

Appendix E3 (cont.) - Piezometer Water Elevations

Piezometer water elevations given in meters above arbitrary datum. See Appendix B1 for monitoring well and piezometer measuring point elevations.

	1995 Survey Date							
Well	7-Oct	13-Oct	18-Oct	2-Nov	5-Nov	9-Nov	12-Nov	16-Nov
1A	99.435	99.334	99.297	99.375	99.319	99.258	99.224	99.175
1B	99.431	99.326	99.289	99.365	99.317	99.247	99.216	99.172
1C	99.439	99.338	99.301	99.376	99.326	99.261	99.228	99.179
1E	99.432	99.333	99.296	99.370	99.325	99.257	99.217	99.172
3A	99.392	99.147	99.135	99.298	99.167	99.090	99.042	98.997
3B	99.404	99.151	99.129	99.293	99.177	99.087	99.055	98.982
3C	99.408	99.146	99.131	99.298	99.176	99.086	99.047	98.988
3E	99.377	99.167	99.158	99.273	99.171	99.087	99.058	98.997
11A	99.277	99.123	99.102	99.209	99.140	99.083	99.039	98.995
11B	99.286	99.132	99.106	99.212	99.168	99.086	99.052	98.994
11C	99.240	99.256	99.120	99.214	99.209	99.087	99.084	98.994
11E	99.066	99.132	99.109	99.247	99.192	99.142	99.090	98.987
14A	99.288	99.097	99.085	99.196	99.111	99.053	99.009	98.955
14B	99.278	99.010	99.075	99.188	99.114	99.040	99.002	98.950
14E	99.269	99.148	99.061	99.174	99.089	99.024	98.986	98.971
21A	99.152	98.985	98.960	99.053	98.998	98.952	98.916	98.879
21B	99.149	98.990	98.964	99.054	99.004	98.954	98.922	98.890
21C	99.130	98.966	98.940	99.034	98.992	98.930	98.902	98.861
21E	99.154	98.978	98.959	99.048	98.992	98.949	98.921	98.880
24A	99.147	98.945	98.929	99.013	98.959	98.909	98.872	98.832
24B	99.166	98.948	98.931	99.014	98.941	98.910	98.894	98.833
24C	99.160	98.942	98.925	99.009	98.969	98.903	98.880	98.833
24E	99.156	98.945	98.929	99.013	98.959	98.907	98.873	98.825
32A	98.679	98.608	98.592	98.610	98.599	98.599	98.591	98.593
32B	98.674	98.603	98.584	98.598	98.591	98.588	98.580	98.594
32C	98.687	98.610	98.591	98.608	98.601	98.598	98.582	98.637
32E	98.684	98.611	98.593	98.608	98.603	98.600	98.590	98.638
34A	98.555	98.461	98.437	98.453	98.438	98.441	98.426	98.419
34B	98.577	98.472	98.441	98.457	98.439	98.437	98.441	98.426
34C	98.549	98.457	98.434	98.448	98.428	98.433	98.426	98.417
34E	98.544	98.452	98.430	98.439	98.424	98.415	98.427	98.406

Appendix E3 (cont.) - Piezometer Water Elevations

Piezometer water elevations given in meters above arbitrary datum. See Appendix B1 for monitoring well and piezometer measuring point elevations.

	1995 Survey Date					1996 Survey Date		
Well	19-Nov	22-Nov	26-Nov	2-Dec	15-Dec	10-Jan	2-Mar	1-Apr
1A	99.158	99.129	99.109	99.077	99.022	98.958	98.908	99.309
1B	99.150	99.119	99.107	99.069	99.011	98.962	98.915	99.304
1C	99.175	99.131	99.126	99.080	99.022	98.984	98.925	99.310
1E	99.157	99.126	99.115	99.081	99.022	98.969	98.922	99.309
3A	98.965	98.930	98.909	98.867	98.806	98.748	98.729	99.106
3B	98.973	98.927	98.907	98.862	98.805	98.750	98.698	99.106
3C	98.977	98.923	98.918	98.859	98.800	98.763	98.702	99.105
3E	98.987	98.935	98.932	98.876	98.817	98.777	98.719	99.129
11A	98.973	98.950	98.919	98.891	98.835	100.055	98.734	99.125
11B	98.990	98.951	98.936	98.894	98.840	98.799	98.759	99.132
11C	98.996	98.951	98.931	98.906	98.891	98.795	98.768	99.144
11E	98.992	98.935	98.944	98.920	98.921	98.802	98.746	99.127
14A	98.942	98.917	98.900	98.853	98.802	98.748	98.697	99.087
14B	98.941	98.899	98.890	98.841	98.789	98.745	98.704	99.088
14E	98.919	98.883	98.863	98.823	98.768	98.713	98.671	99.073
21A	98.863	98.836	98.820	98.788	98.745	98.703	98.667	99.009
21B	98.871	98.842	98.829	98.792	98.749	98.708	98.675	99.012
21C	98.842	98.820	98.801	98.766	98.723	100.052	98.650	98.991
21E	98.865	98.836	98.823	98.789	98.741	98.700	98.664	99.007
24A	98.815	98.792	98.774	98.748	98.702	98.661	98.622	98.967
24B	98.832	98.799	98.793	98.745	98.702	98.688	98.643	98.981
24C	98.815	98.788	98.777	98.741	98.697	98.671	98.626	98.963
24E	98.820	98.796	98.785	98.744	98.701	98.659	98.633	98.938
32A	98.583	98.570	98.555	98.549	98.535	98.525	98.515	98.645
32B	98.575	98.558	98.551	98.537	98.524	98.520	98.509	98.639
32C	98.577	98.568	98.554	98.544	98.532	98.524	98.524	98.645
32E	98.580	98.569	98.555	98.547	98.533	98.525	98.518	98.651
34A	98.413	98.411	98.393	98.386	98.371	98.362	98.354	98.498
34B	98.435	98.407	98.414	98.387	98.367	98.385	98.368	98.509
34C	98.421	98.404	98.389	98.379	98.364	98.359	98.356	98.495
34E	98.409	98.397	98.383	98.369	98.357	98.346	98.347	98.487

Appendix E4 - Vertical Gradients

Piezometer gradients given in percent (meters/meter x 100). Negative values represent downward flow (total head decreasing with depth). Positive values represent upward flow (total head increasing with depth).

		1995 Survey Date							
Nest	Wells	22-Jan	29-Jan	16-Feb	22-Mar	15-May	30-May	9-Jun	16-Jun
1	A-B	1.23	0.06	0.78	0.48	0.71	1.11	13.87	6.92
	B-C	-1.42	-0.72	-0.60	-0.84	-----	9.86	-1.01	-1.42
	C-E	0.67	0.24	-0.22	0.29	-----	-0.69	0.03	0.50
3	A-B	0.36	-0.45	0.46	0.16	12.22	12.19	13.53	12.75
	B-C	-0.12	0.37	0.25	0.13	-9.26	0.37	0.13	-0.06
	C-E	0.21	-1.15	-1.20	1.16	-1.56	0.11	-1.66	-2.41
11	A-B	0.37	0.03	0.52	0.09	0.15	-0.03	12.07	10.57
	B-C	1.09	-1.09	0.13	-1.70	1.96	13.44	-1.09	0.30
	C-E	-1.78	0.84	0.76	1.32	-----	-0.47	0.64	0.48
14	A-B	0.58	0.22	0.29	0.78	10.96	11.09	10.71	10.56
	B-E	0.62	0.77	0.57	0.42	0.15	0.30	0.40	0.12
21	A-B	-0.62	-1.07	-0.58	-0.14	12.02	15.81	14.87	14.27
	B-C	1.59	2.01	2.84	1.52	3.12	0.13	0.76	0.90
	C-E	-0.70	-0.91	-1.32	-0.74	-1.87	-0.50	-0.56	-0.50
24	A-B	-0.01	-0.80	-0.63	-0.77	0.21	7.46	10.20	9.97
	B-C	0.34	0.22	0.86	1.24	0.34	3.80	0.92	0.60
	C-E	-0.49	0.09	-0.34	-0.20	4.92	0.09	-0.02	-0.31
32	A-B	0.93	-----	-----	-----	-----	-----	-----	-----
	B-C	-0.12	-0.36	-0.77	-0.30	-0.24	0.77	-0.30	-0.42
	C-E	-0.17	-0.09	0.02	-0.09	1.61	-0.60	-6.13	-0.13
34	A-B	0.73	-0.63	0.64	0.84	0.17	13.09	12.55	12.62
	B-C	0.20	1.15	0.61	0.38	0.14	-7.08	0.67	0.38
	C-E	0.46	0.24	0.13	0.20	0.64	6.98	0.13	0.35

----- No data

Appendix E4 (cont.) - Vertical Gradients

Piezometer gradients given in percent (meters/meter x 100). Negative values represent downward flow (total head decreasing with depth). Positive values represent upward flow (total head increasing with depth).

		1995 Survey Date							
Nest	Wells	26-Jun	7-Jul	14-Jul	21-Jul	31-Jul	11-Aug	18-Aug	5-Sep
1	A-B	13.78	0.44	0.33	0.34	0.32	0.65	-0.10	-0.18
	B-C	-0.48	-0.37	-1.54	-0.90	-1.01	0.40	-0.42	-1.01
	C-E	-0.05	0.07	0.62	0.24	0.41	-0.43	-0.69	0.50
3	A-B	13.47	5.50	0.19	-0.26	-0.52	1.36	0.13	-0.46
	B-C	0.49	-6.01	0.49	0.06	1.35	-0.12	0.06	-6.26
	C-E	-1.41	-0.55	-0.70	-0.65	-1.05	0.31	-0.50	6.30
11	A-B	13.04	0.08	1.94	-0.79	0.43	0.77	-0.13	-0.08
	B-C	-1.09	-0.13	-1.00	-1.00	-2.31	-2.13	-0.05	-3.26
	C-E	0.33	0.44	0.56	0.76	0.13	0.52	0.33	0.68
14	A-B	11.26	0.33	0.36	0.13	0.21	0.62	0.35	0.22
	B-E	0.32	0.35	0.45	0.40	0.42	0.54	0.25	0.59
21	A-B	8.55	-1.41	-0.80	-0.69	-0.40	0.88	0.07	-0.27
	B-C	1.66	1.03	1.52	7.57	1.52	1.45	1.03	1.73
	C-E	-0.56	-0.60	-0.43	-3.76	-0.63	-0.77	-0.74	-0.67
24	A-B	10.53	-1.25	-1.01	-0.31	-0.63	0.65	-4.43	-0.68
	B-C	-0.49	0.60	1.24	0.47	0.41	-1.51	6.04	1.05
	C-E	0.67	0.95	-0.23	-0.13	0.20	0.85	-0.34	-0.34
32	A-B		2.87	0.22	0.46	0.53	0.38	0.50	0.26
	B-C	-0.54	-3.14	-0.12	-0.24	-0.48	-0.54	-1.13	-0.06
	C-E	-0.13	-0.05	-0.13	0.06	-0.17	-0.02	-0.05	0.41
34	A-B	12.74	-0.65	-1.67	-0.89	2.69	0.88	-0.16	-1.66
	B-C	0.97	0.32	1.69	0.61	0.67	-0.04	0.55	0.97
	C-E	0.09	0.56	0.31	-0.09	0.35	0.16	0.49	0.49

Appendix E4 (cont.) - Vertical Gradients

Piezometer gradients given in percent (meters/meter x 100). Negative values represent downward flow (total head decreasing with depth). Positive values represent upward flow (total head increasing with depth).

		1995 Survey Date							
Nest	Wells	7-Oct	13-Oct	18-Oct	2-Nov	5-Nov	9-Nov	12-Nov	16-Nov
1	A-B	0.21	0.46	0.48	0.57	0.11	0.67	0.50	0.18
	B-C	-0.48	-0.72	-0.72	-0.66	-0.54	-0.84	-0.72	-0.42
	C-E	0.29	0.20	0.20	0.24	0.03	0.16	0.46	0.29
3	A-B	-0.61	-0.21	0.40	0.30	-0.57	0.22	-0.81	1.03
	B-C	-0.24	0.31	-0.12	-0.30	0.06	0.06	0.49	-0.37
	C-E	1.57	-1.05	-1.36	1.26	0.26	-0.05	-0.55	-0.45
11	A-B	-0.49	-0.53	-0.26	-0.19	-1.58	-0.20	-0.80	0.03
	B-C	4.04	-10.75	-1.18	-0.13	-3.53	-0.05	-2.74	0.04
	C-E	6.91	4.93	0.44	-1.30	0.68	-2.17	-0.23	0.29
14	A-B	0.44	4.30	0.49	0.37	-0.16	0.65	0.35	0.25
	B-E	0.22	-3.41	0.35	0.35	0.62	0.40	0.40	-0.52
21	A-B	0.21	-0.35	-0.28	-0.06	-0.42	-0.14	-0.43	-0.81
	B-C	1.31	1.66	1.66	1.38	0.83	1.66	1.38	2.01
	C-E	-0.84	-0.43	-0.67	-0.50	-0.01	-0.67	-0.67	-0.67
24	A-B	-0.85	-0.11	-0.06	-0.01	0.97	-0.01	-1.14	-0.01
	B-C	0.34	0.34	0.34	0.28	-1.83	0.41	0.86	-0.04
	C-E	0.16	-0.09	-0.13	-0.13	0.38	-0.13	0.27	0.31
32	A-B	0.30	0.32	0.52	0.77	0.51	0.71	0.71	-0.07
	B-C	-0.77	-0.42	-0.42	-0.59	-0.59	-0.59	-0.12	-2.55
	C-E	0.10	-0.05	-0.09	-0.02	-0.09	-0.09	-0.32	-0.05
34	A-B	-1.38	-0.72	-0.24	-0.24	-0.03	0.31	-1.01	-0.46
	B-C	1.69	0.91	0.44	0.55	0.67	0.26	0.91	0.55
	C-E	0.16	0.16	0.13	0.31	0.13	0.64	-0.06	0.38

Appendix E4 (cont.) - Vertical Gradients

Piezometer gradients given in percent (meters/meter x 100). Negative values represent downward flow (total head decreasing with depth). Positive values represent upward flow (total head increasing with depth).

Nest	Wells	19-Nov	22-Nov	26-Nov	2-Dec	15-Dec	10-Jan	2-Mar	1-Apr
1	A-B	0.52	0.67	0.12	0.55	0.79	-0.33	-0.58	0.35
	B-C	-1.48	-0.72	-1.13	-0.66	-0.66	-1.31	-0.60	-0.37
	C-E	0.75	0.20	0.46	-0.05	-0.01	0.62	0.12	0.03
3	A-B	-0.51	0.24	0.18	0.40	0.11	-0.12	2.56	0.04
	B-C	-0.24	0.25	-0.67	0.19	0.31	-0.80	-0.24	0.06
	C-E	-0.50	-0.60	-0.70	-0.85	-0.85	-0.70	-0.85	-1.20
11	A-B	-1.07	-0.09	-1.11	-0.23	-0.37	-----	-1.83	-0.57
	B-C	-0.48	0.04	0.48	-1.00	-4.40	0.39	-0.74	-1.00
	C-E	0.17	0.64	-0.51	-0.55	-1.18	-0.27	0.88	0.68
14	A-B	0.04	0.97	0.54	0.66	0.74	0.16	-0.45	-0.09
	B-E	0.54	0.40	0.67	0.45	0.52	0.79	0.82	0.37
21	A-B	-0.59	-0.45	-0.68	-0.30	-0.30	-0.39	-0.64	-0.21
	B-C	2.01	1.52	1.94	1.80	1.80	-----	1.73	1.45
	C-E	-0.81	-0.56	-0.77	-0.81	-0.63	-----	-0.50	-0.56
24	A-B	-0.90	-0.35	-1.04	0.22	0.05	-1.60	-1.26	-0.92
	B-C	1.05	0.66	0.98	0.22	0.28	1.05	1.05	1.11
	C-E	-0.16	-0.27	-0.27	-0.09	-0.13	0.45	-0.23	-0.16
32	A-B	0.52	0.79	0.26	0.80	0.74	0.34	0.41	0.44
	B-C	-0.12	-0.59	-0.18	-0.42	-0.48	-0.24	-0.89	-0.36
	C-E	-0.13	-0.05	-0.05	-0.13	-0.05	-0.05	0.22	-0.25
34	A-B	-1.52	0.32	-1.47	-0.04	0.33	-1.65	-1.00	-0.89
	B-C	0.85	0.20	1.51	0.49	0.20	1.57	0.73	0.85
	C-E	0.42	0.24	0.20	0.35	0.24	0.46	0.31	0.27

----- No data

Appendix E5 - Water Table Elevation Contour Maps

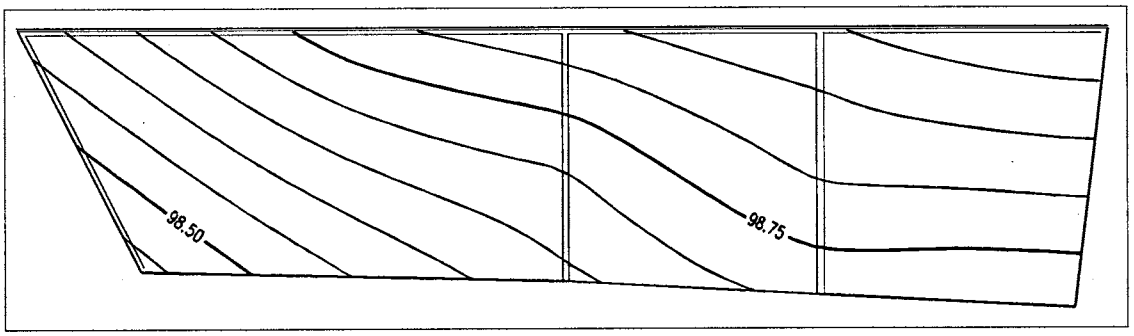

January 22, 1995

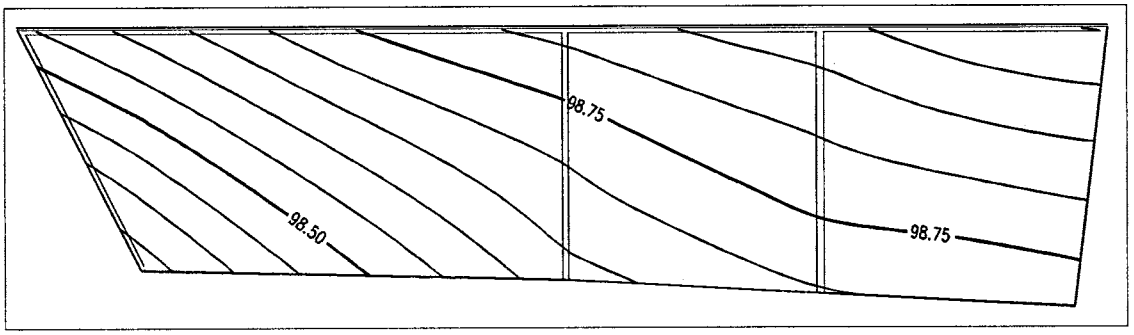

January 29, 1995

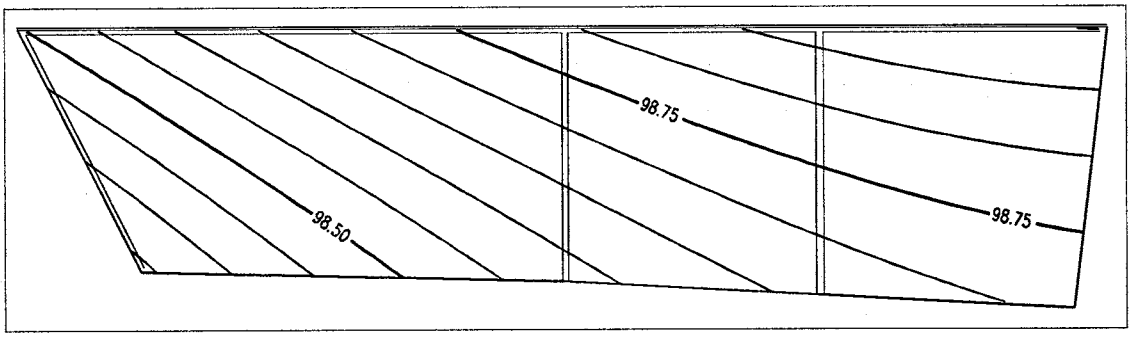

February 16, 1995

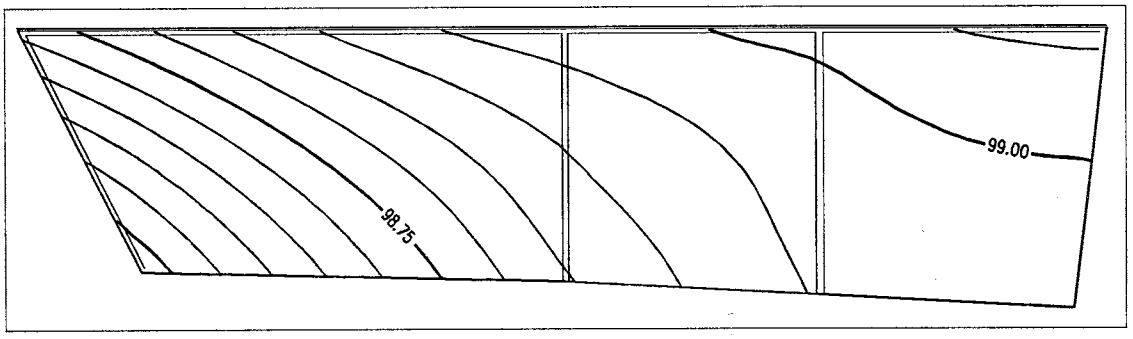

March 22, 1995

Contour interval 0.05 m, arbitrary vertical datum.

Appendix E5 (cont.) - Water Table Elevation Contour Maps

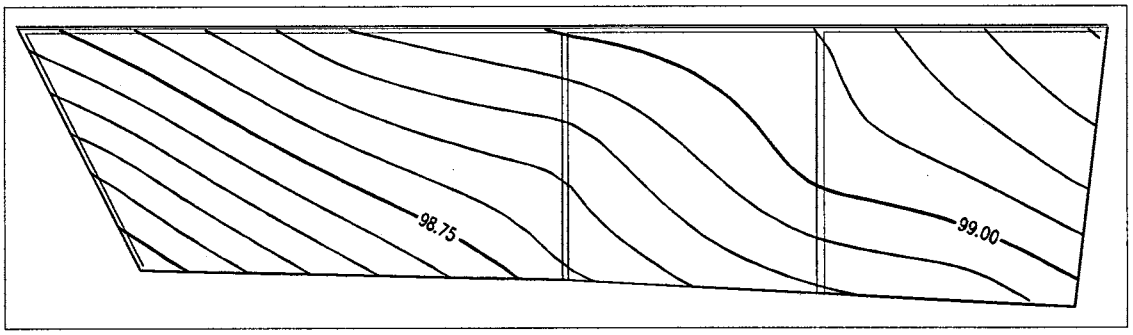

May 15, 1995

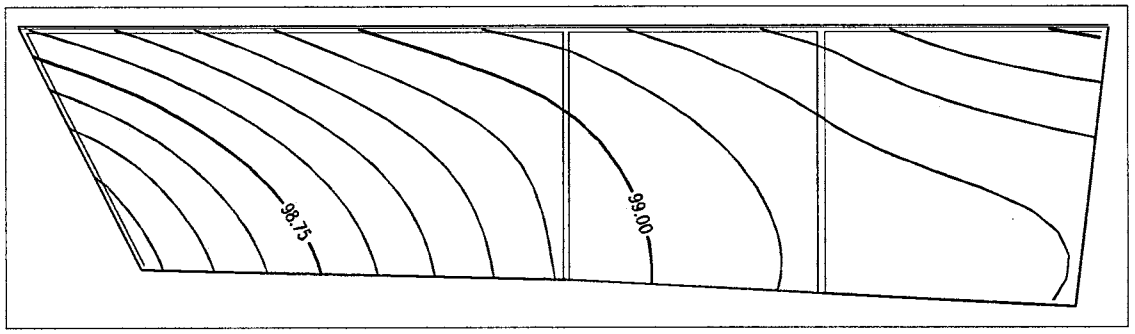

May 30, 1995

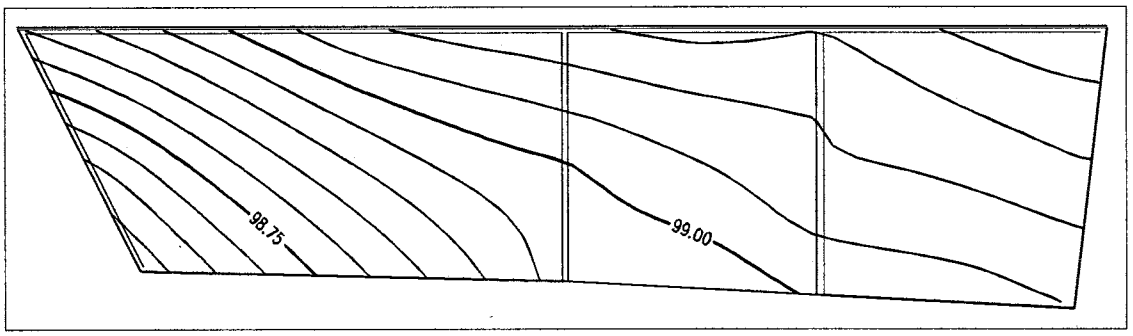

June 9, 1995

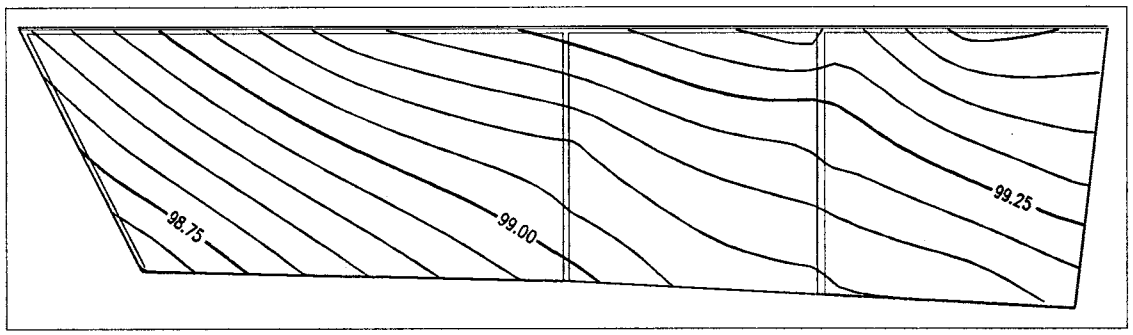

June 16, 1995

Contour interval 0.05 m, arbitrary vertical datum.

Appendix E5 (cont.) - Water Table Elevation Contour Maps

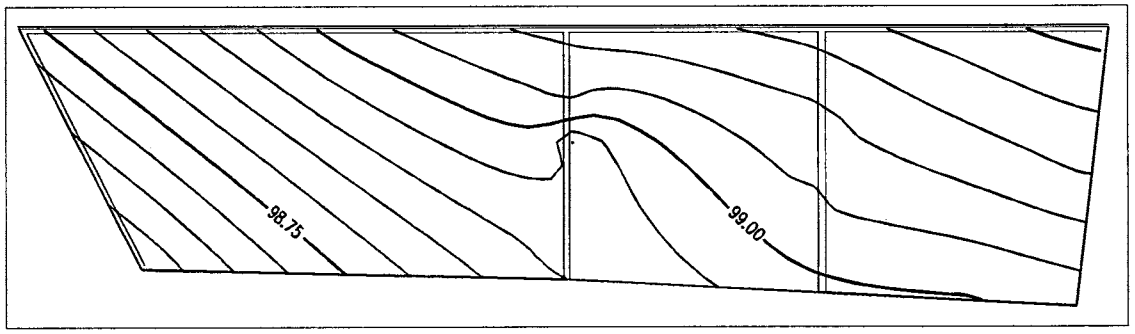

June 26, 1995

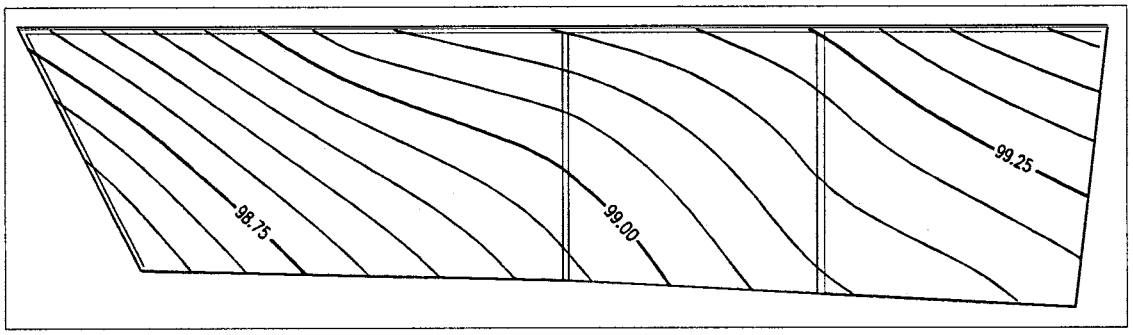

July 7, 1995

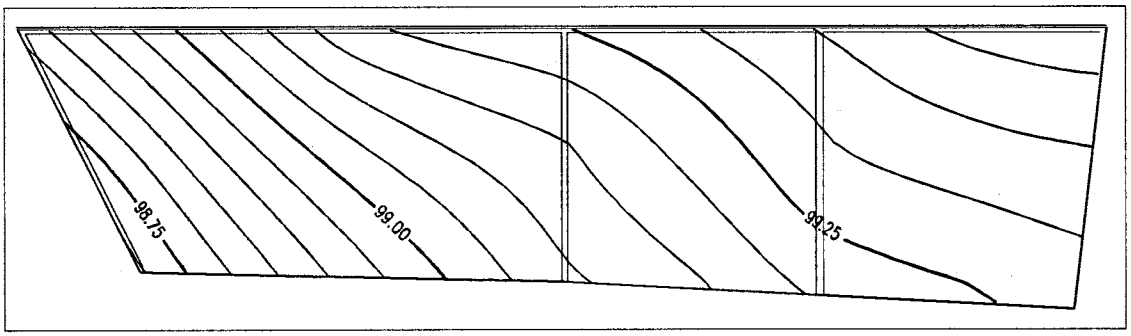

July 14, 1995

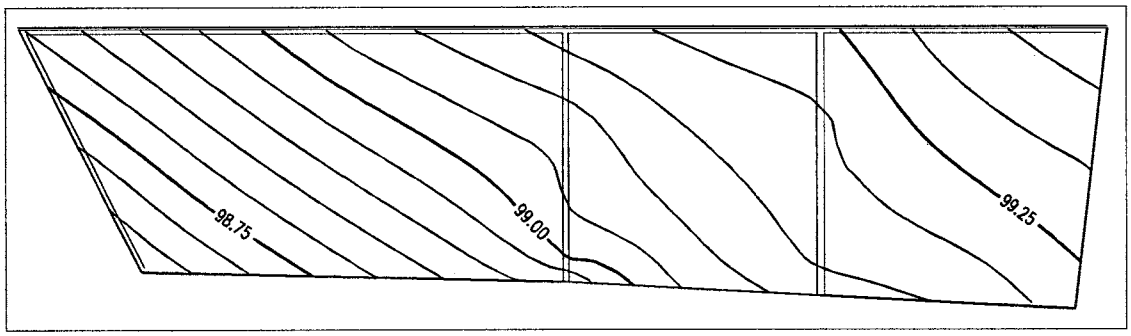

July 21, 1995

Contour interval 0.05 m, arbitrary vertical datum

Appendix E5 (cont.) - Water Table Elevation Contour Maps

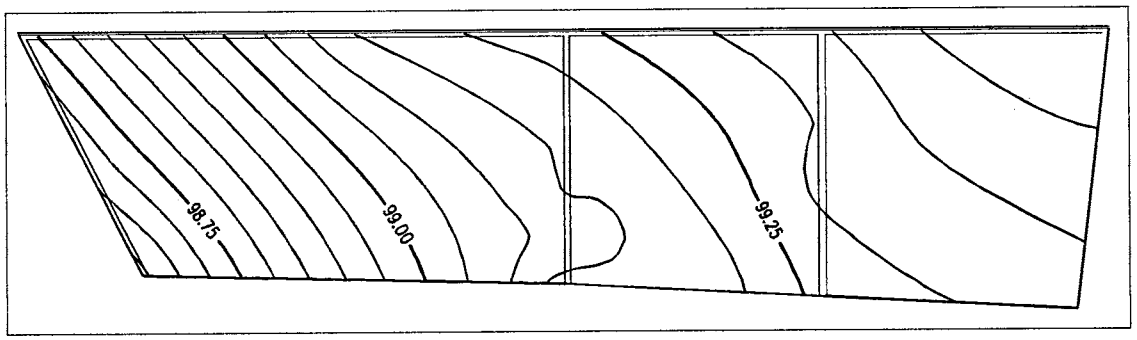

July 31, 1995

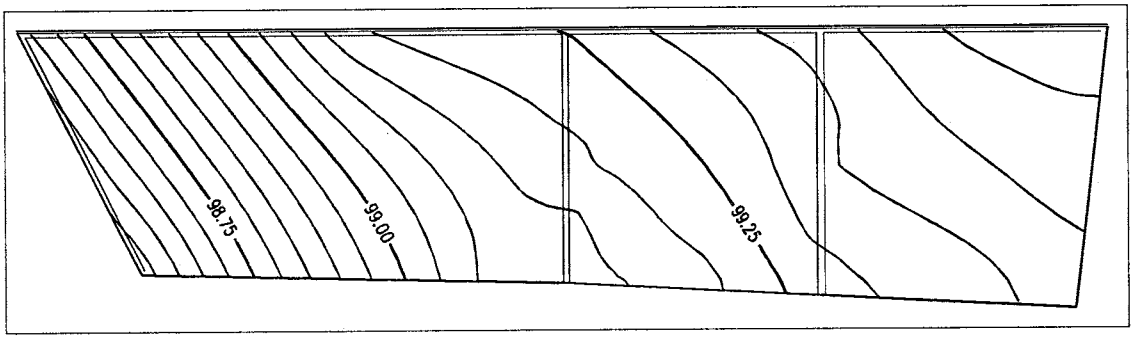

August 11, 1995

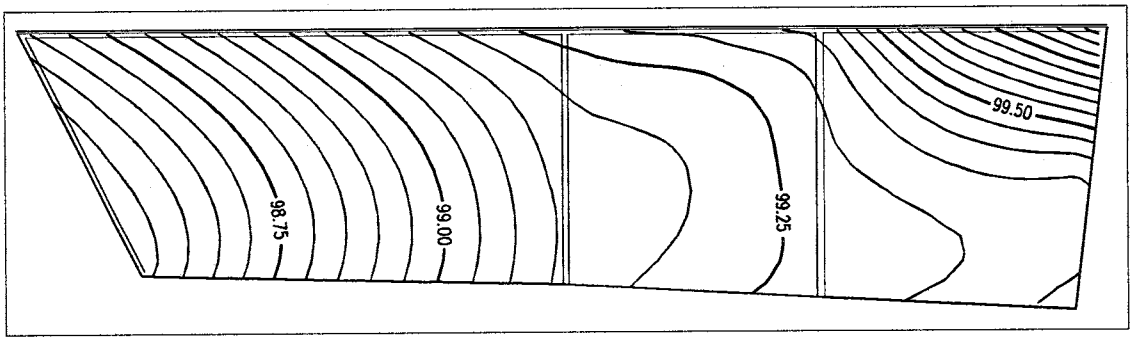

August 18, 1995

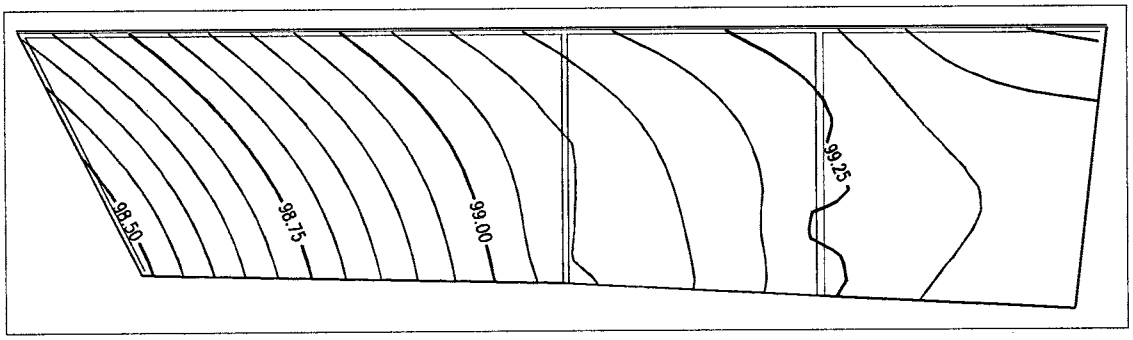

September 5, 1995

Contour interval 0.05 m, arbitrary vertical datum

Appendix E5 (cont.) - Water Table Elevation Contour Maps

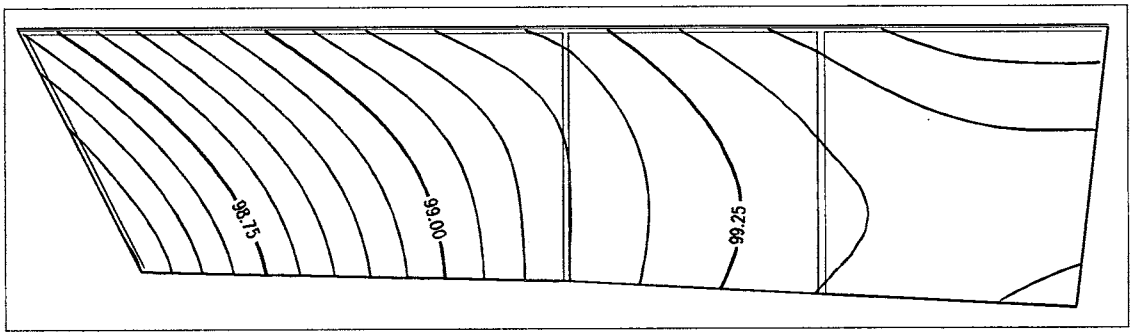

October 7, 1995

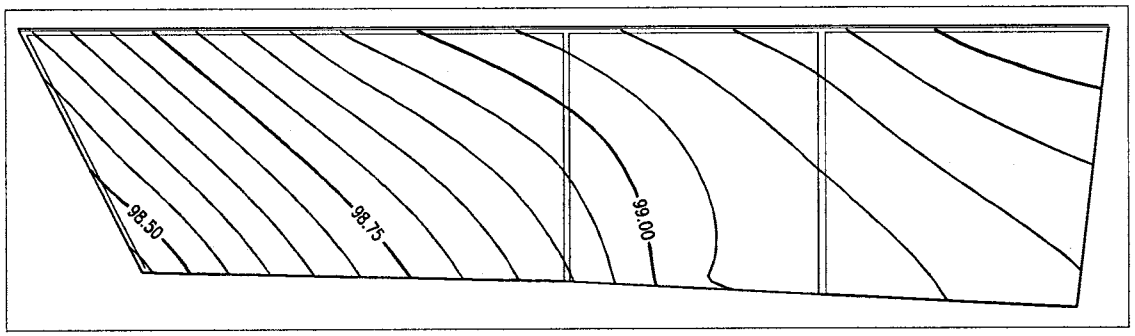

October 18, 1995

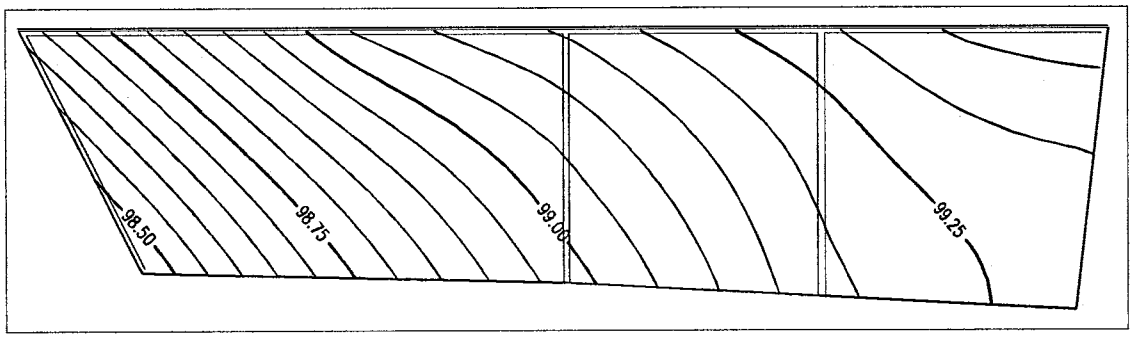

November 2, 1995

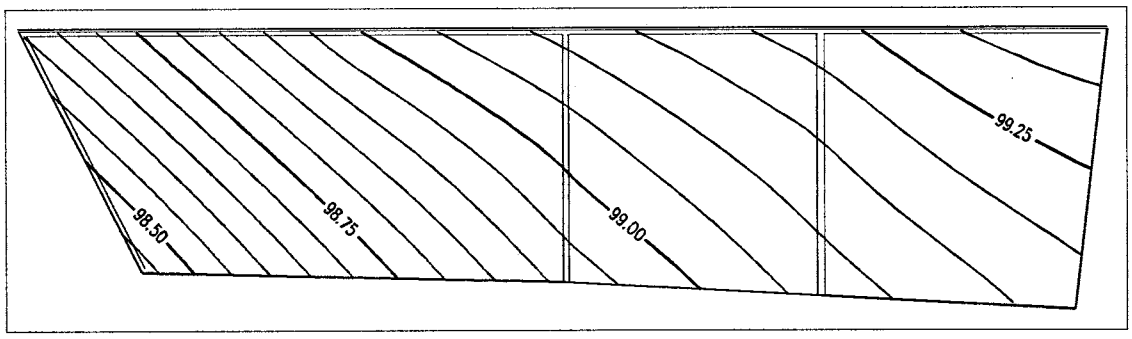

November 5, 1995

Contour interval 0.05 m, arbitrary vertical datum.

Appendix E5 (cont.) - Water Table Elevation Contour Maps

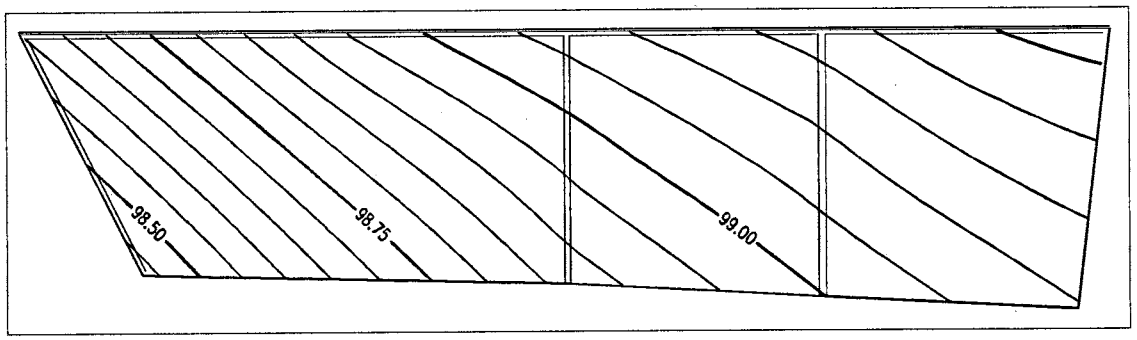

November 9, 1995

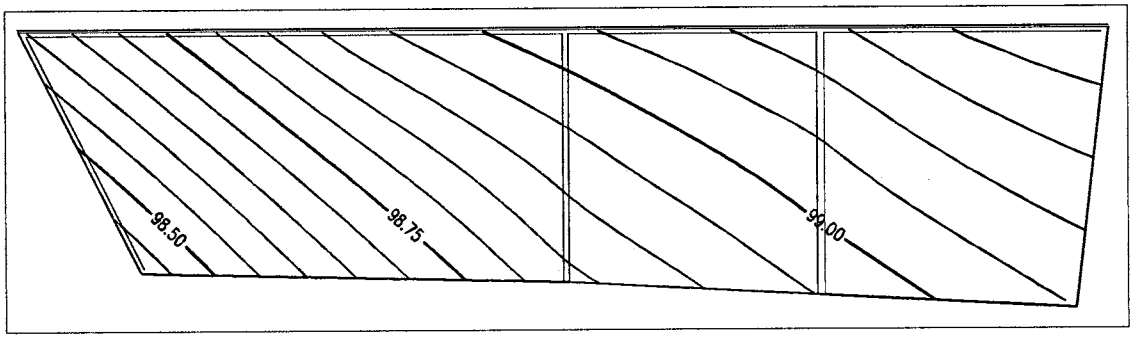

November 12, 1995

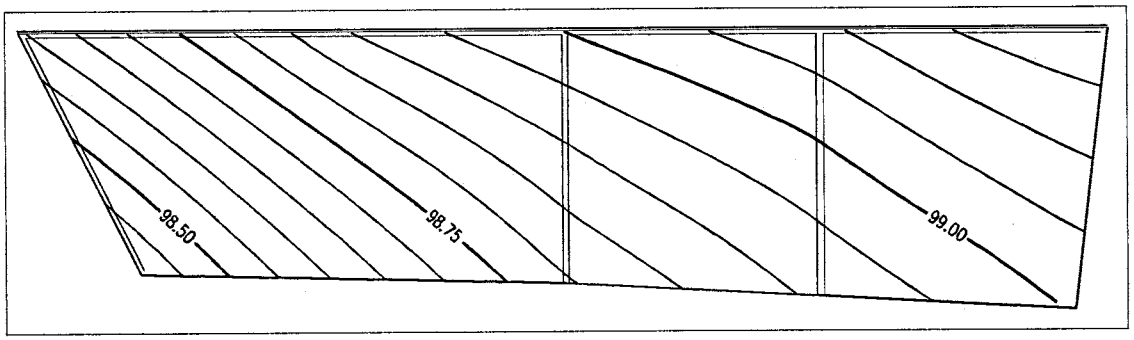

November 16, 1995

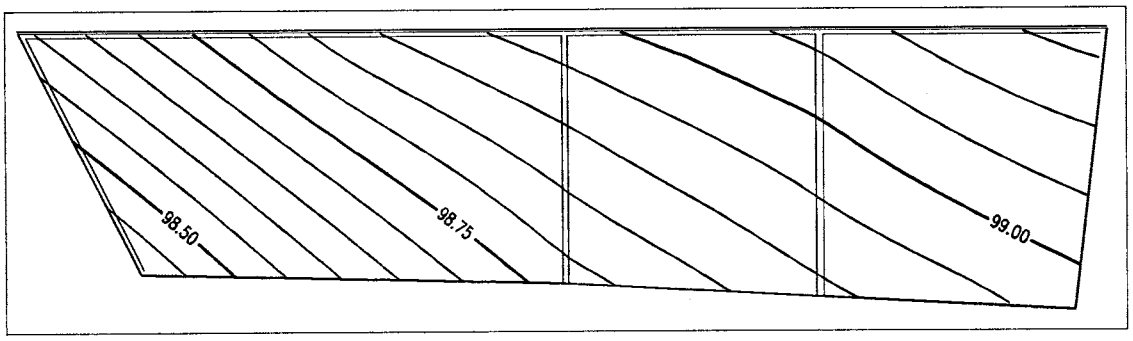

November 19, 1995

Contour interval 0.05 m, arbitrary vertical datum.

Appendix E5 (cont.) - Water Table Elevation Contour Maps

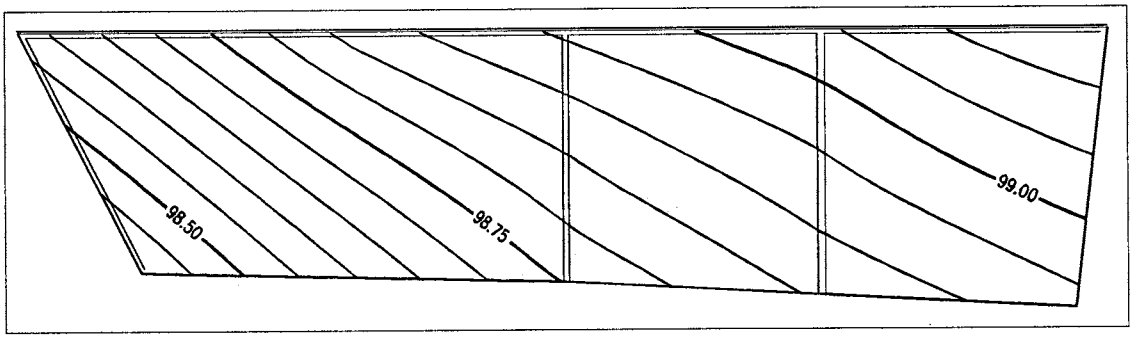

November 22, 1995

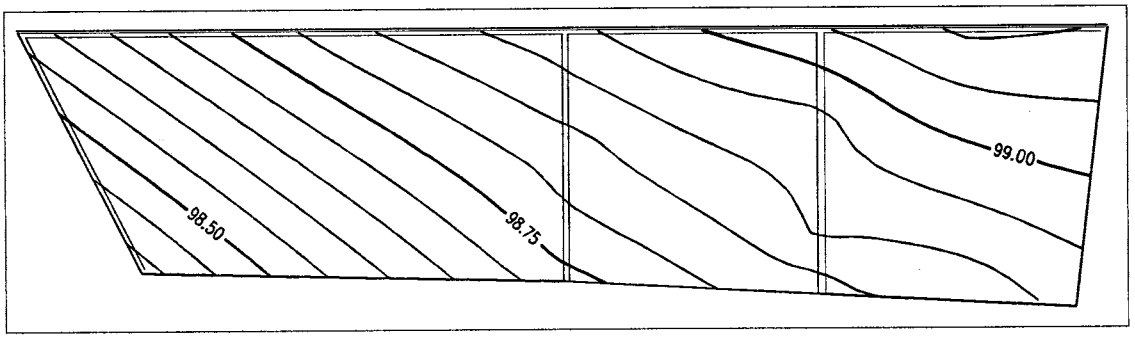

November 26, 1995

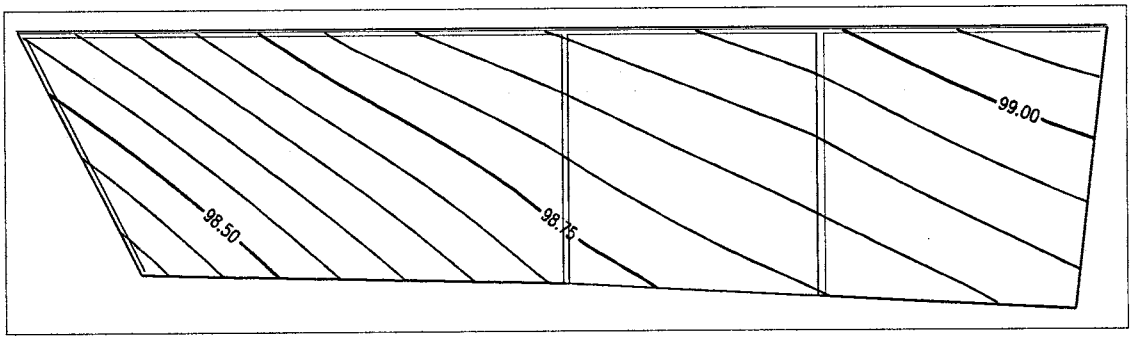

December 2, 1995

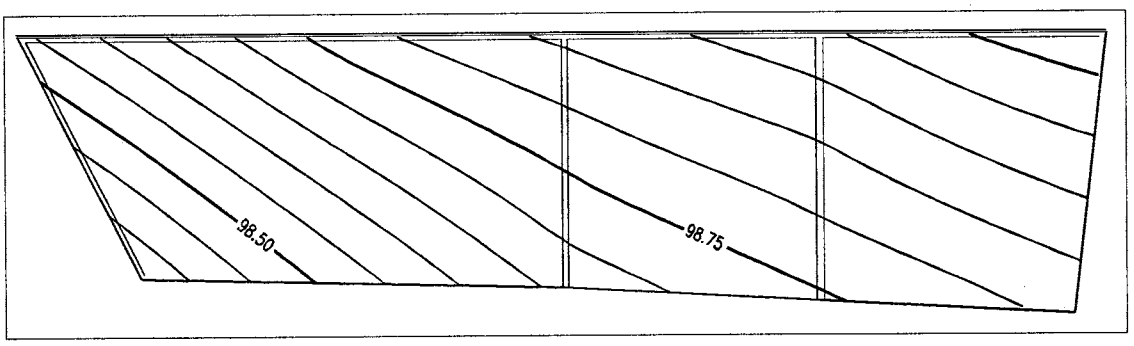

December 15, 1995

Contour interval 0.05 m, arbitrary vertical datum.

Appendix E5 (cont.) - Water Table Elevation Contour Maps

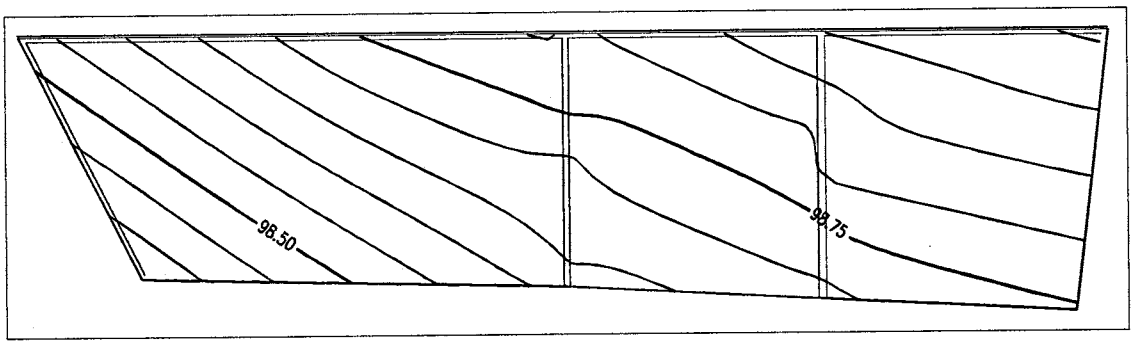

January 10, 1996

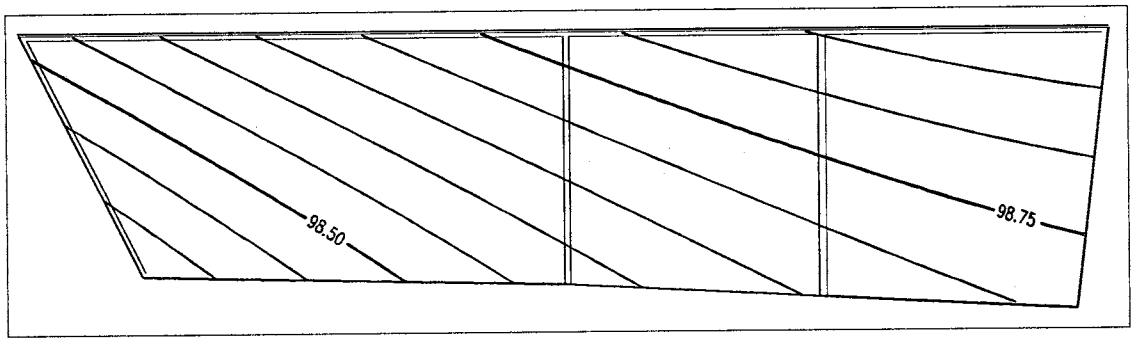

March 2, 1996

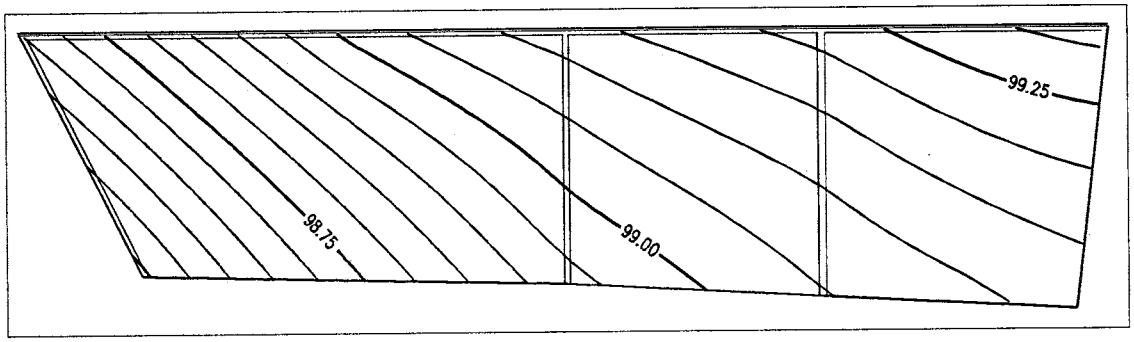

April 1, 1996

Contour interval 0.05 m, arbitrary vertical datum.

Appendix F1 - Pressure Transducer Calibration Data

The following table lists the calibration parameters for the pressure transducers used in the well slug tests:

Transducer	m (meters/volt)	b (meters)	r^2
1	0.716215	-0.161902	0.999985
2	0.704002	-0.013746	0.999991
3	0.704767	-0.080455	0.999999
4	0.706154	-0.115061	0.999980
5	0.712485	0.113358	0.999991

where:

$$y = mx + b$$

y = water depth (m)
x = pressure transducer voltage (v)

Appendix F2 - Slug Test Data

Monitoring Well 1A					
t (sec)	s (m)	t (sec)	s (m)	t (sec)	s (m)
0.0	0.000	22.0	0.086	61.0	0.014
0.5	-0.124	22.5	0.083	62.0	0.013
1.0	0.226	23.0	0.082	63.0	0.012
1.5	0.224	23.5	0.080	64.0	0.011
2.0	0.218	24.0	0.078	65.0	0.010
2.5	0.213	24.5	0.077	66.0	0.009
3.0	0.208	25.0	0.075	67.0	0.008
3.5	0.202	25.5	0.073	68.0	0.008
4.0	0.197	26.0	0.071	69.0	0.007
4.5	0.194	26.5	0.069	70.0	0.007
5.0	0.188	27.0	0.068	71.0	0.006
5.5	0.184	28.0	0.065	72.0	0.006
6.0	0.180	29.0	0.062	73.0	0.006
6.5	0.176	30.0	0.060	74.0	0.005
7.0	0.172	31.0	0.057	75.0	0.005
7.5	0.168	32.0	0.054	76.0	0.005
8.0	0.164	33.0	0.052	77.0	0.004
8.5	0.161	34.0	0.050	78.0	0.004
9.0	0.157	35.0	0.048	79.0	0.004
9.5	0.153	36.0	0.045	80.0	0.004
10.0	0.150	37.0	0.043	81.0	0.003
10.5	0.147	38.0	0.042	82.0	0.003
11.0	0.143	39.0	0.040	83.0	0.002
11.5	0.140	40.0	0.038	84.0	0.002
12.0	0.137	41.0	0.036	85.0	0.002
12.5	0.134	42.0	0.034	86.0	0.001
13.0	0.131	43.0	0.032	87.0	0.001
13.5	0.128	44.0	0.031	88.0	0.001
14.0	0.125	45.0	0.029	89.0	0.001
14.5	0.122	46.0	0.028	90.0	0.001
15.0	0.119	47.0	0.027	91.0	0.001
15.5	0.117	48.0	0.026	92.0	0.001
16.0	0.114	49.0	0.025	93.0	0.001
16.5	0.112	50.0	0.023	94.0	0.001
17.0	0.109	51.0	0.023	95.0	0.000
17.5	0.106	52.0	0.022	96.0	0.000
18.0	0.103	53.0	0.020	97.0	0.000
18.5	0.101	54.0	0.020		
19.0	0.099	55.0	0.018		
19.5	0.096	56.0	0.018		
20.0	0.094	57.0	0.017		
20.5	0.092	58.0	0.016		
21.0	0.090	59.0	0.015		
21.5	0.088	60.0	0.015		

Monitoring Well 2A			
t (sec)	s (m)	t (sec)	s (m)
0.0	0.000	22.0	0.035
0.5	-0.041	22.5	0.033
1.0	0.281	23.0	0.031
1.5	0.261	23.5	0.030
2.0	0.247	24.0	0.029
2.5	0.235	24.5	0.027
3.0	0.223	25.0	0.025
3.5	0.212	25.5	0.025
4.0	0.202	26.0	0.023
4.5	0.191	26.5	0.022
5.0	0.182	27.0	0.021
5.5	0.173	27.5	0.020
6.0	0.164	28.0	0.019
6.5	0.156	29.0	0.018
7.0	0.149	30.0	0.016
7.5	0.141	31.0	0.015
8.0	0.135	32.0	0.013
8.5	0.127	33.0	0.012
9.0	0.121	34.0	0.010
9.5	0.115	35.0	0.010
10.0	0.109	36.0	0.009
10.5	0.105	37.0	0.008
11.0	0.100	38.0	0.007
11.5	0.095	39.0	0.006
12.0	0.091	40.0	0.006
12.5	0.086	41.0	0.005
13.0	0.082	42.0	0.005
13.5	0.078	43.0	0.004
14.0	0.075	44.0	0.004
14.5	0.070	45.0	0.003
15.0	0.067	46.0	0.003
15.5	0.063	47.0	0.002
16.0	0.060	48.0	0.002
16.5	0.058	49.0	0.001
17.0	0.055	50.0	0.001
17.5	0.052	51.0	0.000
18.0	0.050	52.0	0.000
18.5	0.049	53.0	0.000
19.0	0.046		
19.5	0.044		
20.0	0.042		
20.5	0.040		
21.0	0.038		
21.5	0.037		

Appendix F2 (cont.) - Slug Test Data

Monitoring Well 3A									
t (sec)	s (m)	t (sec)	s (m)	t (sec)	s (m)	t (sec)	s (m)	t (sec)	s (m)
0.0	0.000	22.0	0.236	60.5	0.142	104.5	0.087	152.5	0.048
0.5	0.424	22.5	0.234	61.5	0.141	105.5	0.086	157.5	0.046
1.0	0.344	23.0	0.233	62.5	0.140	106.5	0.085	162.5	0.043
1.5	0.316	23.5	0.231	63.5	0.137	107.5	0.084	167.5	0.040
2.0	0.311	24.0	0.229	64.5	0.136	108.5	0.083	172.5	0.038
2.5	0.308	24.5	0.228	65.5	0.134	109.5	0.082	177.5	0.037
3.0	0.305	25.0	0.226	66.5	0.133	110.5	0.081	182.5	0.034
3.5	0.303	25.5	0.225	67.5	0.131	111.5	0.080	187.5	0.032
4.0	0.300	26.0	0.223	68.5	0.130	112.5	0.080	192.5	0.030
4.5	0.298	26.5	0.222	69.5	0.128	113.5	0.078	197.5	0.029
5.0	0.296	27.0	0.220	70.5	0.126	114.5	0.077	202.5	0.026
5.5	0.293	27.5	0.220	71.5	0.125	115.5	0.077	207.5	0.025
6.0	0.292	28.5	0.216	72.5	0.124	116.5	0.075	212.5	0.023
6.5	0.289	29.5	0.214	73.5	0.122	117.5	0.075	217.5	0.023
7.0	0.288	30.5	0.210	74.5	0.121	118.5	0.073	222.5	0.022
7.5	0.286	31.5	0.208	75.5	0.119	119.5	0.073	227.5	0.020
8.0	0.283	32.5	0.205	76.5	0.118	120.5	0.072	232.5	0.020
8.5	0.281	33.5	0.203	77.5	0.117	121.5	0.071	237.5	0.019
9.0	0.280	34.5	0.200	78.5	0.115	122.5	0.070	242.5	0.018
9.5	0.278	35.5	0.197	79.5	0.114	123.5	0.069	247.5	0.017
10.0	0.275	36.5	0.195	80.5	0.113	124.5	0.069	252.5	0.014
10.5	0.274	37.5	0.192	81.5	0.112	125.5	0.068	257.5	0.013
11.0	0.272	38.5	0.189	82.5	0.111	126.5	0.067	262.5	0.012
11.5	0.271	39.5	0.186	83.5	0.109	127.5	0.066	267.5	0.011
12.0	0.268	40.5	0.184	84.5	0.108	128.5	0.065	272.5	0.010
12.5	0.267	41.5	0.181	85.5	0.107	129.5	0.064	277.5	0.010
13.0	0.265	42.5	0.179	86.5	0.106	130.5	0.064	282.5	0.009
13.5	0.264	43.5	0.176	87.5	0.105	131.5	0.063	287.5	0.008
14.0	0.262	44.5	0.174	88.5	0.103	132.5	0.062	292.5	0.008
14.5	0.260	45.5	0.172	89.5	0.103	133.5	0.061	297.5	0.008
15.0	0.258	46.5	0.170	90.5	0.101	134.5	0.061	302.5	0.008
15.5	0.257	47.5	0.168	91.5	0.100	135.5	0.060	307.5	0.008
16.0	0.255	48.5	0.165	92.5	0.099	136.5	0.060	312.5	0.007
16.5	0.253	49.5	0.163	93.5	0.098	137.5	0.059	317.5	0.006
17.0	0.252	50.5	0.161	94.5	0.097	138.5	0.058	322.5	0.005
17.5	0.250	51.5	0.158	95.5	0.096	139.5	0.057	327.5	0.005
18.0	0.248	52.5	0.156	96.5	0.095	140.5	0.056	332.5	0.004
18.5	0.247	53.5	0.154	97.5	0.093	141.5	0.056	337.5	0.004
19.0	0.245	54.5	0.152	98.5	0.093	142.5	0.055	342.5	0.003
19.5	0.243	55.5	0.150	99.5	0.092	143.5	0.054	347.5	0.003
20.0	0.242	56.5	0.149	100.5	0.091	144.5	0.053	352.5	0.003
20.5	0.240	57.5	0.147	101.5	0.090	145.5	0.053	357.5	0.002
21.0	0.238	58.5	0.145	102.5	0.088	146.5	0.053	372.5	0.001
21.5	0.238	59.5	0.144	103.5	0.088	147.5	0.052	402.5	0.000

Appendix F2 (cont.) - Slug Test Data

Monitoring Well 4A									
t (sec)	s (m)	t (sec)	s (m)	t (sec)	s (m)	t (sec)	s (m)	t (sec)	s (m)
0.0	0.000	22.0	0.192	62.5	0.093	106.5	0.048	170.5	0.007
0.5	1.030	22.5	0.190	63.5	0.091	107.5	0.048	175.5	0.005
1.0	0.285	23.0	0.189	64.5	0.090	108.5	0.047	180.5	0.004
1.5	0.290	23.5	0.187	65.5	0.088	109.5	0.046	185.5	0.003
2.0	0.284	24.0	0.185	66.5	0.088	110.5	0.045	190.5	0.002
2.5	0.280	24.5	0.184	67.5	0.086	111.5	0.044	195.5	0.002
3.0	0.277	25.0	0.181	68.5	0.085	112.5	0.044	200.5	0.001
3.5	0.274	25.5	0.180	69.5	0.084	113.5	0.043	205.5	0.001
4.0	0.271	26.5	0.177	70.5	0.083	114.5	0.042	210.5	0.002
4.5	0.268	27.5	0.173	71.5	0.082	115.5	0.041	215.5	0.001
5.0	0.265	28.5	0.170	72.5	0.081	116.5	0.040	220.5	0.001
5.5	0.262	29.5	0.167	73.5	0.080	117.5	0.039	225.5	0.001
6.0	0.260	30.5	0.164	74.5	0.078	118.5	0.038	230.5	0.000
6.5	0.257	31.5	0.161	75.5	0.077	119.5	0.037		
7.0	0.255	32.5	0.158	76.5	0.076	120.5	0.037		
7.5	0.252	33.5	0.155	77.5	0.075	121.5	0.037		
8.0	0.249	34.5	0.151	78.5	0.074	122.5	0.035		
8.5	0.247	35.5	0.148	79.5	0.073	123.5	0.035		
9.0	0.245	36.5	0.145	80.5	0.073	124.5	0.034		
9.5	0.242	37.5	0.142	81.5	0.071	125.5	0.033		
10.0	0.240	38.5	0.140	82.5	0.070	126.5	0.032		
10.5	0.239	39.5	0.138	83.5	0.069	127.5	0.031		
11.0	0.236	40.5	0.135	84.5	0.068	128.5	0.030		
11.5	0.234	41.5	0.133	85.5	0.067	129.5	0.030		
12.0	0.232	42.5	0.130	86.5	0.066	130.5	0.029		
12.5	0.230	43.5	0.127	87.5	0.065	131.5	0.029		
13.0	0.227	44.5	0.125	88.5	0.065	132.5	0.028		
13.5	0.225	45.5	0.123	89.5	0.064	133.5	0.028		
14.0	0.223	46.5	0.120	90.5	0.063	134.5	0.027		
14.5	0.221	47.5	0.118	91.5	0.062	135.5	0.026		
15.0	0.219	48.5	0.117	92.5	0.061	136.5	0.025		
15.5	0.217	49.5	0.114	93.5	0.060	137.5	0.025		
16.0	0.215	50.5	0.112	94.5	0.060	138.5	0.024		
16.5	0.213	51.5	0.110	95.5	0.059	139.5	0.023		
17.0	0.212	52.5	0.109	96.5	0.059	140.5	0.022		
17.5	0.209	53.5	0.107	97.5	0.058	141.5	0.022		
18.0	0.207	54.5	0.105	98.5	0.057	142.5	0.022		
18.5	0.205	55.5	0.104	99.5	0.055	143.5	0.022		
19.0	0.203	56.5	0.102	100.5	0.055	144.5	0.021		
19.5	0.202	57.5	0.101	101.5	0.053	145.5	0.020		
20.0	0.200	58.5	0.099	102.5	0.053	150.5	0.017		
20.5	0.198	59.5	0.097	103.5	0.052	155.5	0.015		
21.0	0.196	60.5	0.095	104.5	0.051	160.5	0.012		
21.5	0.194	61.5	0.095	105.5	0.050	165.5	0.009		

Appendix F2 (cont.) - Slug Test Data

Monitoring Well 5A									
t (sec)	s (m)	t (sec)	s (m)	t (sec)	s (m)	t (sec)	s (m)	t (sec)	s (m)
0.0	0.000	22.0	0.176	60.5	0.047	104.5	0.013	152.5	0.006
0.5	0.430	22.5	0.173	61.5	0.045	105.5	0.012	157.5	0.005
1.0	0.337	23.0	0.170	62.5	0.043	106.5	0.012	162.5	0.003
1.5	0.329	23.5	0.167	63.5	0.043	107.5	0.012	167.5	0.001
2.0	0.323	24.0	0.165	64.5	0.042	108.5	0.012	172.5	0.000
2.5	0.318	24.5	0.162	65.5	0.040	109.5	0.012		
3.0	0.313	25.0	0.159	66.5	0.039	110.5	0.011		
3.5	0.308	25.5	0.157	67.5	0.037	111.5	0.011		
4.0	0.303	26.0	0.154	68.5	0.036	112.5	0.011		
4.5	0.299	26.5	0.151	69.5	0.035	113.5	0.011		
5.0	0.295	27.0	0.149	70.5	0.034	114.5	0.011		
5.5	0.291	27.5	0.146	71.5	0.032	115.5	0.011		
6.0	0.287	28.5	0.141	72.5	0.032	116.5	0.011		
6.5	0.282	29.5	0.137	73.5	0.031	117.5	0.011		
7.0	0.278	30.5	0.133	74.5	0.030	118.5	0.011		
7.5	0.273	31.5	0.127	75.5	0.030	119.5	0.010		
8.0	0.270	32.5	0.123	76.5	0.028	120.5	0.010		
8.5	0.266	33.5	0.118	77.5	0.027	121.5	0.010		
9.0	0.263	34.5	0.114	78.5	0.026	122.5	0.010		
9.5	0.259	35.5	0.110	79.5	0.026	123.5	0.009		
10.0	0.255	36.5	0.107	80.5	0.025	124.5	0.009		
10.5	0.251	37.5	0.103	81.5	0.024	125.5	0.009		
11.0	0.247	38.5	0.100	82.5	0.023	126.5	0.008		
11.5	0.243	39.5	0.096	83.5	0.023	127.5	0.008		
12.0	0.240	40.5	0.093	84.5	0.022	128.5	0.008		
12.5	0.236	41.5	0.089	85.5	0.022	129.5	0.008		
13.0	0.232	42.5	0.087	86.5	0.022	130.5	0.008		
13.5	0.229	43.5	0.084	87.5	0.021	131.5	0.008		
14.0	0.225	44.5	0.081	88.5	0.021	132.5	0.008		
14.5	0.222	45.5	0.078	89.5	0.020	133.5	0.008		
15.0	0.219	46.5	0.075	90.5	0.019	134.5	0.008		
15.5	0.215	47.5	0.073	91.5	0.019	135.5	0.008		
16.0	0.213	48.5	0.070	92.5	0.018	136.5	0.007		
16.5	0.209	49.5	0.068	93.5	0.018	137.5	0.007		
17.0	0.205	50.5	0.065	94.5	0.018	138.5	0.008		
17.5	0.202	51.5	0.063	95.5	0.017	139.5	0.007		
18.0	0.200	52.5	0.061	96.5	0.017	140.5	0.007		
18.5	0.196	53.5	0.059	97.5	0.016	141.5	0.007		
19.0	0.194	54.5	0.057	98.5	0.015	142.5	0.007		
19.5	0.190	55.5	0.055	99.5	0.015	143.5	0.007		
20.0	0.187	56.5	0.053	100.5	0.015	144.5	0.007		
20.5	0.184	57.5	0.052	101.5	0.014	145.5	0.007		
21.0	0.181	58.5	0.051	102.5	0.014	146.5	0.007		
21.5	0.179	59.5	0.048	103.5	0.013	147.5	0.006		

Appendix F2 (cont.) - Slug Test Data

Monitoring Well 6A											
t (sec)	s (m)	t (sec)	s (m)	t (sec)	s (m)	t (sec)	s (m)	t (sec)	s (m)	t (sec)	s (m)
0.0	0.000	22.0	0.308	64.0	0.237	108.0	0.167	184.0	0.098	504.0	0.023
0.5	0.531	22.5	0.307	65.0	0.235	109.0	0.165	189.0	0.094	519.0	0.021
1.0	0.405	23.0	0.306	66.0	0.233	110.0	0.164	194.0	0.089	534.0	0.016
1.5	0.367	23.5	0.306	67.0	0.232	111.0	0.162	199.0	0.086	549.0	0.010
2.0	0.367	24.0	0.305	68.0	0.230	112.0	0.162	204.0	0.082	564.0	0.010
2.5	0.351	25.0	0.303	69.0	0.228	113.0	0.161	209.0	0.078	579.0	0.010
3.0	0.357	26.0	0.302	70.0	0.226	114.0	0.160	214.0	0.074	594.0	0.006
3.5	0.352	27.0	0.299	71.0	0.225	115.0	0.158	219.0	0.072	609.0	0.003
4.0	0.350	28.0	0.297	72.0	0.223	116.0	0.158	224.0	0.071	624.0	0.000
4.5	0.356	29.0	0.296	73.0	0.221	117.0	0.156	229.0	0.069		
5.0	0.348	30.0	0.294	74.0	0.220	118.0	0.155	234.0	0.067		
5.5	0.346	31.0	0.293	75.0	0.218	119.0	0.154	239.0	0.064		
6.0	0.344	32.0	0.291	76.0	0.217	120.0	0.153	244.0	0.061		
6.5	0.342	33.0	0.289	77.0	0.215	121.0	0.152	249.0	0.061		
7.0	0.341	34.0	0.287	78.0	0.213	122.0	0.151	254.0	0.059		
7.5	0.340	35.0	0.285	79.0	0.211	123.0	0.150	259.0	0.059		
8.0	0.339	36.0	0.284	80.0	0.209	124.0	0.148	264.0	0.057		
8.5	0.339	37.0	0.281	81.0	0.207	125.0	0.147	269.0	0.056		
9.0	0.336	38.0	0.281	82.0	0.206	126.0	0.146	274.0	0.056		
9.5	0.335	39.0	0.279	83.0	0.205	127.0	0.144	279.0	0.053		
10.0	0.334	40.0	0.277	84.0	0.202	128.0	0.144	284.0	0.051		
10.5	0.333	41.0	0.275	85.0	0.201	129.0	0.143	289.0	0.048		
11.0	0.332	42.0	0.273	86.0	0.199	130.0	0.142	294.0	0.046		
11.5	0.330	43.0	0.272	87.0	0.198	131.0	0.141	299.0	0.042		
12.0	0.329	44.0	0.269	88.0	0.197	132.0	0.139	304.0	0.039		
12.5	0.328	45.0	0.268	89.0	0.196	133.0	0.138	309.0	0.038		
13.0	0.326	46.0	0.266	90.0	0.194	134.0	0.137	314.0	0.037		
13.5	0.326	47.0	0.265	91.0	0.193	135.0	0.136	319.0	0.035		
14.0	0.325	48.0	0.263	92.0	0.190	136.0	0.135	324.0	0.032		
14.5	0.323	49.0	0.261	93.0	0.188	137.0	0.134	329.0	0.030		
15.0	0.322	50.0	0.259	94.0	0.187	138.0	0.133	334.0	0.027		
15.5	0.321	51.0	0.258	95.0	0.185	139.0	0.132	339.0	0.026		
16.0	0.320	52.0	0.256	96.0	0.183	140.0	0.131	344.0	0.024		
16.5	0.319	53.0	0.254	97.0	0.182	141.0	0.129	349.0	0.023		
17.0	0.319	54.0	0.253	98.0	0.181	142.0	0.129	354.0	0.024		
17.5	0.317	55.0	0.251	99.0	0.179	143.0	0.128	369.0	0.025		
18.0	0.316	56.0	0.250	100.0	0.178	144.0	0.127	384.0	0.026		
18.5	0.314	57.0	0.249	101.0	0.176	149.0	0.123	399.0	0.027		
19.0	0.314	58.0	0.247	102.0	0.175	154.0	0.120	414.0	0.026		
19.5	0.313	59.0	0.245	103.0	0.174	159.0	0.117	429.0	0.028		
20.0	0.312	60.0	0.243	104.0	0.172	164.0	0.113	444.0	0.025		
20.5	0.311	61.0	0.242	105.0	0.171	169.0	0.110	459.0	0.025		
21.0	0.310	62.0	0.240	106.0	0.169	174.0	0.107	474.0	0.026		
21.5	0.309	63.0	0.238	107.0	0.168	179.0	0.102	489.0	0.025		

Appendix F2 (cont.) - Slug Test Data

Monitoring Well 7A									
t (sec)	s (m)	t (sec)	s (m)	t (sec)	s (m)	t (sec)	s (m)	t (sec)	s (m)
0.0	0.000	22.0	0.221	61.5	0.115	105.5	0.060	161.5	0.029
0.5	0.419	22.5	0.219	62.5	0.113	106.5	0.059	166.5	0.027
1.0	0.320	23.0	0.218	63.5	0.112	107.5	0.058	171.5	0.024
1.5	0.316	23.5	0.217	64.5	0.109	108.5	0.058	176.5	0.023
2.0	0.312	24.0	0.214	65.5	0.107	109.5	0.057	181.5	0.023
2.5	0.309	24.5	0.212	66.5	0.106	110.5	0.056	186.5	0.022
3.0	0.305	25.0	0.211	67.5	0.104	111.5	0.055	191.5	0.020
3.5	0.303	25.5	0.209	68.5	0.102	112.5	0.055	196.5	0.018
4.0	0.299	26.0	0.207	69.5	0.101	113.5	0.053	201.5	0.016
4.5	0.296	26.5	0.205	70.5	0.100	114.5	0.053	206.5	0.015
5.0	0.294	27.5	0.202	71.5	0.099	115.5	0.052	211.5	0.014
5.5	0.291	28.5	0.199	72.5	0.097	116.5	0.052	216.5	0.013
6.0	0.289	29.5	0.195	73.5	0.095	117.5	0.051	221.5	0.011
6.5	0.286	30.5	0.192	74.5	0.094	118.5	0.050	226.5	0.010
7.0	0.283	31.5	0.189	75.5	0.092	119.5	0.050	231.5	0.009
7.5	0.281	32.5	0.185	76.5	0.091	120.5	0.049	236.5	0.008
8.0	0.279	33.5	0.182	77.5	0.090	121.5	0.049	241.5	0.008
8.5	0.276	34.5	0.180	78.5	0.089	122.5	0.048	246.5	0.007
9.0	0.274	35.5	0.176	79.5	0.087	123.5	0.047	251.5	0.006
9.5	0.272	36.5	0.174	80.5	0.086	124.5	0.047	256.5	0.004
10.0	0.270	37.5	0.171	81.5	0.085	125.5	0.046	261.5	0.003
10.5	0.268	38.5	0.168	82.5	0.083	126.5	0.046	266.5	0.001
11.0	0.265	39.5	0.166	83.5	0.083	127.5	0.045	271.5	0.001
11.5	0.263	40.5	0.162	84.5	0.081	128.5	0.045	276.5	0.000
12.0	0.261	41.5	0.159	85.5	0.080	129.5	0.044		
12.5	0.259	42.5	0.157	86.5	0.079	130.5	0.044		
13.0	0.257	43.5	0.154	87.5	0.078	131.5	0.043		
13.5	0.254	44.5	0.152	88.5	0.077	132.5	0.042		
14.0	0.253	45.5	0.150	89.5	0.075	133.5	0.042		
14.5	0.250	46.5	0.146	90.5	0.075	134.5	0.042		
15.0	0.249	47.5	0.145	91.5	0.073	135.5	0.040		
15.5	0.246	48.5	0.142	92.5	0.072	136.5	0.040		
16.0	0.245	49.5	0.140	93.5	0.071	137.5	0.040		
16.5	0.242	50.5	0.137	94.5	0.070	138.5	0.039		
17.0	0.240	51.5	0.136	95.5	0.068	139.5	0.039		
17.5	0.239	52.5	0.133	96.5	0.068	140.5	0.038		
18.0	0.236	53.5	0.131	97.5	0.067	141.5	0.037		
18.5	0.234	54.5	0.129	98.5	0.066	142.5	0.037		
19.0	0.233	55.5	0.127	99.5	0.065	143.5	0.037		
19.5	0.231	56.5	0.124	100.5	0.064	144.5	0.035		
20.0	0.229	57.5	0.122	101.5	0.062	145.5	0.035		
20.5	0.227	58.5	0.120	102.5	0.062	146.5	0.035		
21.0	0.226	59.5	0.119	103.5	0.061	151.5	0.032		
21.5	0.224	60.5	0.117	104.5	0.060	156.5	0.030		

Appendix F2 (cont.) - Slug Test Data

Monitoring Well 8A					
t (sec)	s (m)	t (sec)	s (m)	t (sec)	s (m)
0.0	0.000	22.0	0.040	62.0	0.002
0.5	0.270	22.5	0.038	63.0	0.002
1.0	0.250	23.0	0.037	64.0	0.002
1.5	0.238	23.5	0.036	65.0	0.002
2.0	0.228	24.0	0.033	66.0	0.002
2.5	0.218	24.5	0.032	67.0	0.001
3.0	0.207	25.0	0.031	68.0	0.001
3.5	0.199	25.5	0.029	69.0	0.001
4.0	0.191	26.0	0.027	70.0	0.001
4.5	0.182	27.0	0.026	71.0	0.001
5.0	0.174	28.0	0.024	72.0	0.001
5.5	0.167	29.0	0.022	73.0	0.001
6.0	0.160	30.0	0.020	74.0	0.001
6.5	0.152	31.0	0.018	75.0	0.001
7.0	0.146	32.0	0.017	76.0	0.001
7.5	0.140	33.0	0.016	77.0	0.000
8.0	0.134	34.0	0.014		
8.5	0.128	35.0	0.013		
9.0	0.123	36.0	0.012		
9.5	0.117	37.0	0.011		
10.0	0.112	38.0	0.010		
10.5	0.107	39.0	0.009		
11.0	0.103	40.0	0.009		
11.5	0.098	41.0	0.008		
12.0	0.094	42.0	0.007		
12.5	0.090	43.0	0.007		
13.0	0.086	44.0	0.007		
13.5	0.082	45.0	0.007		
14.0	0.079	46.0	0.007		
14.5	0.075	47.0	0.006		
15.0	0.072	48.0	0.005		
15.5	0.069	49.0	0.005		
16.0	0.066	50.0	0.004		
16.5	0.063	51.0	0.004		
17.0	0.061	52.0	0.003		
17.5	0.058	53.0	0.003		
18.0	0.055	54.0	0.003		
18.5	0.053	55.0	0.003		
19.0	0.051	56.0	0.003		
19.5	0.049	57.0	0.003		
20.0	0.047	58.0	0.002		
20.5	0.045	59.0	0.002		
21.0	0.043	60.0	0.003		
21.5	0.041	61.0	0.002		

Monitoring Well 9A					
t (sec)	s (m)	t (sec)	s (m)	t (sec)	s (m)
0.0	0.000	22.0	0.086	62.5	0.005
0.5	0.259	22.5	0.082	63.5	0.004
1.0	0.401	23.0	0.079	64.5	0.004
1.5	0.427	23.5	0.076	65.5	0.004
2.0	0.400	24.0	0.074	66.5	0.003
2.5	0.383	24.5	0.071	67.5	0.003
3.0	0.366	25.0	0.069	68.5	0.002
3.5	0.351	25.5	0.067	69.5	0.002
4.0	0.336	26.5	0.062	70.5	0.002
4.5	0.323	27.5	0.058	71.5	0.002
5.0	0.310	28.5	0.053	72.5	0.002
5.5	0.298	29.5	0.050	73.5	0.001
6.0	0.287	30.5	0.047	74.5	0.001
6.5	0.276	31.5	0.044	75.5	0.001
7.0	0.265	32.5	0.041	76.5	0.001
7.5	0.255	33.5	0.038	77.5	0.000
8.0	0.245	34.5	0.036		
8.5	0.236	35.5	0.034		
9.0	0.227	36.5	0.031		
9.5	0.218	37.5	0.029		
10.0	0.209	38.5	0.028		
10.5	0.201	39.5	0.026		
11.0	0.194	40.5	0.024		
11.5	0.187	41.5	0.023		
12.0	0.179	42.5	0.022		
12.5	0.172	43.5	0.020		
13.0	0.166	44.5	0.019		
13.5	0.159	45.5	0.018		
14.0	0.154	46.5	0.017		
14.5	0.149	47.5	0.016		
15.0	0.142	48.5	0.015		
15.5	0.137	49.5	0.014		
16.0	0.132	50.5	0.013		
16.5	0.127	51.5	0.012		
17.0	0.123	52.5	0.011		
17.5	0.118	53.5	0.011		
18.0	0.114	54.5	0.009		
18.5	0.110	55.5	0.009		
19.0	0.105	56.5	0.008		
19.5	0.102	57.5	0.008		
20.0	0.098	58.5	0.006		
20.5	0.095	59.5	0.006		
21.0	0.092	60.5	0.006		
21.5	0.089	61.5	0.005		

Appendix F2 (cont.) - Slug Test Data

Monitoring Well 10A							
t (sec)	s (m)	t (sec)	s (m)	t (sec)	s (m)	t (sec)	s (m)
0.0	0.000	22.0	0.158	60.5	0.029	104.5	0.003
0.5	1.802	22.5	0.155	61.5	0.028	105.5	0.002
1.0	0.451	23.0	0.152	62.5	0.027	106.5	0.002
1.5	0.418	23.5	0.148	63.5	0.025	107.5	0.002
2.0	0.404	24.0	0.145	64.5	0.024	108.5	0.002
2.5	0.393	24.5	0.142	65.5	0.023	109.5	0.001
3.0	0.382	25.0	0.139	66.5	0.023	110.5	0.001
3.5	0.373	25.5	0.135	67.5	0.021	111.5	0.000
4.0	0.364	26.0	0.133	68.5	0.021		
4.5	0.355	26.5	0.129	69.5	0.019		
5.0	0.347	27.0	0.126	70.5	0.019		
5.5	0.339	27.5	0.124	71.5	0.017		
6.0	0.331	28.5	0.118	72.5	0.017		
6.5	0.322	29.5	0.113	73.5	0.017		
7.0	0.315	30.5	0.109	74.5	0.016		
7.5	0.308	31.5	0.104	75.5	0.015		
8.0	0.301	32.5	0.099	76.5	0.014		
8.5	0.294	33.5	0.095	77.5	0.014		
9.0	0.286	34.5	0.091	78.5	0.013		
9.5	0.281	35.5	0.088	79.5	0.013		
10.0	0.274	36.5	0.084	80.5	0.012		
10.5	0.268	37.5	0.080	81.5	0.012		
11.0	0.261	38.5	0.076	82.5	0.011		
11.5	0.256	39.5	0.073	83.5	0.011		
12.0	0.250	40.5	0.071	84.5	0.010		
12.5	0.245	41.5	0.067	85.5	0.009		
13.0	0.239	42.5	0.064	86.5	0.009		
13.5	0.234	43.5	0.061	87.5	0.009		
14.0	0.228	44.5	0.058	88.5	0.008		
14.5	0.223	45.5	0.057	89.5	0.008		
15.0	0.218	46.5	0.054	90.5	0.008		
15.5	0.213	47.5	0.051	91.5	0.008		
16.0	0.208	48.5	0.049	92.5	0.007		
16.5	0.204	49.5	0.047	93.5	0.007		
17.0	0.199	50.5	0.045	94.5	0.006		
17.5	0.195	51.5	0.043	95.5	0.006		
18.0	0.190	52.5	0.041	96.5	0.006		
18.5	0.186	53.5	0.039	97.5	0.006		
19.0	0.182	54.5	0.038	98.5	0.005		
19.5	0.178	55.5	0.036	99.5	0.005		
20.0	0.174	56.5	0.034	100.5	0.004		
20.5	0.170	57.5	0.033	101.5	0.004		
21.0	0.166	58.5	0.031	102.5	0.004		
21.5	0.162	59.5	0.030	103.5	0.004		

Appendix F2 (cont.) - Slug Test Data

Monitoring Well 11A									
t (sec)	s (m)	t (sec)	s (m)	t (sec)	s (m)	t (sec)	s (m)	t (sec)	s (m)
0.0	0.000	22.0	0.253	60.0	0.097	104.0	0.030	148.0	0.008
0.5	0.493	22.5	0.250	61.0	0.095	105.0	0.029	153.0	0.006
1.0	0.409	23.0	0.246	62.0	0.093	106.0	0.028	158.0	0.005
1.5	0.402	23.5	0.244	63.0	0.090	107.0	0.027	163.0	0.003
2.0	0.397	24.0	0.241	64.0	0.088	108.0	0.027	168.0	0.001
2.5	0.393	24.5	0.238	65.0	0.086	109.0	0.027	173.0	0.000
3.0	0.388	25.0	0.236	66.0	0.083	110.0	0.025		
3.5	0.383	25.5	0.232	67.0	0.082	111.0	0.025		
4.0	0.379	26.0	0.230	68.0	0.080	112.0	0.023		
4.5	0.375	26.5	0.227	69.0	0.077	113.0	0.023		
5.0	0.370	27.0	0.224	70.0	0.075	114.0	0.023		
5.5	0.366	27.5	0.222	71.0	0.074	115.0	0.022		
6.0	0.362	28.0	0.218	72.0	0.072	116.0	0.022		
6.5	0.358	29.0	0.213	73.0	0.070	117.0	0.020		
7.0	0.354	30.0	0.208	74.0	0.068	118.0	0.020		
7.5	0.350	31.0	0.202	75.0	0.066	119.0	0.020		
8.0	0.346	32.0	0.198	76.0	0.065	120.0	0.019		
8.5	0.342	33.0	0.192	77.0	0.062	121.0	0.020		
9.0	0.339	34.0	0.188	78.0	0.060	122.0	0.018		
9.5	0.335	35.0	0.183	79.0	0.059	123.0	0.017		
10.0	0.331	36.0	0.179	80.0	0.058	124.0	0.017		
10.5	0.327	37.0	0.175	81.0	0.057	125.0	0.017		
11.0	0.324	38.0	0.170	82.0	0.055	126.0	0.016		
11.5	0.320	39.0	0.166	83.0	0.053	127.0	0.016		
12.0	0.317	40.0	0.162	84.0	0.052	128.0	0.015		
12.5	0.313	41.0	0.157	85.0	0.050	129.0	0.015		
13.0	0.310	42.0	0.153	86.0	0.050	130.0	0.014		
13.5	0.307	43.0	0.150	87.0	0.048	131.0	0.014		
14.0	0.303	44.0	0.146	88.0	0.047	132.0	0.013		
14.5	0.299	45.0	0.142	89.0	0.045	133.0	0.013		
15.0	0.296	46.0	0.139	90.0	0.044	134.0	0.013		
15.5	0.293	47.0	0.134	91.0	0.043	135.0	0.012		
16.0	0.290	48.0	0.131	92.0	0.042	136.0	0.012		
16.5	0.287	49.0	0.128	93.0	0.040	137.0	0.011		
17.0	0.282	50.0	0.125	94.0	0.040	138.0	0.011		
17.5	0.280	51.0	0.122	95.0	0.038	139.0	0.010		
18.0	0.277	52.0	0.119	96.0	0.037	140.0	0.010		
18.5	0.274	53.0	0.115	97.0	0.036	141.0	0.010		
19.0	0.270	54.0	0.113	98.0	0.035	142.0	0.010		
19.5	0.267	55.0	0.110	99.0	0.034	143.0	0.009		
20.0	0.265	56.0	0.107	100.0	0.034	144.0	0.009		
20.5	0.262	57.0	0.104	101.0	0.032	145.0	0.008		
21.0	0.259	58.0	0.102	102.0	0.031	146.0	0.008		
21.5	0.256	59.0	0.099	103.0	0.030	147.0	0.008		

Appendix F2 (cont.) - Slug Test Data

Monitoring Well 12A											
t (sec)	s (m)	t (sec)	s (m)	t (sec)	s (m)	t (sec)	s (m)	t (sec)	s (m)	t (sec)	s (m)
0.0	0.000	22.0	0.207	63.0	0.173	107.0	0.141	175.0	0.102	475.0	0.013
0.5	0.730	22.5	0.207	64.0	0.173	108.0	0.139	180.0	0.099	490.0	0.010
1.0	0.299	23.0	0.206	65.0	0.173	109.0	0.136	185.0	0.097	505.0	0.012
1.5	0.265	23.5	0.206	66.0	0.171	110.0	0.133	190.0	0.094	520.0	0.012
2.0	0.259	24.0	0.205	67.0	0.171	111.0	0.132	195.0	0.091	535.0	0.011
2.5	0.250	24.5	0.204	68.0	0.170	112.0	0.132	200.0	0.088	550.0	0.010
3.0	0.189	25.0	0.204	69.0	0.169	113.0	0.132	205.0	0.084	565.0	0.009
3.5	0.189	26.0	0.204	70.0	0.168	114.0	0.131	210.0	0.082	580.0	0.008
4.0	0.184	27.0	0.203	71.0	0.166	115.0	0.131	215.0	0.079	595.0	0.008
4.5	0.194	28.0	0.203	72.0	0.166	116.0	0.131	220.0	0.076	610.0	0.008
5.0	0.199	29.0	0.203	73.0	0.166	117.0	0.131	225.0	0.078	625.0	0.006
5.5	0.203	30.0	0.201	74.0	0.166	118.0	0.130	230.0	0.075	640.0	0.005
6.0	0.204	31.0	0.201	75.0	0.165	119.0	0.129	235.0	0.074	655.0	0.004
6.5	0.206	32.0	0.200	76.0	0.164	120.0	0.129	240.0	0.071	670.0	0.003
7.0	0.207	33.0	0.198	77.0	0.164	121.0	0.129	245.0	0.068	685.0	0.002
7.5	0.208	34.0	0.197	78.0	0.164	122.0	0.129	250.0	0.066	700.0	0.000
8.0	0.209	35.0	0.196	79.0	0.164	123.0	0.128	255.0	0.063		
8.5	0.209	36.0	0.196	80.0	0.163	124.0	0.128	260.0	0.061		
9.0	0.209	37.0	0.195	81.0	0.162	125.0	0.127	265.0	0.060		
9.5	0.210	38.0	0.194	82.0	0.162	126.0	0.127	270.0	0.057		
10.0	0.210	39.0	0.193	83.0	0.161	127.0	0.126	275.0	0.056		
10.5	0.211	40.0	0.192	84.0	0.160	128.0	0.126	280.0	0.054		
11.0	0.211	41.0	0.192	85.0	0.159	129.0	0.126	285.0	0.053		
11.5	0.211	42.0	0.189	86.0	0.159	130.0	0.126	290.0	0.053		
12.0	0.211	43.0	0.189	87.0	0.159	131.0	0.126	295.0	0.057		
12.5	0.211	44.0	0.188	88.0	0.158	132.0	0.126	300.0	0.057		
13.0	0.211	45.0	0.187	89.0	0.157	133.0	0.126	305.0	0.055		
13.5	0.211	46.0	0.186	90.0	0.157	134.0	0.126	310.0	0.053		
14.0	0.211	47.0	0.186	91.0	0.157	135.0	0.126	315.0	0.051		
14.5	0.211	48.0	0.185	92.0	0.157	136.0	0.126	320.0	0.049		
15.0	0.211	49.0	0.186	93.0	0.156	137.0	0.126	325.0	0.045		
15.5	0.211	50.0	0.186	94.0	0.154	138.0	0.126	330.0	0.042		
16.0	0.211	51.0	0.184	95.0	0.153	139.0	0.126	335.0	0.038		
16.5	0.210	52.0	0.183	96.0	0.152	140.0	0.127	340.0	0.033		
17.0	0.210	53.0	0.182	97.0	0.152	141.0	0.127	345.0	0.030		
17.5	0.209	54.0	0.181	98.0	0.151	142.0	0.127	350.0	0.029		
18.0	0.209	55.0	0.181	99.0	0.150	143.0	0.127	355.0	0.027		
18.5	0.209	56.0	0.180	100.0	0.150	144.0	0.126	370.0	0.027		
19.0	0.209	57.0	0.179	101.0	0.149	145.0	0.126	385.0	0.027		
19.5	0.208	58.0	0.178	102.0	0.147	150.0	0.123	400.0	0.023		
20.0	0.208	59.0	0.177	103.0	0.147	155.0	0.120	415.0	0.021		
20.5	0.207	60.0	0.176	104.0	0.145	160.0	0.116	430.0	0.020		
21.0	0.207	61.0	0.174	105.0	0.144	165.0	0.112	445.0	0.018		
21.5	0.207	62.0	0.174	106.0	0.143	170.0	0.106	460.0	0.016		

Appendix F2 (cont.) - Slug Test Data

Monitoring Well 13A									
t (sec)	s (m)	t (sec)	s (m)	t (sec)	s (m)	t (sec)	s (m)	t (sec)	s (m)
0.0	0.000	22.0	0.224	60.5	0.065	104.5	0.018	152.5	0.008
0.5	1.807	22.5	0.221	61.5	0.062	105.5	0.017	157.5	0.008
1.0	0.465	23.0	0.219	62.5	0.060	106.5	0.017	162.5	0.008
1.5	0.417	23.5	0.216	63.5	0.058	107.5	0.017	167.5	0.008
2.0	0.406	24.0	0.213	64.5	0.057	108.5	0.017	172.5	0.007
2.5	0.396	24.5	0.210	65.5	0.054	109.5	0.017	177.5	0.008
3.0	0.386	25.0	0.208	66.5	0.054	110.5	0.016	182.5	0.008
3.5	0.377	25.5	0.205	67.5	0.051	111.5	0.017	187.5	0.008
4.0	0.369	26.0	0.202	68.5	0.050	112.5	0.016	192.5	0.008
4.5	0.363	26.5	0.200	69.5	0.049	113.5	0.016	197.5	0.008
5.0	0.356	27.0	0.197	70.5	0.047	114.5	0.016	202.5	0.008
5.5	0.351	27.5	0.195	71.5	0.046	115.5	0.016	207.5	0.008
6.0	0.345	28.5	0.189	72.5	0.044	116.5	0.015	212.5	0.008
6.5	0.340	29.5	0.184	73.5	0.042	117.5	0.015	217.5	0.007
7.0	0.334	30.5	0.179	74.5	0.042	118.5	0.015	222.5	0.006
7.5	0.327	31.5	0.174	75.5	0.040	119.5	0.014	227.5	0.006
8.0	0.322	32.5	0.168	76.5	0.039	120.5	0.014	232.5	0.005
8.5	0.318	33.5	0.164	77.5	0.038	121.5	0.013	237.5	0.004
9.0	0.313	34.5	0.159	78.5	0.037	122.5	0.013	242.5	0.003
9.5	0.308	35.5	0.153	79.5	0.035	123.5	0.013	247.5	0.003
10.0	0.304	36.5	0.150	80.5	0.034	124.5	0.012	252.5	0.002
10.5	0.300	37.5	0.144	81.5	0.033	125.5	0.012	257.5	0.002
11.0	0.296	38.5	0.139	82.5	0.032	126.5	0.012	262.5	0.000
11.5	0.292	39.5	0.136	83.5	0.031	127.5	0.012		
12.0	0.289	40.5	0.131	84.5	0.030	128.5	0.011		
12.5	0.285	41.5	0.126	85.5	0.029	129.5	0.011		
13.0	0.281	42.5	0.123	86.5	0.029	130.5	0.011		
13.5	0.278	43.5	0.118	87.5	0.029	131.5	0.011		
14.0	0.275	44.5	0.115	88.5	0.028	132.5	0.011		
14.5	0.271	45.5	0.110	89.5	0.026	133.5	0.010		
15.0	0.268	46.5	0.107	90.5	0.026	134.5	0.009		
15.5	0.264	47.5	0.102	91.5	0.025	135.5	0.010		
16.0	0.261	48.5	0.099	92.5	0.025	136.5	0.010		
16.5	0.258	49.5	0.095	93.5	0.024	137.5	0.009		
17.0	0.254	50.5	0.092	94.5	0.023	138.5	0.009		
17.5	0.251	51.5	0.089	95.5	0.023	139.5	0.009		
18.0	0.248	52.5	0.086	96.5	0.023	140.5	0.009		
18.5	0.245	53.5	0.084	97.5	0.022	141.5	0.009		
19.0	0.241	54.5	0.080	98.5	0.021	142.5	0.009		
19.5	0.239	55.5	0.077	99.5	0.021	143.5	0.009		
20.0	0.236	56.5	0.075	100.5	0.020	144.5	0.008		
20.5	0.232	57.5	0.072	101.5	0.020	145.5	0.008		
21.0	0.230	58.5	0.069	102.5	0.020	146.5	0.008		
21.5	0.227	59.5	0.068	103.5	0.019	147.5	0.008		

Appendix F2 (cont.) - Slug Test Data

Monitoring Well 14A			
t (sec)	s (m)	t (sec)	s (m)
0.0	0.000	22.0	0.040
0.5	0.509	22.5	0.037
1.0	0.392	23.0	0.035
1.5	0.373	23.5	0.032
2.0	0.354	24.0	0.030
2.5	0.335	24.5	0.029
3.0	0.317	25.0	0.027
3.5	0.301	25.5	0.025
4.0	0.287	26.0	0.023
4.5	0.272	26.5	0.022
5.0	0.258	27.0	0.021
5.5	0.246	27.5	0.019
6.0	0.233	28.5	0.016
6.5	0.222	29.5	0.015
7.0	0.210	30.5	0.013
7.5	0.200	31.5	0.011
8.0	0.190	32.5	0.009
8.5	0.180	33.5	0.007
9.0	0.172	34.5	0.007
9.5	0.163	35.5	0.005
10.0	0.155	36.5	0.005
10.5	0.147	37.5	0.004
11.0	0.139	38.5	0.003
11.5	0.132	39.5	0.002
12.0	0.125	40.5	0.001
12.5	0.118	41.5	0.001
13.0	0.113	42.5	0.000
13.5	0.107		
14.0	0.101		
14.5	0.095		
15.0	0.090		
15.5	0.085		
16.0	0.081		
16.5	0.076		
17.0	0.073		
17.5	0.068		
18.0	0.064		
18.5	0.060		
19.0	0.057		
19.5	0.054		
20.0	0.050		
20.5	0.047		
21.0	0.045		
21.5	0.042		

Monitoring Well 15A					
t (sec)	s (m)	t (sec)	s (m)	t (sec)	s (m)
0.0	0.000	22.0	0.107	65.5	0.008
0.5	0.458	22.5	0.103	66.5	0.008
1.0	0.374	23.5	0.097	67.5	0.008
1.5	0.360	24.5	0.091	68.5	0.007
2.0	0.350	25.5	0.085	69.5	0.008
2.5	0.339	26.5	0.080	70.5	0.007
3.0	0.330	27.5	0.074	71.5	0.006
3.5	0.322	28.5	0.070	72.5	0.007
4.0	0.312	29.5	0.065	73.5	0.006
4.5	0.303	30.5	0.061	74.5	0.006
5.0	0.295	31.5	0.057	75.5	0.006
5.5	0.287	32.5	0.053	76.5	0.007
6.0	0.278	33.5	0.050	77.5	0.006
6.5	0.270	34.5	0.047	78.5	0.007
7.0	0.262	35.5	0.044	79.5	0.006
7.5	0.255	36.5	0.040	80.5	0.006
8.0	0.248	37.5	0.039	81.5	0.007
8.5	0.240	38.5	0.036	82.5	0.007
9.0	0.233	39.5	0.034	83.5	0.007
9.5	0.227	40.5	0.032	84.5	0.007
10.0	0.220	41.5	0.029	85.5	0.007
10.5	0.214	42.5	0.027	86.5	0.007
11.0	0.208	43.5	0.025	87.5	0.008
11.5	0.202	44.5	0.023	88.5	0.008
12.0	0.196	45.5	0.022	89.5	0.008
12.5	0.190	46.5	0.020	90.5	0.008
13.0	0.184	47.5	0.019	91.5	0.008
13.5	0.179	48.5	0.018	92.5	0.007
14.0	0.173	49.5	0.018		
14.5	0.169	50.5	0.016		
15.0	0.163	51.5	0.015		
15.5	0.158	52.5	0.015		
16.0	0.154	53.5	0.013		
16.5	0.149	54.5	0.013		
17.0	0.145	55.5	0.013		
17.5	0.140	56.5	0.012		
18.0	0.137	57.5	0.011		
18.5	0.132	58.5	0.010		
19.0	0.128	59.5	0.010		
19.5	0.124	60.5	0.010		
20.0	0.120	61.5	0.010		
20.5	0.117	62.5	0.009		
21.0	0.113	63.5	0.009		
21.5	0.109	64.5	0.008		

Appendix F2 (cont.) - Slug Test Data

Monitoring Well 16A			
t (sec)	s (m)	t (sec)	s (m)
0.0	0.000	22.0	0.105
0.5	0.471	22.5	0.101
1.0	0.409	23.0	0.098
1.5	0.393	23.5	0.094
2.0	0.381	24.0	0.091
2.5	0.369	24.5	0.089
3.0	0.357	25.0	0.085
3.5	0.347	25.5	0.082
4.0	0.336	26.0	0.079
4.5	0.326	27.0	0.075
5.0	0.315	28.0	0.069
5.5	0.304	29.0	0.064
6.0	0.296	30.0	0.060
6.5	0.287	31.0	0.055
7.0	0.278	32.0	0.052
7.5	0.269	33.0	0.048
8.0	0.260	34.0	0.045
8.5	0.252	35.0	0.041
9.0	0.244	36.0	0.038
9.5	0.236	37.0	0.035
10.0	0.229	38.0	0.033
10.5	0.222	39.0	0.030
11.0	0.214	40.0	0.027
11.5	0.208	41.0	0.025
12.0	0.201	42.0	0.023
12.5	0.195	43.0	0.021
13.0	0.188	44.0	0.019
13.5	0.182	45.0	0.017
14.0	0.177	46.0	0.016
14.5	0.171	47.0	0.014
15.0	0.166	48.0	0.013
15.5	0.161	49.0	0.011
16.0	0.156	50.0	0.010
16.5	0.150	51.0	0.009
17.0	0.145	52.0	0.008
17.5	0.141	53.0	0.006
18.0	0.136	54.0	0.005
18.5	0.132	55.0	0.004
19.0	0.127	56.0	0.004
19.5	0.123	57.0	0.002
20.0	0.119	58.0	0.002
20.5	0.116	59.0	0.001
21.0	0.112	60.0	0.001
21.5	0.108	61.0	0.000

Monitoring Well 17A			
t (sec)	s (m)	t (sec)	s (m)
0.0	0.000	22.0	0.008
0.5	0.457	22.5	0.007
1.0	0.543	23.0	0.006
1.5	0.356	23.5	0.005
2.0	0.323	24.0	0.003
2.5	0.294	24.5	0.002
3.0	0.269	25.0	0.001
3.5	0.246	25.5	0.000
4.0	0.226		
4.5	0.206		
5.0	0.189		
5.5	0.173		
6.0	0.160		
6.5	0.146		
7.0	0.135		
7.5	0.124		
8.0	0.114		
8.5	0.105		
9.0	0.097		
9.5	0.089		
10.0	0.082		
10.5	0.076		
11.0	0.070		
11.5	0.065		
12.0	0.060		
12.5	0.055		
13.0	0.051		
13.5	0.047		
14.0	0.044		
14.5	0.040		
15.0	0.037		
15.5	0.034		
16.0	0.030		
16.5	0.029		
17.0	0.026		
17.5	0.024		
18.0	0.021		
18.5	0.020		
19.0	0.018		
19.5	0.016		
20.0	0.015		
20.5	0.012		
21.0	0.011		
21.5	0.010		

Appendix F2 (cont.) - Slug Test Data

Monitoring Well 18A					
t (sec)	s (m)	t (sec)	s (m)	t (sec)	s (m)
0.0	0.000	22.0	0.042	61.0	0.003
0.5	0.779	22.5	0.040	62.0	0.003
1.0	0.365	23.0	0.039	63.0	0.003
1.5	0.342	23.5	0.036	64.0	0.003
2.0	0.322	24.0	0.034	65.0	0.003
2.5	0.306	24.5	0.033	66.0	0.003
3.0	0.290	25.0	0.031	67.0	0.003
3.5	0.274	25.5	0.030	68.0	0.003
4.0	0.261	26.0	0.029	69.0	0.003
4.5	0.248	26.5	0.028	70.0	0.003
5.0	0.238	27.0	0.026	71.0	0.003
5.5	0.227	28.0	0.024	72.0	0.003
6.0	0.216	29.0	0.022	73.0	0.003
6.5	0.207	30.0	0.020	74.0	0.003
7.0	0.198	31.0	0.018	75.0	0.003
7.5	0.186	32.0	0.017	76.0	0.003
8.0	0.177	33.0	0.016	77.0	0.003
8.5	0.169	34.0	0.014	78.0	0.003
9.0	0.161	35.0	0.014	79.0	0.003
9.5	0.151	36.0	0.013	80.0	0.002
10.0	0.144	37.0	0.012	81.0	0.002
10.5	0.138	38.0	0.011	82.0	0.002
11.0	0.130	39.0	0.011	83.0	0.001
11.5	0.124	40.0	0.009	84.0	0.001
12.0	0.118	41.0	0.009	85.0	0.001
12.5	0.111	42.0	0.008	86.0	0.001
13.0	0.106	43.0	0.008	87.0	0.000
13.5	0.100	44.0	0.007		
14.0	0.095	45.0	0.007		
14.5	0.091	46.0	0.006		
15.0	0.086	47.0	0.006		
15.5	0.082	48.0	0.006		
16.0	0.078	49.0	0.005		
16.5	0.074	50.0	0.005		
17.0	0.070	51.0	0.005		
17.5	0.067	52.0	0.005		
18.0	0.063	53.0	0.005		
18.5	0.060	54.0	0.005		
19.0	0.057	55.0	0.004		
19.5	0.054	56.0	0.004		
20.0	0.051	57.0	0.003		
20.5	0.049	58.0	0.003		
21.0	0.046	59.0	0.003		
21.5	0.044	60.0	0.003		

Monitoring Well 19A				
t (sec)	s (m)	t (sec)	s (m)	
0.0	0.000	22.0	0.011	
0.5	0.559	22.5	0.010	
1.0	0.344	23.0	0.009	
1.5	0.297	23.5	0.009	
2.0	0.279	24.0	0.008	
2.5	0.261	24.5	0.007	
3.0	0.243	25.0	0.007	
3.5	0.226	25.5	0.007	
4.0	0.209	26.5	0.005	
4.5	0.193	27.5	0.004	
5.0	0.178	28.5	0.003	
5.5	0.165	29.5	0.003	
6.0	0.152	30.5	0.002	
6.5	0.140	31.5	0.001	
7.0	0.129	32.5	0.001	
7.5	0.119	33.5	0.001	
8.0	0.110	34.5	0.000	
8.5	0.100			
9.0	0.093			
9.5	0.086			
10.0	0.079			
10.5	0.072			
11.0	0.067			
11.5	0.062			
12.0	0.057			
12.5	0.053			
13.0	0.048			
13.5	0.045			
14.0	0.041			
14.5	0.038			
15.0	0.035			
15.5	0.032			
16.0	0.030			
16.5	0.027			
17.0	0.024			
17.5	0.023			
18.0	0.021			
18.5	0.020			
19.0	0.018			
19.5	0.017			
20.0	0.015			
20.5	0.014			
21.0	0.012			
21.5	0.012			

Appendix F2 (cont.) - Slug Test Data

Monitoring Well 20A			
t (sec)	s (m)	t (sec)	s (m)
0.0	0.000	22.0	0.051
0.5	0.316	22.5	0.048
1.0	0.466	23.0	0.046
1.5	0.339	23.5	0.043
2.0	0.330	24.0	0.041
2.5	0.318	24.5	0.039
3.0	0.303	25.0	0.037
3.5	0.290	25.5	0.035
4.0	0.276	26.0	0.033
4.5	0.264	26.5	0.032
5.0	0.251	27.0	0.030
5.5	0.239	27.5	0.028
6.0	0.229	28.0	0.027
6.5	0.217	28.5	0.025
7.0	0.208	29.0	0.023
7.5	0.198	29.5	0.022
8.0	0.189	30.5	0.020
8.5	0.180	31.5	0.017
9.0	0.172	32.5	0.015
9.5	0.164	33.5	0.012
10.0	0.157	34.5	0.011
10.5	0.150	35.5	0.009
11.0	0.143	36.5	0.008
11.5	0.136	37.5	0.006
12.0	0.130	38.5	0.004
12.5	0.124	39.5	0.003
13.0	0.118	40.5	0.002
13.5	0.113	41.5	0.002
14.0	0.107	42.5	0.000
14.5	0.103		
15.0	0.099		
15.5	0.095		
16.0	0.089		
16.5	0.086		
17.0	0.082		
17.5	0.078		
18.0	0.074		
18.5	0.071		
19.0	0.068		
19.5	0.064		
20.0	0.061		
20.5	0.058		
21.0	0.056		
21.5	0.053		

Monitoring Well 21A				
t (sec)	s (m)	t (sec)	s (m)	
0.0	0.000	22.0	0.027	
0.5	0.004	22.5	0.025	
1.0	0.554	23.0	0.023	
1.5	0.371	23.5	0.021	
2.0	0.338	24.0	0.020	
2.5	0.313	24.5	0.019	
3.0	0.291	25.0	0.017	
3.5	0.271	25.5	0.016	
4.0	0.254	26.0	0.015	
4.5	0.239	26.5	0.015	
5.0	0.226	27.0	0.014	
5.5	0.214	27.5	0.013	
6.0	0.202	28.0	0.012	
6.5	0.189	28.5	0.011	
7.0	0.178	29.0	0.011	
7.5	0.167	29.5	0.010	
8.0	0.156	30.5	0.009	
8.5	0.146	31.5	0.008	
9.0	0.137	32.5	0.007	
9.5	0.128	33.5	0.006	
10.0	0.120	34.5	0.006	
10.5	0.113	35.5	0.005	
11.0	0.107	36.5	0.004	
11.5	0.100	37.5	0.004	
12.0	0.093	38.5	0.004	
12.5	0.087	39.5	0.004	
13.0	0.082	40.5	0.003	
13.5	0.077	41.5	0.003	
14.0	0.073	42.5	0.002	
14.5	0.067	43.5	0.002	
15.0	0.064	44.5	0.002	
15.5	0.059	45.5	0.002	
16.0	0.056	46.5	0.001	
16.5	0.053	47.5	0.001	
17.0	0.049	48.5	0.001	
17.5	0.046	49.5	0.001	
18.0	0.044	50.5	0.001	
18.5	0.041	51.5	0.001	
19.0	0.038	52.5	0.001	
19.5	0.036	53.5	0.000	
20.0	0.034			
20.5	0.032			
21.0	0.030			
21.5	0.028			

Appendix F2 (cont.) - Slug Test Data

Monitoring Well 22A											
t (sec)	s (m)	t (sec)	s (m)	t (sec)	s (m)	t (sec)	s (m)	t (sec)	s (m)	t (sec)	s (m)
0.0	0.000	22.0	0.305	60.5	0.177	104.5	0.096	152.5	0.046	402.5	0.005
0.5	1.167	22.5	0.303	61.5	0.174	105.5	0.095	157.5	0.042	417.5	0.005
1.0	0.221	23.0	0.301	62.5	0.172	106.5	0.095	162.5	0.040	432.5	0.001
1.5	0.427	23.5	0.298	63.5	0.169	107.5	0.093	167.5	0.037	447.5	0.000
2.0	0.418	24.0	0.296	64.5	0.168	108.5	0.091	172.5	0.034		
2.5	0.415	24.5	0.294	65.5	0.166	109.5	0.090	177.5	0.032		
3.0	0.410	25.0	0.292	66.5	0.163	110.5	0.088	182.5	0.030		
3.5	0.406	25.5	0.290	67.5	0.161	111.5	0.086	187.5	0.028		
4.0	0.402	26.0	0.288	68.5	0.158	112.5	0.085	192.5	0.027		
4.5	0.398	26.5	0.286	69.5	0.156	113.5	0.083	197.5	0.026		
5.0	0.395	27.0	0.284	70.5	0.155	114.5	0.082	202.5	0.024		
5.5	0.392	27.5	0.282	71.5	0.152	115.5	0.081	207.5	0.023		
6.0	0.388	28.5	0.278	72.5	0.150	116.5	0.080	212.5	0.023		
6.5	0.385	29.5	0.274	73.5	0.148	117.5	0.079	217.5	0.023		
7.0	0.382	30.5	0.270	74.5	0.146	118.5	0.077	222.5	0.022		
7.5	0.378	31.5	0.266	75.5	0.144	119.5	0.077	227.5	0.020		
8.0	0.376	32.5	0.262	76.5	0.142	120.5	0.075	232.5	0.019		
8.5	0.373	33.5	0.258	77.5	0.139	121.5	0.074	237.5	0.019		
9.0	0.370	34.5	0.255	78.5	0.138	122.5	0.073	242.5	0.019		
9.5	0.367	35.5	0.251	79.5	0.136	123.5	0.071	247.5	0.017		
10.0	0.364	36.5	0.248	80.5	0.134	124.5	0.070	252.5	0.018		
10.5	0.362	37.5	0.244	81.5	0.133	125.5	0.069	257.5	0.017		
11.0	0.359	38.5	0.241	82.5	0.131	126.5	0.068	262.5	0.017		
11.5	0.356	39.5	0.237	83.5	0.129	127.5	0.067	267.5	0.017		
12.0	0.354	40.5	0.234	84.5	0.127	128.5	0.065	272.5	0.016		
12.5	0.351	41.5	0.231	85.5	0.125	129.5	0.064	277.5	0.015		
13.0	0.349	42.5	0.227	86.5	0.123	130.5	0.063	282.5	0.015		
13.5	0.346	43.5	0.224	87.5	0.122	131.5	0.063	287.5	0.014		
14.0	0.344	44.5	0.221	88.5	0.120	132.5	0.062	292.5	0.013		
14.5	0.340	45.5	0.218	89.5	0.118	133.5	0.061	297.5	0.013		
15.0	0.339	46.5	0.215	90.5	0.116	134.5	0.060	302.5	0.013		
15.5	0.336	47.5	0.212	91.5	0.115	135.5	0.059	307.5	0.012		
16.0	0.333	48.5	0.209	92.5	0.113	136.5	0.058	312.5	0.012		
16.5	0.331	49.5	0.206	93.5	0.112	137.5	0.057	317.5	0.012		
17.0	0.329	50.5	0.203	94.5	0.110	138.5	0.056	322.5	0.012		
17.5	0.326	51.5	0.200	95.5	0.109	139.5	0.055	327.5	0.012		
18.0	0.324	52.5	0.198	96.5	0.107	140.5	0.053	332.5	0.011		
18.5	0.321	53.5	0.196	97.5	0.107	141.5	0.053	337.5	0.011		
19.0	0.319	54.5	0.192	98.5	0.105	142.5	0.053	342.5	0.010		
19.5	0.317	55.5	0.190	99.5	0.103	143.5	0.052	347.5	0.010		
20.0	0.314	56.5	0.187	100.5	0.102	144.5	0.051	352.5	0.009		
20.5	0.312	57.5	0.184	101.5	0.101	145.5	0.050	357.5	0.009		
21.0	0.309	58.5	0.182	102.5	0.099	146.5	0.050	372.5	0.006		
21.5	0.307	59.5	0.179	103.5	0.098	147.5	0.049	387.5	0.006		

Appendix F2 (cont.) - Slug Test Data

Monitoring Well 23A											
t (sec)	s (m)	t (sec)	s (m)	t (sec)	s (m)	t (sec)	s (m)	t (sec)	s (m)	t (sec)	s (m)
0.0	0.000	22.0	0.360	58.0	0.278	102.0	0.209	146.0	0.155	350.0	0.055
0.5	0.313	22.5	0.358	59.0	0.275	103.0	0.209	147.0	0.153	355.0	0.054
1.0	0.695	23.0	0.357	60.0	0.274	104.0	0.207	148.0	0.152	360.0	0.052
1.5	0.433	23.5	0.356	61.0	0.272	105.0	0.206	149.0	0.152	375.0	0.049
2.0	0.427	24.0	0.355	62.0	0.270	106.0	0.204	150.0	0.151	390.0	0.047
2.5	0.423	24.5	0.354	63.0	0.268	107.0	0.203	155.0	0.146	405.0	0.043
3.0	0.419	25.0	0.353	64.0	0.266	108.0	0.202	160.0	0.142	420.0	0.040
3.5	0.417	25.5	0.351	65.0	0.264	109.0	0.200	165.0	0.138	435.0	0.038
4.0	0.414	26.0	0.350	66.0	0.262	110.0	0.198	170.0	0.133	450.0	0.036
4.5	0.412	26.5	0.348	67.0	0.261	111.0	0.197	175.0	0.130	465.0	0.035
5.0	0.410	27.0	0.348	68.0	0.259	112.0	0.195	180.0	0.125	480.0	0.033
5.5	0.408	27.5	0.346	69.0	0.258	113.0	0.194	185.0	0.121	495.0	0.030
6.0	0.407	28.0	0.345	70.0	0.256	114.0	0.192	190.0	0.118	510.0	0.027
6.5	0.405	28.5	0.344	71.0	0.254	115.0	0.192	195.0	0.116	525.0	0.025
7.0	0.404	29.0	0.342	72.0	0.252	116.0	0.190	200.0	0.113	540.0	0.022
7.5	0.402	29.5	0.342	73.0	0.251	117.0	0.189	205.0	0.111	555.0	0.021
8.0	0.400	30.0	0.340	74.0	0.249	118.0	0.187	210.0	0.107	570.0	0.019
8.5	0.398	31.0	0.338	75.0	0.247	119.0	0.187	215.0	0.104	585.0	0.017
9.0	0.396	32.0	0.335	76.0	0.246	120.0	0.186	220.0	0.102	600.0	0.016
9.5	0.395	33.0	0.333	77.0	0.244	121.0	0.184	225.0	0.099	615.0	0.015
10.0	0.393	34.0	0.331	78.0	0.243	122.0	0.183	230.0	0.097	630.0	0.013
10.5	0.391	35.0	0.330	79.0	0.241	123.0	0.181	235.0	0.093	645.0	0.013
11.0	0.390	36.0	0.327	80.0	0.240	124.0	0.180	240.0	0.092	660.0	0.012
11.5	0.389	37.0	0.325	81.0	0.238	125.0	0.179	245.0	0.090	675.0	0.010
12.0	0.387	38.0	0.323	82.0	0.237	126.0	0.177	250.0	0.087	690.0	0.010
12.5	0.385	39.0	0.321	83.0	0.235	127.0	0.176	255.0	0.085	705.0	0.011
13.0	0.384	40.0	0.318	84.0	0.234	128.0	0.175	260.0	0.083	720.0	0.013
13.5	0.383	41.0	0.317	85.0	0.232	129.0	0.174	265.0	0.080	735.0	0.012
14.0	0.381	42.0	0.314	86.0	0.231	130.0	0.173	270.0	0.078	750.0	0.012
14.5	0.380	43.0	0.312	87.0	0.230	131.0	0.171	275.0	0.077	765.0	0.011
15.0	0.378	44.0	0.310	88.0	0.228	132.0	0.171	280.0	0.075	780.0	0.012
15.5	0.377	45.0	0.308	89.0	0.227	133.0	0.169	285.0	0.073	795.0	0.010
16.0	0.375	46.0	0.305	90.0	0.225	134.0	0.168	290.0	0.071	810.0	0.009
16.5	0.374	47.0	0.303	91.0	0.224	135.0	0.167	295.0	0.070	825.0	0.004
17.0	0.373	48.0	0.301	92.0	0.222	136.0	0.166	300.0	0.068	840.0	0.004
17.5	0.371	49.0	0.299	93.0	0.221	137.0	0.165	305.0	0.066	855.0	0.005
18.0	0.370	50.0	0.296	94.0	0.219	138.0	0.164	310.0	0.065	870.0	0.005
18.5	0.369	51.0	0.294	95.0	0.219	139.0	0.162	315.0	0.064	885.0	0.006
19.0	0.367	52.0	0.291	96.0	0.217	140.0	0.161	320.0	0.062	900.0	0.005
19.5	0.366	53.0	0.289	97.0	0.217	141.0	0.160	325.0	0.060	915.0	0.003
20.0	0.365	54.0	0.287	98.0	0.215	142.0	0.159	330.0	0.059	930.0	0.002
20.5	0.363	55.0	0.284	99.0	0.214	143.0	0.158	335.0	0.058	945.0	0.001
21.0	0.362	56.0	0.282	100.0	0.213	144.0	0.157	340.0	0.057		
21.5	0.361	57.0	0.279	101.0	0.211	145.0	0.156	345.0	0.056		

Appendix F2 (cont.) - Slug Test Data

Monitoring Well 24A									
t (sec)	s (m)	t (sec)	s (m)	t (sec)	s (m)	t (sec)	s (m)	t (sec)	s (m)
0.0	0.000	22.0	0.205	58.5	0.067	102.5	0.017	146.5	0.004
0.5	1.242	22.5	0.202	59.5	0.066	103.5	0.017	147.5	0.004
1.0	0.403	23.0	0.199	60.5	0.064	104.5	0.016	148.5	0.004
1.5	0.399	23.5	0.196	61.5	0.061	105.5	0.015	149.5	0.003
2.0	0.391	24.0	0.193	62.5	0.060	106.5	0.015	154.5	0.002
2.5	0.385	24.5	0.191	63.5	0.059	107.5	0.015	159.5	0.001
3.0	0.378	25.0	0.187	64.5	0.057	108.5	0.014	164.5	0.001
3.5	0.372	25.5	0.184	65.5	0.055	109.5	0.013	169.5	0.001
4.0	0.365	26.0	0.182	66.5	0.053	110.5	0.013	174.5	0.000
4.5	0.359	26.5	0.179	67.5	0.052	111.5	0.013		
5.0	0.353	27.0	0.176	68.5	0.051	112.5	0.013		
5.5	0.347	27.5	0.173	69.5	0.050	113.5	0.012		
6.0	0.341	28.0	0.171	70.5	0.048	114.5	0.012		
6.5	0.335	28.5	0.169	71.5	0.047	115.5	0.012		
7.0	0.330	29.0	0.165	72.5	0.045	116.5	0.011		
7.5	0.324	29.5	0.163	73.5	0.044	117.5	0.011		
8.0	0.320	30.5	0.158	74.5	0.043	118.5	0.010		
8.5	0.315	31.5	0.154	75.5	0.042	119.5	0.010		
9.0	0.309	32.5	0.148	76.5	0.040	120.5	0.010		
9.5	0.305	33.5	0.144	77.5	0.038	121.5	0.010		
10.0	0.300	34.5	0.140	78.5	0.037	122.5	0.009		
10.5	0.295	35.5	0.135	79.5	0.036	123.5	0.009		
11.0	0.290	36.5	0.131	80.5	0.035	124.5	0.009		
11.5	0.286	37.5	0.127	81.5	0.034	125.5	0.009		
12.0	0.281	38.5	0.123	82.5	0.032	126.5	0.009		
12.5	0.277	39.5	0.119	83.5	0.032	127.5	0.009		
13.0	0.272	40.5	0.116	84.5	0.030	128.5	0.008		
13.5	0.268	41.5	0.112	85.5	0.029	129.5	0.008		
14.0	0.264	42.5	0.109	86.5	0.028	130.5	0.007		
14.5	0.260	43.5	0.105	87.5	0.028	131.5	0.007		
15.0	0.255	44.5	0.102	88.5	0.027	132.5	0.007		
15.5	0.252	45.5	0.098	89.5	0.027	133.5	0.007		
16.0	0.248	46.5	0.095	90.5	0.025	134.5	0.007		
16.5	0.244	47.5	0.094	91.5	0.024	135.5	0.007		
17.0	0.240	48.5	0.090	92.5	0.024	136.5	0.006		
17.5	0.236	49.5	0.088	93.5	0.023	137.5	0.006		
18.0	0.233	50.5	0.085	94.5	0.022	138.5	0.006		
18.5	0.230	51.5	0.082	95.5	0.022	139.5	0.006		
19.0	0.225	52.5	0.080	96.5	0.021	140.5	0.006		
19.5	0.223	53.5	0.078	97.5	0.021	141.5	0.006		
20.0	0.219	54.5	0.075	98.5	0.020	142.5	0.006		
20.5	0.215	55.5	0.073	99.5	0.019	143.5	0.005		
21.0	0.212	56.5	0.071	100.5	0.018	144.5	0.004		
21.5	0.209	57.5	0.069	101.5	0.017	145.5	0.004		

Appendix F2 (cont.) - Slug Test Data

Monitoring Well 25A									
t (sec)	s (m)	t (sec)	s (m)	t (sec)	s (m)	t (sec)	s (m)	t (sec)	s (m)
0.0	0.000	22.0	0.336	64.5	0.233	108.5	0.154	188.5	0.081
0.5	1.206	22.5	0.335	65.5	0.231	109.5	0.152	193.5	0.079
1.0	0.487	23.0	0.334	66.5	0.228	110.5	0.151	198.5	0.077
1.5	0.416	23.5	0.332	67.5	0.226	111.5	0.150	203.5	0.074
2.0	0.411	24.5	0.330	68.5	0.224	112.5	0.148	208.5	0.071
2.5	0.407	25.5	0.326	69.5	0.222	113.5	0.147	213.5	0.070
3.0	0.403	26.5	0.324	70.5	0.219	114.5	0.146	218.5	0.068
3.5	0.400	27.5	0.321	71.5	0.217	115.5	0.144	223.5	0.066
4.0	0.398	28.5	0.317	72.5	0.216	116.5	0.144	228.5	0.064
4.5	0.396	29.5	0.315	73.5	0.213	117.5	0.142	233.5	0.062
5.0	0.393	30.5	0.313	74.5	0.211	118.5	0.141	238.5	0.061
5.5	0.391	31.5	0.310	75.5	0.210	119.5	0.140	243.5	0.059
6.0	0.389	32.5	0.307	76.5	0.207	120.5	0.139	248.5	0.057
6.5	0.387	33.5	0.304	77.5	0.206	121.5	0.138	253.5	0.055
7.0	0.385	34.5	0.302	78.5	0.204	122.5	0.137	258.5	0.054
7.5	0.384	35.5	0.300	79.5	0.201	123.5	0.135	263.5	0.051
8.0	0.381	36.5	0.297	80.5	0.200	124.5	0.135	268.5	0.049
8.5	0.379	37.5	0.295	81.5	0.197	125.5	0.133	273.5	0.047
9.0	0.377	38.5	0.292	82.5	0.195	126.5	0.132	278.5	0.046
9.5	0.375	39.5	0.289	83.5	0.194	127.5	0.131	283.5	0.043
10.0	0.374	40.5	0.287	84.5	0.192	128.5	0.129	288.5	0.041
10.5	0.372	41.5	0.285	85.5	0.190	129.5	0.129	293.5	0.038
11.0	0.370	42.5	0.282	86.5	0.188	130.5	0.128	298.5	0.036
11.5	0.369	43.5	0.280	87.5	0.186	131.5	0.127	303.5	0.033
12.0	0.367	44.5	0.278	88.5	0.184	132.5	0.126	308.5	0.031
12.5	0.366	45.5	0.276	89.5	0.183	133.5	0.125	313.5	0.030
13.0	0.363	46.5	0.274	90.5	0.181	134.5	0.123	318.5	0.028
13.5	0.362	47.5	0.271	91.5	0.180	135.5	0.123	323.5	0.027
14.0	0.361	48.5	0.268	92.5	0.178	136.5	0.121	328.5	0.026
14.5	0.360	49.5	0.267	93.5	0.177	137.5	0.120	333.5	0.025
15.0	0.358	50.5	0.264	94.5	0.175	138.5	0.120	338.5	0.023
15.5	0.356	51.5	0.261	95.5	0.174	139.5	0.119	343.5	0.023
16.0	0.355	52.5	0.259	96.5	0.172	140.5	0.117	348.5	0.021
16.5	0.354	53.5	0.257	97.5	0.170	141.5	0.117	353.5	0.020
17.0	0.352	54.5	0.255	98.5	0.168	142.5	0.116	368.5	0.017
17.5	0.350	55.5	0.252	99.5	0.167	143.5	0.114	383.5	0.012
18.0	0.349	56.5	0.250	100.5	0.166	148.5	0.110	398.5	0.007
18.5	0.347	57.5	0.248	101.5	0.164	153.5	0.106	413.5	0.003
19.0	0.346	58.5	0.246	102.5	0.163	158.5	0.102	428.5	0.000
19.5	0.344	59.5	0.243	103.5	0.161	163.5	0.098		
20.0	0.343	60.5	0.241	104.5	0.159	168.5	0.093		
20.5	0.341	61.5	0.239	105.5	0.158	173.5	0.090		
21.0	0.340	62.5	0.237	106.5	0.157	178.5	0.087		
21.5	0.338	63.5	0.234	107.5	0.155	183.5	0.085		

Appendix F2 (cont.) - Slug Test Data

Monitoring Well 26A											
t (sec)	s (m)	t (sec)	s (m)	t (sec)	s (m)	t (sec)	s (m)	t (sec)	s (m)	t (sec)	s (m)
0.0	0.000	22.0	0.299	61.0	0.201	105.0	0.129	157.0	0.074	417.0	0.011
0.5	0.173	22.5	0.298	62.0	0.200	106.0	0.128	162.0	0.070	432.0	0.010
1.0	0.504	23.0	0.297	63.0	0.197	107.0	0.126	167.0	0.068	447.0	0.009
1.5	0.399	23.5	0.295	64.0	0.196	108.0	0.125	172.0	0.065	462.0	0.010
2.0	0.393	24.0	0.293	65.0	0.194	109.0	0.124	177.0	0.061	477.0	0.010
2.5	0.389	24.5	0.291	66.0	0.192	110.0	0.123	182.0	0.059	492.0	0.008
3.0	0.385	25.0	0.290	67.0	0.190	111.0	0.121	187.0	0.057	507.0	0.007
3.5	0.381	25.5	0.288	68.0	0.189	112.0	0.120	192.0	0.056	522.0	0.007
4.0	0.378	26.0	0.286	69.0	0.186	113.0	0.119	197.0	0.055	537.0	0.008
4.5	0.376	26.5	0.284	70.0	0.184	114.0	0.117	202.0	0.052	552.0	0.008
5.0	0.372	27.0	0.283	71.0	0.183	115.0	0.116	207.0	0.049	567.0	0.007
5.5	0.369	28.0	0.280	72.0	0.181	116.0	0.115	212.0	0.048	582.0	0.005
6.0	0.366	29.0	0.277	73.0	0.179	117.0	0.114	217.0	0.045	597.0	0.007
6.5	0.364	30.0	0.274	74.0	0.178	118.0	0.113	222.0	0.044	612.0	0.006
7.0	0.361	31.0	0.271	75.0	0.175	119.0	0.112	227.0	0.043	627.0	0.005
7.5	0.359	32.0	0.268	76.0	0.175	120.0	0.111	232.0	0.042	642.0	0.003
8.0	0.356	33.0	0.265	77.0	0.172	121.0	0.111	237.0	0.041	657.0	0.000
8.5	0.353	34.0	0.263	78.0	0.170	122.0	0.110	242.0	0.040		
9.0	0.351	35.0	0.261	79.0	0.168	123.0	0.109	247.0	0.040		
9.5	0.348	36.0	0.257	80.0	0.167	124.0	0.108	252.0	0.038		
10.0	0.348	37.0	0.255	81.0	0.165	125.0	0.106	257.0	0.037		
10.5	0.344	38.0	0.252	82.0	0.163	126.0	0.105	262.0	0.037		
11.0	0.342	39.0	0.249	83.0	0.161	127.0	0.104	267.0	0.037		
11.5	0.340	40.0	0.247	84.0	0.160	128.0	0.104	272.0	0.035		
12.0	0.338	41.0	0.244	85.0	0.158	129.0	0.103	277.0	0.034		
12.5	0.335	42.0	0.242	86.0	0.156	130.0	0.102	282.0	0.033		
13.0	0.334	43.0	0.240	87.0	0.154	131.0	0.100	287.0	0.031		
13.5	0.332	44.0	0.237	88.0	0.154	132.0	0.100	292.0	0.030		
14.0	0.329	45.0	0.235	89.0	0.151	133.0	0.098	297.0	0.030		
14.5	0.327	46.0	0.233	90.0	0.150	134.0	0.097	302.0	0.030		
15.0	0.326	47.0	0.231	91.0	0.149	135.0	0.096	307.0	0.030		
15.5	0.324	48.0	0.228	92.0	0.147	136.0	0.094	312.0	0.030		
16.0	0.321	49.0	0.226	93.0	0.146	137.0	0.094	317.0	0.029		
16.5	0.320	50.0	0.224	94.0	0.145	138.0	0.092	322.0	0.027		
17.0	0.318	51.0	0.221	95.0	0.142	139.0	0.091	327.0	0.027		
17.5	0.316	52.0	0.219	96.0	0.141	140.0	0.090	332.0	0.025		
18.0	0.314	53.0	0.217	97.0	0.140	141.0	0.089	337.0	0.024		
18.5	0.312	54.0	0.215	98.0	0.139	142.0	0.088	342.0	0.023		
19.0	0.310	55.0	0.213	99.0	0.138	143.0	0.087	347.0	0.021		
19.5	0.308	56.0	0.211	100.0	0.136	144.0	0.086	352.0	0.020		
20.0	0.307	57.0	0.209	101.0	0.135	145.0	0.085	357.0	0.019		
20.5	0.305	58.0	0.207	102.0	0.134	146.0	0.084	372.0	0.018		
21.0	0.303	59.0	0.205	103.0	0.132	147.0	0.083	387.0	0.015		
21.5	0.301	60.0	0.204	104.0	0.131	152.0	0.079	402.0	0.011		

Appendix F2 (cont.) - Slug Test Data

Mon. Well 27A	
t (sec)	s (m)
0.0	0.000
0.5	1.078
1.0	0.435
1.5	0.317
2.0	0.279
2.5	0.248
3.0	0.223
3.5	0.201
4.0	0.180
4.5	0.161
5.0	0.143
5.5	0.399
6.0	0.198
6.5	0.101
7.0	0.090
7.5	0.080
8.0	0.072
8.5	0.063
9.0	0.059
9.5	0.052
10.0	0.047
10.5	0.042
11.0	0.037
11.5	0.033
12.0	0.029
12.5	0.027
13.0	0.023
13.5	0.021
14.0	0.018
14.5	0.016
15.0	0.014
15.5	0.013
16.0	0.011
16.5	0.009
17.0	0.008
17.5	0.007
18.0	0.006
18.5	0.004
19.0	0.004
19.5	0.003
20.0	0.003
20.5	0.002
21.0	0.001
21.5	0.000

Monitoring Well 28A									
t (sec)	s (m)	t (sec)	s (m)	t (sec)	s (m)	t (sec)	s (m)	t (sec)	s (m)
0.0	0.000	22.0	0.330	60.5	0.243	104.5	0.181	152.5	0.126
0.5	0.098	22.5	0.328	61.5	0.242	105.5	0.180	157.5	0.121
1.0	1.101	23.0	0.328	62.5	0.239	106.5	0.178	162.5	0.117
1.5	0.494	23.5	0.326	63.5	0.238	107.5	0.177	167.5	0.111
2.0	0.413	24.0	0.324	64.5	0.236	108.5	0.176	172.5	0.106
2.5	0.406	24.5	0.323	65.5	0.234	109.5	0.175	177.5	0.101
3.0	0.400	25.0	0.321	66.5	0.233	110.5	0.173	182.5	0.098
3.5	0.396	25.5	0.320	67.5	0.231	111.5	0.172	187.5	0.093
4.0	0.392	26.0	0.319	68.5	0.229	112.5	0.171	192.5	0.091
4.5	0.390	26.5	0.318	69.5	0.229	113.5	0.170	197.5	0.086
5.0	0.387	27.0	0.316	70.5	0.227	114.5	0.169	202.5	0.083
5.5	0.385	27.5	0.315	71.5	0.226	115.5	0.168	207.5	0.079
6.0	0.382	28.5	0.312	72.5	0.224	116.5	0.167	212.5	0.075
6.5	0.381	29.5	0.310	73.5	0.223	117.5	0.165	217.5	0.072
7.0	0.379	30.5	0.307	74.5	0.221	118.5	0.164	222.5	0.068
7.5	0.376	31.5	0.305	75.5	0.220	119.5	0.163	227.5	0.065
8.0	0.375	32.5	0.302	76.5	0.218	120.5	0.162	232.5	0.063
8.5	0.373	33.5	0.300	77.5	0.217	121.5	0.160	237.5	0.061
9.0	0.371	34.5	0.297	78.5	0.216	122.5	0.160	242.5	0.059
9.5	0.369	35.5	0.294	79.5	0.214	123.5	0.159	247.5	0.056
10.0	0.368	36.5	0.292	80.5	0.213	124.5	0.157	252.5	0.054
10.5	0.366	37.5	0.290	81.5	0.211	125.5	0.157	257.5	0.053
11.0	0.364	38.5	0.288	82.5	0.210	126.5	0.155	262.5	0.051
11.5	0.362	39.5	0.285	83.5	0.208	127.5	0.154	267.5	0.049
12.0	0.361	40.5	0.283	84.5	0.207	128.5	0.152	272.5	0.048
12.5	0.358	41.5	0.281	85.5	0.206	129.5	0.152	277.5	0.046
13.0	0.358	42.5	0.278	86.5	0.204	130.5	0.150	282.5	0.046
13.5	0.356	43.5	0.276	87.5	0.203	131.5	0.150	287.5	0.043
14.0	0.353	44.5	0.274	88.5	0.201	132.5	0.148	292.5	0.042
14.5	0.353	45.5	0.272	89.5	0.200	133.5	0.147	297.5	0.041
15.0	0.351	46.5	0.269	90.5	0.199	134.5	0.145	302.5	0.040
15.5	0.350	47.5	0.267	91.5	0.198	135.5	0.144	307.5	0.038
16.0	0.348	48.5	0.265	92.5	0.196	136.5	0.144	312.5	0.036
16.5	0.347	49.5	0.262	93.5	0.195	137.5	0.142	317.5	0.034
17.0	0.345	50.5	0.261	94.5	0.193	138.5	0.141	322.5	0.033
17.5	0.343	51.5	0.259	95.5	0.192	139.5	0.140	327.5	0.032
18.0	0.342	52.5	0.257	96.5	0.191	140.5	0.139	332.5	0.031
18.5	0.340	53.5	0.256	97.5	0.190	141.5	0.139	337.5	0.029
19.0	0.338	54.5	0.254	98.5	0.188	142.5	0.137	342.5	0.028
19.5	0.337	55.5	0.251	99.5	0.187	143.5	0.136	347.5	0.025
20.0	0.335	56.5	0.250	100.5	0.186	144.5	0.135	352.5	0.025
20.5	0.335	57.5	0.248	101.5	0.185	145.5	0.134	357.5	0.022
21.0	0.333	58.5	0.246	102.5	0.184	146.5	0.133	372.5	0.016
21.5	0.331	59.5	0.245	103.5	0.182	147.5	0.132	387.5	0.013

Appendix F2 (cont.) - Slug Test Data

Monitoring Well 30A			
t (sec)	s (m)	t (sec)	s (m)
0.0	0.000	22.0	0.029
0.5	1.726	22.5	0.029
1.0	0.341	23.0	0.029
1.5	0.307	23.5	0.028
2.0	0.279	24.0	0.027
2.5	0.228	24.5	0.027
3.0	0.209	25.0	0.027
3.5	0.191	25.5	0.027
4.0	0.179	26.0	0.027
4.5	0.165	26.5	0.027
5.0	0.153	27.0	0.027
5.5	0.144	27.5	0.027
6.0	0.134	28.0	0.027
6.5	0.125	28.5	0.027
7.0	0.116	29.5	0.027
7.5	0.109	30.5	0.027
8.0	0.102	31.5	0.027
8.5	0.095	32.5	0.027
9.0	0.089	33.5	0.027
9.5	0.083	34.5	0.027
10.0	0.078		
10.5	0.072		
11.0	0.068		
11.5	0.065		
12.0	0.060		
12.5	0.056		
13.0	0.053		
13.5	0.051		
14.0	0.048		
14.5	0.045		
15.0	0.043		
15.5	0.042		
16.0	0.040		
16.5	0.038		
17.0	0.036		
17.5	0.035		
18.0	0.034		
18.5	0.033		
19.0	0.032		
19.5	0.032		
20.0	0.031		
20.5	0.030		
21.0	0.030		
21.5	0.029		

Monitoring Well 32A							
t (sec)	s (m)	t (sec)	s (m)	t (sec)	s (m)	t (sec)	s (m)
0.0	0.000	22.0	0.064	59.5	0.026	103.5	0.010
0.5	0.688	22.5	0.064	60.5	0.026	104.5	0.010
1.0	0.102	23.0	0.063	61.5	0.025	105.5	0.008
1.5	0.101	23.5	0.063	62.5	0.024	106.5	0.008
2.0	0.100	24.0	0.061	63.5	0.023	107.5	0.008
2.5	0.099	24.5	0.061	64.5	0.022	108.5	0.007
3.0	0.098	25.0	0.061	65.5	0.022	109.5	0.007
3.5	0.096	25.5	0.060	66.5	0.022	110.5	0.006
4.0	0.096	26.0	0.059	67.5	0.022	111.5	0.006
4.5	0.095	26.5	0.058	68.5	0.021	112.5	0.006
5.0	0.094	27.0	0.058	69.5	0.021	113.5	0.005
5.5	0.093	27.5	0.058	70.5	0.021	114.5	0.004
6.0	0.093	28.0	0.057	71.5	0.020	115.5	0.004
6.5	0.092	28.5	0.056	72.5	0.020	116.5	0.004
7.0	0.091	29.5	0.055	73.5	0.020	117.5	0.004
7.5	0.090	30.5	0.054	74.5	0.019	118.5	0.004
8.0	0.089	31.5	0.052	75.5	0.018	119.5	0.004
8.5	0.088	32.5	0.052	76.5	0.018	120.5	0.003
9.0	0.087	33.5	0.051	77.5	0.016	121.5	0.003
9.5	0.086	34.5	0.050	78.5	0.015	122.5	0.003
10.0	0.085	35.5	0.049	79.5	0.015	123.5	0.002
10.5	0.083	36.5	0.048	80.5	0.015	124.5	0.001
11.0	0.083	37.5	0.047	81.5	0.015	125.5	0.001
11.5	0.081	38.5	0.046	82.5	0.015	126.5	0.001
12.0	0.080	39.5	0.045	83.5	0.014	127.5	0.000
12.5	0.080	40.5	0.044	84.5	0.014		
13.0	0.079	41.5	0.043	85.5	0.013		
13.5	0.078	42.5	0.042	86.5	0.013		
14.0	0.077	43.5	0.041	87.5	0.013		
14.5	0.076	44.5	0.040	88.5	0.012		
15.0	0.075	45.5	0.038	89.5	0.012		
15.5	0.075	46.5	0.036	90.5	0.012		
16.0	0.073	47.5	0.036	91.5	0.012		
16.5	0.073	48.5	0.036	92.5	0.012		
17.0	0.072	49.5	0.034	93.5	0.012		
17.5	0.072	50.5	0.033	94.5	0.012		
18.0	0.070	51.5	0.032	95.5	0.012		
18.5	0.070	52.5	0.031	96.5	0.012		
19.0	0.068	53.5	0.030	97.5	0.012		
19.5	0.068	54.5	0.029	98.5	0.012		
20.0	0.067	55.5	0.028	99.5	0.012		
20.5	0.066	56.5	0.028	100.5	0.011		
21.0	0.065	57.5	0.027	101.5	0.011		
21.5	0.065	58.5	0.027	102.5	0.010		

Appendix F2 (cont.) - Slug Test Data

Monitoring Well 33A			
t (sec)	s (m)	t (sec)	s (m)
0.0	0.000	22.0	0.029
0.5	0.002	22.5	0.027
1.0	0.251	23.0	0.026
1.5	0.239	23.5	0.025
2.0	0.227	24.0	0.023
2.5	0.215	24.5	0.022
3.0	0.205	25.0	0.021
3.5	0.195	25.5	0.019
4.0	0.186	26.0	0.019
4.5	0.177	26.5	0.018
5.0	0.168	27.0	0.016
5.5	0.161	27.5	0.016
6.0	0.153	28.0	0.015
6.5	0.146	29.0	0.014
7.0	0.139	30.0	0.012
7.5	0.132	31.0	0.010
8.0	0.125	32.0	0.009
8.5	0.119	33.0	0.008
9.0	0.113	34.0	0.007
9.5	0.108	35.0	0.006
10.0	0.102	36.0	0.005
10.5	0.097	37.0	0.005
11.0	0.093	38.0	0.005
11.5	0.088	39.0	0.003
12.0	0.084	40.0	0.003
12.5	0.080	41.0	0.003
13.0	0.075	42.0	0.002
13.5	0.072	43.0	0.002
14.0	0.068	44.0	0.002
14.5	0.065	45.0	0.002
15.0	0.062	46.0	0.001
15.5	0.058	47.0	0.000
16.0	0.055		
16.5	0.052		
17.0	0.050		
17.5	0.047		
18.0	0.044		
18.5	0.042		
19.0	0.040		
19.5	0.038		
20.0	0.036		
20.5	0.035		
21.0	0.033		
21.5	0.031		

Monitoring Well 34A			
t (sec)	s (m)	t (sec)	s (m)
0.0	0.000	22.0	0.064
0.5	-0.301	22.5	0.063
1.0	0.252	23.0	0.060
1.5	0.239	23.5	0.059
2.0	0.230	24.0	0.057
2.5	0.221	24.5	0.056
3.0	0.215	25.0	0.054
3.5	0.208	25.5	0.051
4.0	0.201	26.0	0.051
4.5	0.195	26.5	0.049
5.0	0.189	27.0	0.047
5.5	0.183	27.5	0.045
6.0	0.177	28.0	0.044
6.5	0.171	28.5	0.043
7.0	0.166	29.5	0.040
7.5	0.161	30.5	0.037
8.0	0.156	31.5	0.036
8.5	0.151	32.5	0.033
9.0	0.146	33.5	0.031
9.5	0.141	34.5	0.029
10.0	0.137	35.5	0.027
10.5	0.133	36.5	0.025
11.0	0.129	37.5	0.024
11.5	0.125	38.5	0.022
12.0	0.122	39.5	0.020
12.5	0.117	40.5	0.019
13.0	0.114	41.5	0.017
13.5	0.111	42.5	0.016
14.0	0.107	43.5	0.015
14.5	0.103	44.5	0.013
15.0	0.100	45.5	0.012
15.5	0.097	46.5	0.010
16.0	0.094	47.5	0.010
16.5	0.092	48.5	0.008
17.0	0.088	49.5	0.007
17.5	0.086	50.5	0.006
18.0	0.083	51.5	0.004
18.5	0.081	52.5	0.003
19.0	0.078	53.5	0.002
19.5	0.075	54.5	0.000
20.0	0.073		
20.5	0.071		
21.0	0.069		
21.5	0.067		

Appendix F2 (cont.) - Slug Test Data

Piezometer 1B			
t (sec)	s (m)	t (sec)	s (m)
0.0	0.000	22.0	0.001
0.5	0.127	22.5	0.002
1.0	0.309	23.0	0.001
1.5	0.436	23.5	0.001
2.0	0.358	24.0	0.001
2.5	0.296	24.5	0.000
3.0	0.248		
3.5	0.208		
4.0	0.176		
4.5	0.148		
5.0	0.125		
5.5	0.106		
6.0	0.089		
6.5	0.076		
7.0	0.064		
7.5	0.055		
8.0	0.047		
8.5	0.039		
9.0	0.034		
9.5	0.029		
10.0	0.024		
10.5	0.021		
11.0	0.017		
11.5	0.015		
12.0	0.013		
12.5	0.011		
13.0	0.009		
13.5	0.008		
14.0	0.007		
14.5	0.006		
15.0	0.005		
15.5	0.004		
16.0	0.004		
16.5	0.004		
17.0	0.004		
17.5	0.003		
18.0	0.003		
18.5	0.002		
19.0	0.002		
19.5	0.002		
20.0	0.002		
20.5	0.002		
21.0	0.002		
21.5	0.002		

Piezometer 1C			
t (sec)	s (m)	t (sec)	s (m)
0.0	0.000	22.0	0.023
0.5	1.272	22.5	0.022
1.0	0.507	23.0	0.019
1.5	0.455	23.5	0.018
2.0	0.418	24.0	0.017
2.5	0.387	24.5	0.016
3.0	0.361	25.0	0.015
3.5	0.334	25.5	0.014
4.0	0.312	26.0	0.012
4.5	0.289	26.5	0.012
5.0	0.268	27.0	0.010
5.5	0.250	28.0	0.010
6.0	0.232	29.0	0.008
6.5	0.216	30.0	0.008
7.0	0.201	31.0	0.006
7.5	0.187	32.0	0.005
8.0	0.174	33.0	0.004
8.5	0.162	34.0	0.003
9.0	0.151	35.0	0.002
9.5	0.140	36.0	0.002
10.0	0.131	37.0	0.002
10.5	0.122	38.0	0.001
11.0	0.113	39.0	0.001
11.5	0.105	40.0	0.001
12.0	0.098	41.0	0.001
12.5	0.092	42.0	0.000
13.0	0.085		
13.5	0.079		
14.0	0.074		
14.5	0.069		
15.0	0.064		
15.5	0.060		
16.0	0.056		
16.5	0.052		
17.0	0.048		
17.5	0.045		
18.0	0.042		
18.5	0.039		
19.0	0.036		
19.5	0.033		
20.0	0.031		
20.5	0.029		
21.0	0.027		
21.5	0.025		

Piezometer 1E			
t (sec)	s (m)	t (sec)	s (m)
0.0	0.000	22.0	0.017
0.5	0.015	22.5	0.017
1.0	0.551	23.0	0.016
1.5	0.384	23.5	0.016
2.0	0.326	24.0	0.017
2.5	0.277	24.5	0.016
3.0	0.234	25.0	0.016
3.5	0.198	25.5	0.015
4.0	0.168	26.0	0.016
4.5	0.142	26.5	0.016
5.0	0.121	27.0	0.016
5.5	0.105		
6.0	0.089		
6.5	0.077		
7.0	0.066		
7.5	0.059		
8.0	0.050		
8.5	0.043		
9.0	0.038		
9.5	0.034		
10.0	0.030		
10.5	0.027		
11.0	0.024		
11.5	0.022		
12.0	0.020		
12.5	0.019		
13.0	0.017		
13.5	0.017		
14.0	0.017		
14.5	0.017		
15.0	0.018		
15.5	0.018		
16.0	0.017		
16.5	0.017		
17.0	0.017		
17.5	0.017		
18.0	0.017		
18.5	0.017		
19.0	0.017		
19.5	0.017		
20.0	0.017		
20.5	0.017		
21.0	0.017		
21.5	0.017		

Appendix F2 (cont.) - Slug Test Data

Piezometer 3B			
t (sec)	s (m)	t (sec)	s (m)
0.0	0.000	22.0	0.020
0.5	0.563	22.5	0.018
1.0	0.484	23.0	0.016
1.5	0.444	23.5	0.015
2.0	0.408	24.0	0.014
2.5	0.374	24.5	0.013
3.0	0.346	25.0	0.012
3.5	0.319	25.5	0.012
4.0	0.294	26.0	0.010
4.5	0.272	26.5	0.010
5.0	0.252	27.0	0.008
5.5	0.234	27.5	0.008
6.0	0.216	28.5	0.007
6.5	0.200	29.5	0.007
7.0	0.186	30.5	0.006
7.5	0.172	31.5	0.005
8.0	0.160	32.5	0.004
8.5	0.149	33.5	0.003
9.0	0.137	34.5	0.003
9.5	0.128	35.5	0.003
10.0	0.119	36.5	0.003
10.5	0.110	37.5	0.002
11.0	0.101	38.5	0.002
11.5	0.094	39.5	0.001
12.0	0.087	40.5	0.002
12.5	0.080	41.5	0.001
13.0	0.074	42.5	0.001
13.5	0.068	43.5	0.001
14.0	0.064	44.5	0.001
14.5	0.059	45.5	0.001
15.0	0.054	46.5	0.001
15.5	0.050	47.5	0.000
16.0	0.046		
16.5	0.043		
17.0	0.039		
17.5	0.037		
18.0	0.034		
18.5	0.031		
19.0	0.029		
19.5	0.028		
20.0	0.026		
20.5	0.024		
21.0	0.022		
21.5	0.021		

Piezometer 3C			
t (sec)	s (m)	t (sec)	s (m)
0.0	0.000	22.0	0.031
0.5	1.879	22.5	0.029
1.0	0.561	23.0	0.027
1.5	0.506	23.5	0.026
2.0	0.460	24.0	0.024
2.5	0.427	24.5	0.023
3.0	0.396	25.0	0.021
3.5	0.369	25.5	0.020
4.0	0.345	26.0	0.018
4.5	0.322	26.5	0.017
5.0	0.301	27.0	0.016
5.5	0.282	27.5	0.015
6.0	0.263	28.5	0.013
6.5	0.246	29.5	0.011
7.0	0.231	30.5	0.009
7.5	0.216	31.5	0.009
8.0	0.202	32.5	0.007
8.5	0.189	33.5	0.007
9.0	0.178	34.5	0.006
9.5	0.166	35.5	0.006
10.0	0.155	36.5	0.004
10.5	0.146	37.5	0.004
11.0	0.136	38.5	0.004
11.5	0.128	39.5	0.003
12.0	0.119	40.5	0.003
12.5	0.112	41.5	0.002
13.0	0.104	42.5	0.002
13.5	0.098	43.5	0.002
14.0	0.092	44.5	0.002
14.5	0.085	45.5	0.002
15.0	0.081	46.5	0.002
15.5	0.075	47.5	0.001
16.0	0.070	48.5	0.002
16.5	0.066	49.5	0.001
17.0	0.061	50.5	0.001
17.5	0.057	51.5	0.002
18.0	0.054	52.5	0.001
18.5	0.051		
19.0	0.047		
19.5	0.044		
20.0	0.041		
20.5	0.039		
21.0	0.036		
21.5	0.034		

Appendix F2 (cont.) - Slug Test Data

Monitoring Well 3E									
t (sec)	s (m)	t (sec)	s (m)	t (sec)	s (m)	t (sec)	s (m)	t (sec)	s (m)
0.0	0.000	22.0	0.408	60.5	0.226	104.5	0.116	152.5	0.059
0.5	0.904	22.5	0.405	61.5	0.221	105.5	0.114	157.5	0.055
1.0	0.613	23.0	0.401	62.5	0.218	106.5	0.112	162.5	0.051
1.5	0.593	23.5	0.399	63.5	0.215	107.5	0.111	167.5	0.048
2.0	0.577	24.0	0.396	64.5	0.211	108.5	0.109	172.5	0.045
2.5	0.570	24.5	0.393	65.5	0.208	109.5	0.107	177.5	0.041
3.0	0.563	25.0	0.389	66.5	0.206	110.5	0.106	182.5	0.038
3.5	0.557	25.5	0.386	67.5	0.202	111.5	0.105	187.5	0.035
4.0	0.551	26.0	0.383	68.5	0.199	112.5	0.104	192.5	0.033
4.5	0.546	26.5	0.380	69.5	0.196	113.5	0.102	197.5	0.030
5.0	0.541	27.0	0.377	70.5	0.193	114.5	0.100	202.5	0.027
5.5	0.536	27.5	0.374	71.5	0.190	115.5	0.099	207.5	0.025
6.0	0.531	28.5	0.368	72.5	0.187	116.5	0.098	212.5	0.024
6.5	0.526	29.5	0.361	73.5	0.184	117.5	0.096	217.5	0.022
7.0	0.521	30.5	0.356	74.5	0.181	118.5	0.095	222.5	0.022
7.5	0.517	31.5	0.351	75.5	0.179	119.5	0.094	227.5	0.020
8.0	0.512	32.5	0.345	76.5	0.175	120.5	0.092	232.5	0.018
8.5	0.507	33.5	0.340	77.5	0.173	121.5	0.091	237.5	0.016
9.0	0.503	34.5	0.334	78.5	0.170	122.5	0.090	242.5	0.015
9.5	0.499	35.5	0.329	79.5	0.169	123.5	0.088	247.5	0.013
10.0	0.495	36.5	0.325	80.5	0.166	124.5	0.087	252.5	0.011
10.5	0.490	37.5	0.319	81.5	0.163	125.5	0.086	257.5	0.011
11.0	0.486	38.5	0.314	82.5	0.160	126.5	0.085	262.5	0.009
11.5	0.483	39.5	0.310	83.5	0.158	127.5	0.084	267.5	0.009
12.0	0.479	40.5	0.305	84.5	0.156	128.5	0.083	272.5	0.008
12.5	0.474	41.5	0.301	85.5	0.154	129.5	0.082	277.5	0.007
13.0	0.471	42.5	0.296	86.5	0.151	130.5	0.081	282.5	0.006
13.5	0.467	43.5	0.291	87.5	0.149	131.5	0.079	287.5	0.005
14.0	0.463	44.5	0.287	88.5	0.147	132.5	0.078	292.5	0.005
14.5	0.459	45.5	0.283	89.5	0.145	133.5	0.077	297.5	0.005
15.0	0.456	46.5	0.279	90.5	0.143	134.5	0.076	302.5	0.004
15.5	0.452	47.5	0.274	91.5	0.140	135.5	0.075	307.5	0.004
16.0	0.449	48.5	0.270	92.5	0.138	136.5	0.074	312.5	0.004
16.5	0.445	49.5	0.266	93.5	0.136	137.5	0.073	317.5	0.003
17.0	0.441	50.5	0.261	94.5	0.134	138.5	0.073	322.5	0.002
17.5	0.438	51.5	0.257	95.5	0.132	139.5	0.071	327.5	0.001
18.0	0.435	52.5	0.254	96.5	0.130	140.5	0.071	332.5	0.001
18.5	0.431	53.5	0.250	97.5	0.129	141.5	0.069	337.5	0.000
19.0	0.428	54.5	0.246	98.5	0.126	142.5	0.068		
19.5	0.425	55.5	0.242	99.5	0.124	143.5	0.067		
20.0	0.421	56.5	0.238	100.5	0.122	144.5	0.065		
20.5	0.418	57.5	0.236	101.5	0.121	145.5	0.066		
21.0	0.414	58.5	0.232	102.5	0.119	146.5	0.065		
21.5	0.411	59.5	0.228	103.5	0.117	147.5	0.064		

Appendix F2 (cont.) - Slug Test Data

Piezometer 11B			
t (sec)	s (m)	t (sec)	s (m)
0.0	0.000	22.0	0.013
0.5	0.812	22.5	0.011
1.0	0.771	23.0	0.011
1.5	0.524	23.5	0.010
2.0	0.472	24.0	0.008
2.5	0.429	24.5	0.007
3.0	0.392	25.0	0.006
3.5	0.358	25.5	0.005
4.0	0.326	26.0	0.005
4.5	0.299	26.5	0.004
5.0	0.272	27.0	0.003
5.5	0.248	27.5	0.003
6.0	0.225	28.0	0.002
6.5	0.207	29.0	0.002
7.0	0.190	30.0	0.002
7.5	0.175	31.0	0.000
8.0	0.162		
8.5	0.149		
9.0	0.137		
9.5	0.127		
10.0	0.116		
10.5	0.107		
11.0	0.098		
11.5	0.090		
12.0	0.083		
12.5	0.076		
13.0	0.071		
13.5	0.064		
14.0	0.059		
14.5	0.054		
15.0	0.050		
15.5	0.046		
16.0	0.042		
16.5	0.037		
17.0	0.035		
17.5	0.032		
18.0	0.029		
18.5	0.026		
19.0	0.023		
19.5	0.022		
20.0	0.020		
20.5	0.018		
21.0	0.016		
21.5	0.014		

Piezometer 11C			
t (sec)	s (m)	t (sec)	s (m)
0.0	0.000	24.0	0.219
0.5	0.829	25.0	0.217
1.0	0.541	26.0	0.216
1.5	0.481	27.0	0.214
2.0	0.458	28.0	0.214
2.5	0.434	29.0	0.213
3.0	0.415	30.0	0.212
3.5	0.396	32.0	0.210
4.0	0.382	34.0	0.209
4.5	0.371	36.0	0.206
5.0	0.358	38.0	0.206
5.5	0.349	40.0	0.204
6.0	0.339	42.0	0.202
6.5	0.333	44.0	0.200
7.0	0.325	46.0	0.199
7.5	0.319	50.0	0.196
8.0	0.313	55.0	0.193
8.5	0.307	60.0	0.189
9.0	0.303	65.0	0.185
9.5	0.297	70.0	0.182
10.0	0.291	75.0	0.178
10.5	0.286	80.0	0.176
11.0	0.280	85.0	0.173
11.5	0.276	90.0	0.169
12.0	0.270	100.0	0.166
12.5	0.267	120.0	0.159
13.0	0.262	130.0	0.156
13.5	0.259	142.0	0.154
14.0	0.256	172.0	0.147
14.5	0.242	202.0	0.146
15.0	0.249	232.0	0.135
15.5	0.246	262.0	0.122
16.0	0.243	292.0	0.109
16.5	0.241	322.0	0.097
17.0	0.239	352.0	0.110
17.5	0.237	382.0	0.099
18.0	0.235	412.0	0.081
18.5	0.233	442.0	0.063
19.0	0.231	472.0	0.046
19.5	0.230	502.0	0.039
20.0	0.228	562.0	0.035
21.0	0.225	612.0	0.034
22.0	0.223	672.0	0.029
23.0	0.221	732.0	0.015

Piezometer 11E			
t (sec)	s (m)	t (sec)	s (m)
0.0	0.000	24.0	0.215
0.5	0.568	25.0	0.213
1.0	0.494	27.5	0.208
1.5	0.457	30.5	0.202
2.0	0.428	35.5	0.194
2.5	0.405	40.5	0.186
3.0	0.385	45.5	0.178
3.5	0.372	50.5	0.170
4.0	0.358	55.5	0.162
4.5	0.348	60.5	0.158
5.0	0.339	65.5	0.154
5.5	0.331	70.5	0.150
6.0	0.323	75.5	0.147
6.5	0.317	80.5	0.143
7.0	0.311	85.5	0.141
7.5	0.305	90.5	0.139
8.0	0.299	100.5	0.137
8.5	0.295	110.5	0.135
9.0	0.290	120.5	0.133
9.5	0.286	153.5	0.134
10.0	0.281	203.5	0.134
10.5	0.278	233.5	0.120
11.0	0.274	263.5	0.111
11.5	0.270	293.5	0.105
12.0	0.265	323.5	0.104
12.5	0.261		
13.0	0.258		
13.5	0.254		
14.0	0.252		
14.5	0.249		
15.0	0.247		
15.5	0.244		
16.0	0.242		
16.5	0.240		
17.0	0.238		
17.5	0.236		
18.0	0.234		
18.5	0.232		
19.0	0.230		
19.5	0.229		
20.0	0.227		
21.0	0.223		
22.0	0.221		
23.0	0.218		

Appendix F2 (cont.) - Slug Test Data

Piezometer 14B			
t (sec)	s (m)	t (sec)	s (m)
0.0	0.000	22.0	0.019
0.5	0.489	22.5	0.018
1.0	0.514	23.0	0.017
1.5	0.457	23.5	0.015
2.0	0.414	24.0	0.015
2.5	0.375	24.5	0.013
3.0	0.345	25.0	0.013
3.5	0.318	25.5	0.012
4.0	0.295	26.0	0.012
4.5	0.272	26.5	0.011
5.0	0.251	27.0	0.011
5.5	0.233	27.5	0.010
6.0	0.214	28.0	0.010
6.5	0.198	29.0	0.009
7.0	0.183	30.0	0.008
7.5	0.168	31.0	0.008
8.0	0.154	32.0	0.006
8.5	0.143	33.0	0.006
9.0	0.133	34.0	0.006
9.5	0.122	35.0	0.005
10.0	0.113	36.0	0.005
10.5	0.105	37.0	0.005
11.0	0.097	38.0	0.004
11.5	0.090	39.0	0.004
12.0	0.084	40.0	0.003
12.5	0.077	41.0	0.003
13.0	0.071	42.0	0.003
13.5	0.066	43.0	0.003
14.0	0.061	44.0	0.003
14.5	0.057	45.0	0.003
15.0	0.053	46.0	0.002
15.5	0.048	47.0	0.002
16.0	0.045	48.0	0.002
16.5	0.042	49.0	0.002
17.0	0.038	50.0	0.002
17.5	0.036	51.0	0.000
18.0	0.033		
18.5	0.031		
19.0	0.029		
19.5	0.027		
20.0	0.026		
20.5	0.024		
21.0	0.022		
21.5	0.021		

Piez. 14E	
t (sec)	s (m)
0.0	0.000
0.5	0.569
1.0	0.342
1.5	0.246
2.0	0.176
2.5	0.124
3.0	0.086
3.5	0.059
4.0	0.038
4.5	0.026
5.0	0.017
5.5	0.011
6.0	0.007
6.5	0.004
7.0	0.003
7.5	0.002
8.0	0.001
8.5	0.000

Appendix F2 (cont.) - Slug Test Data

Piez. 21B	
t (sec)	s (m)
0.0	0.000
0.5	0.985
1.0	0.460
1.5	0.378
2.0	0.310
2.5	0.256
3.0	0.212
3.5	0.176
4.0	0.146
4.5	0.122
5.0	0.101
5.5	0.083
6.0	0.070
6.5	0.057
7.0	0.047
7.5	0.038
8.0	0.032
8.5	0.026
9.0	0.021
9.5	0.017
10.0	0.013
10.5	0.010
11.0	0.008
11.5	0.006
12.0	0.004
12.5	0.003
13.0	0.001
13.5	0.001
14.0	0.000

Piez. 21C	
t (sec)	s (m)
0.0	0.000
0.5	0.559
1.0	0.391
1.5	0.355
2.0	0.291
2.5	0.238
3.0	0.193
3.5	0.156
4.0	0.125
4.5	0.099
5.0	0.080
5.5	0.062
6.0	0.049
6.5	0.038
7.0	0.029
7.5	0.022
8.0	0.015
8.5	0.011
9.0	0.007
9.5	0.004
10.0	0.002
10.5	0.000

Piez. 21E	
t (sec)	s (m)
0.0	0.000
0.5	0.932
1.0	0.471
1.5	0.392
2.0	0.325
2.5	0.264
3.0	0.213
3.5	0.168
4.0	0.136
4.5	0.108
5.0	0.086
5.5	0.068
6.0	0.055
6.5	0.043
7.0	0.034
7.5	0.027
8.0	0.021
8.5	0.017
9.0	0.013
9.5	0.010
10.0	0.008
10.5	0.006
11.0	0.005
11.5	0.004
12.0	0.003
12.5	0.003
13.0	0.002
13.5	0.002
14.0	0.002
14.5	0.001
15.0	0.001
15.5	0.001
16.0	0.001
16.5	0.000

Appendix F2 (cont.) - Slug Test Data

Piezometer 24B			
t (sec)	s (m)	t (sec)	s (m)
0.0	0.000	22.0	0.067
0.5	1.585	22.5	0.063
1.0	0.578	23.0	0.061
1.5	0.536	23.5	0.057
2.0	0.503	24.0	0.055
2.5	0.475	24.5	0.052
3.0	0.449	25.0	0.049
3.5	0.425	25.5	0.048
4.0	0.402	26.0	0.045
4.5	0.380	26.5	0.042
5.0	0.360	27.0	0.040
5.5	0.341	27.5	0.039
6.0	0.323	28.0	0.037
6.5	0.307	29.0	0.034
7.0	0.291	30.0	0.031
7.5	0.274	31.0	0.028
8.0	0.260	32.0	0.025
8.5	0.246	33.0	0.024
9.0	0.234	34.0	0.022
9.5	0.222	35.0	0.021
10.0	0.211	36.0	0.019
10.5	0.201	37.0	0.017
11.0	0.192	38.0	0.016
11.5	0.183	39.0	0.015
12.0	0.174	40.0	0.014
12.5	0.166	42.0	0.011
13.0	0.158	44.0	0.010
13.5	0.150	46.0	0.009
14.0	0.144	48.0	0.008
14.5	0.137	50.0	0.007
15.0	0.130	54.0	0.005
15.5	0.124	58.0	0.004
16.0	0.118	62.0	0.004
16.5	0.112	66.0	0.003
17.0	0.108	70.0	0.002
17.5	0.102	74.0	0.001
18.0	0.098		
18.5	0.092		
19.0	0.089		
19.5	0.085		
20.0	0.080		
20.5	0.077		
21.0	0.073		
21.5	0.070		

Piez. 24C	
t (sec)	s (m)
0.0	0.000
0.5	1.180
1.0	0.489
1.5	0.401
2.0	0.335
2.5	0.282
3.0	0.239
3.5	0.200
4.0	0.167
4.5	0.142
5.0	0.121
5.5	0.103
6.0	0.087
6.5	0.074
7.0	0.063
7.5	0.054
8.0	0.046
8.5	0.040
9.0	0.034
9.5	0.029
10.0	0.025
10.5	0.021
11.0	0.018
11.5	0.016
12.0	0.014
12.5	0.012
13.0	0.010
13.5	0.009
14.0	0.008
14.5	0.008
15.0	0.006
15.5	0.006
16.0	0.006
16.5	0.004
17.0	0.004
17.5	0.004
18.0	0.003
18.5	0.003
19.0	0.002

Piez. 24E	
t (sec)	s (m)
0.0	0.000
0.5	1.276
1.0	1.229
1.5	0.475
2.0	0.329
2.5	0.279
3.0	0.235
3.5	0.199
4.0	0.169
4.5	0.145
5.0	0.123
5.5	0.107
6.0	0.091
6.5	0.080
7.0	0.070
7.5	0.060
8.0	0.054
8.5	0.048
9.0	0.043
9.5	0.039
10.0	0.036
10.5	0.033
11.0	0.030
11.5	0.029
12.0	0.027
12.5	0.026
13.0	0.024
13.5	0.023
14.0	0.024
14.5	0.022
15.0	0.022
15.5	0.021
16.0	0.022
16.5	0.022
17.0	0.021
17.5	0.021
18.0	0.020

Appendix F2 (cont.) - Slug Test Data

Piezometer 32B			
t (sec)	s (m)	t (sec)	s (m)
0.00	0.000	11.00	0.006
0.25	0.007	11.25	0.005
0.50	1.180	11.50	0.004
0.75	0.459	11.75	0.004
1.00	0.400	12.00	0.003
1.25	0.358	12.25	0.003
1.50	0.323	12.50	0.003
1.75	0.292	12.75	0.002
2.00	0.263	13.00	0.002
2.25	0.235	13.25	0.002
2.50	0.211	13.50	0.001
2.75	0.190	13.75	0.001
3.00	0.171	14.00	0.001
3.25	0.153	14.25	0.001
3.50	0.138	14.50	0.001
3.75	0.124	14.75	0.001
4.00	0.112	15.00	0.001
4.25	0.101	15.25	0.001
4.50	0.091	15.50	0.000
4.75	0.081		
5.00	0.074		
5.25	0.066		
5.50	0.059		
5.75	0.053		
6.00	0.048		
6.25	0.044		
6.50	0.039		
6.75	0.035		
7.00	0.031		
7.25	0.028		
7.50	0.026		
7.75	0.023		
8.00	0.020		
8.25	0.018		
8.50	0.016		
8.75	0.015		
9.00	0.013		
9.25	0.011		
9.50	0.011		
9.75	0.008		
10.00	0.008		
10.25	0.007		
10.50	0.006		
10.75	0.006		

Piez. 32C	
t (sec)	s (m)
0.00	0.000
0.25	2.493
0.50	0.597
0.75	0.369
1.00	0.285
1.25	0.233
1.50	0.194
1.75	0.162
2.00	0.136
2.25	0.113
2.50	0.095
2.75	0.079
3.00	0.066
3.25	0.055
3.50	0.045
3.75	0.038
4.00	0.032
4.25	0.027
4.50	0.022
4.75	0.019
5.00	0.016
5.25	0.013
5.50	0.011
5.75	0.010
6.00	0.008
6.25	0.007
6.50	0.007
6.75	0.005
7.00	0.005
7.25	0.005
7.50	0.004
7.75	0.004
8.00	0.003
8.25	0.003
8.50	0.003
8.75	0.003
9.00	0.003
9.25	0.002
9.50	0.002
9.75	0.002
10.00	0.002
10.25	0.002
10.50	0.002
11.00	0.001

Piez. 32E	
t (sec)	s (m)
0.00	0.000
0.25	4.133
0.50	0.878
0.75	0.435
1.00	0.337
1.25	0.284
1.50	0.246
1.75	0.217
2.00	0.193
2.25	0.171
2.50	0.152
2.75	0.135
3.00	0.121
3.25	0.106
3.50	0.095
3.75	0.083
4.00	0.074
4.25	0.065
4.50	0.058
4.75	0.051
5.00	0.045
5.25	0.039
5.50	0.035
5.75	0.031
6.00	0.027
6.25	0.024
6.50	0.020
6.75	0.018
7.00	0.015
7.25	0.013
7.50	0.011
7.75	0.010
8.00	0.009
8.25	0.008
8.50	0.006
8.75	0.005
9.00	0.004
9.25	0.004
9.50	0.003
9.75	0.002
10.00	0.001
10.25	0.001
10.50	0.000

Appendix F2 (cont.) - Slug Test Data

Piezometer 34B					
t (sec)	s (m)	t (sec)	s (m)	t (sec)	s (m)
0.0	0.000	22.0	0.148	60.0	0.031
0.5	0.557	22.5	0.144	61.0	0.029
1.0	0.500	23.0	0.141	62.0	0.028
1.5	0.480	23.5	0.137	63.0	0.027
2.0	0.463	24.0	0.133	64.0	0.027
2.5	0.447	24.5	0.130	65.0	0.026
3.0	0.432	25.0	0.126	66.0	0.025
3.5	0.418	25.5	0.124	67.0	0.025
4.0	0.406	26.0	0.121	68.0	0.025
4.5	0.393	26.5	0.118	69.0	0.023
5.0	0.381	27.0	0.114	70.0	0.023
5.5	0.370	27.5	0.112	71.0	0.023
6.0	0.358	28.0	0.110	72.0	0.023
6.5	0.348	29.0	0.104	73.0	0.023
7.0	0.339	30.0	0.099	74.0	0.022
7.5	0.328	31.0	0.095	75.0	0.022
8.0	0.319	32.0	0.091	76.0	0.022
8.5	0.310	33.0	0.087	77.0	0.021
9.0	0.301	34.0	0.083	78.0	0.021
9.5	0.293	35.0	0.080	79.0	0.021
10.0	0.285	36.0	0.077	80.0	0.021
10.5	0.277	37.0	0.074	81.0	0.021
11.0	0.269	38.0	0.071	82.0	0.021
11.5	0.261	39.0	0.067	83.0	0.021
12.0	0.255	40.0	0.065	84.0	0.021
12.5	0.248	41.0	0.063	85.0	0.021
13.0	0.241	42.0	0.060	86.0	0.021
13.5	0.234	43.0	0.057	87.0	0.021
14.0	0.228	44.0	0.055	88.0	0.021
14.5	0.221	45.0	0.053	89.0	0.021
15.0	0.216	46.0	0.051	90.0	0.021
15.5	0.210	47.0	0.049	91.0	0.021
16.0	0.204	48.0	0.048	92.0	0.021
16.5	0.199	49.0	0.046	93.0	0.021
17.0	0.193	50.0	0.044	94.0	0.021
17.5	0.187	51.0	0.042	95.0	0.021
18.0	0.183	52.0	0.041	96.0	0.021
18.5	0.178	53.0	0.040	97.0	0.021
19.0	0.173	54.0	0.038	98.0	0.021
19.5	0.169	55.0	0.037	99.0	0.021
20.0	0.164	56.0	0.036	100.0	0.020
20.5	0.160	57.0	0.034	101.0	0.020
21.0	0.156	58.0	0.033	102.0	0.020
21.5	0.152	59.0	0.031	103.0	0.020

Piez. 34C	
t (sec)	s (m)
0.00	0.000
0.25	0.050
0.50	3.169
0.75	0.511
1.00	0.370
1.25	0.312
1.50	0.275
1.75	0.245
2.00	0.219
2.25	0.194
2.50	0.172
2.75	0.153
3.00	0.136
3.25	0.122
3.50	0.108
3.75	0.096
4.00	0.087
4.25	0.077
4.50	0.069
4.75	0.061
5.00	0.054
5.25	0.049
5.50	0.043
5.75	0.038
6.00	0.034
6.25	0.031
6.50	0.028
6.75	0.025
7.00	0.022
7.25	0.020
7.50	0.018
7.75	0.016
8.00	0.014
8.25	0.013
8.50	0.011
8.75	0.010
9.00	0.010
9.25	0.008
9.50	0.008
9.75	0.006
10.00	0.006
10.25	0.006
10.50	0.005
10.75	0.005

Piez. 34E	
t (sec)	s (m)
0.00	0.000
0.25	-0.019
0.50	3.341
0.75	0.760
1.00	0.466
1.25	0.373
1.50	0.325
1.75	0.287
2.00	0.260
2.25	0.235
2.50	0.213
2.75	0.193
3.00	0.176
3.25	0.159
3.50	0.144
3.75	0.131
4.00	0.118
4.25	0.107
4.50	0.096
4.75	0.087
5.00	0.079
5.25	0.072
5.50	0.064
5.75	0.058
6.00	0.053
6.25	0.046
6.50	0.042
6.75	0.037
7.00	0.034
7.25	0.029
7.50	0.026
7.75	0.023
8.00	0.020
8.25	0.019
8.50	0.016
8.75	0.015
9.00	0.012
9.25	0.012
9.50	0.010
9.75	0.009
10.00	0.008
10.25	0.006
10.50	0.005
10.75	0.004

Appendix G1 - Irrigation Data

Irrigation Date April 10, 1995				
time	weir gauge depth (cm)	calculated flow rate (gal/min)	elapsed time (min)	flow increment (gal)
7:30	52.00	4170	1	4170
7:45	52.00	4170	15	62557
8:00	52.00	4170	15	62557
8:15	54.00	4768	15	71525
8:30	54.00	4768	15	71525
8:50	56.00	5214	20	104278
9:00	56.00	5214	10	52139
9:15	55.50	5100	15	76503
9:30	55.00	4988	15	74821
9:45	53.00	4555	15	68319
10:00	52.00	4170	15	62557
10:15	52.00	4170	15	62557
10:30	52.00	4170	15	62557
10:45	51.75	4296	15	64438
11:00	53.50	4661	15	69911
11:20	53.50	4661	20	93215
11:30	50.50	4046	10	40462
11:45	51.00	4145	15	62175
12:00	54.00	4768	15	71525
12:15	55.00	4988	15	74821
12:30	55.00	4988	15	74821
12:45	55.50	5100	15	76503
13:00	55.50	5100	15	76503
13:20	54.50	4877	20	97549
13:30	54.25	4823	10	48227
13:35	54.00	4768	5	23842
		TOTAL	366	1,710,061

Appendix G1 (cont.) - Irrigation Data

Irrigation Date April 24, 1995				
time	weir gauge depth (cm)	calculated flow rate (gal/min)	elapsed time (min)	flow increment (gal)
7:26	37.0	1829	1	1829
7:31	39.5	2140	5	10700
7:36	40.0	2206	5	11029
7:43	52.0	4170	7	29193
7:48	52.0	4170	5	20852
8:07	53.5	4661	19	88554
8:23	53.0	4555	16	72874
8:43	48.0	3431	20	68614
9:03	50.5	4046	20	80925
9:29	51.0	4145	26	107770
9:45	52.5	4269	16	68308
10:00	48.5	3518	15	52776
10:15	52.5	4269	15	64038
10:30	52.0	4170	15	62557
10:43	52.5	4269	13	55500
10:45	52.5	4269	2	8538
11:00	53.0	4555	15	68319
11:15	53.0	4555	15	68319
11:30	53.0	4555	15	68319
11:45	52.5	4269	15	64038
12:00	52.0	4170	15	62557
12:15	51.0	4145	15	62175
12:30	46.5	3176	15	47636
12:46	47.5	3344	16	53510
13:00	45.5	3012	14	42173
13:15	41.5	2411	15	36160
13:30	36.5	1770	15	26551
13:45	25.0	723	15	10848
14:00	16.5	279	15	4190
14:05	10.5	104	5	519
		TOTAL	400	1,419,371

Appendix G1 (cont.) - Irrigation Data

Irrigation Date May 15, 1995				
time	weir gauge depth (cm)	calculated flow rate (gal/min)	elapsed time (min)	flow increment (gal)
13:20	51.0	4145	1	4145
13:25	52.5	4269	5	21346
13:30	53.5	4661	5	23304
13:40	53.5	4661	10	46607
13:50	53.5	4661	10	46607
14:05	54.0	4768	15	71525
14:20	54.0	4768	15	71525
14:35	54.0	4768	15	71525
14:50	55.5	5100	15	76503
15:05	55.5	5100	15	76503
15:20	55.5	5100	15	76503
15:35	55.0	4988	15	74821
15:50	55.0	4988	15	74821
16:05	55.0	4988	15	74821
16:20	55.0	4988	15	74821
16:35	55.0	4988	15	74821
16:50	54.5	4877	15	73162
17:05	54.5	4877	15	73162
17:20	55.0	4988	15	74821
17:35	55.0	4988	15	74821
17:50	55.0	4988	15	74821
18:00	55.0	4988	15	74821
18:15	55.0	4988	15	74821
18:30	53.5	4661	15	69911
18:40	53.0	4555	10	45546
18:45	52.5	4269	5	21346
18:50	52.0	4170	5	20852
18:55	51.5	4073	5	20366
19:00	52.5	4269	5	21346
19:05	53.0	4555	5	22773
19:10	53.5	4661	5	23304
19:15	53.5	4661	5	23304
19:20	54.0	4768	5	23842
19:22	54.0	4768	2	9537
19:23	54.0	4768	1	4768
		TOTAL	369	1,787,525

Appendix G1 (cont.) - Irrigation Data

Irrigation Date June 5, 1995				
time	weir gauge depth (cm)	calculated flow rate (gal/min)	elapsed time (min)	flow increment (gal)
13:13	26.5	829	1	829
13:16	45.5	3012	3	9037
13:23	52.5	4269	7	29885
13:31	54.5	4678	8	37427
13:46	54.5	4678	15	70175
14:01	54.5	4678	15	70175
14:16	54.5	4678	15	70175
14:31	53.5	4471	15	67064
14:45	54.5	4678	14	65497
15:00	54.5	4678	15	70175
15:15	54.5	4678	15	70175
15:30	54.5	4678	15	70175
15:45	54.5	4678	15	70175
16:00	54.0	4574	15	68609
16:15	54.5	4678	15	70175
16:30	54.0	4574	15	68609
16:45	53.5	4471	15	67064
17:00	53.5	4471	15	67064
17:15	53.5	4471	15	67064
17:30	53.5	4471	15	67064
17:45	54.0	4574	15	68609
18:00	54.0	4574	15	68609
18:15	54.0	4574	15	68609
18:30	54.0	4574	15	68609
18:45	54.5	4678	15	70175
19:00	54.5	4678	15	70175
19:10	50.0	3790	10	37896
		TOTAL	358	1,629,299

Appendix G1 (cont.) - Irrigation Data

Irrigation Date June 19, 1995				
time	weir gauge depth (cm)	calculated flow rate (gal/min)	elapsed time (min)	flow increment (gal)
11:40	36.5	1770	10	17700
11:45	36.0	1713	5	8563
12:00	34.0	1494	15	22408
12:15	33.0	1391	15	20869
12:30	32.5	1342	15	20124
12:45	34.0	1494	15	22408
13:00	37.0	1829	15	27431
13:15	42.0	2481	15	37221
13:30	43.0	2627	15	39401
13:45	49.5	3698	15	55467
14:00	51.0	3977	15	59659
14:15	52.0	4170	15	62557
14:30	52.5	4269	15	64038
14:45	52.5	4269	15	64038
15:00	53.5	4269	15	64038
15:15	53.0	4369	15	65541
15:30	53.0	4369	15	65541
15:45	53.0	4369	15	65541
16:00	53.0	4369	15	65541
16:15	53.0	4369	15	65541
16:30	52.5	4269	15	64038
16:45	53.0	4369	15	65541
17:00	52.5	4269	15	64038
17:15	53.5	4471	15	67064
17:30	53.0	4369	15	65541
17:45	53.0	4369	15	65541
18:00	53.5	4471	15	67064
18:15	53.5	4471	15	67064
18:30	53.0	4369	15	65541
18:45	53.0	4369	15	65541
18:55	51.0	3977	10	39773
19:00	41.0	2341	5	11706
19:05	33.0	1391	5	6956
19:10	27.0	866	5	4329
		TOTAL	460	1633360

Appendix G1 (cont.) - Irrigation Data

Irrigation Date July 28, 1995				
time	weir gauge depth (cm)	calculated flow rate (gal/min)	elapsed time (min)	flow increment (gal)
12:39	50.0	3790	1	3790
12:40	51.0	3977	1	3977
12:45	53.0	4369	5	21847
13:00	54.0	4574	15	68609
13:15	54.0	4574	15	68609
13:30	53.5	4471	15	67064
13:45	53.0	4369	15	65541
14:00	53.5	4471	15	67064
14:15	53.0	4369	15	65541
14:30	52.5	4269	15	64038
14:45	53.0	4369	15	65541
15:00	52.5	4269	15	64038
15:15	52.0	4170	15	62557
15:30	52.0	4170	15	62557
15:45	51.0	3977	15	59659
16:00	50.5	3883	15	58241
16:15	50.0	3790	15	56844
16:30	49.0	3607	15	54111
16:45	48.0	3431	15	51460
17:00	49.0	3607	15	54111
17:15	50.0	3790	15	56844
17:30	50.5	3883	15	58241
17:45	51.0	3977	15	59659
18:00	51.0	3977	15	59659
18:15	52.0	4170	15	62557
18:30	52.0	4170	15	62557
18:45	52.5	4269	15	64038
19:00	53.0	4369	15	65541
19:15	53.5	4471	15	67064
19:30	54.0	4574	15	68609
19:45	40.5	2273	15	34092
19:50	33.0	1391	5	6956
19:55	27.0	866	5	4329
20:00	19.5	408	5	2038
		TOTAL	442	1757384

Appendix G1 (cont.) - Irrigation Data

Irrigation Date July 10, 1995				
time	weir gauge depth (cm)	calculated flow rate (gal/min)	elapsed time (min)	flow increment (gal)
14:24	34.0	1494	1	1494
14:25	45.5	3012	1	3012
14:30	52.0	4170	5	20852
14:35	52.0	4170	5	20852
14:40	54.0	4574	5	22870
14:45	54.0	4574	5	22870
15:00	54.5	4678	15	70175
15:15	50.0	3790	15	56844
15:30	47.0	3259	15	48891
15:45	43.5	2701	15	40519
16:00	46.0	3093	15	46401
16:15	50.5	3883	15	58241
16:30	52.5	4269	15	64038
16:45	52.5	4269	15	64038
17:00	54.0	4574	15	68609
17:15	53.5	4471	15	67064
17:30	53.0	4369	15	65541
17:45	52.5	4269	15	64038
18:00	52.0	4170	15	62557
18:15	52.5	4269	15	64038
18:30	52.5	4269	15	64038
18:45	52.0	4170	15	62557
19:00	52.0	4170	15	62557
19:15	52.0	4170	15	62557
19:30	52.0	4170	15	62557
19:45	51.5	4073	15	61098
20:00	52.5	4269	15	64038
20:15	54.0	4574	15	68609
20:30	54.5	4678	15	70175
20:45	54.5	4678	15	70175
20:52	54.5	4678	7	32749
20:54	55.0	4784	2	9568
21:00	54.5	4678	6	28070
21:10	54.5	4678	10	46784
21:15	54.0	4574	5	22870
21:25	54.0	4574	10	45739
21:35	44.0	2777	5	13886
		TOTAL	435	1808134

Appendix G1 (cont.) - Irrigation Data

Irrigation Date August 8, 1995				
time	weir gauge depth (cm)	calculated flow rate (gal/min)	elapsed time (min)	flow increment (gal)
12:30	34.0	1494	1	1494
12:31	36.0	1713	1	1713
12:32	38.5	2012	1	2012
12:33	42.0	2481	1	2481
12:34	45.0	2933	1	2933
12:35	47.5	3344	1	3344
12:40	51.5	4073	5	20366
13:04	54.5	4678	24	112281
13:26	54.5	4678	22	102924
14:00	54.5	4678	34	159064
14:15	54.5	4678	15	70175
14:30	55.0	4784	15	71764
14:45	55.0	4784	15	71764
15:00	54.5	4678	15	70175
15:15	54.5	4678	15	70175
15:30	54.5	4678	15	70175
15:45	54.5	4678	15	70175
16:00	54.5	4678	15	70175
16:15	54.0	4574	15	68609
16:30	54.5	4678	15	70175
16:45	54.0	4574	15	68609
17:00	53.5	4471	15	67064
17:15	53.5	4471	15	67064
		TOTAL	286	1314713

Appendix G1 (cont.) - Irrigation Data

Irrigation Date September 9, 1995				
time	weir gauge depth (cm)	calculated flow rate (gal/min)	elapsed time (min)	flow increment (gal)
15:15	35.0	1601	1	1601
15:30	48.0	3431	15	51460
15:45	52.0	4170	15	62557
16:00	51.5	4073	15	61098
16:15	51.5	4073	15	61098
16:30	51.5	4073	15	61098
16:45	51.5	4073	15	61098
17:00	51.5	4073	15	61098
17:15	48.0	3431	15	51460
17:30	48.0	3431	15	51460
17:45	51.5	4073	15	61098
18:00	48.0	3431	15	51460
18:15	48.5	3518	15	52776
18:30	52.5	4269	15	64038
18:45	49.0	3607	15	54111
19:00	52.5	4269	15	64038
19:15	53.0	4369	15	65541
19:30	52.5	4269	15	64038
19:45	53.0	4369	15	65541
19:48	53.0	4369	3	13108
		TOTAL	273	1079777

Appendix G1 (cont.) - Irrigation Data

Irrigation Date September 26, 1995				
time	weir gauge depth (cm)	calculated flow rate (gal/min)	elapsed time (min)	flow increment (gal)
13:30	55.0	4784	1	4784
13:45	54.5	4678	15	70175
14:00	54.5	4678	15	70175
14:15	54.0	4574	15	68609
14:30	54.5	4678	15	70175
14:45	54.5	4678	15	70175
15:00	54.0	4574	15	68609
15:15	55.0	4784	15	71764
15:30	54.5	4678	15	70175
15:45	54.5	4678	15	70175
16:00	55.0	4784	15	71764
16:15	54.0	4574	15	68609
16:30	54.5	4678	15	70175
16:45	54.5	4678	15	70175
17:00	54.5	4678	15	70175
17:15	54.5	4678	15	70175
17:30	54.5	4678	15	70175
17:45	54.5	4678	15	70175
18:00	54.5	4678	15	70175
18:15	54.5	4678	15	70175
18:18	30.0	1110	3	3329
		TOTAL	289	1339924

Appendix G2 - Weir Calibration Data

The flow velocity data tabled below was gathered using a Marsh-McBirney FLOWMATE® electronic water velocity meter. Measurements were made at the 20, 60, and 80% depths (measured from the water surface).

Depth (ft)	Area (ft^2)	20% depth (ft/sec)	80% depth (ft/sec)	60% depth (ft/sec)	Average (ft/sec)	Meter (gpm)	Weir (gpm)	Diff (%)
1.7	3.4	3.01	2.58	2.93	2.86	4368	4574	4.5
1.7	3.4	2.98	2.67	2.89	2.86	4361	4574	4.7
1.7	3.4	2.95	2.60	2.93	2.85	4353	4574	4.8
1.7	3.4	2.95	2.55	2.91	2.83	4319	4574	5.6
1.7	3.4	2.89	2.55	2.82	2.77	4227	4471	5.5
1.7	3.4	2.90	2.60	2.78	2.77	4219	4369	3.4

$$AVERAGE = \frac{\left(\frac{20\%depth + 80\%depth}{2}\right) + 60\%depth}{2}$$

Appendix G1 (cont.) - Irrigation Data

Irrigation Date October 23, 1995				
time	weir gauge depth (cm)	calculated flow rate (gal/min)	elapsed time (min)	flow increment (gal)
11:30	54.75*	4730	1	4730
11:45	54.75*	4730	15	70950
12:00	54.75*	4730	15	70950
12:15	54.75*	4730	15	70950
12:30	54.75*	4730	15	70950
12:45	54.75*	4730	15	70950
13:00	54.75*	4730	15	70950
13:15	54.75*	4730	15	70950
13:30	54.75*	4730	15	70950
13:45	54.75*	4730	15	70950
14:00	54.75*	4730	15	70950
14:15	54.75*	4730	15	70950
14:30	54.75*	4730	15	70950
14:45	54.75*	4730	15	70950
15:00	54.75*	4730	15	70950
15:15	54.75*	4730	15	70950
15:30	54.75*	4730	15	70950
15:45	54.5	4678	15	70175
16:00	54.5	4678	15	70175
16:15	54.5	4678	15	70175
16:30	55.0	4784	15	71764
16:45	55.0	4784	15	71764
17:00	55.0	4784	15	71764
17:15	55.0	4784	15	71764
17:30	55.0	4784	15	71764
17:45	54.5	4678	15	70175
18:00	54.5	4678	15	70175
18:15	54.5	4678	15	70175
18:30	55.0	4784	15	71764
18:35	54.5	4678	5	23392
18:40	46.5	3176	5	15879
18:45	39.0	2075	5	10376
18:50	29.0	1024	5	5121
18:55	27.5	904	5	4520
19:00	19.5	408	5	2038
		TOTAL	456	2054287

* Project field personnel were not on site until 15:45. Irrigation start time as per irrigator. Water depths prior to 15:45 are the average flow rate for 15:45 to 18:35.

Appendix H1 - West Manhole Flow Calibration Data

Comparison of manual vs. metered flow rates. Data gathered on April 7, 1995, with 1 inch ID flow control section installed in the west manhole.

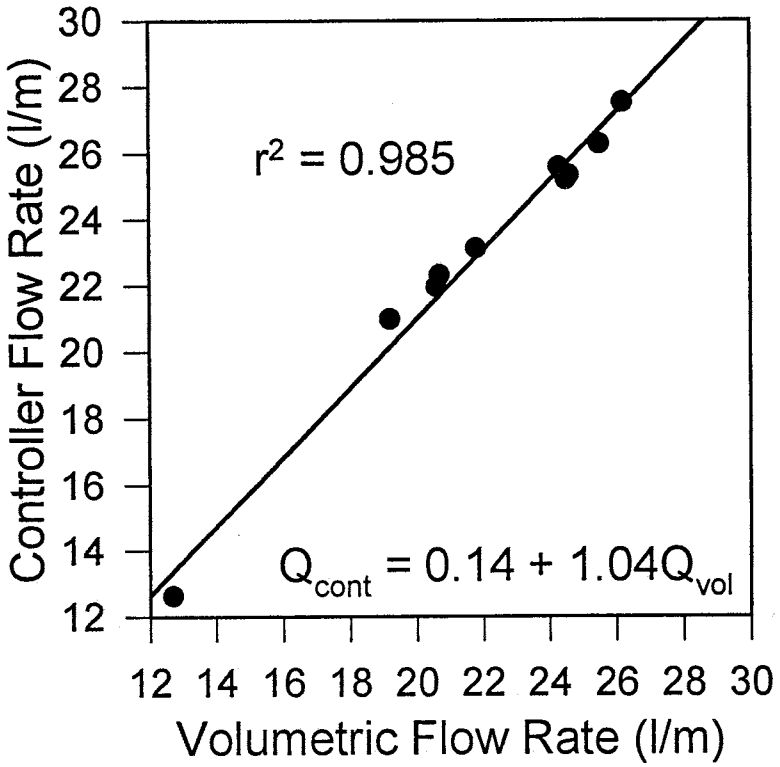

Q_{vol}	Q_{cont}	% difference
12.6	12.7	-0.6
21.0	19.2	8.5
22.0	20.6	6.2
22.3	20.7	7.2
23.1	21.8	5.7
25.6	24.3	5.0
25.2	24.5	2.7
25.3	24.6	2.8
26.3	25.5	3.0
27.5	26.2	4.8
	Average	4.5

Appendix H2 - Impact of Flow Measurement System on Head

Measurement of tile-drain water levels before (1994) and after (1995) installation of the flow measurement system. Values are given in terms of the average head measured in monitoring wells 22 and 23, which straddle the tile-drain line at the west manhole.

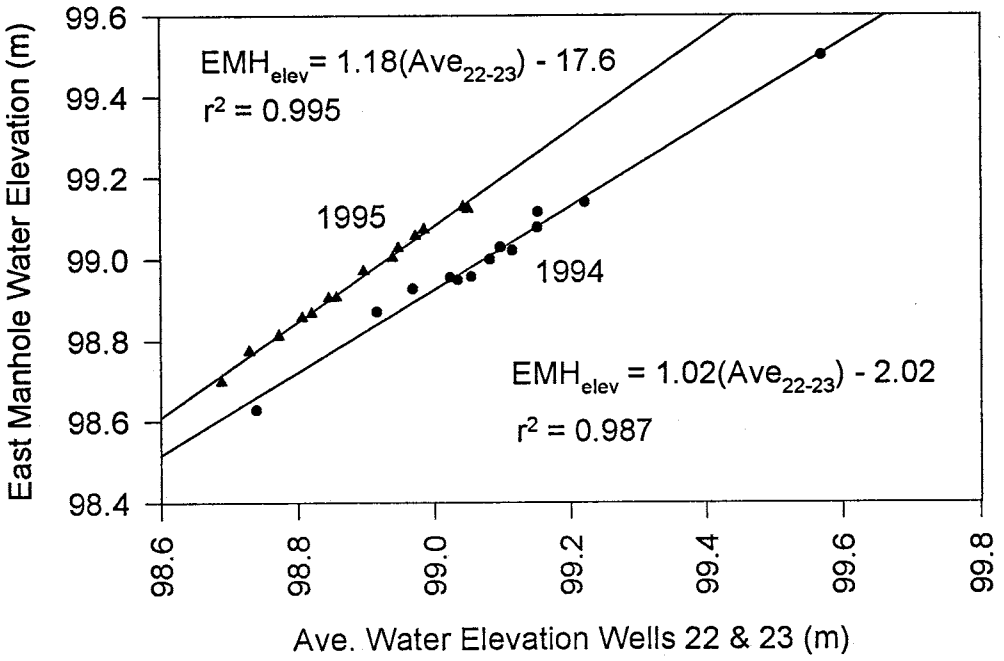

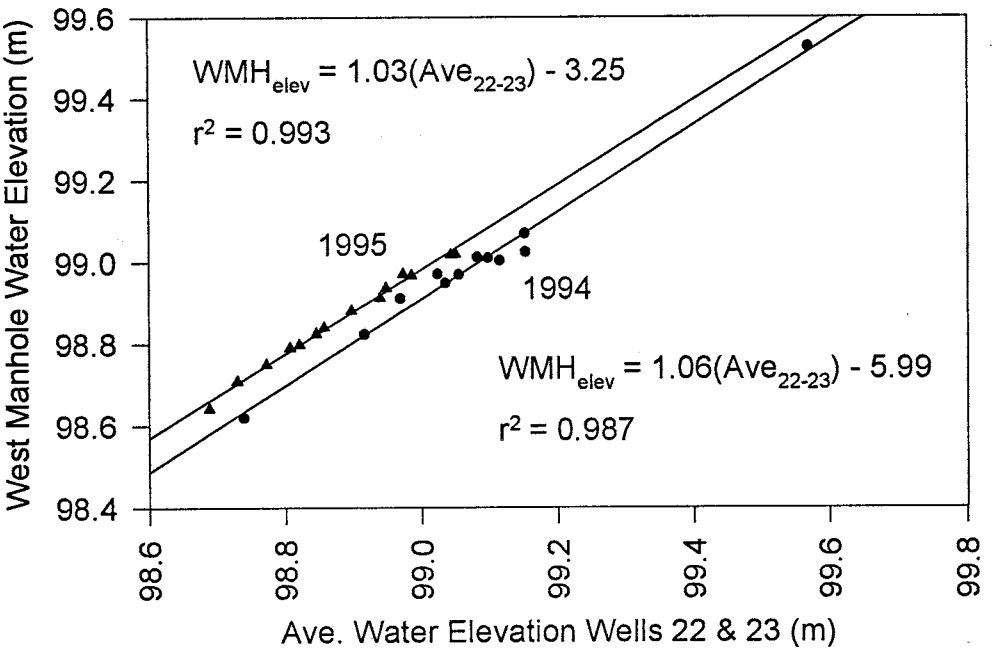

Appendix H3 - Tile-Drain Flow Rates

The following pages present graphical month-long records of the tile-drain flow rate data collected in the east and west manholes. Tile-drain flow rates were recorded at time intervals ranging from 3 to 10 minutes. The data plotted on the graphs represent flow rates averaged over the previous 0.5-hr interval.

Flow rate curves are labeled with "East" and "West" to indicate flow rates measured in the east and west manholes, respectively. Thicker-lined flow rate curves labeled "Difference" are the result of subtracting the east manhole flow rate from the west manhole flow rate to provide the net center bench flow to the tile-drain. Difference curves are ommited during periods of missing data and, for clarity, during periods of erratic flow behavior.

Dashed vertical lines represent the starting time of an irrigation event. Dashed lines are labeled at the top of the graph with the bench sequence of irrigation. For example: "East - Center - West" indicates three sequential irrigations in that order while "East & West - Center" indicates two sequential irrigations, with water applied to east and west benches simultaneously. Question marks (?) following a bench irrigation text indicate either an unknown (if not accompanied by a dashed line) or approximated (if accompanied by a dashed line) irrigation starting time.

Circular symbols appearing on the date axis indicate a monitoring well and piezometer water level survey was conducted on that date.

Appendix H3 (cont.) - Tile-Drain Flow Rates

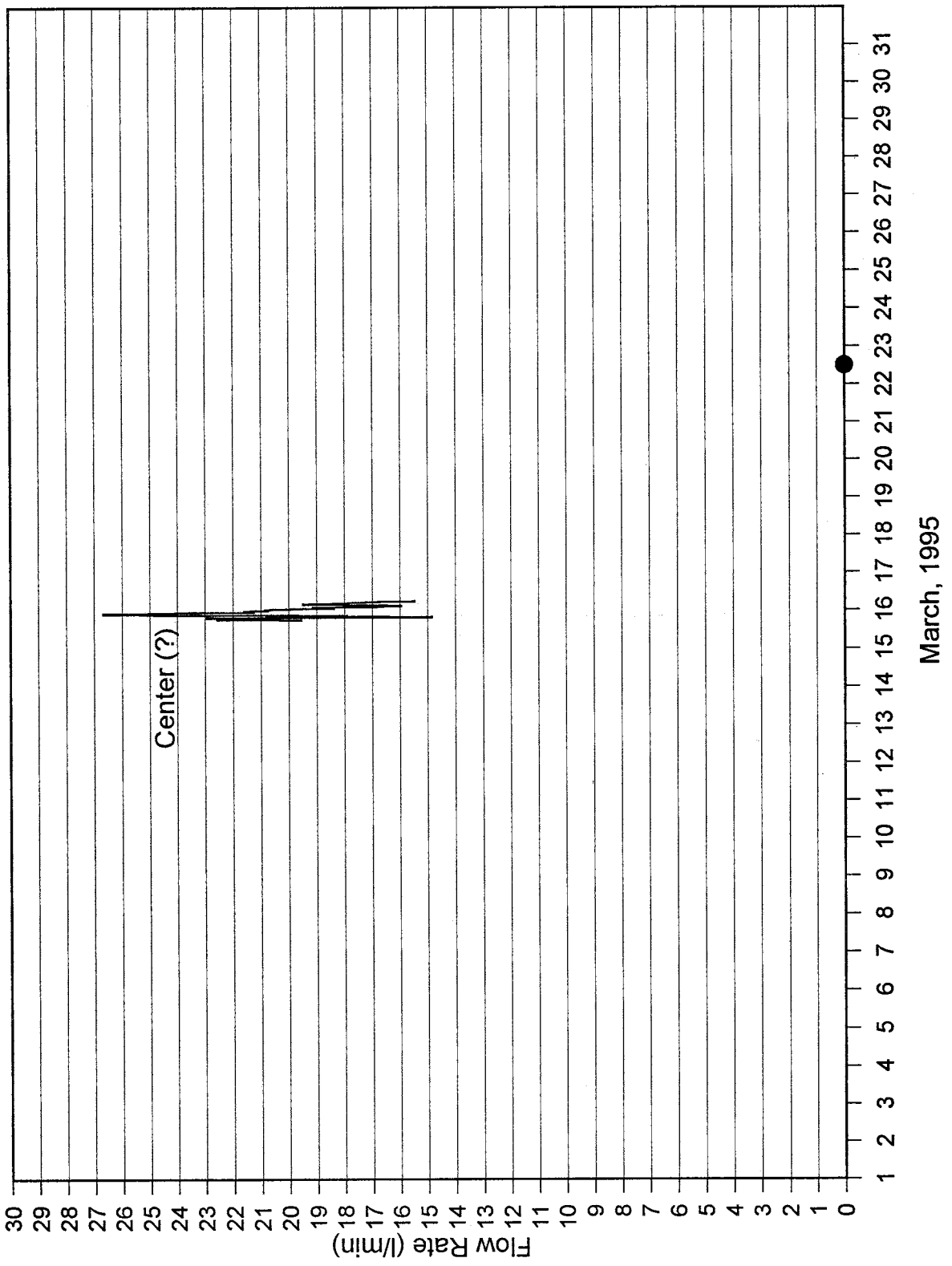

Appendix H3 (cont.) - Tile-Drain Flow Rates

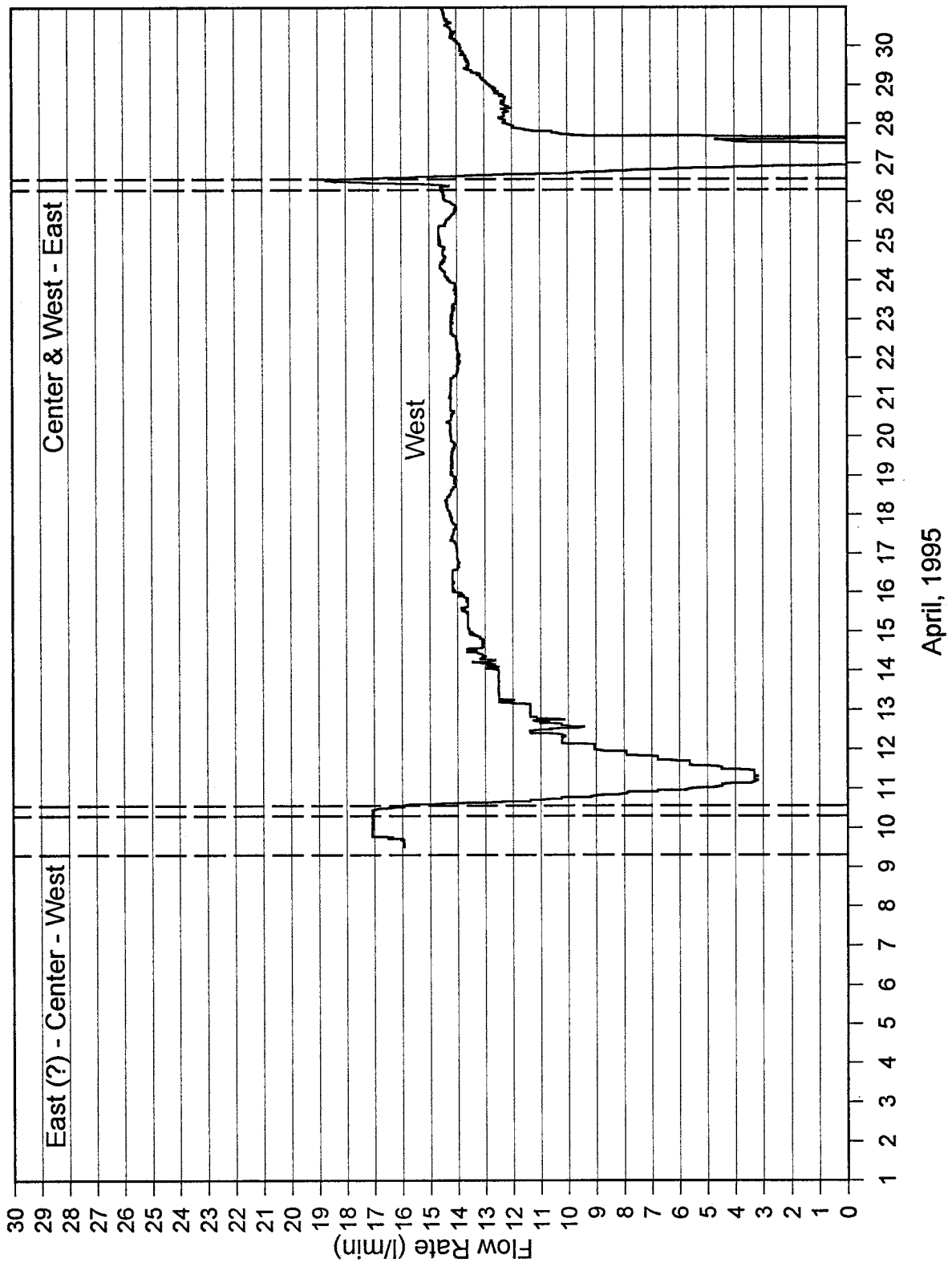

Appendix H3 (cont.) - Tile-Drain Flow Rates

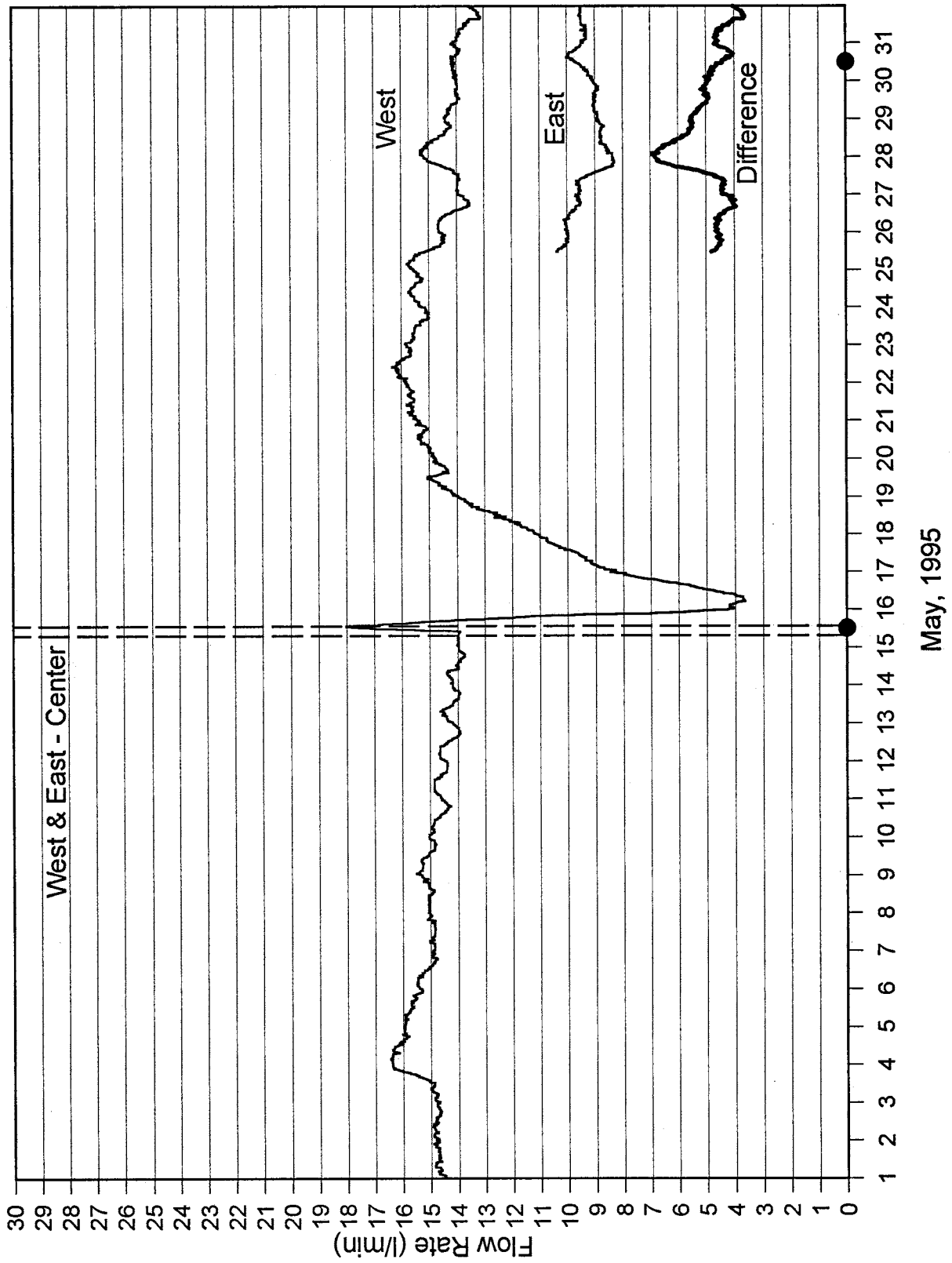

Appendix H3 (cont.) - Tile-Drain Flow Rates

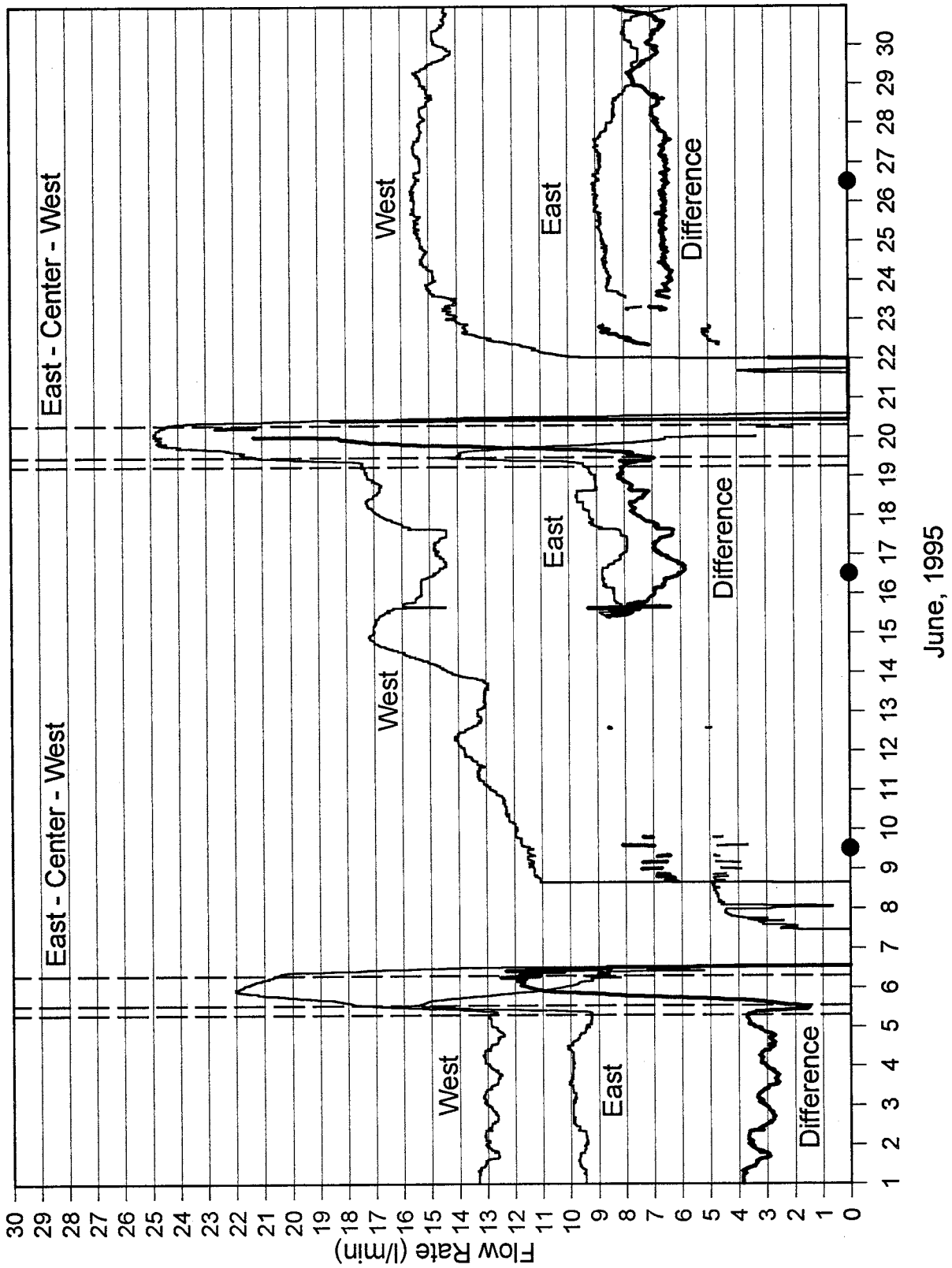

Appendix H3 (cont.) - Tile-Drain Flow Rates

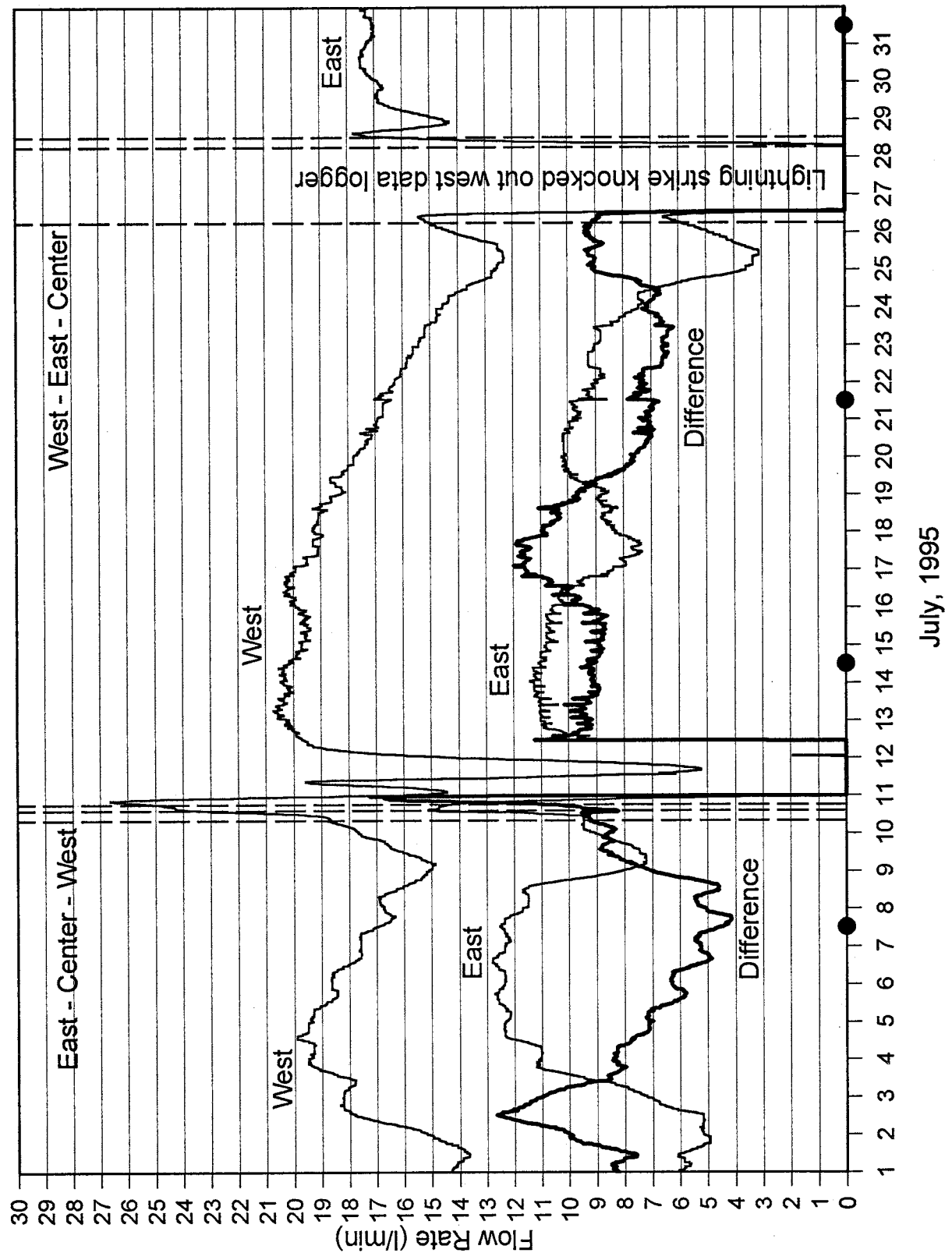

Appendix H3 (cont.) - Tile-Drain Flow Rates

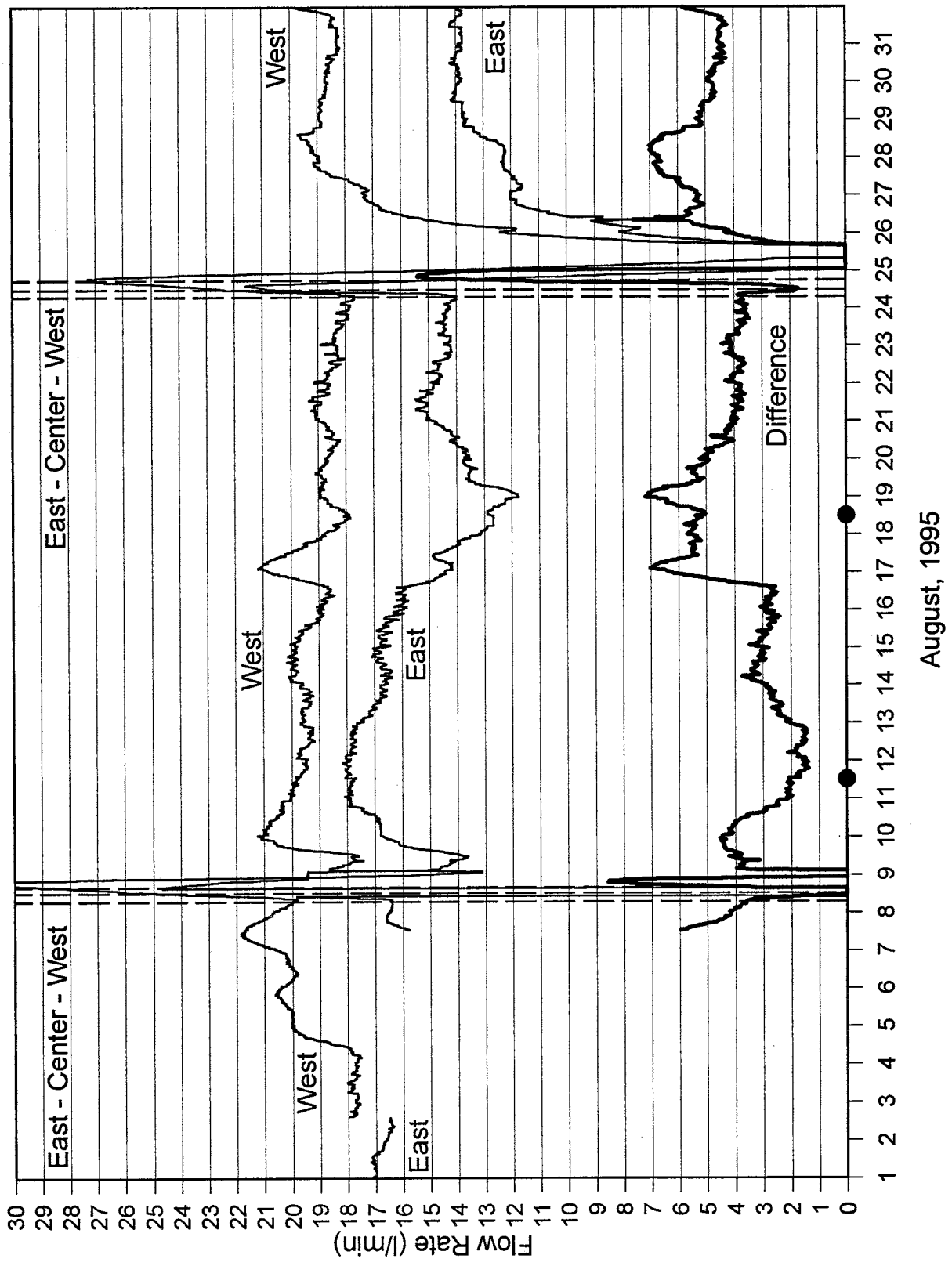

Appendix H3 (cont.) - Tile-Drain Flow Rates

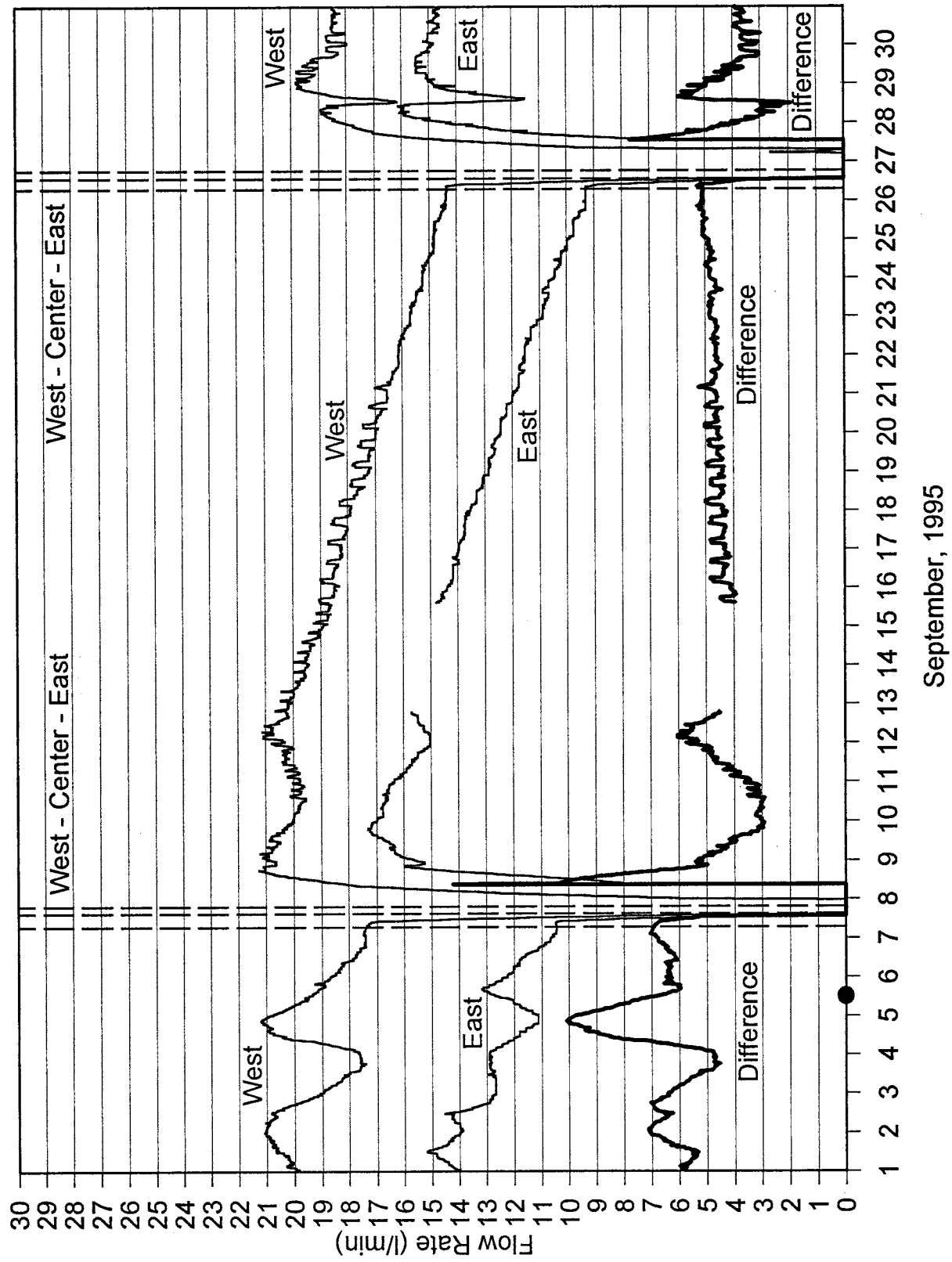

Appendix H3 (cont.) - Tile-Drain Flow Rates

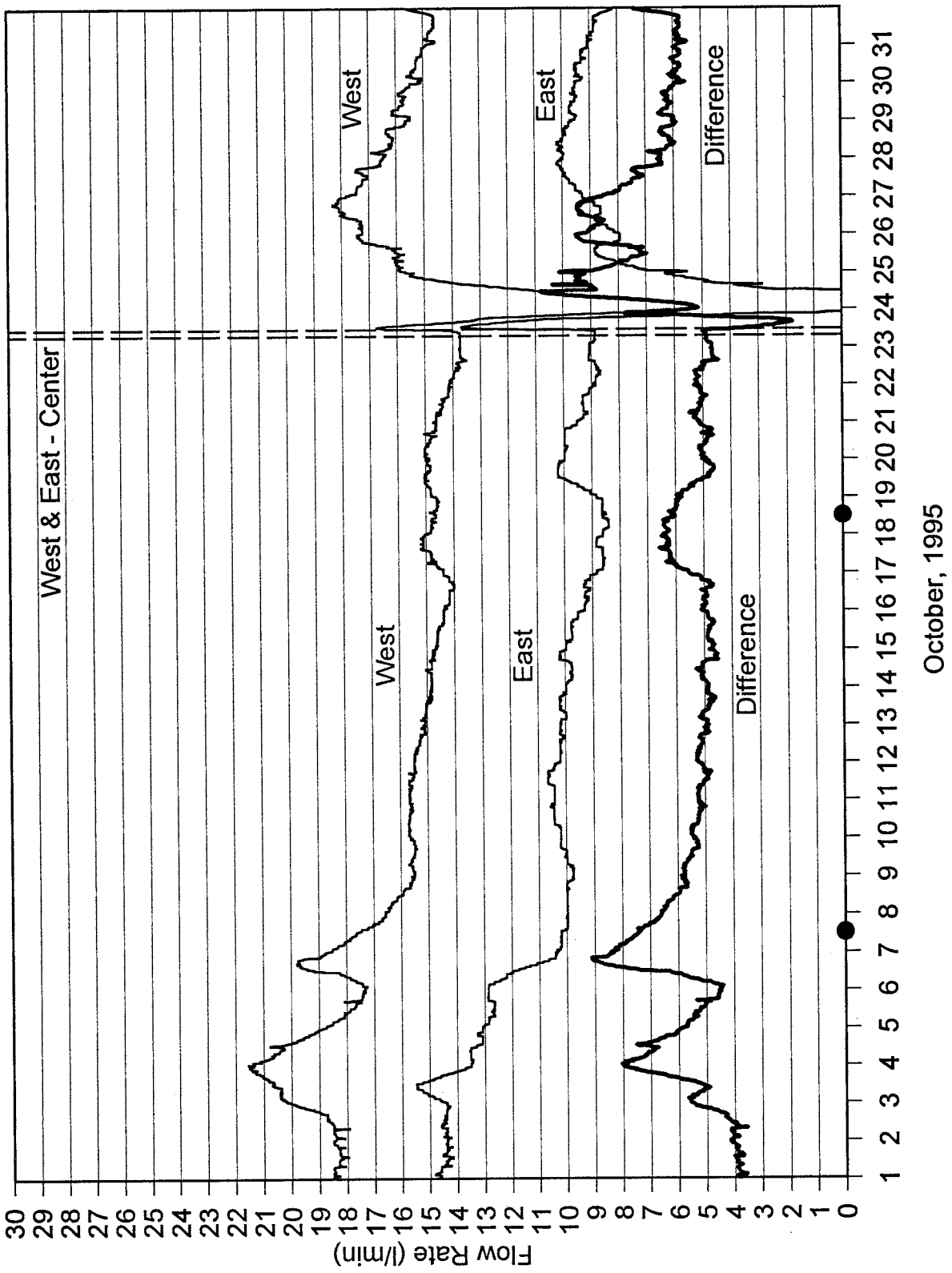

Appendix H3 (cont.) - Tile-Drain Flow Rates

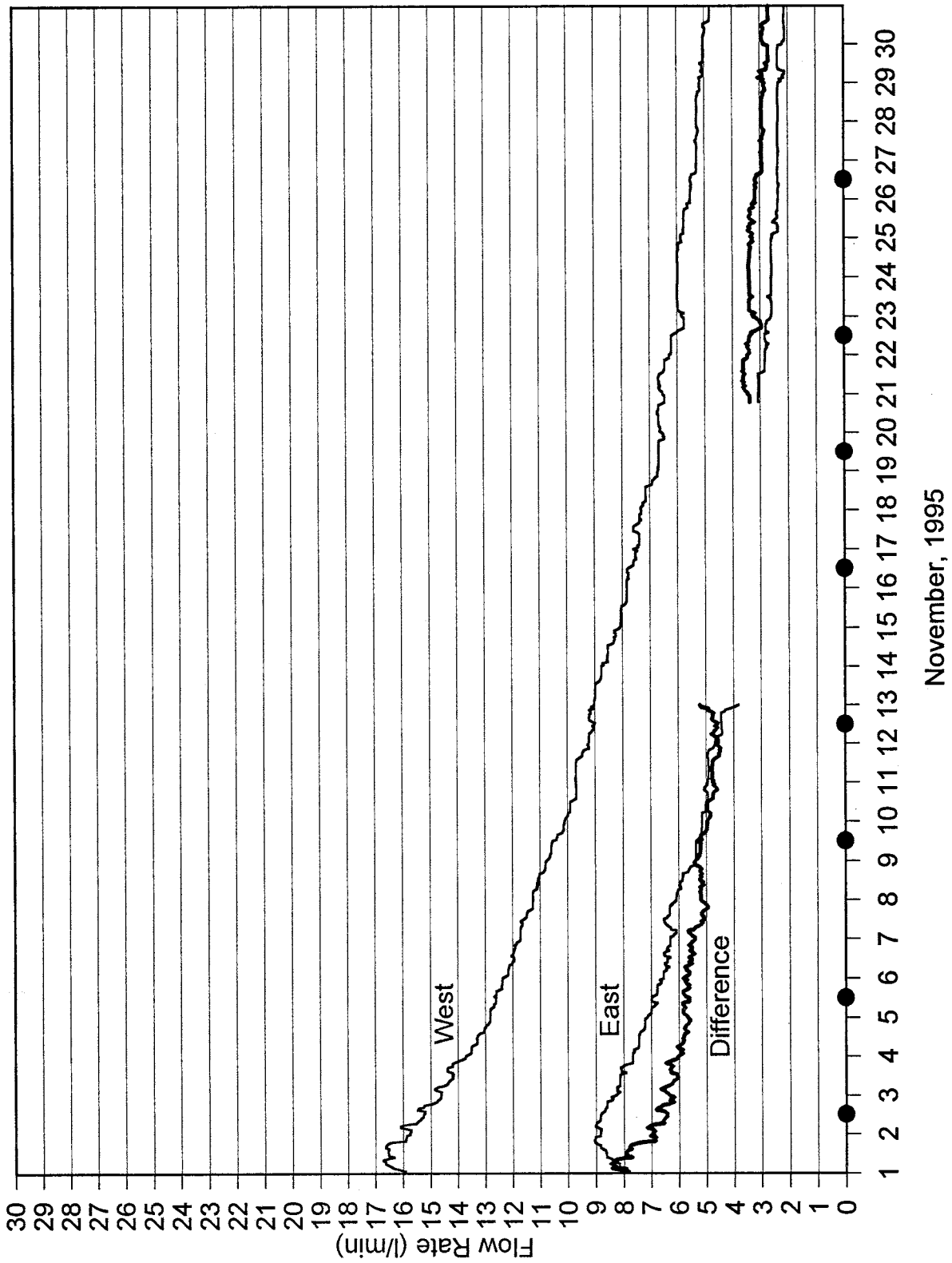

Appendix H3 (cont.) - Tile-Drain Flow Rates

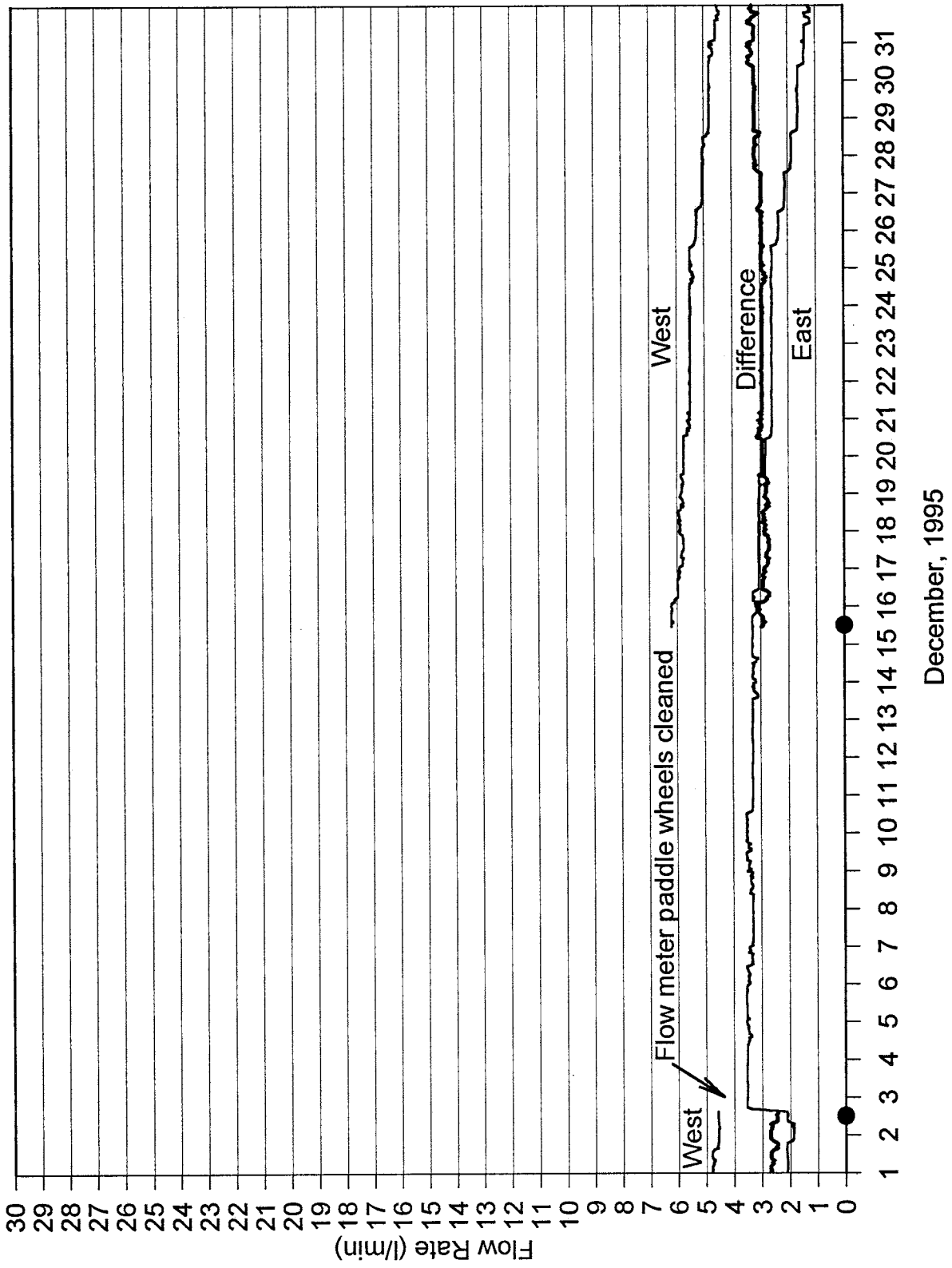

Appendix H3 (cont.) - Tile-Drain Flow Rates

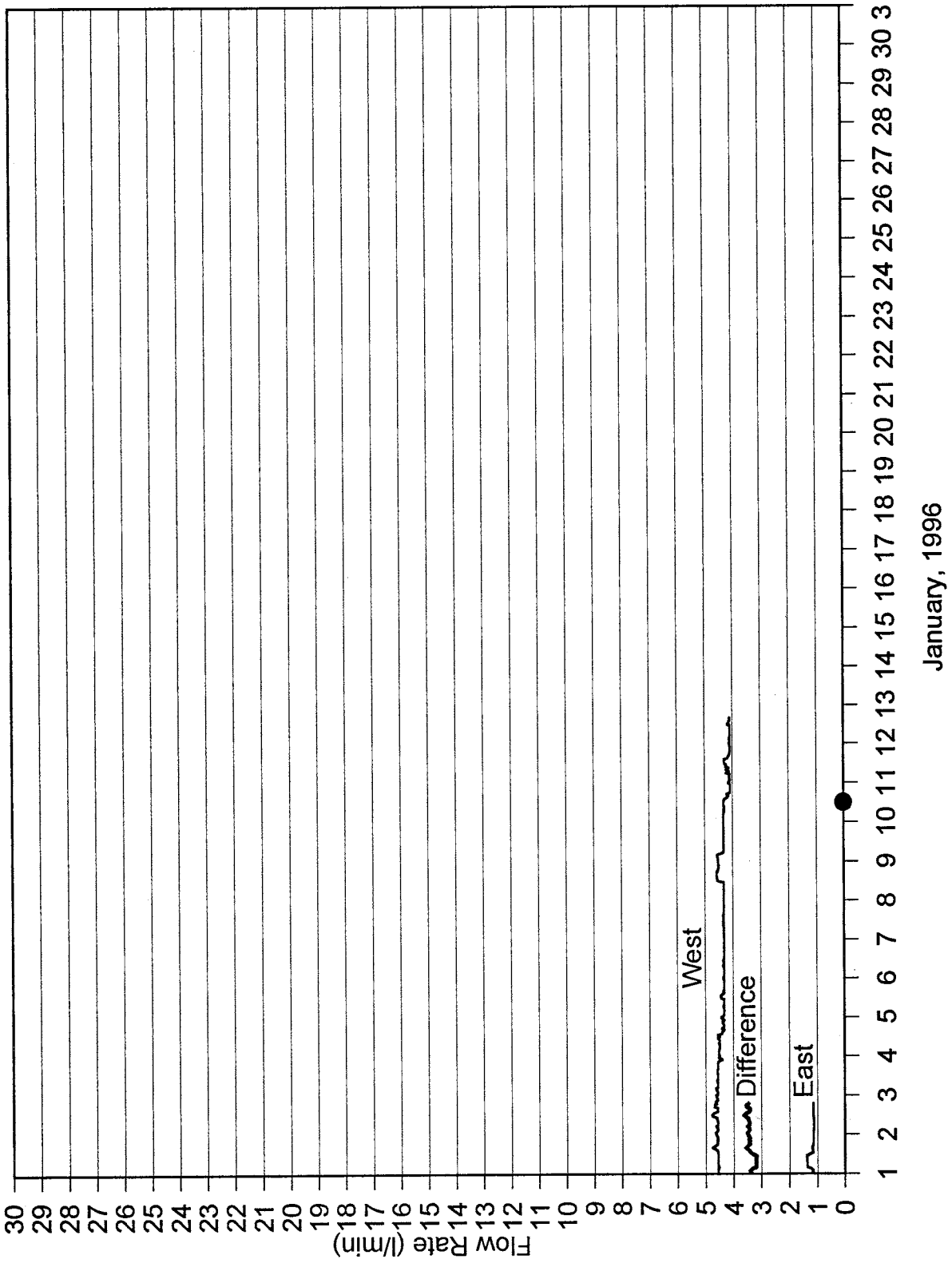

Appendix H3 (cont.) - Tile-Drain Flow Rates

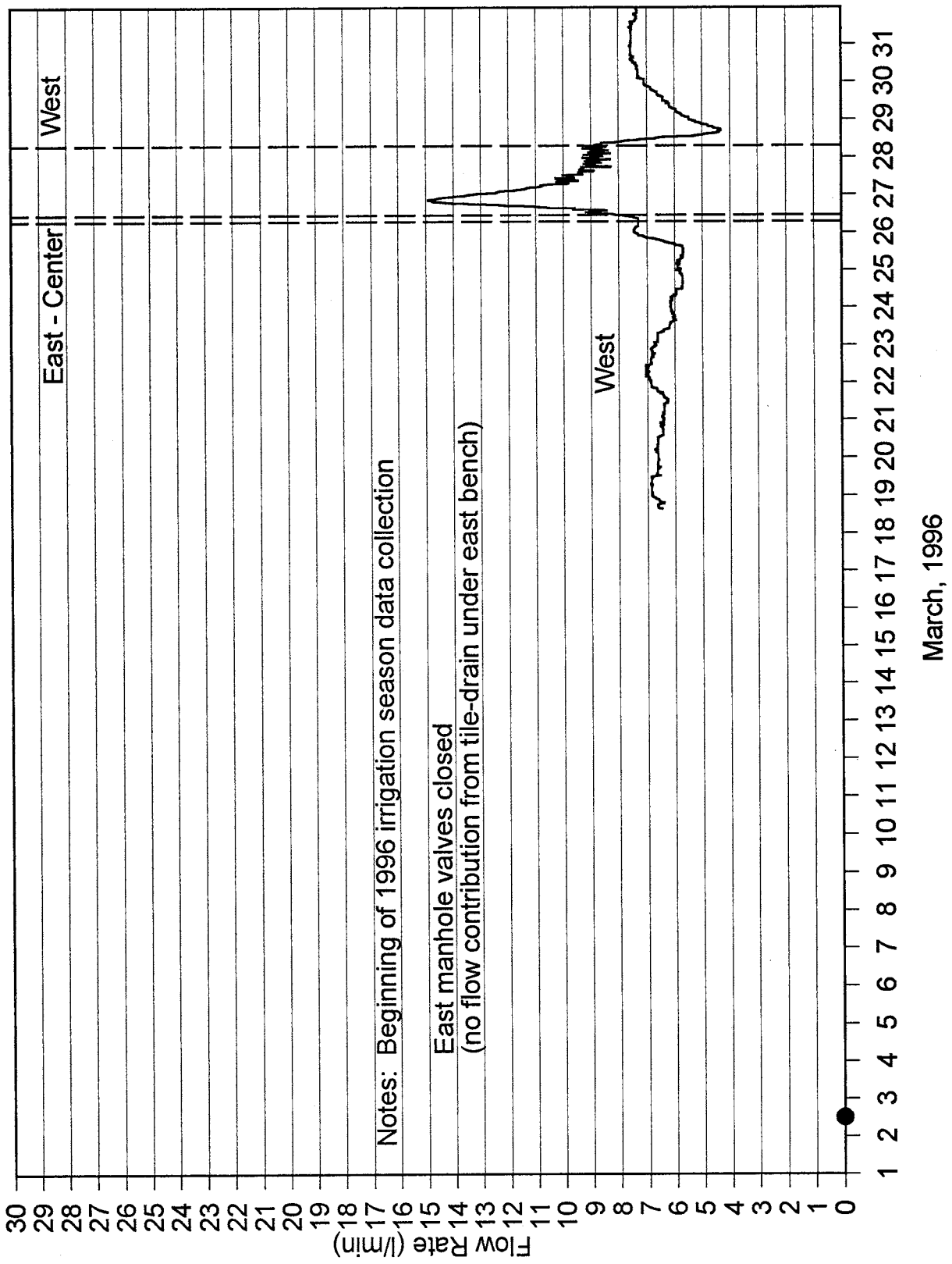

Appendix H3 (cont.) - Tile-Drain Flow Rates

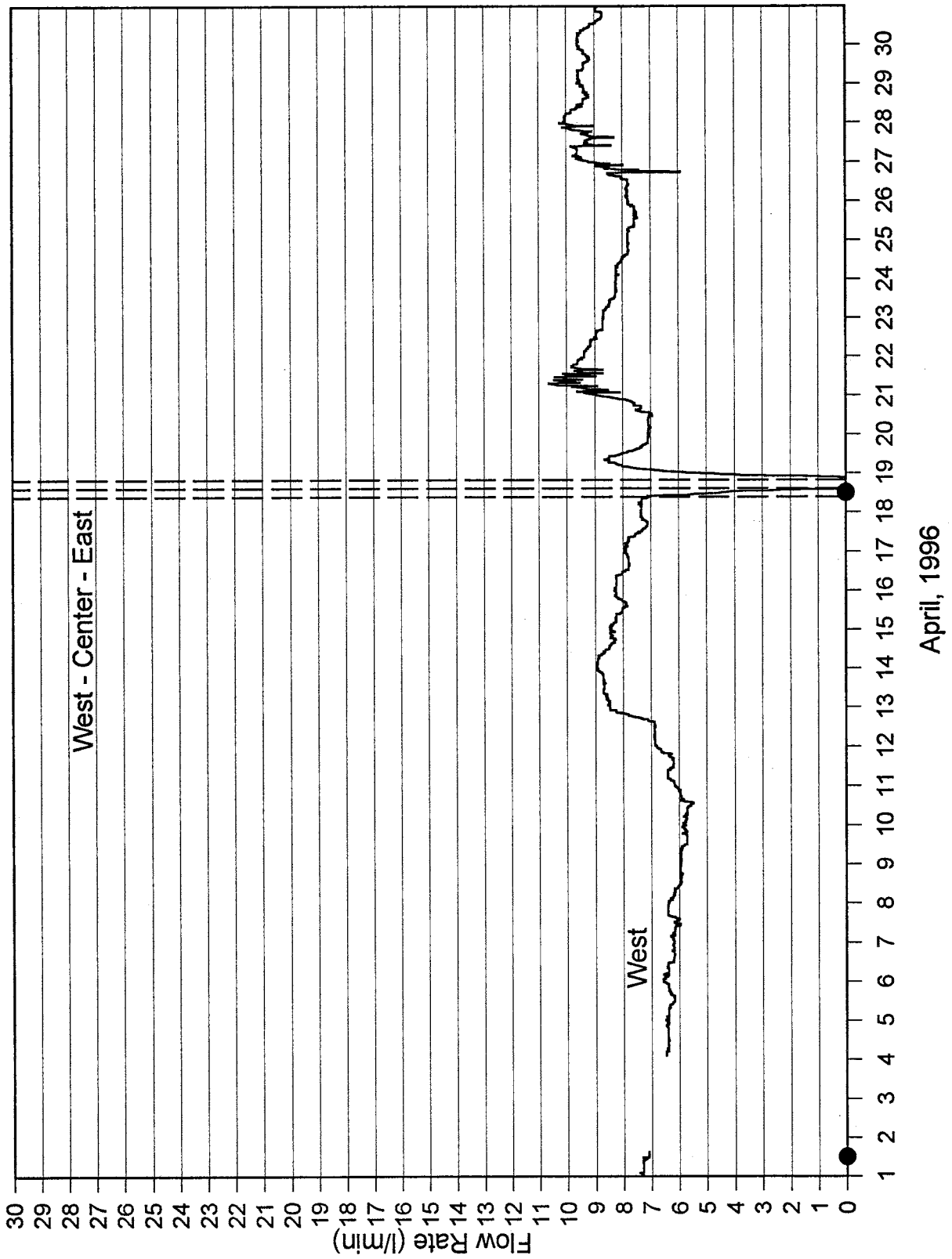

Appendix H3 (cont.) - Tile-Drain Flow Rates

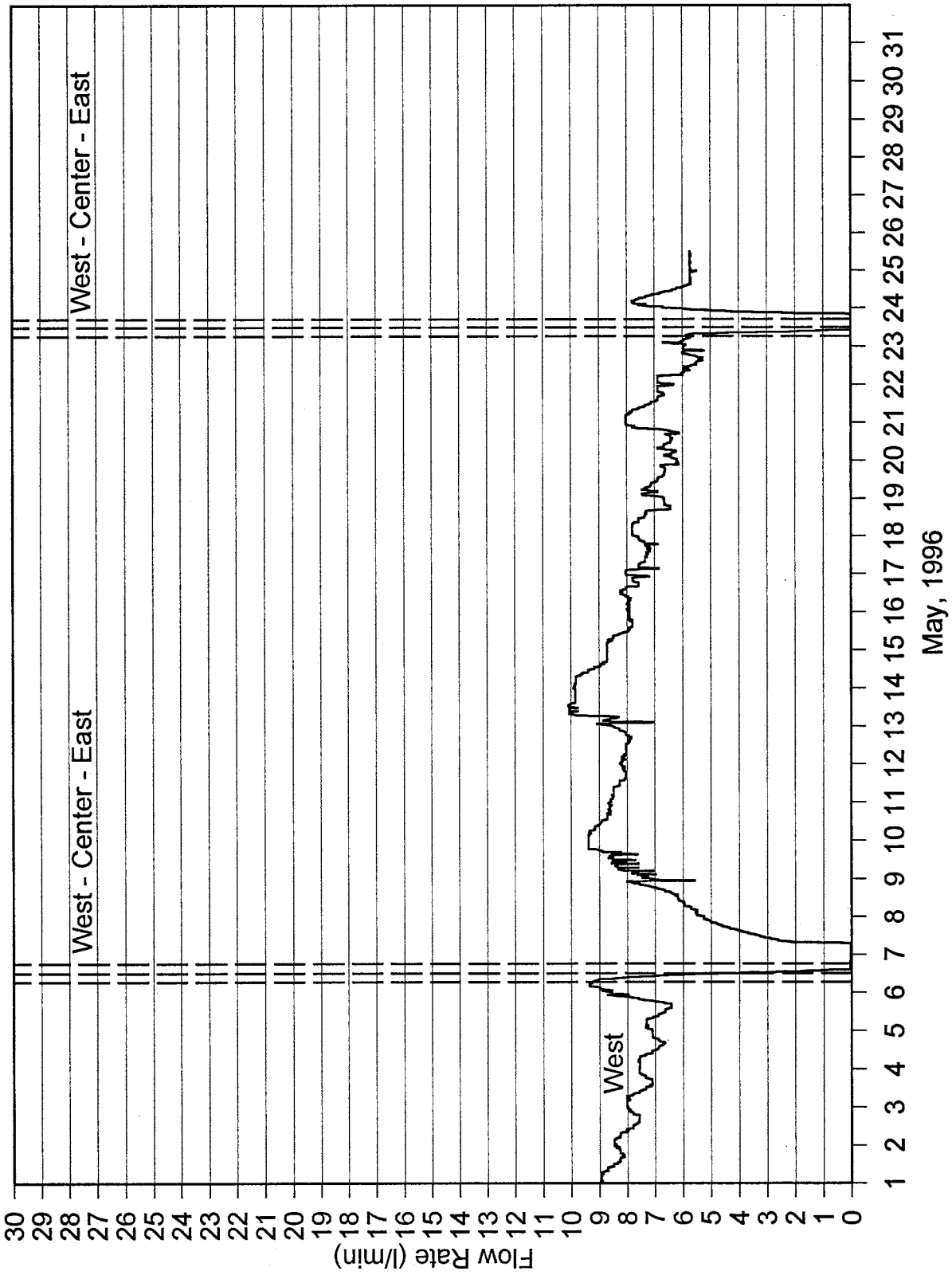

Appendix I - Center Bench Ground Survey Data

[1]X (m)	[1]Y (m)	[2]Z (m)
1000.000	1022.180	99.985
1000.000	1071.830	100.024
1000.000	1091.261	100.015
1000.000	1122.080	100.052
1000.000	1171.480	100.104
1000.000	1221.980	100.113
1017.908	999.232	99.890
1018.159	1021.540	99.942
1018.717	1071.193	99.960
1019.281	1121.394	100.009
1019.836	1170.816	100.049
1020.407	1221.517	100.085
1020.600	1238.680	100.061
1068.233	996.719	99.909
1068.477	1019.767	99.927
1069.005	1069.483	99.966
1069.536	1119.608	100.012
1070.063	1169.139	100.043
1070.606	1220.379	100.079
1070.800	1238.680	100.091
1117.951	994.517	99.906
1118.196	1018.015	99.948
1118.715	1067.790	99.985
1119.238	1117.841	99.994

X (m)	Y (m)	Z (m)
1119.757	1167.478	100.040
1120.298	1219.251	100.073
1120.500	1238.680	100.082
1168.017	991.502	99.912
1168.265	1016.250	99.939
1168.766	1066.087	99.957
1169.269	1116.062	99.982
1169.768	1165.805	100.027
1170.294	1218.116	100.091
1170.500	1238.680	100.098
1217.792	988.396	99.927
1218.085	1014.494	99.951
1218.645	1064.390	99.982
1219.205	1114.288	99.997
1219.764	1164.134	100.034
1220.356	1216.981	100.088
1220.601	1238.680	100.085
1236.600	1013.841	99.942
1236.600	1063.779	99.954
1236.600	1081.850	99.957
1236.600	1113.669	99.976
1236.600	1163.571	100.003
1236.600	1216.612	100.043

[1] Coordinates are based on local coordinate system (same as for wells)

[2] Elevations are based on arbitrary vertical datum (same as for wells)

This thesis is accepted on behalf of the faculty
of the Institute by the following committee:

Advisor

8/8/96
Date

I release this document to the New Mexico Institute of Mining and Technology.

Student's Signature

8/8/96
Date